Akademia Górniczo-Hutnicza im. Stanisława Staszica w Krakowie

DZIEDZINA NAUK INŻYNIERYJNO-TECHNICZNYCH
DYSCYPLINA INŻYNIERIA BIOMEDYCZNA

ROZPRAWA DOKTORSKA

Nieorganiczno-organiczne materiały hybrydowe dla inżynierii tkanki kostnej

Autor: Piotr Robert Pańtak

Promotor rozprawy: dr hab. inż. Aneta Zima, prof. AGH
Promotor pomocniczy: dr inż. Joanna Czechowska

Praca wykonana: Akademia Górniczo-Hutnicza im. S. Staszica w Krakowie
Wydział Inżynierii Materiałowej i Ceramiki
Katedra Ceramiki i Materiałów Ogniotrwałych

Kraków 2025

AGH University of Krakow

FIELD OF ENGINEERING AND TECHNICAL SCIENCES
DISCIPLINE OF BIOMEDICAL ENGINEERING

DOCTORAL DISSERTATION

Inorganic-organic hybrid materials for bone tissue engineering

Author: Piotr Robert Pańtak

First supervisor: dr hab. inż. Aneta Zima, prof. AGH
Auxiliary supervisor: dr inż. Joanna Czechowska

Completed at: AGH University of Kraków
Faculty of Materials Science and Ceramics
Department of Ceramics and Refractories

Kraków 2025

Podziękowania

Pragnę wyrazić swoją serdeczną wdzięczność promotor pracy, dr hab. inż. Anecie Zimie, prof. AGH oraz promotor pomocniczej dr inż. Joannie Czechowskiej za stworzenie mi warunków do rozwoju naukowego, wsparcie merytoryczne, cenne wskazówki oraz zaangażowanie na każdym etapie realizacji rozprawy doktorskiej.

Szczególne podziękowania kieruję do Władz, Pracowników i Koleżanek oraz Kolegów z Wydziału Inżynierii Materiałowej i Ceramiki AGH, którzy umożliwili mi prowadzenie badań. Z wyjątkowym sentymentem wspominam śp. prof. dr hab. inż. Annę Ślósarczyk, która rozbudziła moje zainteresowanie tematyką bioceramiki fosforanowo-wapniowej.

Dziękuję także dr inż. Ewelinie Cichoń, mgr inż. Szymonowi Skibińskiemu oraz mgr inż. Kindze Kowalskiej za życzliwą atmosferę w laboratorium oraz wsparcie w trakcie realizacji pracy.

Jestem również wdzięczny wszystkim osobom, których pomoc i obecność przyczyniły się do powstania niniejszej rozprawy.

Na końcu pragnę podziękować z całego serca mojej Rodzinie i Bliskim za nieustanne wsparcie, cierpliwość i motywację. Wasza obecność miała dla mnie ogromne znaczenie.

Spis treści

Streszczenie

W obliczu rosnącego zapotrzebowania na zaawansowane materiały kościozastępcze, wynikającego z konieczności rekonstrukcji uszkodzonej tkanki twardej, niniejsza rozprawa doktorska koncentruje się na opracowaniu i kompleksowej charakterystyce innowacyjnych, hybrydowych biomateriałów przeznaczonych do regeneracji kości. W prowadzonych badaniach, w celu ograniczenia wad fosforanowo-wapniowych cementów kostnych, zastosowano wieloaspektowe podejście do modyfikacji ich wyjściowego składu poprzez wykorzystanie polimerów naturalnych, silanowych środków sprzęgających, a także wprowadzenie pierwiastków o korzystnym działaniu biologicznym.

Głównym celem rozprawy było zaprojektowanie składu, synteza wyjściowych materiałów, wytworzenie oraz kompleksowa ocena właściwości fizykochemicznych i biologicznych nowych, hybrydowych materiałów kościozastępczych typu cementowego. Dążono do uzyskania biomateriałów charakteryzujących się odpowiednimi właściwościami fizykochemicznymi i biologicznymi, które pozwoliłyby na ich zastosowanie w efektywnej regeneracji tkanki kostnej. Prowadzone badania miały na celu ustalenie zależności pomiędzy wprowadzonymi modyfikacjami składów materiałów wyjściowych, a końcowymi właściwościami otrzymanych hybrydowych materiałów wiązanych chemicznie. Założono również, że opracowane biomateriały będą mogły pełnić rolę nośników substancji o korzystnym działaniu biologicznym oraz będą przydatne do wytwarzania spersonalizowanych implantów z wykorzystaniem nowoczesnych technik formowania.

Opracowano nowoczesne biomateriały wiązane chemicznie tzw. biomikrobetony zawierające w składzie wyjściowym wysokoreaktywny proszek α-fosforanu (V) wapnia (α-TCP), hybrydowe granule hydroksyapatytowo-chitozanowe (HA/CTS) oraz żel pektynowy. Potwierdzono podwójny mechanizm wiązania otrzymanych materiałów, opierający się na hydrolizie α-TCP oraz sieciowaniu zastosowanych polimerów. W badaniach wykorzystano również zmodyfikowane tytanem lub miedzią hybrydowe granule hydroksyapatytowo-chitozanowe. Wykazano, że biomateriały te wykazały najwyższą aktywność antybakteryjną, skutecznie ograniczając adhezję i wzrost *Escherichia coli* oraz *Staphylococcus aureus*.

Kluczowym i dotychczas niestosowanym podejściem do otrzymywania biomateriałów wiązanych chemicznie było wykorzystanie powierzchniowej metody modyfikacji proszku α-TCP przy użyciu dwóch silanowych środków sprzęgających, a mianowicie: tetraetoksysilanu (TEOS) i 3-glicydoksypropylotrimetoksysilanu (GPTMS). Działanie to pozwoliło na otrzymanie biomateriałów o wyższej wytrzymałości na ściskanie dzięki wytworzeniu dodatkowych wiązań chemicznych w ich strukturze. Opracowano także nowatorskie rusztowania kostne otrzymane z wykorzystaniem robocastingu. Pasty do druku 3D zawierały w swym wyjściowym składzie: α-TCP (zmodyfikowany lub

niemodyfikowany silanowymi środkami sprzęgającymi), hybrydowy proszek HA/CTS oraz fazę ciekłą stanowiącą mieszaninę pektyny cytrusowej i wodorofosforanu (V) sodu. W ramach prowadzonych badań zaprojektowano i przebadano szereg składów past bioceramicznych o korzystnych właściwościach reologicznych, umożliwiających precyzyjne wytwarzanie trójwymiarowych struktur o kontrolowanej porowatości, charakteryzujących się dobrymi właściwościami biologicznymi, potwierdzonymi w testach *in vitro*.

Podsumowując, przedstawione w niniejszej rozprawie wyniki badań stanowią wartościowe źródło inspiracji dla projektowania wysoko sfunkcjonalizowanych materiałów hybrydowych typu cementowego, które mogą znaleźć szerokie zastosowanie w inżynierii tkanki kostnej oraz stanowić solidny fundament dla dalszych badań, zwłaszcza biologicznych *in vivo*.

Abstract

In response to the increasing demand for advanced bone substitute materials arising from the need to reconstruct damaged hard tissue, this doctoral dissertation focuses on the development and comprehensive characterization of innovative hybrid biomaterials intended for bone regeneration. In the conducted research, a multifaceted strategy was employed to address the limitations of calcium phosphate bone cements by modifying their initial composition through the incorporation of natural polymers, silane coupling agents, and chemical elements known for their beneficial biological activity.

The main aim of this dissertation was to obtain and develop novel hybrid cementitious-type bone substitutes, followed by their comprehensive physicochemical and biological characterization. Emphasis was placed on developing biomaterials with improved functional properties that would enable their effective application in bone tissue regeneration. The study further sought to elucidate the relationships between the modifications introduced into the initial compositions and the resulting properties of the cementitious materials. Additionally, it was assumed that the developed biomaterials could serve as carriers for biologically active substances and be suitable for the fabrication of personalized implants using advanced manufacturing techniques.

Novel biomaterials, referred to as biomicroconcretes, consisting of highly reactive α-tricalcium phosphate (α-TCP), hybrid hydroxyapatite–chitosan (HA/CTS) granules, and citrus-pectin-based gel, were obtained and developed. A dual setting mechanism was confirmed, involving α-TCP hydrolysis and polymer crosslinking. In addition, titanium- and copper-modified HA/CTS granules were incorporated into selected formulations. These biomaterials demonstrated antibacterial activity, effectively inhibiting the adhesion and proliferation of *Escherichia coli* and *Staphylococcus aureus*.

A key and previously unexplored approach implemented in this dissertation was the surface modification of α-TCP powder using two silane coupling agents—tetraethoxysilane (TEOS) and 3-glycidoxypropyltrimethoxysilane (GPTMS). This strategy enabled the development of biomaterials with significantly enhanced compressive strength due to the formation of additional chemical bonds within the material's structure. Furthermore, innovative bone scaffolds were fabricated using robocasting. The 3D-printing pastes comprised α-TCP (either unmodified or silane-modified), hybrid HA/CTS powder, and a liquid phase composed of citrus pectin and disodium phosphate. A series of bioceramic paste formulations with favourable rheological properties were designed and evaluated, enabling the precise fabrication of three-dimensional scaffolds with controlled porosity and demonstrating promising biological performance *in vitro*.

In conclusion, the findings presented in this dissertation demonstrate that the obtained and developed biomaterials possess properties that make them strong candidates

for application in bone tissue substitution. Moreover, they provide a valuable foundation for the development of highly functionalized hybrid biomaterials with broad potential in bone tissue engineering and constitute a solid basis for further research, particularly *in vivo* studies.

Wykaz publikacji wchodzących w skład cyklu

Rozprawę doktorską stanowi cykl sześciu oryginalnych, spójnych tematycznie artykułów naukowych opublikowanych w latach 2021-2025, o łącznym współczynniku oddziaływania IF = 26,42 oraz o łącznej punktacji MNiSW = 720 punktów.

Publikacja 1

Tytuł: Novel Double Hybrid-Type Bone Cements Based on Calcium Phosphates, Chitosan and Citrus Pectin

Autorzy: Piotr Pańtak, Joanna P. Czechowska, Ewelina Cichoń, Aneta Zima

Dane bibliograficzne: International Journal of Molecular Sciences; ISSN 1422-0067. — 2023 — vol. 24 iss. 17 art. no. 13455, s. 1–15, doi: 10.3390/ijms241713455.

IF= 5,6; **Punkty MNiSW=** 140

Publikacja 2

Tytuł: Influence of Natural Polysaccharides on Properties of the Biomicroconcrete-Type Bioceramics

Autorzy: Piotr Pańtak, Ewelina Cichoń, Joanna P. Czechowska, Aneta Zima

Dane bibliograficzne: Materials; ISSN 1996-1944. — 2021 — vol. 14 iss. 24 art. no. 7496, s. 1–14, doi: 10.3390/ma14247496.

IF= 3,62; **Punkty MNiSW=** 140

Publikacja 3

Tytuł: The Influence of Silane Coupling Agents on the Properties α-TCP-Based Ceramic Bone Substitutes for Orthopaedic Applications

Autorzy: Piotr Pańtak, Joanna P. Czechowska, Aneta Zima

Dane bibliograficzne: RSC Advances; ISSN 2046-2069. — 2023 — vol. 13 iss. 48, s. 34020–34031, doi: 10.1039/d3ra06027f

IF= 3,9; **Punkty MNiSW=** 100

Publikacja 4

Tytuł: The Synergistic Effect of Polysaccharides and Silane Coupling Agents on the Properties of Calcium Phosphate-Based Bone Substitutes

Autorzy: Piotr Pańtak, Joanna P. Czechowska, Vladyslav Vivcharenko, Annett Dorner-Reisel, Aneta Zima

Dane bibliograficzne: International Journal of Molecular Sciences; ISSN 1422-0067. — 2025 — vol. 26 iss. 18 art. no. 8910, s. 1–18, doi: 10.3390/ijms26188910

IF= 4,9; **Punkty MNiSW=** 140

Publikacja 5

Tytuł: The Influence of Titanium and Cooper on Physiochemical and Antibacterial Properties of Bioceramic-Based Composites for Orthopaedic Applications

Autorzy: Piotr Pańtak, Joanna P. Czechowska, Anna Belcarz, Aneta Zima

Dane bibliograficzne: Ceramics International; ISSN 0272-8842. — Tytuł poprz.: Ceramurgia International; ISSN: 0390-5519. — 2025 — vol. 51 iss. 1, s. 1214–1226.0, doi: 1016/j.ceramint.2024.11.102.

IF= 5,1; **Punkty MNiSW=** 100

Publikacja 6

Tytuł: Improving the Processability and Mechanical Strength of Self-Hardening Robocasted Hydroxyapatite Scaffolds with Silane Coupling Agents

Autorzy: Piotr Pańtak, Joanna P. Czechowska, Adelia Kashimbetova, Ladislav Čelko, Edgar B. Montufar, Łukasz Wójcik, Aneta Zima

Dane bibliograficzne: Journal of the Mechanical Behavior of Biomedical Materials; ISSN 1751-6161. — 2025 — vol. 161 art. no. 106792, s. 1–11. — Bibliogr. s. 9–1, doi: 10.1016/j.jmbbm.2024.106792.

IF= 3,3; **Punkty MNiSW=** 100

Opis osiągnięcia stanowiącego podstawę do nadania stopnia doktora

Krótki wstęp teoretyczny

Biomateriały do leczenia ubytków kostnych

W ostatnich latach obserwuje się wyraźny wzrost liczby przypadków uszkodzeń tkanki kostnej, co stanowi konsekwencję zwiększonej zapadalności na choroby cywilizacyjne, takie jak nowotwory czy osteoporoza, a także rosnącej liczby urazów mechanicznych [1]. Pomimo faktu, że tkanka kostna wykazuje naturalną zdolność do regeneracji bez tworzenia tkanki bliznowatej, proces ten przebiega efektywnie wyłącznie w przypadku niewielkich ubytków oraz u pacjentów pozostających w dobrym stanie ogólnym [2]. W sytuacji defektów przekraczających tzw. rozmiar krytyczny, a także u osób starszych lub obciążonych chorobami przewlekłymi, mechanizmy naprawcze kości okazują się niewystarczające lub całkowicie nieskuteczne. W takich przypadkach konieczne staje się zastosowanie odpowiednio zaprojektowanych biomateriałów kościozastępczych [3,4].

Zgodnie z definicją *Europejskiego Stowarzyszenia Biomateriałów*, biomateriał to każda substancja inna niż lek albo kombinacja substancji naturalnych lub syntetycznych, która może być użyta w dowolnym okresie, a której zadaniem jest uzupełnienie lub zastąpienie tkanek narządu, albo jego części lub spełnienie ich funkcji. Biomateriały wykorzystuje się do otrzymywania wyrobów medycznych oraz implantów pełniących rolę terapeutyczną i/lub diagnostyczną. Współczesne biomateriały projektowane są z myślą o zapewnieniu bezpiecznego i przewidywalnego oddziaływania z żywą tkanką, zarówno jako samodzielne jednostki funkcjonalne, jak i składniki zintegrowanych systemów leczniczych. Ich zadaniem może być wypełnienie ubytków, aktywne stymulowanie procesów naprawczych lub kontrolowane dostarczanie substancji biologicznie czynnych [5,6]. Z tego względu stanowią one kluczowy element nowoczesnej inżynierii tkankowej oraz medycyny regeneracyjnej, której celem jest nie tylko tymczasowe wsparcie funkcji organizmu, lecz również trwała rekonstrukcja jego struktur [7].

Spośród wielu biomateriałów stosowanych w substytucji kości, niezwykłe interesujące są materiały oparte na fosforanach (V) wapnia. Ta szczególna grupa wyróżnia się wysokim podobieństwem składu chemicznego do nieorganicznej części tkanki kostnej, co sprawia, że fosforany (V) wapnia wykazują najwyższą biozgodność spośród wszystkich biomateriałów kościozastępczych, a dodatkowo również charakteryzują się wysoką bioaktywnością. Kolejnym atutem tych materiałów jest możliwość wytwarzania ich w różnych formach oraz składach, co czyni je materiałami uniwersalnymi i szeroko stosowanymi w leczeniu ubytków kostnych o zróżnicowanej wielkości, kształcie oraz rozmiarze [8,9]. Poza wspomnianymi wcześniej korzystnymi właściwościami biologicznymi, substytuty

kostne na bazie fosforanów (V) wapnia z uwagi na przynależność do grupy materiałów bioceramicznych, są kruche oraz wykazują stosunkowo niską wytrzymałość mechaniczną, co uniemożliwia ich wykorzystanie w miejscach narażonych na znaczne obciążenia. Ponadto, w przypadku materiałów na bazie fosforanów (V) wapnia, niekiedy po implantacji występują również problemy z odpowiednim dopasowaniem tempa degradacji materiału do tempa odbudowy tkanki kostnej. Dodatkowo, niektóre formy tych materiałów wykazują ograniczoną integrację z otaczającymi tkankami.

Cementy kostne oparte na wysoko reaktywnym proszku α-fosforanu (V) wapnia (α-TCP, $\alpha\text{-}Ca_3(PO_4)_2$) są ciekawą i intensywnie rozwijaną w ostatnich latach grupą materiałów bioceramicznych stosowanych w substytucji tkanki kostnej. Cementy fosforanowo-wapniowe składają się z fazy proszkowej i ciekłej, które po zmieszaniu tworzą jednorodną, łatwą do aplikacji pastę ulegającą następnie procesowi wiązania i twardnienia *in situ*. Mechanizm wiązania tych materiałów opiera się na zdolności proszku α-TCP do hydrolizy, prowadzącej do precypitacji hydroksyapatytu z niedoborem wapnia (CDHA, *ang.* ***C****alcium-****D****eficient* ***H****ydroxy****A****patite*) w warunkach pH zbliżonych do wartości fizjologicznych [10]. Pomimo faktu, że cementy oparte na α-TCP od lat 80-tych XX wieku stanowią skuteczne rozwiązanie w leczeniu ubytków i rekonstrukcji tkanki kostnej, głównie dzięki swojej bioaktywności i biokompatybilności, ich zastosowanie pozostaje ograniczone do miejsc nie przenoszących znacznych obciążeń mechanicznych. W przypadku mocowania endoprotez za pomocą cementów kostnych, wypełniania rozległych ubytków kostnych czy rekonstrukcji trzonów kręgów ich parametry wytrzymałościowe są niewystarczające [11,12]. Wartości wytrzymałości na ściskanie dla tych cementów, uzyskiwane w warunkach laboratoryjnych, mieszczą się w zakresie od około 5 do 12 MPa. W celu poprawy właściwości mechanicznych cementów fosforanowo-wapniowych stosuje się wiele modyfikacji ich składów wyjściowych, zarówno w fazie stałej jak i ciekłej [13–15]. Najczęściej wzrost wytrzymałości tego typu biomateriałów można uzyskać poprzez dodatek polimerów pochodzenia naturalnego lub syntetycznego, zastosowanie włókien lub cząstek wzmacniających, czy też zmniejszenie porowatości cementów poprzez zmianę stosunku fazy ciekłej do stałej. Dobór konkretnej strategii modyfikacji właściwości materiałów cementowych powinien być dostosowany do planowanego zastosowania klinicznego oraz techniki aplikacji materiału. Należy jednak pamiętać, że większość z tych modyfikacji wiąże się z koniecznością uzyskania kompromisu pomiędzy właściwościami fizykochemicznymi materiałów cementowych, a ich właściwościami biologicznymi. Kolejną istotną przeszkodą w szerszym zastosowaniu cementów kostnych na bazie α-TCP jest ich ograniczona wstrzykiwalność.

Dynamiczny rozwój technik małoinwazyjnych (metod zabiegowych ograniczających ingerencję w organizm w porównaniu z tradycyjnymi operacjami), sprzyjających skróceniu czasu hospitalizacji pacjentów, ograniczeniu ryzyka powikłań po zabiegach chirur-

gicznych oraz umożliwiających szybszy powrót do pełnej sprawności, generuje rosnące zapotrzebowanie na biomateriały o wysokiej poręczności chirurgicznej, możliwe do łatwej aplikacji na przykład poprzez wstrzykiwanie. W tym kontekście kluczowym kierunkiem badawczym stały się wstrzykiwalne cementy fosforanowo-wapniowe, które mogą być podawane przy użyciu standardowych strzykawek lub dedykowanych systemów dozujących [16].

Pomimo intensywnych badań nad opracowaniem substytutów kostnych spełniających zarówno warunek biozgodności, jak i wymagania dotyczące właściwości fizykochemicznych oraz biologicznych, które będą równocześnie łatwe do aplikacji przez lekarzy, dotychczas nie udało się opracować uniwersalnego materiału typu cementowego na bazie fosforanów (V) wapnia spełniającego wszystkie powyższe kryteria. Analiza istniejących rozwiązań w zakresie dostępnych na rynku implantacyjnym materiałów wiązanych chemicznie, jednoznacznie wskazuje na potrzebę dalszego rozwoju tego typu materiałów, które nie tylko zapewniałyby odpowiednią stabilność mechaniczną w miejscu ubytku, lecz także aktywnie wspomagałyby procesy biologicznej odbudowy tkanki. Z tego powodu szczególnie obiecującym kierunkiem badań jest wykorzystanie materiałów hybrydowych w celu połączenia ich korzystnych właściwości fizykochemicznych i biologicznych z możliwością łatwej aplikacji do ubytku kostnego.

Materiały hybrydowe

Spośród obecnie rozwijanych fosforanowo-wapniowych materiałów kościozastępczych szczególnie obiecującą grupę stanowią materiały hybrydowe. Reprezentują one odrębną klasę biomateriałów, w których celowo i w sposób kontrolowany łączy się komponenty nieorganiczne z organicznymi, prowadząc do otrzymania nowych materiałów o złożonym składzie. Tak zaprojektowane układy łączą korzystne właściwości obu tych składników, co pozwala uzyskać unikalne cechy fizykochemiczne i biologiczne materiałów, niedostępne dla poszczególnych składników stosowanych oddzielnie [17].

Zgodnie z definicją przyjętą przez Międzynarodową Unię Chemii Czystej i Stosowanej (IUPAC), materiał hybrydowy to jednorodna mieszanina składników organicznych, nieorganicznych lub obu tych typów, w której poszczególne komponenty wzajemnie się przenikają w skali poniżej jednego mikrometra [18]. Choć definicja ta stanowi powszechnie uznany standard terminologiczny, jej ogólny charakter może być niewystarczający do precyzyjnego opisu złożoności strukturalnej materiałów hybrydowych. W praktyce badawczej i inżynierskiej często konieczne jest doprecyzowanie tej definicji o dodatkowe kryteria związane z właściwościami fizykochemicznymi, typem interakcji międzyfazowych oraz sposobem otrzymywania danego układu.

Uzupełnieniem wspomnianej powyżej definicji IUPAC jest klasyfikacja zaproponowana przez Judeinsteina i Sancheza [19], która uwzględnia nie tylko typ materiału, lecz tak-

że charakter oddziaływań między jego składnikami. Zgodnie z tą koncepcją, materiał hybrydowy to układ złożony z co najmniej dwóch komponentów – organicznych i/lub nieorganicznych – połączonych ze sobą za pomocą oddziaływań fizycznych lub poprzez trwałe wiązania chemiczne. Taki podział pozwala na wyróżnienie dwóch głównych klas materiałów hybrydowych:

- klasy I, obejmującej układy zdominowane przez oddziaływania słabe (tj. wiązania wodorowe, siły elektrostatyczne czy oddziaływania van der Waalsa), oraz
- klasy II, w których komponenty łączą się za pomocą wiązań trwałych (jonowych lub kowalencyjnych).

Rozróżnienie to ma istotne znaczenie przy projektowaniu materiałów funkcjonalnych, ponieważ występujące w strukturze materiału wiązania warunkują jego właściwości.

Drugim istotnym kryterium klasyfikacyjnym, poza określeniem rodzaju oddziaływań w strukturze materiału hybrydowego, jest typ dominującej fazy, a więc rodzaj matrycy oraz wprowadzanego składnika dodatkowego. W tym ujęciu wyróżnia się [20]:

- materiały organiczno-nieorganiczne (OI – *ang.* ***O****rganic-****I****norganic*) – z osnową organiczną i komponentem nieorganicznym,
- materiały nieorganiczno-organiczne (IO – *ang.* ***I****norganic-****O****rganic)* – z osnową nieorganiczną i fazą organiczną osadzoną w tej osnowie.

Dodatkowo, do materiałów hybrydowych zalicza się również układy złożone wyłącznie ze składników nieorganicznych (II – *ang.* ***I****norganic-****I****norganic*), a także struktury oparte wyłącznie na składnikach organicznych (OO – *ang.* ***O****rganic-****O****rganic*).

W przypadku większości materiałów hybrydowych zachowana zostaje odrębność faz poszczególnych składników. Natomiast w bardziej zaawansowanych układach – tzw. nanohybrydach – może dojść do dyspersji jednej z faz w drugiej, co skutkuje uzyskaniem wysoce jednorodnej mikrostruktury [21].

W inżynierii tkanki kostnej materiały hybrydowe znajdują zastosowanie m.in. do wytwarzania implantów, powłok o właściwościach bioaktywnych, trójwymiarowych rusztowań wspierających regenerację kości oraz systemów do kontrolowanego uwalniania leków [22]. Mimo szerokiego zakresu potencjalnych zastosowań, analiza dostępnej literatury wskazuje, że dominującą grupę stanowią hybrydy organiczno–nieorganiczne, w których osnowę tworzą biodegradowalne polimery, wzmacniane odpowiednio dobraną fazą nieorganiczną. Z kolei hybrydy nieorganiczno–organiczne, oparte na nieorganicznej osnowie zawierającej wbudowane komponenty organiczne, są znacznie rzadziej opisywane i wciąż stanowią stosunkowo słabo rozpoznaną klasę biomateriałów kościozastępczych.

Szczególne zainteresowanie badaczy budzą układy hybrydowe oparte na fosforanach (V) wapnia oraz naturalnych polimerach. Przykładem takich rozwiązań są materiały hydroksyapatytowo-chitozanowe (HA/CTS) o podwyższonej wytrzymałości mechanicznej otrzymywane z wykorzystaniem zmodyfikowanej mokrej metody syntezy [23]. W wytworzonych nieorganiczno-organicznych granulach HA/CTS, oddziaływania elektrostatyczne pomiędzy grupami aminowymi chitozanu a anionami fosforanowymi pozwoliły na uzyskanie materiałów hybrydowych klasy pierwszej, o jednorodnej mikrostrukturze oraz efektywnej integracji obu faz. Zaletą zaproponowanej metody otrzymywania jest jej elastyczność – umożliwia ona modyfikację właściwości hybrydowych granul poprzez użycie innych polimerów, takich jak np. metyloceluloza [24] lub wprowadzenie składników o działaniu antybakteryjnym, w postaci jonów lub nanocząstek srebra lub złota [25, 26]. Co istotne, hybrydowe granule ceramiczno-polimerowe mogą pełnić nie tylko rolę samodzielnego materiału implantacyjnego, lecz również stanowić fazę wzmacniającą w samowiążących materiałach cementowych – tzw. biomikrobetonach. W takich zastosowaniach, podobnie jak w przypadku tradycyjnych betonów, obecność granul poprawia odporność materiału na kruche pękanie poprzez mechanizm zatrzymywania propagacji mikropęknięć [27].

Nieorganiczno-organiczne materiały hybrydowe są wytwarzane również z wykorzystaniem związków innych niż fosforany (V) wapnia, takich jak na przykład krzemionka – łączona m.in. z chitozanem [28] lub alginianem sodu [29]. Połączenie tych składników pozwala uzyskać biomateriały o podwyższonej bioaktywności, sprzyjające adhezji komórek, indukujące mineralizację macierzy zewnątrzkomórkowej czy ulegające kontrolowanej degradacji.

Przeważająca część badań nad hybrydowymi materiałami kościozastępczymi koncentruje się na układach organiczno-nieorganicznych, w których dominującą fazę stanowią polimery naturalne, takie jak chitozan [30], kolagen [31], żelatyna [32,33], alginian sodu [34], lub polimery syntetyczne, np. poli(kwas mlekowy) (PLA) [35], czy poli(ε-kaprolakton) (PCL) [36]. Obecność składnika organicznego nadaje takim biomateriałom elastyczność i wysoką poręczność chirurgiczną. Niemniej jednak, ich wytrzymałość mechaniczna wciąż pozostaje niewystarczająca, co ogranicza możliwość ich stosowania do miejsc, które nie są narażone na znaczne obciążenia mechaniczne. Obecnie nieorganiczno–organiczne układy hybrydowe, w których faza mineralna pełni dominującą rolę stanowią preferowaną opcję w terapii ubytków kostnych.

Pomimo znaczącego postępu w projektowaniu biomateriałów i licznych badań nad poprawą ich właściwości, wciąż nie udało się opracować materiału łączącego w sposób kompleksowy odpowiednie cechy biologiczne, wytrzymałość mechaniczną i poręczność chirurgiczną. W związku z tym istnieje pilna potrzeba opracowywania nowych metod modyfikacji biomateriałów. Jedną z obiecujących strategii wydaje się być zastosowanie silanowych środków sprzęgających w inżynierii tkanki kostnej.

Silanowe środki sprzęgające

Silanowe środki sprzęgające to związki organokrzemowe, które zawierają w swojej strukturze zarówno grupy funkcyjne zdolne do reakcji z substancjami nieorganicznymi, jak i te, które są kompatybilne z fazą organiczną danego układu. Dzięki tej podwójnej naturze umożliwiają one tworzenie trwałych wiązań chemicznych pomiędzy różnymi komponentami materiału, co prowadzi do poprawy adhezji międzyfazowej pomiędzy nimi, zwiększenia jednorodności materiału, poprawy jego właściwości mechanicznych oraz trwałości [37].

Mechanizm działania silanowych środków sprzęgających obejmuje [38, 39]:

- Zwilżanie powierzchni – silanowe środki sprzęgające charakteryzują się niskim napięciem powierzchniowym oraz odpowiednią lepkością, co umożliwia ich równomierne rozprowadzenie na powierzchni materiału i zapewnia efektywne jego zwilżenie, stanowiące niezbędny warunek dla dalszych oddziaływań międzyfazowych.
- Hydrolizę grup alkoksysilanowych – w środowisku wilgotnym, grupy alkoksysilanowe ulegają reakcji hydrolizy, prowadzącej do powstania reaktywnych grup silanolowych
- (–Si–OR → –Si–OH), które stanowią kluczowe ogniwo w procesie wiązania chemicznego z podłożem.
- Tworzenie wiązań wodorowych z podłożem – grupy silanolowe wytworzone w poprzednim etapie mogą oddziaływać z grupami hydroksylowymi obecnymi na powierzchni materiałów nieorganicznych poprzez tworzenie wiązań wodorowych lub kondensację, prowadząc do utworzenia kowalencyjnych wiązań ($Si–OH + HO–M \rightarrow Si–O–M + H_2O$), gdzie M oznacza atomy występujące na powierzchni podłoża (np. Ca, Si, Al, Ti). Równocześnie segmenty organiczne cząsteczki silanu orientują się w kierunku fazy organicznej, umożliwiając oddziaływanie z dalszymi komponentami systemu hybrydowego.
- Polikondensacja i sieciowanie – niezwiązane grupy silanolowe (–Si–OH) mogą ulegać wzajemnej kondensacji, prowadząc do powstania przestrzennie usieciowanej struktury siloksanowej (–Si–O–Si–). Tworząca się w ten sposób trójwymiarowa sieć stabilizuje warstwę pośrednią i wzmacnia połączenie pomiędzy poszczególnymi fazami poprzez zwiększenie wytrzymałości mechanicznej oraz odporności chemicznej układu.

Silanowe środki sprzęgające znajdują szerokie zastosowanie w przemyśle, przede wszystkim jako dodatki poprawiające adhezję i trwałość chemiczną w produkcji kompozytów konstrukcyjnych, farb i powłok ochronnych, klejów, uszczelniaczy oraz laminatów [40, 41]. Obecnie, ze względu na swoje właściwości adhezyjne, związane z możliwością tworzenia wiązań chemicznych pomiędzy składnikami organicznymi i nieorganicznymi, coraz częściej znajdują również zastosowanie w inżynierii biomateriałów. Szczególne znaczenie przypisuje się im w syntezie hybrydowych materiałów hydrożelowo-elastomerowych [42], hydrożeli responsywnych [43], hydrożeli hialuronianowych [44], materiałach ma-

jących kontakt z krwią [45], metalowych stentów biodegradowalnych ze stopów Zn-Mg [46] czy pokryć na implantach metalowych [47,48]. Zastosowanie silanowych środków sprzęgających w projektowaniu materiałów kościozastępczych także wydaje się w pełni uzasadnione. Przykładowo, Suppakarn i wsp. [49] dokonali modyfikacji proszków hydroksyapatytu (HA) za pomocą różnych silanów, w tym γ-aminopropylotrimethoksysilanem (APES, *γ-minopropyltriethoxysilane*), metylotrimetoksysilanem (MTMS, *methyltrimethoxysilane*) oraz γ-glicydoksypopropylotrimethoksysilanem (GPMS, *γ-glycidoxypropyltrimethoxysilane*), w celu otrzymania kompozytów HA/polipropylen. Otrzymane wyniki badań wykazały, że zastosowanie środków silanowych poprawiło interakcje pomiędzy hydroksyapatytem a polipropylenem, prowadząc do wzrostu sztywności materiału kompozytowego. Z kolei Ji i wsp. [50] opracowali rusztowania kostne oparte na HA, modyfikując jego powierzchnię trzema różnymi środkami sprzęgającymi: 3-metakryloksypropylotrimetoksysilanem (3-MPS, *3-methacryloxypropyltrimethoxysilane*), 3-aminopropylotrimethoksysilanem (APTES, *3-aminopropyltrimethoxysilane*) oraz 3-karboksyetylosilanotrialkilosodowym (3-CES-trialkoxysilane*, 3-carboxyethyltrimethoxysilane*). Zastosowanie tych związków przyczyniło się do poprawy właściwości mechanicznych rusztowań hydroksyapatytowych z wartości około 20 do 30 MPa, co wynikało z obecności wiązań elektrostatycznych między komponentami kompozytu. Ponadto, modyfikowane powierzchnie wykazywały bardzo dobrą biokompatybilność. Ghorbani i wsp. [51] wykorzystali 3-glicydoksypopropylotrimethoksysilan (GPTMS, *3-glycidyloxypropyltrimethoxysilane*) jako nieorganiczny środek sieciujący w rusztowaniach złożonych z chitozanu i polichlorku winylu. W wyniku przeprowadzonych badań wykazano, że obecność GPTMS poprawiła właściwości mechaniczne rusztowań, zwiększyła zdolność do absorpcji wody oraz wpłynęła na kontrolowaną biodegradację materiału. Z kolei Fuh i wsp. [52] opisali metodę modyfikacji hydroksyapatytu z zastosowaniem tetraetoksysilanu (TEOS, *tetraethoxysilane*), która pozwalała na zmianę mikrostruktury tworzywa poprzez zwiększenie jego mikroporowatości, zmniejszenie skurczu wypalania oraz poprawę tempa biodegradacji rusztowań ceramicznych.

Przytoczone powyżej przykłady wskazują na rosnące znaczenie silanowych środków sprzęgających w inżynierii biomateriałów. Dzięki zdolności do tworzenia trwałych wiązań kowalencyjnych między fazą nieorganiczną a organiczną, związki te umożliwiają istotną poprawę właściwości mechanicznych, stabilności chemicznej oraz funkcjonalności materiałów przeznaczonych do kontaktu z tkankami i płynami ustrojowymi.

Pomimo swojej wszechstronności, silanowe środki sprzęgające nie były jeszcze stosowane do modyfikacji fosforanowo-wapniowych cementów kostnych. Ich wykorzystanie stwarza nowe możliwości projektowania zaawansowanych materiałów wiązanych chemicznie do regeneracji tkanki kostnej i może przynieść szereg potencjalnych korzyści, takich jak [37]:

- **poprawę właściwości mechanicznych** – dzięki **połączeniu** fazy ceramicznej z polimerami następuje ograniczenie propagacji pęknięć i wzrost wytrzymałości na ściskanie oraz modułu sprężystości.
- **wspomaganie adhezji do tkanek i innych materiałów** – grupy funkcyjne silanowych środków sprzęgających można dobrać pod kątem interakcji z białkami macierzy zewnątrzkomórkowej, co może sprzyjać osteointegracji.
- **możliwość nadania funkcji antybakteryjnych lub osteoindukcyjnych** – poprzez użycie silanów oraz substancji zawierających jony miedzi, cynku czy bioaktywne ligandy, można nadać cementom fosforanowo-wapniowym właściwości zapobiegające powstawaniu biofilmów lub stymulujące różnicowanie komórek progenitorowych w kierunku osteoblastów.
- **możliwość dalszej funkcjonalizacji** – poprzez użycie silanowych środków sprzęgających można w łatwy sposób funkcjonalizować cementy fosforanowo-wapniowe środkami o korzystnym działaniu biologicznym, na przykład lekami.

Ze uwagi na niewielką liczbę badań poświęconych zastosowaniu silanowych środków sprzęgających w cementowych materiałach kościozastępczych, obszar ten pozostaje w dużej mierze niezbadany, mimo że wykazuje istotny potencjał rozwojowy. Stanowi tym samym obiecujący kierunek dalszych prac badawczych, który może znacząco przyczynić się do poprawy właściwości funkcjonalnych oraz poszerzenia zastosowań współczesnych biomateriałów kościozastępczych.

Czynniki aktywne terapeutycznie do modyfikacji cementów kostnych

Wprowadzenie czynników o korzystnym działaniu biologicznym do cementów fosforanowo-wapniowych stanowi powszechnie stosowaną strategię mającą na celu ograniczenie ryzyka wystąpienia zakażeń pooperacyjnych, które pozostają jedną z głównych przyczyn niepowodzeń w chirurgii ortopedycznej oraz stomatologicznej [53,54]. Do najczęstszych patogenów odpowiedzialnych za infekcje związane z implantami kostnymi należą: *Staphylococcus aureus*, *Escherichia coli* oraz *Pseudomonas aeruginosa*, których zdolność do kolonizacji powierzchni biomateriału i tworzenia opornych biofilmów bakteryjnych stanowi poważne zagrożenie dla powodzenia leczenia [55]. W odpowiedzi na te wyzwania opracowano szereg metod funkcjonalizacji cementów fosforanowo-wapniowych, umożliwiających nadanie im właściwości antybakteryjnych. Do najczęściej stosowanych podejść należą modyfikacje z wykorzystaniem: antybiotyków, nanocząstek metali, związków pochodzenia naturalnego oraz pierwiastków o udokumentowanym działaniu antybakteryjnym.

Jedną z najbardziej konwencjonalnych i szeroko stosowanych metod jest inkorporacja do matrycy cementowej antybiotyków, takich jak gentamycyna [56] czy wankomycyna [57]. Takie podejście umożliwia miejscowe uwalnianie substancji czynnej, co zwiększa skutecz-

ność działania leku i jednocześnie ogranicza ryzyko ogólnoustrojowych działań niepożądanych. Pomimo tych zalet, zastosowanie antybiotyków wiąże się z istotnymi ograniczeniami. Niektóre antybiotyki mogą wykazywać działanie cytotoksyczne wobec komórek gospodarza, a także negatywnie oddziaływać na procesy gojenia i mineralizacji tkanki kostnej. Dodatkową trudność stanowi niejednorodność dystrybucji substancji aktywnej w materiale oraz trudna do przewidzenia kinetyka uwalniania leku z matrycy cementowej, co ogranicza skuteczność i bezpieczeństwo tego typu rozwiązań. W świetle wskazanych ograniczeń intensywnie poszukuje się alternatywnych metod nadawania cementom właściwości antybakteryjnych, które mogłyby uzupełniać lub zastępować klasyczne podejścia oparte na wykorzystaniu antybiotyków w leczeniu zakażeń bakteryjnych.

Nanotechnologia jest jedną z bardziej obiecujących dziedzin nauki i inżynierii, która zajmuje się projektowaniem, syntezą, analizą i zastosowaniem struktur oraz materiałów na poziomie nanometrycznym, które wykazują niezwykłe właściwości fizyczne, chemiczne i biologiczne. Nanotechnologia w medycynie oferuje nowe podejście do diagnostyki oraz leczenia wielu chorób, zwłaszcza nowotworów, chorób przewlekłych, a także wspomaga leczenie zakażeń bakteryjnych poprzez wykorzystanie nanocząstek. Do najczęściej stosowanych nanocząstek o działaniu antybakteryjnym należą nanocząstki srebra (AgNPs) [58], tlenku cynku (ZnONPs) [59], miedzi (CuNPs) [60] oraz tlenku tytanu (TiO_2NPs) [61]. Zaletą ich zastosowania jest ich stabilność w mikrostrukturze biomateriałów cementowych, a także możliwość uzyskania długotrwałego efektu antybakteryjnego bez konieczności stosowania dużych dawek antybiotyków. Nanocząstki oddziałują na bakterie wielokierunkowo, m.in. poprzez uszkadzanie błon komórkowych, zaburzenia funkcji enzymatycznych oraz generowanie reaktywnych form tlenu [62]. Pomimo licznych zalet, wprowadzenie nanocząstek do materiałów implantacyjnych wiąże się także z pewnymi ograniczeniami. Wykazano, że w zbyt wysokich stężeniach mogą one działać toksycznie wobec komórek gospodarza, wywoływać reakcje zapalne, a także indukować niepożądane zmiany biologiczne. Wciąż trwają badania nad ich długoterminowym bezpieczeństwem, w tym nad potencjalną zdolnością do przekraczania bariery krew–mózg, co budzi obawy dotyczące ich negatywnego wpływu na układ nerwowy [63, 64].

W odpowiedzi na powyższe wyzwania, coraz większe zainteresowanie naukowców koncentruje się na naturalnych związkach biologicznie czynnych, wykazujących aktywność antybakteryjną. Do tej grupy należą m.in. chitozan, olejki eteryczne, flawonoidy, kwasy fenolowe oraz ekstrakty roślinne [62–64]. Związki te charakteryzują się wysoką biokompatybilnością, biodegradowalnością oraz potencjalnym działaniem wspomagającym regenerację tkanki kostnej. Ich ograniczeniem jest jednak często niższa skuteczność terapeutyczna w porównaniu do antybiotyków lub nanocząstek.

Kolejną interesującą strategią uzyskania materiałów o działaniu antybakteryjnym jest wprowadzenie w strukturę biomateriału pierwiastków o udokumentowanym działaniu prze-

ciwdrobnoustrojowym. Najczęściej dotuje się biomateriały jonami: Ag^{+}, Cu^{2+}, Zn^{2+} czy Ce^{3+}/Ce^{4+} [65–67], które w sposób kontrolowany są uwalniane w miejscu implantacji, zapewniając długotrwałe działanie antybakteryjne. Oprócz tego, niektóre jony wykazują również korzystne działanie osteokondukcyjne, co dodatkowo zwiększa ich znaczenie w kontekście regeneracji tkanki kostnej [68, 69].

Podsumowanie

Intensywny rozwój inżynierii biomateriałów stawia przed środowiskiem naukowym i przemysłem medycznym coraz wyższe wymagania w zakresie projektowania, modyfikacji oraz wdrażania innowacyjnych materiałów implantacyjnych. Wśród nich szczególną grupę stanowią samowiążące cementy kostne oparte na fosforanach (V) wapnia, których zadaniem jest nie tylko wypełnianie ubytków, lecz także aktywne wspieranie procesów regeneracji i osteointegracji.

Pomimo licznych zalet, dostępne komercyjnie cementy fosforanowo-wapniowe wykazują ograniczoną wytrzymałość mechaniczną i niewystarczającą wstrzykiwalność, co ogranicza ich zastosowanie do miejsc nieprzenoszących znacznych obciążeń mechanicznych. Konieczne jest zatem opracowanie nowoczesnych materiałów cementowych, które – przy zachowaniu korzystnych właściwości biologicznych – będą charakteryzowały się zwiększoną wytrzymałością, lepszą poręcznością chirurgiczną i możliwością pełnienia roli nośników substancji o korzystnym działaniu biologicznym.

Najnowsze trendy w inżynierii biomateriałów kościozastępczych wskazują na integrację bioaktywnej ceramiki fosforanowo-wapniowej z polimerami naturalnymi, prowadzącą do wytworzenia nieorganiczno-organicznych układów hybrydowych o ulepszonych właściwościach. Choć brak jest bezpośrednich doniesień dotyczących zastosowania silanowych środków sprzęgających w cementach kostnych, ich wykorzystanie wydaje się uzasadnione ze względu na zdolność do tworzenia przez te związki trwałych wiązań chemicznych pomiędzy fazą nieorganiczną a organiczną. Badania nad innymi układami kompozytowymi potwierdzają, że związki te zwiększają adhezję międzyfazową, ograniczają propagację mikropęknięć oraz poprawiają integralność materiału, co w przełożeniu na cementy kostne może przynieść szereg korzyści.

Połączenie bioaktywnej ceramiki fosforanowo-wapniowej, polimerów naturalnych i silanowych środków sprzęgających stanowi zatem innowacyjne podejście do projektowania cementów kostnych nowej generacji, umożliwiające uzyskanie materiałów wstrzykiwalnych, o podwyższonej wytrzymałości mechanicznej.

Cel i tezy pracy

Głównym celem niniejszej rozprawy doktorskiej było zaprojektowanie, wytworzenie oraz charakterystyka nowoczesnych hybrydowych materiałów kościozastępczych typu cementowego opartych na fosforanach (V) wapnia, polimerach pochodzenia naturalnego oraz silanowych środkach sprzęgających. Zaproponowano kompleksowe podejście do modyfikacji zarówno fazy stałej jak i ciekłej opracowanych hybrydowych materiałów dla inżynierii tkanki kostnej. W ramach realizacji celu głównego wyznaczono również cele szczegółowe, które obejmowały określenie rodzaju interakcji chemicznych i/lub fizykochemicznych występujących w wytworzonych materiałach hybrydowych, a także ocenę wpływu zastosowanych modyfikatorów na właściwości fizykochemiczne, biologiczne oraz aplikacyjne opracowanych biomateriałów.

W oparciu o tak zdefiniowany cel pracy sformułowano następujące tezy badawcze:

1. Połączenie nieorganiczno-organicznych hybrydowych granul hydroksyapatytowo-chitozanowych, polimerów pochodzenia naturalnego oraz niemodyfikowanego lub modyfikowanego powierzchniowo za pomocą silanowych środków sprzęgających wysokoreaktywnego proszku α-TCP umożliwia otrzymanie nowoczesnych materiałów implantacyjnych wiązanych chemicznie o czasach wiązania oraz parametrach mechanicznych odpowiednich do zastosowań w inżynierii tkanki kostnej.
2. Połączenie materiałów o działaniu przeciwdrobnoustrojowym takich jak polimery o udokumentowanej aktywności antybakteryjnej (chitozan) z fosforanowo-wapniowymi materiałami, do których wprowadzono jony o działaniu antybakteryjnym (jony miedzi) umożliwia otrzymanie materiałów implantacyjnych o rozszerzonym i wzmocnionym działaniu bakteriobójczym.
3. Modyfikacja powierzchni proszku α-TCP przy pomocy silanowych środków sprzęgających oraz wykorzystanie żelu pektyny cytrusowej jako dodatku do fazy ciekłej materiałów umożliwia otrzymanie wielofunkcyjnych, hybrydowych past ceramicznych przeznaczonych do wytwarzania spersonalizowanych implantów kostnych z wykorzystaniem technik formowania przyrostowego.

Zakres prowadzonych badań

W celu weryfikacji tez pracy oraz realizacji założonych celów badawczych przeprowadzono szereg działań obejmujących zarówno projektowanie wyjściowych składów, jak i kompleksową charakterystykę otrzymanych wiązanych chemicznie materiałów hybrydowych. W ramach prowadzonych prac zaproponowano szereg sposobów modyfikacji zarówno fazy stałej jak i ciekłej materiałów cementowych. Zakres badań obejmował następujące etapy:

- Syntezę wysokoreaktywnego proszku α-TCP oraz hybrydowych materiałów hydroksyapatytowo-chitozanowych (HA/CTS) z wykorzystaniem mokrej metody chemicznej oraz charakterystykę materiałów wyjściowych.
- Modyfikację fazy stałej cementów kostnych opartych na proszku α-TCP poprzez wprowadzenie do wyjściowego składu cementu hybrydowych granul HA/CTS oraz ocenę ich wpływu na właściwości fizykochemiczne biomikrobetonów.
- Modyfikację fazy stałej fosforanowo-wapniowych cementów kostnych poprzez dodatek polimerów naturalnych takich jak: alginianu sodu i/lub hydroksypropylometyloceluloza lub powierzchniową funkcjonalizację proszku α-TCP z użyciem silanowych środków sprzęgających – tetraetoksysilanu (TEOS) lub 3-glicydoksylopropylotrimetoksysilanu (GPTMS).
- Modyfikację fazy ciekłej poprzez wprowadzenie do roztworu wodorofosforanu (V) sodu żelu pektyny cytrusowej jako naturalnego dodatku polimerowego, a następnie ocenę wpływu jednoczesnej modyfikacji obu faz (stałej i ciekłej) na właściwości otrzymanych samowiążących materiałów kościozastępczych.
- Modyfikację hybrydowych granul HA/CTS pierwiastkami o udokumentowanym korzystnym działaniu terapeutycznym – miedzią i tytanem – oraz analizę ich wpływu na właściwości strukturalne, mechaniczne i biologiczne otrzymanych biomateriałów.
- Zaprojektowanie składów i otrzymanie nowoczesnych past cementowych opartych na fosforanach (V) wapnia, polimerach pochodzenia naturalnego i silanowych środkach sprzęgających, dedykowanych do wytwarzania trójwymiarowych rusztowań kostnych metodą robocastingu oraz ich charakterystyka.

Zastosowana metodyka badawcza

W celu dokonania kompleksowej oceny otrzymanych biomateriałów wiązanych chemicznie, z uwagi na ich zróżnicowaną formę, a także potencjalne zastosowanie w medycynie regeneracyjnej, wykorzystano szereg metod pozwalających na ocenę ich właściwości fizykochemicznych oraz biologicznych.

1. Powierzchnię właściwą wyjściowych oraz zmodyfikowanych z wykorzystaniem silanowych środków sprzęgających proszków fosforanowo-wapniowych określono

metodą fizycznej adsorpcji azotu z zastosowaniem izotermy Brunauera-Emmetta-Tellera (BET).

2. Potencjał elektrokinetyczny proszków wyznaczono przy użyciu analizatora elektroforetycznego.
3. Rozkład wielkości cząstek proszków ceramicznych określono z zastosowaniem techniki dynamicznego rozpraszania światła (DLS).
4. Skład fazowy oraz chemiczny otrzymanych materiałów został określony przy użyciu technik takich jak rentgenowska spektroskopia fluorescencyjna (XRF), rentgenowska analiza dyfrakcyjna (XRD), spektroskopia w podczerwieni z transformacją Fouriera (FTIR) oraz spektroskopia Ramana.
5. Czasy wiązania, zarówno początkowe jak i końcowe, otrzymanych materiałów cementowych zmierzono za pomocą aparatu Gillmore'a zgodnie z normą ASTM C266-20.
6. Wstrzykiwalność opracowanych materiałów oceniano przez ekstrudowanie pasty cementowej przez dyszę 2 mm ze strzykawki do cylindra z płynem SBF, podgrzanym do temperatury 37°C. Siła przyłożona do tłoka strzykawki została zmierzona za pomocą maszyny wytrzymałościowej przy prędkości przesuwu głowicy wynoszącej 1,0 mm/min.
7. Reologię past ceramicznych przeznaczonych do druku badano w zależności od czasu przy stałej szybkości ścinania $1s^{-1}$ z wykorzystaniem reometru wyposażonego w przystawkę typu płytka-płytka.
8. Mikrostrukturę uzyskanych materiałów zbadano za pomocą skaningowego mikroskopu elektronowego (SEM) połączonego ze spektrometrem dyspersji energii promieniowania rentgenowskiego (EDS), umożliwiającego analizę składu chemicznego w mikroobszarach. W celu zbadania porowatości oraz rozkładu wielkości porów wykorzystano metodę porozymetrii rtęciowej.
9. Właściwości mechaniczne otrzymanych materiałów cementowych oceniono na podstawie statycznej próby ściskania, wyznaczając takie parametry jak wytrzymałość na ściskanie oraz moduł Younga.
10. Potencjał bioaktywny *in vitro* otrzymanych biomateriałów, rozumiany jako zdolność formowania się na powierzchni materiału apatytowej warstwy fosforanowo-wapniowej, oceniano przez inkubację tworzyw w sztucznym płynie fizjologicznym (SBF) o składzie jonowym zbliżonym do ludzkiego osocza. Zmiany morfologii oraz składu chemicznego powierzchni materiałów po inkubacji obserwowano z wykorzystaniem techniki SEM/EDS. Dodatkowo, w celu oceny zmian strukturalnych powierzchni materiałów oraz potwierdzenia formowania się na nich niestechiometrycznego hydroksyapatytu wykorzystano spektroskopię w podczerwieni (FTIR).
11. Ocenę stabilności chemicznej *in vitro* oraz procesów degradacji i uwalniania jonów

z otrzymanych materiałów przeprowadzono na podstawie analizy zmian pH i przewodnictwa jonowego symulowanego płynu fizjologicznego (SBF) oraz wody destylowanej, a także z wykorzystaniem spektrofotometrii UV/Vis.

12. Ocena właściwości przeciwbakteryjnych materiałów modyfikowanych jonami o potencjale terapeutycznym wobec *Staphylococcus aureus* (ATCC 25923) oraz *Escherichia coli* (ATCC 25922) została przeprowadzona z wykorzystaniem metody dyfuzyjno-krążkowej.
13. Ocena cytotoksyczności biomateriałów *in vitro* wobec linii komórkowej MC3T3-E1 opierała się na analizie żywotności komórek po ekspozycji na ekstrakty materiałów zgodnie z normą ISO 10993-5. Cytotoksyczność oceniono za pomocą testów WST-8, LDH oraz zestawu do barwienia Live/Dead, a także przy użyciu mikroskopii konfokalnej po inkubacji komórek na próbkach biomateriałów przez 48 godzin.
14. Aktywność antybakteryjną oceniono metodą AATCC 100-2004 na podstawie liczby komórek tworzących kolonie po inkubacji, natomiast test przyczepności bakterii przeprowadzono poprzez ocenę obecności żywych komórek bakteryjnych związanych z powierzchnią materiałów, wizualizowanych metodą mikroskopii konfokalnej.

Omówienie wyników badań

Etap I – Modyfikacja fazy stałej materiałów cementowych z wykorzystaniem hybrydowych granul hydroksyapatytowo-chitozanowych

Pierwszym etapem przeprowadzonych badań było wytworzenie oraz charakterystyka samowiążących materiałów kościozastępczych na bazie wysokoreaktywnego proszku α-fosforanu (V) wapnia (α-TCP), zawierających dodatkowo hybrydowy komponent w postaci granul hydroksyapatytowo-chitozanowych (HA/CTS). Fazę ciekłą tych materiałów stanowił 2% mas. roztwór wodorofosforanu (V) sodu (Na_2HPO_4). Celem modyfikacji fazy stałej poprzez wprowadzenie do wyjściowego składu cementu kostnego granul była poprawa właściwości mechanicznych cementu kostnego opartego wyłącznie na proszku α-TCP. W jej wyniku otrzymano biomikrobetony – materiały kościozastępcze typu cementowego, w którym hybrydowe granule pełnią funkcję analogiczną do kruszyw wykorzystywanych w klasycznej technologii betonu. (Publikacja 1, Materiał MC1).

Pomiar czasu wiązania, będącego jednym z podstawowych parametrów oceny fosforanowo-wapniowych cementów kostnych, wykazał, że przeprowadzona modyfikacja nie wpłynęła istotnie ani na początkowy, ani na końcowy czas wiązania. Uzyskane wartości wynosiły odpowiednio 4,5 ± 1,0 minuty oraz 7,5 ± 0,5 minuty i mieściły się w zakresie zapewniającym wystarczający czas na przygotowanie i aplikację cementowej pasty, przy jednoczesnym szybkim jej związaniu w miejscu implantacji (Publikacja 1, Tabela 1, Materiał MC1). Proces wiązania opracowanych biomikrobetonów przebiegał analogicznie do wiązania klasycznych apatytowych cementów kostnych, tj. w oparciu o hydrolizę α-TCP do niestechiometrycznego hydroksyapatytu.

Zgodnie z oczekiwaniami, analiza składu fazowego otrzymanych biomateriałów wykazała obecność dwóch faz krystalicznych: α-TCP oraz hydroksyapatytu. Ich ilościowy udział zależał od warunków w jakich materiały były przechowywane po związaniu i stwardnieniu. Inkubacja w warunkach symulujących środowisko biologiczne spowodowała niemalże całkowitą hydrolizę α-TCP, potwierdzając metastabilny charakter tego związku w środowisku wodnym. Jedyną zidentyfikowaną fazą krystaliczną w badaniu dyfrakcji rentgenowskiej w tych materiałach był hydroksyapatyt (Publikacja 1, Rysunek 2A, Tabela 2, Materiał MC1). Analiza składu chemicznego opracowanych substytutów kostnych metodą FTIR potwierdziła obecność charakterystycznych grup funkcyjnych zarówno dla fosforanów (V) wapnia, jak i chitozanu zawartego w hybrydowych granulach HA/CTS. Zidentyfikowane pasma w zakresie około 565 i 605 cm^{-1} przypisano potrójnie zdegenerowanym drganiom zginającym

wiązania P–O–P, natomiast silny dublet w okolicach 600 i 670 cm^{-1} odpowiadał draniom zginającym jonów HPO_4^{2-}. Zauważono także koincydencję pasm zginających HPO_4^{2-} i PO_4^{3-} w okolicy 603 cm^{-1}. Istotne pasma w zakresie 1040–1060 cm^{-1} przypisano asymetrycznym drganiom rozciągającym P–O, natomiast pasmo w okolicy 962 cm^{-1} odpowiadało symetrycznym drganiom rozciągającym P–O. Dla chitozanu zaobserwowano charakterystyczne pasma w zakresie 2928–2933 cm^{-1} (drgania rozciągające C–H grup alkilowych) oraz w okolicach 1649–1650 cm^{-1} (wibracje zginające N–H I-rzędowych grup aminowych) a także pasma w zakresie 1315–1320 cm^{-1} (rozciągające C–N) oraz około 3573 cm^{-1} (rozciągające O–H) (Publikacja 1, Rysunek 2B, Materiał MC1).

Jednym z głównych celów wprowadzenia hybrydowych granul HA/CTS do fazy stałej cementów kostnych na bazie α-TCP było otrzymanie materiałów wiązanych chemicznie o lepszych parametrach mechanicznych. Jak wykazały badania, wytrzymałość na ściskanie otrzymanego biomikrobetonu wynosiła 5,8 ± 1,1 MPa (Publikacja 1, Rysunek 4, Materiał MC1). Tym samym można stwierdzić, że przeprowadzona modyfikacja nie tylko nie przyczyniła się do zwiększenia wytrzymałości materiału w porównaniu do cementów opartych wyłącznie na proszku α-TCP, ale wręcz spowodowała jej obniżenie o około 20% (Publikacja 3, Rysunek 6, Materiał Control). Za główną przyczynę tego niekorzystnego efektu należy uznać słabą adhezję na granicy pomiędzy hybrydowymi granulami a matrycą cementową, co zostało potwierdzone obserwacjami mikrostruktury przełamów otrzymanych materiałów (Publikacja 1, Rysunek 3, Materiał MC1).

Ponadto, sprawdzono również czy modyfikacja fazy stałej cementu kostnego za pomocą materiałów hybrydowych nie wpływa negatywnie na jego właściwości biologiczne *in vitro*. Wyniki badań stabilności chemicznej materiału, pomiary przewodnictwa jonowego właściwego roztworów inkubacyjnych wokół przetrzymywanych próbek cementowych, jak również ocena potencjału bioaktywnego *in vitro*, potwierdziły korzystne właściwości zaprojektowanego i otrzymanego nowego materiału typu biomikrobetonu (Publikacja 1, Rysunek 5-7, Materiał MC1).

Pierwsza modyfikacja fazy stałej cementu kostnego na bazie α-TCP za pomocą hybrydowych granul HA/CTS nie doprowadziła do uzyskania wszystkich założonych celów badawczych. Pomimo tego, że umożliwiła otrzymanie materiału kompozytowego zawierającego komponent hybrydowy, który spełniał kliniczne kryteria w zakresie czasów wiązania, nie zaobserwowano jednak poprawy pozostałych kluczowych właściwości fizykochemicznych i aplikacyjnych, jakich oczekuje się od nowoczesnych materiałów kościozastępczych. W związku z tym konieczne okazało się zaproponowanie kolejnej, uzupełniającej strategii modyfikacji, ukierunkowanej na dalszą poprawę właściwości fosforanowo-wapniowych materiałów cementowych.

Etap II – Modyfikacja fazy stałej i ciekłej materiałów cementowych z wykorzystaniem polimerów naturalnych

Kolejnym etapem badań było wykorzystanie polimerów naturalnych w celu poprawy wytrzymałości mechanicznej opracowanych wcześniej biomikrobetonów. W tym celu przeprowadzono równoczesną modyfikację zarówno fazy stałej jak i ciekłej cementów kostnych opartych na proszku α-TCP oraz materiałach hybrydowych HA/CTS.

Na podstawie analizy publikacji naukowych dotyczących polimerów mogących korzystnie wpłynąć na właściwości nowych materiałów wiązanych chemicznie, do dalszych badań wytypowano trzy różne polisacharydy, a mianowicie: pektynę cytrusową, alginian sodu oraz hydroksypropylometylocelulozę (HPMC). Kluczowym kryterium wyboru modyfikatorów było udokumentowane w literaturze występowanie oddziaływań pomiędzy chitozanem – będącym polisacharydem o charakterze polikationowym – a innymi polisacharydami wykazującymi charakter polianionowy. Głównym celem badań było wytworzenie materiałów hybrydowych, które na skutek oddziaływań elektrostatycznych pomiędzy składnikami wyjściowymi charakteryzowałyby się korzystnymi właściwościami fizykochemicznymi, biologicznymi oraz aplikacyjnymi.

Faza stała badanych biomateriałów została zmodyfikowana poprzez dodatek polimerów w postaci alginianu sodu lub hydroksypropylometylocelulozy (HPMC) w ilości 2 lub 4% mas. Fazę ciekłą w tych materiałów stanowił natomiast 5% mas. żel pektyny cytrusowej (Publikacja 2, Tabela 1).

Jednym z pierwszych zauważalnych efektów przeprowadzonych modyfikacji była poprawa właściwości użytkowych past cementowych. Wprowadzenie polimerów naturalnych zdolnych do tworzenia hydrożeli wpłynęło korzystnie na właściwości reologiczne past, podnosząc ich lepkość i tym samym umożliwiając aplikację materiału poprzez wstrzykiwanie, co jest szczególnie pożądane w małoinwazyjnych procedurach chirurgicznych (Publikacja 2, Rysunek 1). Zastosowanie dodatków polimerowych miało jednak niekorzystny wpływ na czasy wiązania otrzymanych substytutów kostnych. Początkowe czasy wiązania tych materiałów mieściły się w przedziale od 28,0 ± 2,0 do 37,0 ± 2,0 minut, natomiast końcowe przekraczały 60 minut (Publikacja 2, Tabela 2) i były wyraźne dłuższe w stosunku do materiałów niemodyfikowanych. Zaobserwowano bezpośrednią korelację pomiędzy ilością polimerów w składzie materiałów wiązanych chemicznie, a czasem wiązania opracowanych materiałów. Na mechanizm wiązania i twardnienia biomikrobetonów znaczący wpływ miało ograniczenie dostępności wody potrzebnej do reakcji hydrolizy α-TCP. Mniejsza ilość wody w układzie związana była z absorpcją wody przez polimery naturalne obecne w składzie materiałów wyjściowych. Uzyskane wyniki badań potwierdziły występowanie podwójnego mechanizmu wiązania opracowanych materiałów kościozastępczych. Efekt ten obejmował jednocześnie hydrolizę α-TCP oraz sieciowanie łańcu-

chów polimerowych jonami wapnia. Co istotne, wprowadzenie polimerów do matrycy cementowej okazało się skuteczną strategią poprawy parametrów mechanicznych badanych materiałów. Opracowane i otrzymane nowe biomikrobetony, przetrzymywane po związaniu i stwardnieniu w powietrzu, osiągały wytrzymałość na ściskanie w zakresie od 9,3 ± 2,1 MPa (dla materiału referencyjnego) do 17,2 ± 2,6 MPa (dla materiału z dodatkiem 4% mas. alginianu sodu). Po inkubacji w roztworze SBF wartości te były nieznacznie niższe – od 6,6 ± 1,2 do 13,2 ± 1,2 MPa – co przypisano częściowej degradacji materiałów w warunkach symulowanego środowiska fizjologicznego (Publikacja 2, Rysunek 5). Poprawa wytrzymałości na ściskanie badanych materiałów była efektem działania podwójnego systemu wiązania (hydroliza α-TCP i sieciowanie polimerów) oraz interakcji między alginianem sodu a pozostałymi dodatkami polimerowymi, a także tworzenia kompleksów polielektrolitowych pomiędzy hybrydowymi granulami hydroksyapatytowo-chitozanowymi i pektyną cytrusową. Otrzymane materiały kościozastępcze sklasyfikowano jako hybrydy klasy I. Wykazano, że najwyższą wartość wytrzymałości na ściskanie osiągnięto dla materiału zawierającego 4% mas. alginianu sodu, co przypisano sieciowaniu polimeru z udziałem jonów Ca^{2+} oraz jego anionowemu charakterowi. Materiały z dodatkiem HPMC wykazywały niższą wytrzymałość na ściskanie, jednakże osiągnięte wartości wytrzymałości na ściskanie były porównywalne z parametrami typowymi dla ludzkiej kości gąbczastej (około 4-12 MPa). W porównaniu do biomikrobetonów opartych wyłącznie na proszku α-TCP oraz hybrydowych granulach HA/CTS, materiały zawierające pektynę cytrusową i dodatki polimerów modyfikujących fazę stałą wykazywały bardziej zwartą i jednorodną mikrostrukturę (Publikacja 2, Rysunek 3). Oprócz równomiernie rozmieszczonych w matrycy cementowej hybrydowych granul HA/CTS, zaobserwowano polimery – zarówno w postaci cienkiej warstwy pokrywającej ziarna fosforanów (V) wapnia, jak i co szczególnie istotne, w formie charakterystycznych mostków polimerowych łączących hybrydowe granule z pozostałymi składnikami cementu kostnego. Co więcej, zastosowanie biokompatybilnych polisacharydów nie wpłynęło istotnie na stabilność chemiczną, przewodnictwo jonowe właściwe roztworów inkubacyjnych wokół próbek ani na bioaktywność *in vitro* (Publikacja 2, Rysunek 4, Rysunek 6).

Podsumowując, mimo wyraźnej poprawy właściwości mechanicznych i aplikacyjnych, czasy wiązania zmodyfikowanych hybrydowych materiałów wiązanych chemicznie nadal przekraczały wartości akceptowalne. Z tego względu dalsze modyfikacje fosforanowo-wapniowych substytutów kostnych koncentrowały się na zmianie składu wyjściowego materiałów w kierunku skrócenia czasu wiązania, przy jednoczesnym zachowaniu korzystnych właściwości aplikacyjnych oraz poprawionej wytrzymałości na ściskanie.

Etap III – Modyfikacja fazy ciekłej materiałów cementowych z wykorzystaniem pektyny cytrusowej w połączeniu z wodorofosforanem (V) sodu

Jak pokazały wyniki wcześniejszych eksperymentów, zastosowanie polimerów naturalnych może przyczynić się do poprawy wstrzykiwalności oraz wytrzymałości na ściskanie fosforanowo-wapniowych materiałów kościozastępczych typu cementowego. Jednocześnie jednak, wprowadzenie modyfikatorów polimerowych skutkowało znacznym wydłużeniem czasów wiązania, co stanowi istotne ograniczenie w kontekście ich zastosowania klinicznego.

W celu skrócenia czasów wiązania, zaproponowano dalsze modyfikacje składu wyjściowego opracowanych biomikrobetonów. Fazę stałą materiałów stanowił proszek α-TCP oraz hybrydowe granule HA/CTS. Fazę ciekłą natomiast stanowiły mieszaniny roztworu wodorofosforanu (V) sodu (Na_2HPO_4), będącego akceleratorem procesu wiązania cementów opartych na α-TCP oraz żelu pektyny cytrusowej o zmiennych proporcjach (Publikacja 1, Tabela 3). Celem tej modyfikacji było skrócenie czasu wiązania, przy jednoczesnym zachowaniu korzystnych właściwości mechanicznych oraz wstrzykiwalności opracowanych nowych materiałów kościozastępczych.

Uzyskane wyniki badań potwierdziły skrócenie zarówno początkowych, jak i końcowych czasów wiązania badanych biomikrobetonów, które mieściły się w przedziałach odpowiednio od 9,0 ± 0,5 do 30,5 ± 0,5 minut oraz od 16,5 ± 1,0 do 55,5 ± 1,0 minut (Publikacja 1, Tabela 1). Obecność pektyny cytrusowej miała ponadto korzystny wpływ na właściwości reologiczne cementowych past, pełniąc funkcję plastyfikatora. Zwiększenie lepkości mieszaniny przyczyniło się do uzyskania materiałów w pełni wstrzykiwalnych. Otrzymane biomikrobetony zachowywały integralność po ekstruzji do roztworu SBF, w przeciwieństwie do materiału kontrolnego pozbawionego pektyny, w którym obserwowano niekorzystne zjawisko separacji faz (Publikacja 1, Rysunek 1). Analiza składu fazowego materiałów, podobnie jak w poprzednich etapach badań, wykazała obecność dwóch faz krystalicznych: α-TCP oraz hydroksyapatytu. Ich udział ilościowy zależał od warunków, w jakich materiały były przetrzymywane po związaniu i stwardnieniu (Publikacja 1, Rysunek 2A, Tabela 2). Potwierdzono, że materiały zawierające w swym składzie wyjściowym pektynę cytrusową w fazie ciekłej charakteryzowały się nieznacznie spowolnioną hydrolizą α-TCP, co można wiązać z intensywną absorpcją wody przez ten polimer. Badania spektroskopowe dostarczyły dodatkowych informacji na temat składu chemicznego opracowanych materiałów. Poza charakterystycznymi pasmami absorpcyjnymi odpowiadającymi grupom PO_4^{3-} oraz HPO_4^{2-}, potwierdzającymi obecność fosforanów (V) wapnia, zidentyfikowano również pasma charakterystyczne dla zastosowanych polimerów – pektyny cytrusowej oraz chitozanu. Pasmo przy 2930 cm^{-1} przypisano wibracjom rozciągającym grup C-H, natomiast pasmo przy 1649 cm^{-1} – drganiom zginającym N-H, wskazującym na obecność grup aminowych typowych za-

równo dla chitozanu, jak i amidowanej pektyny. Dodatkowo, obserwowane pasma w zakresie 1315 cm^{-1} i 3573 cm^{-1} odpowiadały odpowiednio wibracjom rozciągającym wiązań C-N oraz O-H, co potwierdzało obecność tych polisacharydów w strukturze materiału (Publikacja 1, Rysunek 2B).

Potwierdzono, że modyfikacja fazy ciekłej biomikrobetonów przyczyniła się do zwiększenia adhezji pomiędzy hybrydowymi granulami HA/CTS a fosforanowo-wapniową osnową cementową (Publikacja 1, Rysunek 3). Zjawisko to było wynikiem formowania się wcześniej zaobserwowanych mostków polimerowych, łączących poszczególne komponenty materiału, przy czym najwięcej zaobserwowano ich w biomikrobetonie o najwyższym stężeniu pektyny cytrusowej w fazie ciekłej.

Oprócz poprawy właściwości reologicznych pasty cementowej, umożliwiającej jej aplikację metodą wstrzykiwania, obecność pektyny cytrusowej przyczyniła się do wzrostu wytrzymałości mechanicznej otrzymanych materiałów. Zgodnie z założeniami, dodatek pektyny cytrusowej istotnie poprawił parametry mechaniczne biomikrobetonów, podnosząc ich wytrzymałość na ściskanie z 5,8 ± 1.1 MPa (dla materiału, w którym fazę ciekłą stanowił wyłącznie roztwór Na_2HPO_4) do 13,2 ± 1.3 MPa (dla materiału zawierającego najwyższy udział pektyny w fazie ciekłej) (Publikacja 1, Rysunek 4). Zaobserwowany wzrost wytrzymałości mechanicznej poza występowaniem podwójnego systemu wiązania (hydroliza α-TCP i sieciowanie polimerów), wynikał dodatkowo z dwóch kluczowych mechanizmów. Po pierwsze – ze zwiększonej homogeniczności past cementowych w obecności pektyny, co potwierdziły analizy mikrostruktury; po drugie – z utworzenia dodatkowych oddziaływań – obejmujących zarówno interakcje elektrostatyczne pomiędzy polikationowym chitozanem a polianionową pektyną, jak i oddziaływań wewnątrz hybrydowych granul.

Ocena stabilności chemicznej, przewodnictwa jonowego właściwego oraz potencjału bioaktywnego w warunkach *in vitro* potwierdziła korzystne właściwości biologiczne opracowanych materiałów cementowych. Pomimo obecności dodatków polimerowych, takich jak pektyna cytrusowa oraz chitozan zawarty w hybrydowych granulach HA/CTS, wartości pH roztworu SBF wokół inkubowanych próbek pozostawały zbliżone do fizjologicznego pH płynów ustrojowych (Publikacja 1, Rysunek 5). Na powierzchni biomikrobetonów po zakończeniu inkubacji zaobserwowano charakterystyczne wytrącenia apatytowe, co potwierdziło potencjał bioaktywny badanych materiałów w teście *in vitro* (Publikacja 1, Rysunek 6). Analiza przewodnictwa jonowego właściwego medium inkubacyjnego wykazała nieznaczny wzrost tego parametru wraz ze zwiększeniem udziału pektyny cytrusowej w fazie ciekłej biomikrobetonów z 65–80 µS/cm do 80–91 µS/cm po 28 dniach inkubacji. Wyższe wartości przewodnictwa jonowego w otoczeniu materiałów zawierających pektynę cytrusową przypisano częściowej degradacji tego polimeru (Publikacja 1, Rysunek 7).

Podsumowując, za najkorzystniejszą modyfikację fazy ciekłej hybrydowych materiałów cementowych uznano mieszaninę zawierająca 1% mas. wodorofosforanu (V) sodu oraz 2,5% mas. pektyny cytrusowej. Taki skład fazy ciekłej pozwolił na uzyskanie w pełni wstrzykiwalnych hybrydowych materiałów kościozastępczych typu cementowego, o podwyższonej wytrzymałości na ściskanie oraz odpowiednich czasach wiązania.

Etap IV – Modyfikacja wyjściowego proszku α-TCP z wykorzystaniem silanowych środków sprzęgających

Jak wykazano w poprzednich etapach badań, zastosowanie polimerów naturalnych może istotnie przyczynić się do poprawy wytrzymałości na ściskanie oraz wstrzykiwalności cementowych materiałów fosforanowo-wapniowych. Kolejnym etapem prac badawczych była modyfikacja właściwości powierzchniowych wyjściowego proszku α-TCP stanowiącego podstawę fazy stałej opracowywanych cementowych materiałów kościozastępczych. W szczególności skupiono się na powierzchniowej funkcjonalizacji proszku α-TCP z wykorzystaniem dwóch silanowych środków sprzęgających o różnych grupach funkcyjnych: tetraetoksysilanu (TEOS) oraz 3-glicydoksypopropylotrimetoksysilanu (GPTMS), stosowanych w ilościach 1% mas., 2% mas. oraz 5% mas. (Publikacja 3, Tabela 1). Ze względu na wysoką reaktywność proszku fosforanowo-wapniowego procedurę modyfikacji powierzchni przeprowadzono w warunkach bezwodnych, aby zapobiec hydrolizie zarówno α-TCP, jak i silanowych środków sprzęgających. Zastosowanie bezwodnego etanolu umożliwiło zachowanie struktury krystalicznej α-TCP oraz wyeliminowało ryzyko przedwczesnej hydrolizy silanów.

Modyfikacja powierzchni α-TCP za pomocą TEOS lub GPTMS wpływała zarówno na powierzchnię właściwą jak również na rozkład wielkości cząstek proszku α-TCP. Powierzchnia właściwa proszków α-TCP mieściła się w zakresie od 1,81 do 3,67 m^2/g i malała wraz ze wzrostem ilości zastosowanego do modyfikacji powierzchniowej środka sprzęgającego (Publikacja 3, Rysunek 1). Średni rozmiar cząstek zmniejszył się z zakresu około 1,0–100,0 μm (dla proszku niemodyfikowanego) do 1,0–10,0 μm w przypadku proszków modyfikowanych silanami (Publikacja 3, Rysunek 2). Efekt ten przypisano obniżeniu energii powierzchniowej oraz poprawie dyspersji, wynikającym z obecności warstw organicznych ograniczających powinowactwo cząstek do medium, w którym badano proszki. Analiza potencjału elektrokinetycznego wykazała, że modyfikacja proszków istotnie wpływała na zmianę ładunku powierzchniowego. Niemodyfikowany proszek α-TCP charakteryzował się najniższym elektroujemnym potencjałem elektrokinetycznym (−4,65 mV). Wartość ta wzrosła do −24,4 mV w przypadku proszku zmodyfikowanego GPTMS przy najwyższym badanym stężeniu (Publikacja 3, Tabela 3). Zwiększona elektroujemność potencjału elektrokinetycznego potwierdziła obecność warstw silanowych na powierzchni ziaren, które zmieniają oddziaływania elektrostatyczne oraz ograniczają tendencję do aglomeracji cząstek.

W celu sprawdzenia wpływu zastosowanych środków sprzęgających na właściwości materiałów cementowych przygotowano cementy kostne o prostym składzie wyjściowym, a mianowicie na bazie wyjściowego proszku α-TCP poddanego modyfikacji powierzchniowej. Jako fazę ciekłą zastosowano wodę destylowaną (Publikacja 3, Tabela 2).

Analiza dyfrakcji rentgenowskiej wykazała, że zarówno wyjściowy proszek α-TCP, jak i proszki modyfikowane silanami, zawierały dwie fazy krystaliczne: α-TCP oraz niewielką ilość hydroksyapatytu. Zgodnie z oczekiwaniami, modyfikacja przeprowadzona w środowisku bezwodnym nie doprowadziła do hydrolizy α-TCP do niestechiometrycznego hydroksyapatytu. Oznacza to, że proces hydrolizy zarówno α-fosforanu (V) wapnia, jak i środka sprzęgającego rozpoczynał się dopiero po połączeniu fazy proszkowej z cieczą zarobową cementu.

Analiza widm w podczerwieni, przeprowadzona dla proszków wyjściowych, cementów po związaniu i stwardnieniu w powietrzu oraz próbek inkubowanych przez 7 dni w roztworze SBF, potwierdziła obecność pasm charakterystycznych dla fosforanów wapnia, jednak nie wykazała wyraźnych pasm odpowiadających grupom Si–O–Si, Si–OH, Si–C ani C–H. Brak ten tłumaczy się niskim stężeniem środków silanowych oraz nakładaniem się pasm absorpcyjnych. Spektroskopia Ramana, poza pasmami typowymi dla fosforanów (V) wapnia, potwierdziła także obecność pasm charakterystycznych dla użytych silanowych środków sprzęgających. W cementach zawierających TEOS zaobserwowano pasma przypisywane wiązaniom Si–O–Si (~1100 cm^{-1}), grupie metylowej (~2940 cm^{-1}) oraz wiązaniu Si–O–CH_3 (~1250 cm^{-1}). Grupy Si–OH obecne w TEOS potwierdzono pasmami w zakresie 3600–3700 cm^{-1}. W przypadku materiałów zawierających GPTMS zidentyfikowano charakterystyczne pasmo przy około 910 cm^{-1}, przypisywane drganiom rozciągającym wiązania CH_2–O, związanym z obecnością grup epoksydowych — szczególnie widoczne po inkubacji próbek. Na widmie materiałów modyfikowanych za pomocą GPTMS również widoczne są pasma pochodzące od drgań grup Si–O–Si (~1100 cm^{-1}), Si–CH_3 (~2940 cm^{-1}) oraz Si–O–CH_2 (~1250 cm^{-1}) (Publikacja 3, Rysunek 4, Rysunek 5).

W kolejnym etapie badań przeprowadzono ocenę czasów wiązania otrzymanych cementów kostnych. Uzyskane wyniki wykazały, że zarówno początkowe jak i końcowe czasy wiązania zależały od ilości zastosowanego silanowego środka sprzęgającego. Początkowy czas wiązania mieścił się w zakresie od 3,5 ± 1,0 do 6,5 ± 0,5 min, natomiast końcowy — od 6,5 ± 0,5 do 11,5 ± 0,5 min (Publikacja 3, Tabela 5).

Modyfikacja powierzchni proszku α-TCP z wykorzystaniem silanowych środków sprzęgających, poza skróceniem czasu wiązania, wpłynęła również korzystnie na właściwości mechaniczne otrzymanych cementów. Wytrzymałość na ściskanie badanych materiałów mieściła się w zakresie od 7,3 ± 0,4 MPa do 12,2 ± 0,5 MPa, przy czym najwyższe wartości odnotowano dla cementu zawierającego 5% mas. GPTMS. Analiza statystyczna potwierdziła istotne różnice pomiędzy materiałami modyfikowanymi

a niemodyfikowanym materiałem referencyjnym (Publikacja 3, Rysunek 6). Poprawa parametrów mechanicznych wynikała z wytworzenia dodatkowych wiązań chemicznych podczas jednoczesnej hydrolizy α-TCP oraz silanowych środków sprzęgających — w szczególności wiązań Si–O–Si, Si–O oraz Si–O–P — świadczących o chemicznej integracji składników cementu i potwierdzających jego hybrydowy charakter. Cementy kostne, niezależnie od rodzaju zastosowanego środka sprzęgającego jako modyfikatora α-TCP, charakteryzowały się zwartą i homogeniczną mikrostrukturą, w której widoczne były mikropory. Po siedmiu dniach inkubacji w symulowanym płynie ustrojowym wszystkie analizowane próbki cementowe zostały całkowicie pokryte charakterystycznymi formami apatytowymi, co potwierdziło ich wysoki potencjał bioaktywny *in vitro* (Publikacja 3, Rysunek 9). Ocena stabilności chemicznej próbek inkubowanych w roztworze SBF nie wykazała również negatywnego wpływu obecności silanowych środków sprzęgających. Zmiany pH roztworu otaczającego badane materiały pozostawały bliskie wartościom fizjologicznym i mieściły się w zakresie 7,34–7,40 (Publikacja 3, Rysunek 10). Przewodnictwo jonowe właściwe dla materiał kontrolnego (bez dodatku środka sprzęgającego) mieściło się w zakresie ~72–81 μS/cm. Obecność silanowych modyfikatorów prowadziła do niewielkiego wzrostu przewodnictwa jonowego właściwego – do ~73–87 μS/cm dla próbek zawierających TEOS oraz ~84–96 μS/cm dla próbek z dodatkiem GPTMS. Zjawisko to tłumaczy się wyższą szybkością degradacji silanowych środków sprzęgających oraz towarzyszącym jej uwalnianiem jonów podczas postępującej hydrolizy w środowisku wodnym (Publikacja 3, Rysunek 11).

Wykazano, że opracowana bezwodna metoda modyfikacji powierzchni proszków α-TCP z wykorzystaniem tetraetoksysilanu oraz 3-glicydyloksypropylotrimetoksysilanu stanowi innowacyjne rozwiązanie, umożliwiające poprawę właściwości fizykochemicznych, w szczególności wytrzymałości mechanicznej, materiałów cementowych na bazie fosforanów (V) wapnia przeznaczonych do regeneracji tkanki kostnej. Zwiększenie wytrzymałości mechanicznej uzyskano dzięki wytworzeniu dodatkowych wiązań chemicznych w strukturze materiału. Kolejnym kierunkiem dalszych badań było zastosowanie zaproponowanej strategii modyfikacji wysoko reaktywnego proszku α-TCP w bardziej złożonych układach, uwzględniających obecność polimerów lub innych komponentów funkcjonalnych.

Etap V – Modyfikacja fazy proszkowej materiałów z wykorzystaniem silanowych środków sprzęgających oraz modyfikacja fazy ciekłej

Bazując na wcześniej przeprowadzonych modyfikacjach ukierunkowanych na poprawę właściwości materiałów kościozastępczych – obejmujących wprowadzenie hybrydowych granul HA/CTS do fazy stałej cementów, modyfikację fazy ciekłej poprzez zastosowanie wodorofosforanu (V) sodu oraz pektyny cytrusowej, a także funkcjonalizację

powierzchni wyjściowych proszków α-TCP za pomocą silanowych środków sprzęgających – w kolejnym etapie badań skoncentrowano się na ich połączeniu i ocenie efektu wynikającego z ich jednoczesnego zastosowania.

Ocenie poddano serię materiałów typu biomikrobetonów, w których fazę proszkową stanowił proszek α-TCP (niemodyfikowany lub poddany modyfikacji z wykorzystaniem silanowych środków sprzęgających) w połączeniu z hybrydowymi granulami HA/CTS. Fazę ciekłą tych kompozytów stanowiła mieszanina 1% mas. roztworu Na_2HPO_4 oraz 2,5% mas. żelu pektyny cytrusowej (Publikacja 4, Tabela 3).

Jednoczesne zastosowanie modyfikacji fazy proszkowej z wykorzystaniem silanowych środków sprzęgających oraz fazy ciekłej z wykorzystaniem żelu pektyny cytrynowej przyczyniło się do uzyskania materiałów o początkowych i końcowych czasach wiązania mieszczących się odpowiednio w zakresie 5,5–12,0 minut oraz 11,5–19,5 minut (Publikacja 4, Tabela 2). Szczególnie istotna okazała się rola silanowych środków sprzęgających, które w zauważalnym stopniu skracały czas wiązania.

Kluczowym elementem oceny opracowanych tworzyw była ich wytrzymałość na ściskanie. Przeprowadzone badania wykazały, że wytrzymałość na ściskanie biomateriałów mieściła się w zakresie od 11,4 ± 1,1 MPa do 19,3 ± 1,0 MPa. Wartości te zależały od ilości wprowadzonego silanowego środka sprzęgającego jako modyfikatora wyjściowego proszku α-TCP. Wzrost stężenia środka sprzęgającego skutkował statystycznie istotną poprawą właściwości mechanicznych, niezależnie od rodzaju zastosowanego silanu (Publikacja 4, Rysunek 3). Najwyższą wytrzymałość mechaniczną zmierzono dla materiału zawierającego 5% mas. GPTMS. Za poprawę parametrów mechanicznych cementów kostnych odpowiadały przede wszystkim dodatkowe wiązania chemiczne powstające pomiędzy składnikami biomikrobetonu oraz zwiększona adhezja pomiędzy matrycą cementową a hybrydowymi granulami. Istotną rolę odegrały także zastosowane biopolimery, których grupy funkcyjne oddziaływały z grupami silanowymi, przyczyniając się do zwiększenia kohezji i stabilności mikrostruktury materiału. Poprawę adhezji pomiędzy poszczególnymi komponentami biomikrobetonów potwierdzono dodatkowo w obserwacjach mikrostruktury. Badania porowatości z wykorzystaniem metody porozymetrii rtęciowej wykazały, że obecność tych modyfikatorów prowadziła do istotnego obniżenia porowatości otwartej w materiałach. Biomateriał niezawierający silanowych środków sprzęgających charakteryzował się porowatością całkowitą na poziomie 58,3 ± 0,5% obj., podczas gdy materiały zawierające TEOS lub GPTMS wykazywały istotnie niższe wartości: odpowiednio 47,6 ± 0,5% obj. oraz 46,4 ± 0,5% obj. (Publikacja 4, Rysunek 4). Opracowane biomikrobetony odznaczały się jednorodną mikrostrukturą, w której granule HA/CTS były równomiernie rozmieszczone w osnowie cementowej. W materiałach modyfikowanych silanowymi środkami sprzęgającymi zaobserwowano lepszą adhezję między cementową matrycą fosforanowo-wapniową a granulami HA/CTS (Publikacja 4, Rysunek 5). Ocena stabilności chemicznej, prze-

wodnictwa jonowego właściwego oraz potencjału bioaktywnego metodą *in vitro* miała na celu wstępną analizę przydatności nowoopracowanych materiałów kościozastępczych przed przystąpieniem do badań komórkowych. Wartości pH roztworu SBF otaczającego próbki pozostawały zbliżone do fizjologicznych i mieściły się w zakresie 7,36–7,42. Obecność silanowych środków sprzęgających miała jedynie marginalny wpływ na odczyn środowiska inkubacyjnego (Publikacja 4, Rysunek 6A). Z kolei przewodnictwo jonowe właściwe roztworu wodnego, w którym inkubowano próbki, zależało od ich składu chemicznego, lecz pozostawało w zakresie typowym dla fosforanowo-wapniowych cementów kostnych, wynoszącym od 100–116 μS/cm do 140–181 μS/cm (Publikacja 4, Rysunek 6B). Po siedmiu dniach inkubacji w roztworze SBF powierzchnia wszystkich badanych próbek została całkowicie pokryta charakterystycznymi formami apatytowymi, co jednoznacznie potwierdziło ich potencjał bioaktywny *in vitro* (Publikacja 4, Rysunek 7).

Ocena cytotoksyczności badanych cementów została przeprowadzona na liniach komórkowych MC3T3-E1 na podstawie aktywności metabolicznej komórek z wykorzystaniem testu WST-8. Uzyskane wyniki wykazały wysoką żywotność komórek, przekraczającą 90% dla wszystkich analizowanych materiałów, co zgodnie z normą ISO 10993-5:2009 potwierdza brak działania toksycznego opracowanych biomateriałów (Publikacja 4, Rysunek 8A). Nieznaczne obniżenie żywotności zaobserwowano w przypadku materiałów niemodyfikowanych oraz modyfikowanych z wykorzystaniem TEOS, co można wiązać z umiarkowanym wpływem składników ekstraktu na aktywność dehydrogenazy mitochondrialnej. Różnice te nie przekroczyły jednak ustalonych progów cytotoksyczności. Bezpieczeństwo biologiczne materiałów potwierdzono również za pomocą testu LDH, oceniającego integralność błon komórkowych. Po lizie komórek nie stwierdzono istotnych różnic w aktywności dehydrogenazy mleczanowej pomiędzy badanymi próbkami a kontrolą negatywną, co dodatkowo potwierdziło brak efektu cytotoksycznego (Publikacja 4, Rysunek 8B).

W dalszej części badań przeprowadzono ocenę adhezji i morfologii komórek na powierzchni opracowanych materiałów cementowych. Obserwacje mikroskopowe po wcześniejszym barwieniu fluorescencyjnym, wykazały, że komórki układały się zgodnie z topografią materiału, penetrując jego mikropory i zagłębienia. Mikrostruktura cementów sprzyjała adhezji i rozprzestrzenianiu się komórek, co wskazuje na korzystny wpływ opracowanych tworzyw na osteointegrację (Publikacja 4, Rysunek 8C, D).

Podsumowując, modyfikacja proszku α-TCP za pomocą silanowych środków sprzęgających oraz zastosowanie mieszaniny wodorofosforanu (V) sodu i pektyny cytrusowej jako fazy ciekłej pozwoliło uzyskać samowiążące materiały implantacyjne o korzystnych właściwościach użytkowych, kontrolowanych czasach wiązania oraz zwiększonej wytrzymałości mechanicznej. Co istotne, obecność silanowych środków sprzęgających nie zmieniła korzystnych właściwości biologicznych charakteryzujących materiały na bazie fosforanów (V) wapnia.

Etap VI – Modyfikacja hybrydowych granul HA/CTS pierwiastkami o korzystnym działaniu biologicznym

Kolejny etap badań obejmował funkcjonalizację hybrydowych granul hydroksyapatytowo-chitozanowych (HA/CTS) za pomocą pierwiastków wykazujących korzystne właściwości biologiczne, ze szczególnym uwzględnieniem działania antybakteryjnego. Na etapie syntezy hybrydowych granul do materiału wprowadzono miedź (Cu-HA/CTS) oraz tytan (Ti-HA/CTS) (Publikacja 5, Rysunek 1).

Następnie zaprojektowano i otrzymano innowacyjne substytuty kostne typu biomikrobetonów w których jako fazę stałą zastosowano proszek α-TCP oraz odpowiednio zmodyfikowane hybrydowe granule Cu-HA/CTS lub Ti-HA/CTS, natomiast jako fazę ciekłą, podobnie jak w poprzednich etapach, wykorzystano 1% mas. roztwór Na_2HPO_4 z dodatkiem 2,5% mas. żelu pektyny cytrusowej (Publikacja 5, Tabela 1).

Skuteczność procesu modyfikacji hybrydowych granul została potwierdzona przy pomocy analizy fluorescencji rentgenowskiej (XRF) oraz metody rentgenowskiej spektroskopii dyspersji energii (EDS). Analiza XRF wykazała obecność w otrzymanych materiałach charakterystycznych sygnałów pochodzących od miedzi i tytanu. Wykazano, że zawartość pierwiastków w otrzymanych granulach wynosiła odpowiednio: 5,11 ± 0,007% mas. dla miedzi oraz 4,87 ± 0,003% mas. dla tytanu, co niemalże w pełni odpowiadało założonym wartościom (5% mas.). Modyfikację przeprowadzono mokrą metodą chemiczną, bez dodatkowych etapów obróbki termicznej. Metoda ta umożliwiła efektywne wprowadzenie pierwiastków o właściwościach przeciwdrobnoustrojowych do składu granul HA/CTS przy jednoczesnym zachowaniu ich hybrydowego charakteru.

Opracowane biomikrobetony, zawierające zmodyfikowane granule (Cu-HA/CTS lub Ti-HA/CTS) oraz naturalne biopolimery – wykazywały akceptowalne czasy wiązania, wynoszące od 11,0 ± 0,5 do 12,0 ± 1,5 minut (czas początkowy) oraz od 18,5 ± 1,0 do 21,0 ± 1,0 minut (czas końcowy) (Publikacja 5, Tabela 2). W przypadku biomikrobetonów zawierających hybrydowe granule HA/CTS zmodyfikowane miedzią, zaobserwowano wydłużenie czasu wiązania, które mogło wynikać z tworzenia się kompleksów pektyny cytrusowej z miedzią.

Ocena profilu uwalniania jonów stanowiła istotny etap charakterystyki opracowanych biomateriałów, umożliwiający prognozowanie ich potencjalnej aktywności biologicznej *in vivo*. W analizowanych biomikrobetonach zaobserwowano wyraźne różnice w dynamice uwalniania miedzi i tytanu (Publikacja 5, Rysunek 12). Proces uwalniania tytanu przebiegał znacznie wolniej niż w przypadku miedzi, przy czym w obu przypadkach najwyższe stężenia w roztworze odnotowano w pierwszym dniu inkubacji.

Ocena aktywności antybakteryjnej opracowanych biomikrobetonów obejmowała testy dyfuzyjne w agarze, oznaczenia liczby żywych komórek bakteryjnych (CFU) oraz ana-

lizę adhezji bakterii do powierzchni materiałów. W klasycznym teście dyfuzji, jedynie próbki zawierające granule modyfikowane miedzią wykazały zdolność hamowania wzrostu *S. aureus* oraz *E. coli*, ze strefami inhibicji wynoszącymi odpowiednio 11 i 10 mm. Charakterystyczne zabarwienie stref zahamowania wzrostu bakteryjnego w przypadku biomikrobetonów przypisano obecności jonów miedzi dyfundujących do podłoża i oddziałującej z komponentami białkowymi agaru (Publikacja 5, Rysunek 13A). Biomikrobetony zawierające niemodyfikowane granule oraz zawierające granule modyfikowane tytanem nie wykazywały aktywności antybakteryjnej w tym teście.

Wyniki oznaczeń CFU dostarczyły danych ilościowych potwierdzających obserwacje jakościowe. Materiał zawierający niemodyfikowane granule HA/CTS, wykazywał niewielką, lecz zauważalną redukcję liczby bakterii, wynikającą z działania antybakteryjnego chitozanu. Natomiast materiały zawierające granule modyfikowane miedzią powodowały całkowitą eliminację komórek bakteryjnych obu szczepów, jednoznacznie wskazując na wysoką skuteczność miedzi jako czynnika przeciwdrobnoustrojowego. W przypadku materiałów zawierających granule modyfikowane tytanem nie zaobserwowano efektu bakteriobójczego – co więcej, dla szczepu *S. aureus* odnotowano wzrost liczby żywych komórek (Publikacja 5, Rysunek 13B,C).

Badanie adhezji komórek bakteryjnych do powierzchni próbek – kluczowe w kontekście zapobiegania tworzeniu biofilmów – potwierdziło korzystny wpływ modyfikacji miedzią i tytanem na redukcję przylegania komórek bakteryjnych Gram-dodatnich. Dla szczepu *S. aureus* udział powierzchni pokrytej komórkami wynosił odpowiednio 0,3% (dla materiału zawierającego granule modyfikowane miedzią), 23,9% (dla materiału zawierającego granule modyfikowane tytanem) i 65,5% (dla materiału zawierającego niemodyfikowane granule). W przypadku *E. coli* różnice były mniej wyraźne – 7,6% (dla materiału zawierającego granule modyfikowane miedzią), 21,7% (dla materiału zawierającego granule modyfikowane tytanem) i 15,6% (dla materiału zawierającego niemodyfikowane granule). Dane te sugerują ograniczony wpływ tytanu na adhezję komórek Gram-ujemnych oraz możliwy efekt sprzyjający kolonizacji (Publikacja 5, Rysunek 14).

Podsumowując, zmodyfikowanie hybrydowych granul HA/CTS pierwiastkami o korzystnych właściwościach biologicznych, w połączeniu z odpowiednio zaprojektowaną fazą ciekłą dla materiałów wiązanych chemicznie, umożliwiło otrzymanie nowoczesnych, w pełni wstrzykiwalnych biomateriałów kościozastępczych o wysokim potencjale antybakteryjnym. Opracowane biomikrobetony cechowały się podwyższoną wytrzymałością na ściskanie oraz korzystnym profilem uwalniania miedzi i tytanu, co wskazuje na możliwość ich zastosowania nie tylko jako pasywnych wypełniaczy ubytków, lecz również jako aktywnych nośników substancji o korzystnym działaniu biologicznym.

Etap VII – Rusztowania kostne otrzymane z wykorzystaniem robocastingu

Cementowe materiały kościozastępcze oparte na fosforanach (V) wapnia mogą być stosowane nie tylko w postaci past przeznaczonych do bezpośredniej aplikacji w miejsce ubytku kostnego, lecz również jako materiały do wytwarzania rusztowań przestrzennych z wykorzystaniem nowoczesnych metod formowania przyrostowego, takich jak robocasting. Aby pasty cementowe mogły być wykorzystane do druku, muszą spełniać określone wymagania, w szczególności w zakresie parametrów reologicznych, które warunkują możliwość ich ekstruzji przez dyszę drukarki 3D.

Ostatni etap badań realizowanych w ramach pracy doktorskiej obejmował otrzymanie oraz charakterystykę samowiążących materiałów kościozastępczych na bazie fosforanów (V) wapnia, polimerów naturalnych i silanowych środków sprzęgających, w formie przestrzennych rusztowań o podwyższonej wytrzymałości mechanicznej przy wykorzystaniu metody robocastingu (Publikacja 6, Tabela 1).

Jak wykazano we wcześniejszych badaniach, obecność polimerów naturalnych istotnie wpływa na wzrost lepkości cementowych mieszanin, co w kontekście technologii przyrostowych jest zjawiskiem pożądanym. Wydłużony czas umożliwia bowiem nieprzerwane formowanie większej liczby rusztowań kostnych bez ryzyka przedwczesnego utwardzenia materiału w dyszy lub konieczności wymiany zbiornika roboczego drukarki 3D. Choć opóźniony proces wiązania może być niekorzystny w przypadku bezpośredniej aplikacji pasty do miejsca ubytku kostnego, w technologiach przyrostowych stanowi zaletę, pozwalającą na uzyskanie precyzyjnych i morfologicznie stabilnych rusztowań przestrzennych. Lepkość otrzymanych past cementowych mieściła się w zakresie od 60 do 390 Pa·s (Publikacja 6, Rysunek 2). Pastom zawierającym hybrydowe proszki HA/CTS towarzyszyła większa stabilność lepkości w porównaniu do układów opartych wyłącznie na proszkach α-TCP, co przekładało się na istotnie dłuższe okno czasowe umożliwiające prowadzenie procesu robocastingu – sięgające do około 3000 sekund.

Przeprowadzono ocenę mikrostruktury rusztowań kostnych otrzymanych metodą robocastingu, w celu określenia ich przydatności do zastosowań w inżynierii tkankowej oraz identyfikacji potencjalnych defektów związanych z techniką druku. Po upływie 24 godzin inkubacji próbek w warunkach 100% wilgotności, rusztowania charakteryzowały się obecnością zarówno makro-, jak i mikroporów. Architektura otrzymanych wydruków pozostawała zgodna z przyjętymi założeniami projektowymi modelu komputerowego.

Nie zaobserwowano negatywnego wpływu ani materiału hybrydowego HA/CTS, ani zastosowanych silanowych środków sprzęgających modyfikujących powierzchnię proszku α-TCP na morfologię otrzymanych rusztowań (Publikacja 6, Rysunek 3). Zastosowanie silanowych środków sprzęgających do modyfikacji proszku α-TCP istotnie poprawiło parametry mechaniczne, niezależnie od zastosowanego typu silanu (Publi-

kacja 6, Rysunek 6). Wytrzymałość na ściskanie rusztowań mieściła się w zakresie od 5,2 ± 0,8 MPa do 9,3 ± 0,5 MPa. Zaobserwowany efekt wzrostu wytrzymałości mechanicznej przypisano oddziaływaniom chemicznym pomiędzy komponentami materiału, w szczególności pomiędzy grupami funkcyjnymi obecnymi w polimerach naturalnych i silanowych środkach sprzęgających. Kluczowe znaczenie miała również obecność chitozanu i pektyny cytrusowej, których przeciwstawne ładunki sprzyjały homogenizacji pasty i stabilizacji struktury poprzez tworzenie fizycznych i chemicznych sieci oddziaływań z hybrydowym proszkiem HA/CTS. Wzrost parametrów mechanicznych zależał od ilości wprowadzonych środków sprzęgających.

Końcowy etap oceny trójwymiarowych rusztowań dotyczył zbadania stabilności chemicznej, przewodnictwa jonowego właściwego oraz potencjału bioaktywnego w testach *in vitro*. Obecność biopolimerów i silanów nie wpływała istotnie na zmiany wartości pH symulowanego płynu ustrojowego który pozostawał stabilny i mieścił się w przedziale 7,33–7,43 przez cały okres badania. (Publikacja 6, Rysunek 7A). Przewodnictwo jonowe właściwe roztworu inkubacyjnego wokół badanych próbek wynosiło od około 111 do 146 μS/cm, przy czym zastosowanie hybrydowego materiału HA/CTS w postaci proszku zamiast granul prowadziło do jego obniżenia do poziomu 65–96 μS/cm (Publikacja 6, Rysunek 7B). Po siedmiu dniach inkubacji próbek w roztworze SBF w temperaturze 37°C, na powierzchni wszystkich analizowanych rusztowań zaobserwowano charakterystyczną warstwę apatytową, co potwierdziło ich wysoki potencjał bioaktywny *in vitro* (Publikacja 6, Rysunek 8).

Podsumowując, zaproponowane szerokie podejście do sposobów modyfikacji składów wyjściowych cementów kostnych na bazie α-TCP – obejmujące zarówno fazę proszkową, jak i ciekłą – stanowi kompleksową i skuteczną strategię poprawy właściwości funkcjonalnych materiałów opartych na fosforanach (V) wapnia. Zastosowanie silanowych środków sprzęgających oraz polimerów naturalnych, takich jak chitozan i pektyna cytrusowa, umożliwiło uzyskanie materiałów samowiążących o wyższej wytrzymałości mechanicznej, lepszej adhezji między osnową cementową a hybrydowymi granulami HA/CTS, poprawę parametrów reologicznych, przy jednoczesnym zachowaniu biozgodności i potencjału bioaktywnego *in vitro*. Potwierdzona skuteczność tych modyfikacji zarówno w materiałach typu biomikrobetonów, jak i w rusztowaniach przestrzennych otrzymanych metodą robocastingu, wskazuje na szerokie możliwości aplikacyjne zaproponowanych rozwiązań materiałowych w inżynierii tkanki kostnej.

Wnioski

W ramach niniejszej rozprawy doktorskiej zaprojektowano, otrzymano i poddano ocenie fizykochemicznej oraz biologicznej nowoczesne materiały hybrydowe przeznaczone do regeneracji tkanki kostnej. Opracowane materiały oparto na fosforanach (V) wapnia które częściowo zostały zmodyfikowane z wykorzystaniem silanowych środków sprzęgających i/lub czynników aktywnych biologicznie (jony tytanu oraz miedzi) oraz polimerach pochodzenia naturalnego. W wyniku przeprowadzonych badań oceniono wpływ różnych modyfikacji składów wyjściowych materiałów typu cementowego na właściwości fizykochemiczne, aplikacyjne oraz biologiczne wytworzonych hybrydowych substytutów kostnych.

Na podstawie przeprowadzonych badań eksperymentalnych oraz analizy zgromadzonych wyników sformułowano następujące wnioski:

1. Główny cel pracy doktorskiej został osiągnięty. Wykazano, że możliwe jest otrzymanie hybrydowych biomateriałów kościozastępczych nowej generacji opartych na fosforanach (V) wapnia, polimerach pochodzenia naturalnego oraz silanowych środkach sprzęgających.
2. Wykazano, że opracowana bezwodna modyfikacja proszku α-fosforanu (V) wapnia z wykorzystaniem dwóch różnych silanowych środków sprzęgających, a mianowicie tetraetoksysilanu oraz 3-glicydoksylopropylotrimetoksysilanu, korzystnie wpływa na powierzchnię właściwą, rozkład wielkości cząstek oraz potencjał elektrokinetyczny wyjściowego proszku α-TCP, a tym samym na proces wiązania oraz poprawę wytrzymałości na ściskanie wytworzonych na jego bazie materiałów typu cementowego.
3. Udowodniono, że zastosowanie pektyny cytrusowej, jako związku modyfikującego fazę ciekłą ma korzystny wpływ na właściwości mechaniczne opracowanych biomateriałów. Efekt ten wynika z występowania podwójnego mechanizmu wiązania, obejmującego jednocześnie hydrolizę α-TCP oraz sieciowanie łańcuchów polimerowych jonami wapnia, a w przypadku biomikrobetonów również z tworzenia mostków polimerowych łączących poszczególne komponenty materiałów.
4. Udowodniono, że poprzez wykorzystanie granul hydroksyapatytowo-chitozanowych modyfikowanych miedzią możliwe jest wytworzenie materiałów wiązanych chemicznie typu biomikrobetonów o wielokierunkowym i wzmocnionym działaniu antybakteryjnym. Jednocześnie wykazano, że biomikrobetony zawierające granule HA/CTS modyfikowane tytanem nie wykazują znaczącej aktywności antybakteryjnej.
5. Wykazano, że odpowiednia modyfikacja fazy stałej oraz ciekłej samowiążących cementów fosforanowo-wapniowych za pomocą silanowych środków sprzęgających

oraz pektyny cytrusowej pozwala na otrzymanie hybrydowych past ceramicznych, z których można metodą robocastingu wydrukować odpowiednio spersonalizowane implanty kostne.

6. Potwierdzono, że wytworzone hybrydowe biomateriały nie mają negatywnego wpływu na rozwój i różnicowanie się ludzkich komórek ostoblastycznych (linia MC3T-3-E1), a w testach *in vitro* w SBF wykazują potencjał bioaktywny.
7. Za najbardziej obiecujące materiały implantacyjne uznano biomikrobetony oraz rusztowania kostne oparte na zmodyfikowanym z wykorzystaniem 5% mas. 3-glicydoksylopropylotrimetoksysilanu wysokoreaktywnym proszku α-TCP oraz hybrydowych materiałach hydroksyapatytowo-chitozanowych, które w fazie ciekłej zawierały mieszaninę 2,5% mas. żelu pektyny cytrusowej i 1% mas. wodorofosforanu (V) sodu. Wykazano, że opracowane biomateriały można wykorzystać jako nośniki pierwiastków o korzystnym działaniu biologicznym, a także do wytwarzania porowatych rusztowań kostnych otrzymywanych przy pomocy technik formowania przyrostowego. Opracowane materiały po przeprowadzeniu pełnych badań biologicznych *in vitro* oraz *in vivo* mogą potencjalnie stanowić grupę biomateriałów hybrydowych typu cementowego, do wykorzystania w medycynie jako kościozastępcze preparaty implantacyjne nowej generacji.

Perspektywy

Rezultaty osiągnięte w ramach niniejszej rozprawy doktorskiej otwierają perspektywy do prowadzenia dalszych badań, koncentrujących się na łączeniu wielu strategii modyfikacji zaawansowanych cementów kostnych w celu otrzymania materiałów poręcznych chirurgicznie o wielotorowym działaniu antybakteryjnym, wspierających regenerację tkanki kostnej. Planowane przyszłe badania powinny być realizowane w trzech głównych kierunkach.

Pierwszy kierunek – to badania nad wykorzystaniem silanowych środków sprzęgających do modyfikacji powierzchni biomateriałów fosforanowo-wapniowych, innych niż zastosowane w niniejszej pracy. Dalsze badania w tym obszarze koncentrowałyby się na poszukiwaniu związków o zróżnicowanej budowie chemicznej i grupach funkcyjnych, które mogłyby oferować jeszcze bardziej precyzyjną kontrolę nad interakcjami pomiędzy materiałem a środowiskiem biologicznym.

Drugi obszar badawczy powinien koncentrować się na modyfikacjach biomateriałów typu cementowego z wykorzystaniem jonów, leków lub substancji aktywnych o korzystnym działaniu biologicznym. W dotychczasowych badaniach wykazano, że wprowadzenie jonów miedzi nadawało materiałom silne właściwości antybakteryjne, co jest kluczowe w profilaktyce zakażeń pooperacyjnych. Materiały modyfikowane tytanem, choć nie wykazały wyraźnej aktywności antybakteryjnej *in vitro*, są cenione za biozgodność i wysoki potencjał osteoindukcyjny. W perspektywie dalszych badań planuje się wprowadzenie innych jonów, takich jak magnezowe (Mg^{2+}), strontowe (Sr^{2+}), bizmutowe (Bi^{3+}) czy cynkowe (Zn^{2+}). Jony te są znane z ich zdolności do wspierania osteogenezy i angiogenezy, co jest kluczowe dla efektywnej regeneracji tkanki kostnej.

Trzeci potencjalny kierunek badawczy obejmuje wykorzystanie poręcznych chirurgicznie past cementowych do otrzymywania skomplikowanych i spersonalizowanych rusztowań kostnych za pomocą nowoczesnych technik formowania przyrostowego. W przyszłości możliwa będzie dalsza modyfikacja parametrów druku w celu uzyskania struktur o gradientowej porowatości, kanałach kapilarnych imitujących naczynia krwionośne czy anatomicznie dopasowane modele ubytków kostnych.

Dorobek naukowy

Wykaz publikacji naukowych

1. PAŃTAK, Piotr, CZECHOWSKA, Joanna, KASHIMBETOVA, Adelia, ČELKO, Ladislav, MONTUFAR, Edgar B., WÓJCIK, Łukasz and ZIMA, Aneta. Improving the processability and mechanical strength of self-hardening robocasted hydroxyapatite scaffolds with silane coupling agents. Journal of the Mechanical Behaviour of Biomedical Materials. 2025. Vol. 161, p. 106792. DOI 10.1016/j.jmbbm.2024.106792.
2. PAŃTAK, Piotr, CZECHOWSKA, Joanna, BELCARZ, Anna and ZIMA, Aneta. The influence of titanium and cooper on physiochemical and antibacterial properties of bioceramic-based composites for orthopaedic applications. Ceramics International. 2025. Vol. 51, p. 1214. DOI 10.1016/j.ceramint.2024.11.102.
3. PAŃTAK, Piotr, CZECHOWSKA, Joanna, VIVCHARENKO, Vladyslav, DORNER-REISEL, Annett and ZIMA, Aneta. The synergistic effect of polysaccharides and silane coupling agents on the properties of calcium phosphate-based bone substitutes. International Journal of Molecular Sciences. 2025. Vol. 26, p. 8910. DOI 10.3390/ijms26188910.
4. PASIUT, Katarzyna, PARTYKA, Janusz, KOZIEŃ, Dawid and PAŃTAK, Piotr. Impact of zinc oxide on the structure and surface properties of magnesium-potassium glass-crystalline glazes. Crystals. 2024. Vol. 14, p. 456. DOI 10.3390/cryst14050456.
5. CICHOŃ, Ewelina, KOSOWSKA, Karolina, PAŃTAK, Piotr, CZECHOWSKA, Joanna, ZIMA, Aneta and ŚLÓSARCZYK, Anna. Physicochemical properties of inorganic and hybrid hydroxyapatite-based granules modified with citric acid or polyethylene glycol. Molecules. 2024. Vol. 29, p. 2018. DOI 10.3390/molecules29092018.
6. CZECHOWSKA, Joanna, PAŃTAK, Piotr, KOWALSKA, Kinga, VEDAIYAN, Jeevitha, BALASUBRAMANIAN, Mareeswari, GANESAN, Sundara Moorthi, KWIECIEŃ, Konrad, PAMUŁA, Elżbieta, KANDASWAMY, Ravichandran and ZIMA, Aneta. The influence of citrus pectin and polyacrylamide modified with plant-derived additives on the properties of alpha-TCP-based bone cements. Polymers (Basel). 2024. Vol. 16, p. 1711. DOI 10.3390/polym16121711.
7. SKIBIŃSKI, Szymon, CICHOŃ, Ewelina, SETA, Martyna, GONDEK, Agata, CZECHOWSKA, Joanna, PAŃTAK, Piotr, GUZIK, Maciej, ŚLÓSARCZYK, Anna and ZIMA, Aneta. Evaluation of beta-tricalcium phosphate and poly(3-hydroxybutyrate) – based scaffolds for bone tissue regeneration. Tissue Engineering Part A [online]. 2023. Vol. 29, p. 660. Available from: https://www.liebertpub.com/toc/tea/29/11-12
8. PAŃTAK, Piotr, CZECHOWSKA, Joanna, CICHOŃ, Ewelina and ZIMA, Aneta. Novel double hybrid-type bone cements based on calcium phosphates, chitosan and citrus pectin. International Journal of Molecular Sciences. 2023. Vol. 24, p. 13455. DOI 10.3390/ijms241713455.

9. CICHOŃ, Ewelina, HARAŹNA, Katarzyna, SKIBIŃSKI, Szymon, PAŃTAK, Piotr, ŚLÓSARCZYK, Anna, CZECHOWSKA, Joanna, GUZIK, Maciej and ZIMA, Aneta. Scaffolds based on tricalcium phosphate and bacteria-derived polyhydroxyoctanoate – cytocompatibility studies. Tissue Engineering Part A [online]. 2023. Vol. 29, p. 1397. Available from: https://www.liebertpub.com/toc/tea/29/11-12
10. PAŃTAK, Piotr, CZECHOWSKA, Joanna and ZIMA, Aneta. The influence of silane coupling agents on the properties of alpha-TCP-based ceramic bone substitutes for orthopaedic applications. RSC Advances. 2023. Vol. 13, p. 34020. DOI 10.1039/D3RA06027F.
11. SKIBIŃSKI, Szymon, PAŃTAK, Piotr, CICHOŃ, Ewelina, GUZIK, Maciej, CZECHOWSKA, Joanna, ŚLÓSARCZYK, Anna and ZIMA, Aneta. Biodegradable tricalcium phosphate/poly(3-hydroxybutyrate) scaffolds for bone tissue regeneration. Inżynieria Biomateriałów = Engineering of Biomaterials [online]. 2021. P. 74. Available from: http://yadda.icm.edu.pl/baztech/element/bwmeta1.element.baztech-9234a-0ae-c284-4c4f-bc64-6b0c93242c43/c/74.pdf
12. CICHOŃ, Ewelina, PRAJSNAR, Justyna, GUZIK, Maciej, CZECHOWSKA, Joanna, SKIBIŃSKI, Szymon, PAŃTAK, Piotr, ŚLÓSARCZYK, Anna and ZIMA, Aneta. Foamed calcium phosphate cements and their behaviour during incubation in distilled water. Inżynieria Biomateriałów = Engineering of Biomaterials [online]. 2021. P. 27. Available from: http://yadda.icm.edu.pl/baztech/element/bwmeta1.element.baztech-e771ecae-8db0-4268-8b93-4b6e80a0e713/c/27.pdf
13. CZECHOWSKA, Joanna, CICHOŃ, Ewelina, BELCARZ, Anna, ŚLÓSARCZYK, Anna, PAŃTAK, Piotr, SKIBIŃSKI, Szymon and ZIMA, Aneta. Gold nanoparticles and silicon as effective modifiers of hybrid\=type, chemically bonded biomaterials. Inżynieria Biomateriałów = Engineering of Biomaterials [online]. 2021. P. 26. Available from: http://yadda.icm.edu.pl/baztech/element/bwmeta1.element.baztech-9154e8a6-90d3-4de5-93ff-8c29fc8b58ab/c/26.pdf
14. PAŃTAK, Piotr, CICHOŃ, Ewelina, CZECHOWSKA, Joanna and ZIMA, Aneta. Influence of natural polysaccharides on properties of the biomicroconcrete-type bioceramics. Materials. 2021. Vol. 14, p. 7496. DOI 10.3390/ma14247496.

Wykaz wystąpień konferencyjnych

1. Pańtak, P., Czechowska, J., Kowalska, K., Chwał, J., Belcarz, A., Zima, A., 2025. *Effect of cooper and titanium on the properties of novel antibacterial biomicroconcretes for bone substitution,* The XIX Conference of European Ceramic Society 2025 (ECerS), Dresden, Germany 31 August–4 September 2026 (wystąpienie ustne).
2. Pańtak, P., Czechowska, J., Kowalska, K., Montufar, E.B., Zima, A., 2024. *The beneficial influence of selected silane coupling agents on the properties of novel*

α-TCP-based robocasted scaffolds, Young Ceramists Additive Manufacturing Forum (yCAM 2024), Tampere, Finland, 6–8 May 2024, *Book of Abstracts*, pp. 81–82 (wystąpienie ustne).

3. Pańtak, P., Czechowska, J., Zima, A., 2023. *How silane coupling agents influenced the properties of bioactive bone substitutes?*, Polish–Scandinavian Symposium on Biomaterials, Kraków, 25 September 2023, *Program and Book of Abstracts*, p. 23 (wystąpienie ustne).
4. Pańtak, P., Czechowska, J., Cichoń, E., Skibiński, S., Zima, A., 2023. *Innowacyjne podejście do modyfikacji fosforanów (V) wapnia z wykorzystaniem silanowych środków sprzęgających*, Biomateriały w medycynie i kosmetologii, IV Sympozjum, 22 lutego 2023 r., Toruń, *Mataeriały konferencyjne*, pp. 21–22 (wystąpienie ustne).
5. Pańtak, P., Czechowska, J., Montufar, E.B., Zima, A., 2023. *Robocasting of novel hybrid α-TCP-based scaffolds for bone tissue engineering applications*, Bioceramics 33, 33rd Conference and Annual Meeting of the International Society for Ceramics in Medicine (ISCM), October 17–20 2023, Solothurn, Switzerland, *Program & Abstracts*, pp. 237–238 (wystąpienie ustne).
6. Pańtak, P., Skibiński, S., Cichoń, E., Czechowska, J., Guzik, M., Ślósarczyk, A., Zima, A., 2022. *Evaluation of β-tricalcium phosphate-based scaffold coated with polyhydroxynonanoate for bone tissue engineering application,* Bioceramics 32, 32nd Symposium and Annual Meeting of the International Society for Ceramics in Medicine, September 20–23 2022, Venice, Italy, *Book of Abstracts*, p. 189 (poster).
7. Pańtak, P., Cichoń, E., Skibiński, S., Czechowska, J., Zima, A., Ślósarczyk, A., 2022. *How liquid phase composition affects the properties of calcium phosphate biomicroconcretes based on α-TCP?,* 2022 Hawaii Joint Symposium, Honolulu, HI, January 8–10 2022, *Final Program*, p. 48 (poster).
8. Pańtak, P., Cichoń, E., Skibiński, S., Czechowska, J., Zima, A., 2022. *Influence of tetraethoxysilane (TEOS) on physicochemical properties of α-tricalcium phosphate-based injectable bone substitutes*, BioMaH 2022, 3rd Biennial International Conference BioMaterials and Novel Technologies for Healthcare, October 18–21 2022, Rome, Italy, *Conference Proceedings*, pp. 170–171 (wystąpienie ustne).
9. Pańtak, P., Cichoń, E., Skibiński, S., Ślósarczyk, A., Czechowska, J., Zima, A., 2022. *Influence of tetraethoxysilane (TEOS) on the properties of calcium phosphate-based biomicroconcrete-type biomaterials*, BIOMATSEN 2022, 7th International Congress on Biomaterials and Biosensors, April 22–28 2022, Oludeniz, Turkey, *Book of Abstracts*, p. 27 (poster).
10. Pańtak, P., Cichoń, E., Skibiński, S., Czechowska, J., Zima, A., 2022. *Influence of various liquid phases on properties of α-TCP-based bioactive bone cements*, Ceramics in Europe 2022, Kraków, 10–14 July, *Abstract Book*, p. 478 (poster).
11. Pańtak, P., Skibiński, S., Czechowska, J., Cichoń, E., Guzik, M., Ślósarczyk, A., Zima,

A., 2022. *Short and medium chain length polyhydroxyalkanoates as coatings of β-tricalcium phosphate scaffolds for bone tissue regeneration*, ScSB 2022, 15th Annual Meeting of the Scandinavian Society for Biomaterials, 13–15 June 2022, Jurmala, Latvia, p. P24 (poster).

12. Pańtak, P., Czechowska, J., Cichoń, E., Skibiński, S., Zima, A., 2022. *The effect of liquid phase on properties of calcium phosphate-based cements containing hybrid hydroxyapatite/chitosan granules*, UK–Poland–Ukraine Bioinspired Materials Conference, 29–30 November 2022, Online, *Book of Abstracts,* p. 37 (wystąpienie ustne).
13. Pańtak, P., Cichoń, E., Skibiński, S., Czechowska, J., Zima, A., Ślósarczyk, A., 2021. *Citrus pectin and its influence on properties of α-TCP-based bone cements*, The 2nd International Conference on Chemistry for Beauty and Health 2021, Poznań–Toruń, May 12–14 2021, *Book of Abstracts*, p. 86 (wystąpienie ustne).
14. Pańtak, P., Cichoń, E., Skibiński, S., Czechowska, J., Zima, A., Ślósarczyk, A., 2021. *Evaluation of liquid phase influence on properties of α-TCP-based biomicroconcrete--type bone substitutes*, ESB 2021, 31st Conference of the European Society for Biomaterials, 5–9 September 2021, Porto, Portugal, *Abstract Book*, pp. 1136–1137 (poster).
15. Pańtak, P., Cichoń, E., Skibiński, S., Czechowska, J., Zima, A., 2021. *Pektyna cytrusowa i inne polisacharydy jako dodatki do wstrzykiwalnych biomikrobetonów kościozastępczych*, Biomateriały w medycynie i kosmetologii, II Sympozjum, 28 stycznia 2021 r., Toruń, *Materiały konferencyjne,* p. 62 (poster).
16. Pańtak, P., Cichoń, E., Czechowska, J., Ślósarczyk, A., Zima, A., 2021. *Wpływ pektyny cytrusowej dodawanej do fazy ciekłej na fosforanowo-wapniowe cementy kostne*, Implanty 2021, III Ogólnopolska Konferencja Naukowa, 18 czerwca 2021, Gdańsk (online), *Książka abstraktów*, p. 73 (poster).
17. Pańtak, P., Cichoń, E., Skibiński, S., Czechowska, J., Zima, A., 2020. *Citrus pectin and other polysaccharides as additives to injectable biomicroconcrete-type bone fillers*, UK–Poland Bioinspired Materials Conference, 23–24 November 2020, Online, *Book of Abstracts,* p. 104 (poster).

Wykaz projektów badawczych

1. Biomikrobetony dla chirurgii kostnej z układu alfa TCP - HAp - chitozan z hybrydowymi granulami – Grant badawczy OPUS NCN Nr 2017/27/B/ST8/01173 – Wykonawca
2. Technologia biorafinacji olejów roślinnych do wytwarzania zaawansowanych materiałów kompozytowych – Grant badawczy Techmatstrateg NCBiR Nr TECHMATSTRATEG2/407507/1/NCBR/2019 – Wykonawca
3. Hybrydowe materiały implantacyjne do zastosowań w inżynierii tkanki kostnej – projekt badawczy Inicjatywa Doskonałości – Uczelnia Badawcza – AGH Nr IDUB/4/18.16.0.4159 – Wykonawca

Wykaz patentów i zgłoszeń patentowych

1. Zima, A., Czechowska, J., Pańtak, P. (2025). Sposób otrzymywania biomateriału kościozastępczego w postaci hybrydowych granul (Patent Nr PL246598B1).
2. Zima, A., Czechowska, J., Pańtak, P. (2024). Sposób otrzymywania hybrydowych granul na bazie hydroksyapatytu (Zgłoszenie Nr PL447485A1).

Wykaz staży i wyjazdów naukowych

1. Otrzymywanie i charakterystyka materiałów z wykorzystaniem druku 3D, Central European Institute of Technology – Staż naukowy z realizacją badań do pracy doktorskiej, finansowanie w ramach Inicjatywa Doskonałości – Uczelnia Badawcza – AGH, Działanie 6, 15.11–16.12.2022, Brno, Czechy
2. Synteza i charakterystyka hybrydowych granul modyfikowanych jonami miedzi, Uniwersytet w Göteborgu – Staż naukowy w ramach programu STER NAWA Umiędzynarodowienie Szkół Doktorskich, 01-30.06.2024, Göteborg, Szwecja
3. Ocena biologiczna kompozytowych biomateriałów kościozastępczych opartych na fosforanach (V) wapnia oraz bioszkłach boranowych, FUNGLASS – Staż naukowy finansowany w ramach stypendium Europejskiego Stowarzyszenia Ceramicznego (ECerS) w ramach projektu JECS Trust, 01.04.2025-30.06.2025, Trenczyn, Słowacja

Wykaz ważniejszych nagród i osiągnięć

1. Laureat XIV edycji Ogólnopolskiego Konkursu Student-Wynalazca (2024)
2. Złoty medal na Międzynarodowej Wystawie Geneva International Exhibition of Inventions (2024)
3. Złoty medal na Międzynarodowej Warszawskiej Wystawie Wynalazków IWIS 2024 (2024)
4. Srebrny medal na Międzynarodowej Wystawie iENA – International Trade Fair „Ideas – Inventions – New Products" (2024)
5. Srebrny medal na Międzynarodowej Wystawie Arca – 20th International Innovation Exhibition (2024)
6. Nagroda specjalna FIRI The first institute of inventors and researchers of Iran przyznana podczas Międzynarodowej Wystawie Geneva International Exhibition of Inventions (2024)
7. Laureat konkursu na wyjazdy stażowe STER NAWA – umiędzynarodowienie szkół doktorskich, finansowanego przez Narodową Agencję Wymiany Akademickiej.
8. Laureat III edycji konkursu zwiększonych stypendiów dla najlepszych doktorantów szkół doktorskich w ramach Projektu Inicjatywa Doskonałości – Uczelnia Badawcza AGH (2024)
9. Laureat konkursu dla najlepszych asystentów lub adiunktów w ramach Projektu Inicjatywa Doskonałości – Uczelnia Badawcza AGH (2024)

Szkoły letnie i szkolenia

1. Szkoła letnia: *Additive Manufacturing for Life Sciences*, 19–22.06.2023, Uppsala, Szwecja
2. Warsztat materiałowy: *Zastosowanie sprzężonych metod analizy termicznej w badaniach materiałowych,* 15–16.02.2023, Gdańsk, Polska
3. Warsztat biomateriałowy: *Antimicrobial biomaterials for orthopaedics/dentistry and beyond* podczas konferencji Bioceramics 32, 22.09.2022, Wenecja, Włochy
4. Warsztat biomateriałowy: *Finceramica – Porous hydroxyapatite cranioplasty Infection efficacy and paediatric indications* na konferencji Bioceramics 32, 21.09.2022, Wenecja, Włochy
5. Warsztat ceramiczny: *Fundamentals and Advanced Technologies of Sintering* podczas konferencji ECerS, Kraków, 2022
6. Kurs szkoleniowy z zakresu prawa własności intelektualnej: „*Ochrona Własności Intelektualnej w AGH – Intellectual Property Protection at AGH*", Organizatorzy: PhD Skills Academy, 1.02.2021, Kraków, Polska
7. Kurs szkoleniowy z zakresu spektroskopii: „*Spektroskopia w podczerwieni FTIR w skali mikro i makro – Micro- and Macro-scale FTIR Spectroscopy*", Organizator: MS Spektrum, 31.05.2022, Kraków, Polska

Stypendia naukowe

1. Stypendium Rektora AGH za osiągnięcia publikacyjne (2022, 2023, 2024)
2. Stypendium Dziekana Wydziału Inżynierii Materiałowej i Ceramiki AGH za osiągnięcia naukowe (2022, 2023, 2024)

Członkostwo w organizacjach

1. Członkostwo w Polskim Stowarzyszeniu Biomateriałów (od 2021 r.)
2. Członkostwo w Polskim Towarzystwie Ceramicznym (od 2021 r.)

Bibliografia

[1] A.-M. Wu, C. Bisignano, S.L. James, G.G. Abady, A. Abedi, E. Abu-Gharbieh, R.K. Alhassan, V. Alipour, J. Arabloo, M. Asaad, W.N. Asmare, A.F. Awedew, M. Banach, S.K. Banerjee, A. Bijani, T.T.M. Birhanu, S.R. Bolla, L.A. Cámera, J.-C. Chang, D.Y. Cho, M.T. Chung, R.A.S. Couto, X. Dai, L. Dandona, R. Dandona, F. Farzadfar, I. Filip, F. Fischer, A.A. Fomenkov, T.K. Gill, B. Gupta, J.A. Haagsma, A. Haj-Mirzaian, S. Hamidi, S.I. Hay, I.M. Ilic, M.D. Ilic, R.Q. Ivers, M. Jürisson, R. Kalhor, T. Kanchan, T. Kavetskyy, R. Khalilov, E.A. Khan, M. Khan, C.J. Kneib, V. Krishnamoorthy, G.A. Kumar, N. Kumar, R. Lalloo, S. Lasrado, S.S. Lim, Z. Liu, A. Manafi, N. Manafi, R.G. Menezes, T.J. Meretoja, B. Miazgowski, T.R. Miller, Y. Mohammad, A. Mohammadian-Hafshejani, A.H. Mokdad, C.J.L. Murray, M. Naderi, M.D. Naimzada, V.C. Nayak, C.T. Nguyen, R. Nikbakhsh, A.T. Olagunju, N. Otstavnov, S.S. Otstavnov, J.R. Padubidri, J. Pereira, H.Q. Pham, M. Pinheiro, S. Polinder, H. Pourchamani, N. Rabiee, A. Radfar, M.H.U. Rahman, D.L. Rawaf, S. Rawaf, M.R. Saeb, A.M. Samy, L. Sanchez Riera, D.C. Schwebel, S. Shahabi, M.A. Shaikh, A. Soheili, R. Tabarés-Seisdedos, M.R. Tovani-Palone, B.X. Tran, R.S. Travillian, P.R. Valdez, T.J. Vasankari, D.Z. Velazquez, N. Venketasubramanian, G.T. Vu, Z.-J. Zhang, T. Vos, Global, regional, and national burden of bone fractures in 204 countries and territories, 1990–2019: a systematic analysis from the Global Burden of Disease Study 2019, Lancet Healthy Longev 2 (2021) e580–e592. https://doi.org/10.1016/S2666-7568(21)00172-0.

[2] H. ElHawary, A. Baradaran, J. Abi-Rafeh, J. Vorstenbosch, L. Xu, J.I. Efanov, Bone Healing and Inflammation: Principles of Fracture and Repair, Semin Plast Surg 35 (2021) 198–203. https://doi.org/10.1055/s-0041-1732334.

[3] C. Gao, S. Peng, P. Feng, C. Shuai, Bone biomaterials and interactions with stem cells, Bone Res 5 (2017) 17059. https://doi.org/10.1038/boneres.2017.59.

[4] J. Wei, X. Chen, Y. Xu, L. Shi, M. Zhang, M. Nie, X. Liu, Significance and considerations of establishing standardized critical values for critical size defects in animal models of bone tissue regeneration, Heliyon 10 (2024) e33768. https://doi.org/10.1016/j.heliyon.2024.e33768.

[5] M.R. Pharaon, T. Scholz, G.R.D. Evans, Tissue Engineering, in: Plast Reconstr Surg, Springer London, London, 2010: pp. 137–157. https://doi.org/10.1007/978-1-84882-513-0_12.

[6] D. Cao, J. Ding, Recent advances in regenerative biomaterials, Regen Biomater 9 (2022). https://doi.org/10.1093/rb/rbac098.

[7] S. Liu, J.-M. Yu, Y.-C. Gan, X.-Z. Qiu, Z.-C. Gao, H. Wang, S.-X. Chen, Y. Xiong, G.-H. Liu, S.-E. Lin, A. McCarthy, J. V. John, D.-X. Wei, H.-H. Hou, Biomimetic natural biomaterials for tissue engineering and regenerative medicine: new biosynthesis methods, recent advances, and emerging applications, Mil Med Res 10 (2023) 16. https://doi.org/10.1186/s40779-023-00448-w.

[8] N. Eliaz, N. Metoki, Calcium Phosphate Bioceramics: A Review of Their History, Structure, Properties, Coating Technologies and Biomedical Applications, Materials 10 (2017) 334. https://doi.org/10.3390/ma10040334.

[9] J. Lu, H. Yu, C. Chen, Biological properties of calcium phosphate biomaterials for bone repair: a review, RSC Adv 8 (2018) 2015–2033. https://doi.org/10.1039/C7RA11278E.

[10] M.C. Tronco, J.B. Cassel, L.A. dos Santos, α-TCP-based calcium phosphate cements: A critical review, Acta Biomater 151 (2022) 70–87. https://doi.org/10.1016/j.actbio.2022.08.040.

[11] A. Robu, R. Ciocoiu, A. Antoniac, I. Antoniac, A.D. Raiciu, H. Dura, N. Forna, M.B. Cristea, I.D. Carstoc, Bone Cements Used for Hip Prosthesis Fixation: The Influence of the Handling Procedures on Functional Properties Observed during In Vitro Study, Materials 15 (2022) 2967. https://doi.org/10.3390/ma15092967.

[12] S. Chaudhry, D. Dunlop, Bone cement in arthroplasty, Orthop Trauma 26 (2012) 391–396. https://doi.org/10.1016/j.mporth.2012.09.004.

[13] J.-H. Jang, S. Shin, H.-J. Kim, J. Jeong, H.-E. Jin, M.S. Desai, S.-W. Lee, S.-Y. Kim, Improvement of physical properties of calcium phosphate cement by elastin-like polypeptide supplementation, Sci Rep 8 (2018) 5216. https://doi.org/10.1038/s41598-018-23577-y.

[14] U. Gbureck, K. Spatz, R. Thull, Improvement of Mechanical Properties of Self Setting Calcium Phosphate Bone Cements Mixed With Different Metal Oxides, Materwiss Werksttech 34 (2003) 1036–1040. https://doi.org/10.1002/mawe.200300700.

[15] A.J. Ambard, L. Mueninghoff, Calcium Phosphate Cement: Review of Mechanical and Biological Properties, Journal of Prosthodontics 15 (2006) 321–328. https://doi.org/10.1111/j.1532-849X.2006.00129.x.

[16] A. Vezenkova, J. Locs, Sudoku of porous, injectable calcium phosphate cements – Path to osteoinductivity, Bioact Mater 17 (2022) 109–124. https://doi.org/10.1016/j.bioactmat.2022.01.001.

[17] H. Gu, C. Liu, J. Zhu, J. Gu, E.K. Wujcik, L. Shao, N. Wang, H. Wei, R. Scaffaro, J. Zhang, Z. Guo, Introducing advanced composites and hybrid materials, Adv Compos Hybrid Mater 1 (2018) 1–5. https://doi.org/10.1007/s42114-017-0017-y.

[18] "Hybrid material," in: The IUPAC Compendium of Chemical Terminology, International Union of Pure and Applied Chemistry (IUPAC), Research Triangle Park, NC, 2014. https://doi.org/10.1351/goldbook.GT07553.

[19] P. Judeinstein, C. Sanchez, Hybrid organic–inorganic materials: a land of multidisciplinarity, J. Mater. Chem. 6 (1996) 511–525. https://doi.org/10.1039/JM9960600511.

[20] P. Gomez-Romero, A. Pokhriyal, D. Rueda-García, L.N. Bengoa, R.M. González-Gil, Hybrid Materials: A Metareview, Chemistry of Materials 36 (2024) 8–27. https://doi.org/10.1021/acs.chemmater.3c01878.

[21] M. Nanko, Definitions and Categories of Hybrid Materials, AZojomo (ISSN 1833-122X) 6 (2009). https://doi.org/10.2240/azojomo0288.

[22] W. Park, H. Shin, B. Choi, W.-K. Rhim, K. Na, D. Keun Han, Advanced hybrid nanomaterials for biomedical applications, Prog Mater Sci 114 (2020) 100686. https://doi.org/10.1016/j.pmatsci.2020.100686.

[23] A. Zima, Hydroxyapatite-chitosan based bioactive hybrid biomaterials with improved mechanical strength, Spectrochim Acta A Mol Biomol Spectrosc 193 (2018) 175–184. https://doi.org/10.1016/j.saa.2017.12.008.

[24] J. Czechowska, Self-assembling, hybrid hydroxyapatite-methylcellulose granules, modified with nano-silver, Mater Lett 300 (2021) 130156. https://doi.org/10.1016/j.matlet.2021.130156.

[25] J.P. Czechowska, A. Dorner-Reisel, A. Zima, Hybrid Bone Substitute Containing Tricalcium Phosphate and Silver Modified Hydroxyapatite–Methylcellulose Granules, J Funct Biomater 15 (2024) 196. https://doi.org/10.3390/jfb15070196.

[26] J. Czechowska, E. Cichoń, A. Belcarz, A. Ślósarczyk, A. Zima, Effect of Gold Nanoparticles and Silicon on the Bioactivity and Antibacterial Properties of Hydroxyapatite/Chitosan/Tricalcium Phosphate-Based Biomicroconcretes, Materials 14 (2021) 3854. https://doi.org/10.3390/ma14143854.

[27] M. Dziadek, A. Zima, E. Cichoń, J. Czechowska, A. Ślósarczyk, Biomicroconcretes based on the hybrid HAp/CTS granules, α-TCP and pectins as a novel injectable bone substitutes, Mater Lett 265 (2020) 127457. https://doi.org/10.1016/j.matlet.2020.127457.

[28] J.-N. Liang, L.-P. Yan, Y.-F. Dong, X. Liu, G. Wu, N.-R. Zhao, Robust and nanostructured chitosan–silica hybrids for bone repair application, J Mater Chem B 8 (2020) 5042–5051. https://doi.org/10.1039/D0TB00009D.

[29] J.A. Sowjanya, J. Singh, T. Mohita, S. Sarvanan, A. Moorthi, N. Srinivasan, N. Selvamurugan, Biocomposite scaffolds containing chitosan/alginate/nano-silica for bone tissue engineering, Colloids Surf B Biointerfaces 109 (2013) 294–300. https://doi.org/10.1016/j.colsurfb.2013.04.006.

[30] J. Gaweł, J. Milan, J. Żebrowski, D. Płoch, I. Stefaniuk, M. Kus-Liśkiewicz, Biomaterial composed of chitosan, riboflavin, and hydroxyapatite for bone tissue regeneration, Sci Rep 13 (2023) 17004. https://doi.org/10.1038/s41598-023-44225-0.

[31] Y. Liu, J. Gu, D. Fan, Fabrication of High-Strength and Porous Hybrid Scaffolds Based on Nano-Hydroxyapatite and Human-Like Collagen for Bone Tissue Regeneration, Polymers (Basel) 12 (2020) 61. https://doi.org/10.3390/polym12010061.

[32] A. Houaoui, A. Szczodra, M. Lallukka, L. El-Guermah, R. Agniel, E. Pauthe, J. Massera, M. Boissiere, New Generation of Hybrid Materials Based on Gelatin and Bioactive Glass Particles for Bone Tissue Regeneration, Biomolecules 11 (2021) 444. https://doi.org/10.3390/biom11030444.

[33] N.R. El-Bahrawy, A. Elmekawy, M.L. Salem, R. Morsy, Gelatin-hydroxyapatite-based hybrid com***posites: Enhanced mechanical and biological characteristics through biomaterials integration for bone*** tissue engineering applications, Int J Biol Macromol 320 (2025) 145772. https://doi.org/10.1016/j.ijbiomac.2025.145772.

[34] S. Iswarya, T. Theivasanthi, S.C.B. Gopinath, Sodium alginate/Hydroxyapatite/nanocellulose composites: Synthesis and Potentials for bone tissue engineering, J Mech Behav Biomed Mater 148 (2023) 106189. https://doi.org/10.1016/j.jmbbm.2023.106189.

[35] A. Magiera, J. Markowski, E. Menaszek, J. Pilch, S. Blazewicz, PLA-Based Hybrid and Composite Electrospun Fibrous Scaffolds as Potential Materials for Tissue Engineering, J Nanomater 2017 (2017) 1–11. https://doi.org/10.1155/2017/9246802.

[36] K.-H. Shin, Y.-H. Koh, H.-E. Kim, Synthesis and Characterization of Drug-Loaded Poly(ε-caprolactone)/Silica Hybrid Nanofibrous Scaffolds, J Nanomater 2013 (2013). https://doi.org/10.1155/2013/351810.

[37] Z. Zhang, K. Ren, J. Ji, Silane coupling agent in biomedical materials, Biointerphases 18 (2023). https://doi.org/10.1116/6.0002712.

[38] J.G. Matisons, Silanes and Siloxanes as Coupling Agents to Glass: A Perspective, in: 2012: pp. 281–298. https://doi.org/10.1007/978-94-007-3876-8_10.

[39] M.-C. Brochier Salon, M.N. Belgacem, Hydrolysis-Condensation Kinetics of Different Silane Coupling Agents, Phosphorus Sulfur Silicon Relat Elem 186 (2011) 240–254. https://doi.org/10.1080/10426507.2010.494644.

[40] S. Shokoohi, A. Arefazar, R. Khosrokhavar, Silane Coupling Agents in Polymer-based Reinforced Composites: A Review, Journal of Reinforced Plastics and Composites 27 (2008) 473–485. https://doi.org/10.1177/0731684407081391.

[41] Y. Xie, C.A.S. Hill, Z. Xiao, H. Militz, C. Mai, Silane coupling agents used for natural fiber/polymer composites: A review, Compos Part A Appl Sci Manuf 41 (2010) 806–819. https://doi.org/10.1016/j.compositesa.2010.03.005.

[42] Q. Liu, G. Nian, C. Yang, S. Qu, Z. Suo, Bonding dissimilar polymer networks in various manufacturing processes, Nat Commun 9 (2018) 846. https://doi.org/10.1038/s41467-018-03269-x.

[43] A. Farooq, A. Farooq, S. Jabeen, A. Islam, N. Gull, R.U. Khan, H.M. Shifa ul Haq, A. Mehmood, N. Hussain, M. Bilal, Designing Kappa-carrageenan/guar gum/polyvinyl alcohol-based pH-responsive silane-crosslinked hydrogels for controlled release of cephradine, J Drug Deliv Sci Technol 67 (2022) 102969. https://doi.org/10.1016/j.jddst.2021.102969.

[44] H.-Y. Lee, H.-E. Kim, S.-H. Jeong, One-pot synthesis of silane-modified hyaluronic acid hydrogels for effective antibacterial drug delivery via sol–gel stabilization, Colloids Surf B Biointerfaces 174 (2019) 308–315. https://doi.org/10.1016/j.colsurfb.2018.11.034.

[45] M. Li, K. Liu, W. Liu, N. Chen, Y. Wang, F. Zhang, Q. Luo, L. Yang, R. Luo, Y. Wang, A universal anti-thrombotic and antibacterial coating: A chemical approach directed by Fenton reaction and silane coupling, Appl Surf Sci 600 (2022) 154143. https://doi.org/10.1016/j.apsusc.2022.154143.

[46] Y. Sheng, J. Yang, R. Hou, L. Chen, J. Xu, H. Liu, X. Zhao, X. Wang, R. Zeng, W. Li, Y. (Mike) Xie, Improved biocompatibility and degradation behavior of biodegradable Zn-1Mg by grafting zwitterionic phosphorylcholine chitosan (PCCs) coating on silane pre-modified surface, Appl Surf Sci 527 (2020) 146914. https://doi.org/10.1016/j.apsusc.2020.146914.

[47] L. Huang, K. Su, Y.-F. Zheng, K.W.-K. Yeung, X.-M. Liu, Construction of TiO2/silane nanofilm on AZ31 magnesium alloy for controlled degradability and enhanced biocompatibility, Rare Metals 38 (2019) 588–600. https://doi.org/10.1007/s12598-018-1187-7.

[48] N. He, J. Li, W. Li, X. Lin, Q. Fu, X. Peng, W. Jin, Z. Yu, P.K. Chu, Poly(lactic acid) coating with a silane transition layer on MgAl LDH-coated biomedical Mg alloys for enhanced corrosion and cytocompatibility, Colloids Surf A Physicochem Eng Asp 661 (2023) 130947. https://doi.org/10.1016/j.colsurfa.2023.130947.

[49] N. Suppakarn, S. Sanmaung, Y. Ruksakulpiwat, W. Sutapun, Effect of Surface Modification on Properties of Natural Hydroxyapatite/Polypropylene Composites, Key Eng Mater 361–363 (2007) 511–514. https://doi.org/10.4028/www.scientific.net/KEM.361-363.511.

[50] E. Ji, Y.H. Song, J.H. Seo, K. Il Joo, Utilization of functionalized silane coatings for enhanced mechanical properties of hydroxyapatite filler, Korean Journal of Chemical Engineering 40 (2023) 1709–1714. https://doi.org/10.1007/s11814-023-1396-0.

[51] F. Ghorbani, M. Pourhaghgouy, T. Mohammadi-hafshehjani, A. Zamanian, Effect of Silane-Coupling Modification on the Performance of chitosan-poly vinyl Alcohol-Hybrid Scaffolds in Bone Tissue Engineering, Silicon 12 (2020) 3015–3026. https://doi.org/10.1007/s12633-020-00397-2.

[52] L.-J. Fuh, Y.-J. Huang, W.-C. Chen, D.-J. Lin, Preparation of micro-porous bioceramic containing silicon-substituted hydroxyapatite and beta-tricalcium phosphate, Materials Science and Engineering: C 75 (2017) 798–806. https://doi.org/10.1016/j.msec.2017.02.065.

[53] R.O. Darouiche, Treatment of Infections Associated with Surgical Implants, New England Journal of Medicine 350 (2004) 1422–1429. https://doi.org/10.1056/NEJMra035415.

[54] S.M. Kurtz, K.L. Ong, E. Lau, K.J. Bozic, D. Berry, J. Parvizi, Prosthetic Joint Infection Risk after TKA in the Medicare Population, Clin Orthop Relat Res 468 (2010) 52–56. https://doi.org/10.1007/s11999-009-1013-5.

[55] A. Mombelli, F. Décaillet, The characteristics of biofilms in peri-implant disease, J Clin Periodontol 38 (2011) 203–213. https://doi.org/10.1111/j.1600-051X.2010.01666.x.

[56] M. Bohner, J. Lemaître, P. Van Landuyt, P.-Y. Zambelli, H.P. Merkle, B. Gander, Gentamicin-Loaded Hydraulic Calcium Phosphate Bone Cement as Antibiotic Delivery System, J Pharm Sci 86 (1997) 565–572. https://doi.org/10.1021/js960405a.

[57] D. Loca, M. Sokolova, J. Locs, A. Smirnova, Z. Irbe, Calcium phosphate bone cements for local vancomycin delivery, Materials Science and Engineering: C 49 (2015) 106–113. https://doi.org/10.1016/j.msec.2014.12.075.

[58] F.M. Abed, S.B. Kotha, H. AlShukairi, F.N. Almotawah, R.A. Alabdulaly, S.K. Mallineni, Effect of Different Concentrations of Silver Nanoparticles on the Quality of the Chemical Bond of Glass Ionomer Cement Dentine in Primary Teeth, Front Bioeng Biotechnol 10 (2022). https://doi.org/10.3389/fbioe.2022.816652.

[59] J.-H. Ryu, U. Mangal, J. Yoo, J.-H. Youm, J.-Y. Kim, J.-Y. Seo, D. Kim, J.-S. Kwon, S.-H. Choi, Low concentration zinc oxide nanoparticles enrichment enhances bacterial and pro-inflammatory resistance of calcium silicate-based cements, J Mech Behav Biomed Mater 151 (2024) 106399. https://doi.org/10.1016/j.jmbbm.2024.106399.

[60] A. Pillai, J. Chakka, N. Heshmathi, Y. Zhang, F. Alkadi, M. Maniruzzaman, Multifunctional Three-Dimensional Printed Copper Loaded Calcium Phosphate Scaffolds for Bone Regeneration, Pharmaceuticals 16 (2023) 352. https://doi.org/10.3390/ph16030352.

[61] J. Jenima, M. Priya Dharshini, M.L. Ajin, J. Jebeen Moses, K.P. Retnam, K.P. Arunachalam, S. Avudaiappan, R.F. Arrue Munoz, A comprehensive review of titanium dioxide nanoparticles in cementitious composites, Heliyon 10 (2024) e39238. https://doi.org/10.1016/j.heliyon.2024.e39238.

[62] M.J. Hajipour, K.M. Fromm, A. Akbar Ashkarran, D. Jimenez de Aberasturi, I.R. de Larramendi, T. Rojo, V. Serpooshan, W.J. Parak, M. Mahmoudi, Antibacterial properties of nanoparticles, Trends Biotechnol 30 (2012) 499–511. https://doi.org/10.1016/j.tibtech.2012.06.004.

[63] A. Nel, T. Xia, L. Mädler, N. Li, Toxic Potential of Materials at the Nanolevel, Science (1979) 311 (2006) 622–627. https://doi.org/10.1126/science.1114397.

[64] B. Fadeel, A.E. Garcia-Bennett, Better safe than sorry: Understanding the toxicological properties of inorganic nanoparticles manufactured for biomedical applications, Adv Drug Deliv Rev 62 (2010) 362–374. https://doi.org/10.1016/j.addr.2009.11.008.

[65] A.A. Gainanova, G.M. Kuz'micheva, R.P. Terekhova, I.I. Pashkin, A.L. Trigub, N.E. Malysheva, R.D. Svetogorov, A.R. Alimguzina, A. V. Koroleva, New antimicrobial materials with cerium ions in the composition of salts, solutions, and composite systems based on $Ce^{3+}(NO_3)_3 \times 6H_2O$, New Journal of Chemistry 46 (2022) 19271–19282. https://doi.org/10.1039/D2NJ03691F.

[66] R. Kamphof, R.N.O. Lima, J.W. Schoones, J.J. Arts, R.G.H.H. Nelissen, G. Cama, B.G.C.W. Pijls, Antimicrobial activity of ion-substituted calcium phosphates: A systematic review, Heliyon 9 (2023) e16568. https://doi.org/10.1016/j.heliyon.2023.e16568.

[67] M. Claudel, J. V. Schwarte, K.M. Fromm, New Antimicrobial Strategies Based on Metal Complexes, Chemistry (Easton) 2 (2020) 849–899. https://doi.org/10.3390/chemistry2040056.

[68] Q. Shen, Y. Qi, Y. Kong, H. Bao, Y. Wang, A. Dong, H. Wu, Y. Xu, Advances in Copper-Based Biomaterials With Antibacterial and Osteogenic Properties for Bone Tissue Engineering, Front Bioeng Biotechnol 9 (2022). https://doi.org/10.3389/fbioe.2021.795425.

[69] T. Lian, Y. Wang, P. Zheng, Research Progress in Medical Biomaterials for Bone Infections, J Funct Biomater 16 (2025) 189. https://doi.org/10.3390/jfb16050189.

Przedruk artykułów

Publikacja 1 – „*Novel Double Hybrid-Type Bone Cements Based on Calcium Phosphates, Chitosan and Citrus Pectin*

International Journal of
Molecular Sciences

MDPI

Article

Novel Double Hybrid-Type Bone Cements Based on Calcium Phosphates, Chitosan and Citrus Pectin

Piotr Pańtak [1,*], Joanna P. Czechowska [1,*], Ewelina Cichoń [2] and Aneta Zima [1]

[1] Faculty of Materials Science and Ceramics, AGH University of Science and Technology, Mickiewicza Av. 30, 30-058 Krakow, Poland
[2] Jerzy Haber Institute of Catalysis and Surface Chemistry, Polish Academy of Sciences, Niezapominajek 8, 30-239 Krakow, Poland; ewelina.cichon@ikifp.edu.pl
* Correspondence: pantak@agh.edu.pl (P.P.); jczech@agh.edu.pl (J.P.C.)

Abstract: In this work, the influence of the liquid phase composition on the physicochemical properties of double hybrid-type bone substitutes was investigated. The solid phase of obtained biomicroconcretes was composed of highly reactive α-tricalcium phosphate powder (α-TCP) and hybrid hydroxyapatite/chitosan granules (HA/CTS). Various combinations of disodium phosphate (Na_2HPO_4) solution and citrus pectin gel were used as liquid phases. The novelty of this study is the development of double-hybrid materials with a dual setting system. The double hybrid phenomenon is due to the interactions between polycationic polymer (chitosan in hybrid granules) and polyanionic polymer (citrus pectin). The chemical and phase composition (FTIR, XRD), setting times (Gillmore needles), injectability, mechanical strength, microstructure (SEM) and chemical stability in vitro were studied. The setting times of obtained materials ranged from 4.5 to 30.5 min for initial and from 7.5 to 55.5 min for final setting times. The compressive strength varied from 5.75 to 13.24 MPa. By incorporating citrus pectin into the liquid phase of the materials, not only did it enhance their physicochemical properties, but it also resulted in the development of fully injectable materials featuring a dual setting system. It has been shown that the properties of materials can be controlled by using the appropriate ratio of citrus pectin in the liquid phase.

Keywords: bone cements; hybrid materials; calcium phosphate; chitosan; dual setting; injectability; polysaccharides

Citation: Pańtak, P.; Czechowska, J.P.; Cichoń, E.; Zima, A. Novel Double Hybrid-Type Bone Cements Based on Calcium Phosphates, Chitosan and Citrus Pectin. *Int. J. Mol. Sci.* **2023**, *24*, 13455. https://doi.org/10.3390/ijms241713455

Academic Editors: Mike Barbeck, Ole Jung and Reinhard Schnettler

Received: 6 July 2023
Revised: 1 August 2023
Accepted: 9 August 2023
Published: 30 August 2023

1. Introduction

Calcium phosphate cements (CPCs) are self-setting ceramic materials commonly used in orthopedic applications. The setting process of α-tricalcium phosphate (α-TCP) containing CPCs is based on its hydrolysis to non-stoichiometric hydroxyapatite in ambient or elevated temperature [1]. CPCs are well known to be biocompatible due to their chemical similarity to the inorganic part of bone [2,3]. Lately, a new group of chemically bonded materials, namely biomicroconcretes, composed of aggregates, e.g., in the form of granules, microspheres or pellets that are embedded in the CPC matrix, has been studied. For example, Russo et al. [4] showed the beneficial influence of carbon nanostructures on the mechanical performance of polymeric composites. The aggregates, similar to those in classic concrete, are supposed to cause microcrack retention. Additionally, granules can enrich material with agents exhibiting antibacterial or bactericidal properties, such as polymers (i.e., chitosan, methylcellulose), ions (i.e., Ag^+, Cu^{2+}) or nanoparticles (such as AgNPs and AuNPs) [5–7]. It is also possible to include active agents in hybrid materials to overcome issues related to bacterial resistance to antibiotics, as showed previously in the study of De Santis et al. [8].

Despite the excellent bioactivity of calcium phosphate-based chemically bonded biomaterials, their injectability is often poor, which hinders their application in minimally

invasive surgery. Moreover, their mechanical properties are not sufficient for load-bearing applications. The improvement in surgical handiness of bone cements can be achieved by introducing polymeric additives, which plasticize the paste and facilitate its application [9,10]. The use of polymers in combination with inorganic calcium phosphates can additionally lead to the formation of organics-in-inorganics hybrids [11]. According to the International Union of Pure and Applied Chemistry (IUPAC) definition, hybrid material is *material composed of an intimate mixture of inorganic components, organic components, or both types of components* [12]. It is believed that in hybrids, the combination of components occurs at the molecular level. For this reason, two classes of hybrids are distinguished. Class I components act together with weak bonds (van der Waals, electrostatic, and hydrogen bonds), while class II components are bonded by strong (covalent or ionic-covalent) chemical bonds [12]. The formation of hybrids in a material's structure can change the properties of the final product, for example by enhancing the mechanical properties of bone cements [13]. A new trend in reinforcing CPCs takes advantage of the interactions between oppositely charged polyelectrolytes such as chitosan and pectin [14]. Chitosan is a linear polycationic polysaccharide obtained by chemical processing of shellfish industry waste [15]. It possesses excellent bioactivity as well as antimicrobial proprieties, so it is commonly used as a compound for wound dressings, membranes or drug carrier systems [16], while citrus pectin is an anionic polysaccharide derived from citrus pectin peel from food industry waste [17]. From a medical point of view, pectin has important features, including its gelling capacity, biocompatibility, and anti-inflammatory and anticancer properties [18]. In the biomaterials industry, pectin can be used in different forms—coatings, films, hydrogels, conjugates, sprays and many more; however, its application in calcium phosphate cements is still under evaluation [19].

The electrostatic interactions occurring between polycation (chitosan) and polyanion (pectin) lead to the formation of class I hybrids. Due to the different nature of the charges, the selection of these natural polymers results in the formation of a rigid gel [20,21]. This phenomenon has been previously applied to obtain membranes, tissue scaffolds and drug delivery systems. De Almeida et al. [22] studied pectin/gold nanoparticles/chitosan superabsorbent hydrogels with a satisfactory elastic modulus for drug delivery purposes. Martins et al. [23] developed water-stable and mechanically resistant membranes based on pectin and chitosan polyelectrolyte complexes, without covalent crosslinking. However, to the best of our knowledge, the simultaneous application of chitosan and pectin in CPCs has not yet been examined [24]. Due to the structure and properties of natural polymers such as chitosan or pectin, they are susceptible to chemical and physical modifications. Such modifications are carried out to change the properties of the initial polymers by, for example, developing their surfaces or functionalizing the functional groups of their individual monomers [25–27].

The aim of this study was to develop, obtain and study new hybrid injectable biomicroconcretes and to determine the effect of citrus pectin introduced in the liquid phase on the physicochemical, applicational and biological properties of those materials. Biomicroconcretes composed of highly reactive α-TCP powder as setting phase, hybrid hydroxyapatite/chitosan (HA/CTS) granules as aggregates, and different liquid phases containing citrus pectin were obtained and investigated. This choice of material composition would allow developing double-hybrid bone substitutes (hybrid in granules, as well as hybrid originated from polyelectrolyte interactions) with a dual-setting mechanism. According to our knowledge, these are the first studies regarding the double-hybrid system in cementitious materials. Other authors have used different dual-setting mechanisms in bone cements. Geffers et al. [28] developed dual-setting brushite-silica gel cements characterized by improved mechanical properties, while Christel et al. [29] studied calcium phosphate-polymethacrylate cements, which were characterized by significantly shortened setting times and improved mechanical strength. However, through careful selection of the liquid phase, it will be possible to obtain fully injectable materials containing hybrid granules for the first time. What is more, due to the use of natural polymers as a modifier of CPCs,

this research will pave the way to further modification of similar materials through their functionalization. In addition, appropriate selection of the liquid phase will allow one to obtain materials characterized by setting times characteristic of calcium phosphate-based bone cements.

2. Results and Discussion

2.1. Setting Times

In clinical practice, cementitious bone substitutes should be characterized by setting times that allow their application by the surgeon to the targeted defect site. This parameter determines how long it takes for the material to set after the liquid and powder phases have been mixed. Optimally, the application should take place during "dough" time, i.e., between the initial and final setting times [30]. Ideally, the initial setting time (t_i) should be approximately 15 min, whereas the final setting time (t_f) should be under 30 min [31,32]. However, in the literature, ranges between 4–8 min for t_i, and up to 15 min for t_f also can be found [33].

It is very important that, in the case of materials with complex compositions, the setting time is not adversely affected by the additives. Thus, the choice of components is crucial when designing cementitious biomaterials, especially injectable ones. In our studies, despite the complex compositions of the biomicroconcretes, their setting times were within an acceptable range (Table 1). However, both the initial and final setting times of the cement pastes were strongly dependent on their liquid phase composition.

Table 1. Setting time of the biomicroconcretes.

Material	Initial Setting Time (t_i) [min]	Final Setting Time (t_f) [min]
MC1	4.5 ± 1.0	7.5 ± 0.5
MC2	9.0 ± 0.5	16.5 ± 1.0
MC3	11.5 ± 0.5	21.0 ± 1.0
MC4	17.5 ± 1.0	32.0 ± 1.5
MC5	30.5 ± 0.5	55.5 ± 1.0

Setting times of MC1, where the liquid phase constituted solely of 2.0 wt% Na_2HPO_4 solution, were the shortest and equal to 4.5 min (t_i) and 7.5 min (t_f). In this case, the setting process of biomicroconcrete was based only on the hydrolysis of α-tricalcium phosphate to calcium-deficient hydroxyapatite (CDHA), according to the following chemical equation (Equation (1)) [34,35].

$$3Ca_3(PO_4)_2 + H_2O \rightarrow Ca_9(PO_4)5(HPO)_4OH \quad (1)$$

It is known that the rate of α-TCP hydrolysis to CDHA depends on many external and internal factors, including: physical conditions during paste formation (e.g., temperature, humidity), the presence of a setting accelerator (e.g., Na_2HPO_4) or inhibitor, as well as the kinds and amounts of polymeric additives. Usually, the addition of polymer to CPCs causes an increase in setting times but, depending on the polymer type, various processes can be responsible for this phenomenon [36]. In the case of materials containing citrus pectin (MC2–MC5), α-TCP hydrolysis is also a second setting reaction, which is directly connected with pectin cross-linking by Ca^{2+} ions that occur [14]. The double-setting mechanism resulted in longer setting times, because the process of α-TCP hydrolysis was disrupted by calcium-mediated cross-linking of the citrus pectin. It was observed that the materials' setting times increased proportionally to the amount of citrus pectin gel in the liquid phase and were in the range of 9.0–17.5 min (t_i) and 16.5–32.0 min (t_f). Similar results were observed elsewhere [37] for low esterified pectin from citrus peels and apple pomace added to the solid phase of cementitious materials. The setting times of biomicroconcretes in which the liquid phase consisted solely of citrus pectin gel (MC5) were the longest—30.5 min for the initial and 55.5 min for the final setting time, respectively. This was probably connected

with the water uptake by citrus pectin, which inhibited the hydrolysis process of tricalcium phosphate, whereas the amount of crosslinked pectin was too small to allow the material to set and maintain its integrity during the measurements. As a result, the material MC5 was excluded from further studies due to exceeding the setting times recommended by clinical practice. The polymeric additives in calcium phosphate-based bone cements acted also as plasticizers. By altering the rheological properties of the paste, pectin favors its injectability.

2.2. Injectability

The injectability, in addition to the setting times, is a key property for cementitious-type bone substitutes, especially for non-invasive surgical applications [38]. Currently, a standard for the injectability of calcium phosphate bone cements is not available. However, based on the literature, the maximum force on the syringe plunger during paste extrusion is determined as 100 N [39]. This force determines the value that the surgeon applies to the syringe plunger with one hand during the surgical procedure. The results of injectability tests and the appearance of the cement pastes after injection directly into SBF are shown in Figure 1.

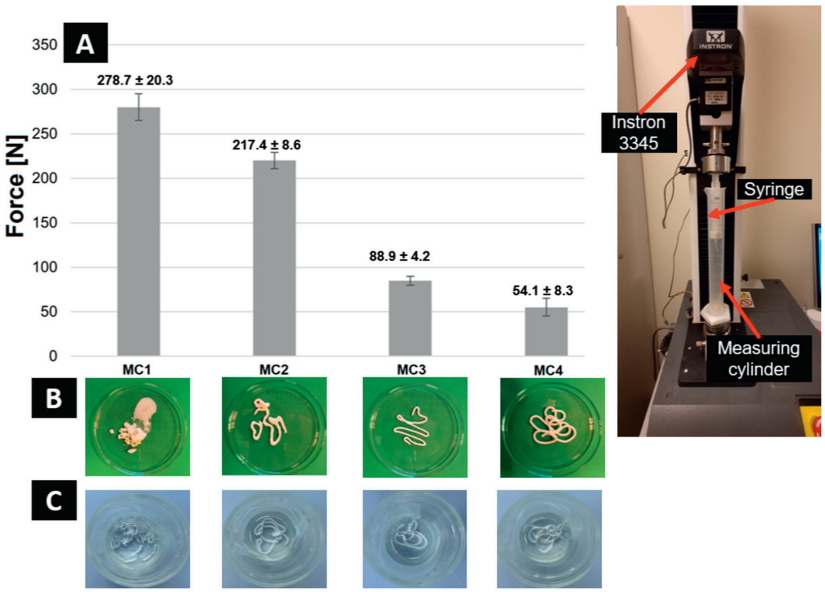

Figure 1. Force required for paste extrusion (**A**), pastes immediately after injection into SBF (**B**), and after 7 days of incubation in SBF (**C**).

The use of citrus pectin allowed for sufficient plasticization of the paste, improving its viscosity. In opposition to CPCs, which are usually non-injectable [40], the obtained biomicroconcretes containing citrus pectin (MC2–MC4) were fully injectable and maintained their cohesion after being extruded into SBF. Phase separation was observed only in the case of MC1, which did not contain added citrus pectin in the liquid phase. The other pastes did not show phase separation during injectability tests. It was also noticed that the force required to inject biomicroconcretes decreased with the increasing amount of citrus pectin. For materials MC3 and MC4, the force was lower than the recommended 100 N [39]. Similar results were obtained by Arkin et al. [41], where a polymer in the form of carboxymethyl cellulose was used as the injectability provider. The presence of citrus pectin in the liquid phase resulted in excellent cohesion of the MC2–MC4 materials, which allowed them to retain their shape in contact with SBF. The double-setting mechanism

including simultaneous hydrolysis of α-TCP to CDHA and calcium-mediated crosslinking of citrus pectin also contributed to the paste cohesion [42,43]. The effect on the injectability of calcium phosphate-based cement pastes is an outcome of their rheological properties. Self-setting materials change their rheological properties over time. Bone cements based on calcium phosphates and biopolymers show a pseudo-thixotropic character [44].

2.3. Phase Composition and Structural Studies

Calcium phosphate ceramics are used in biomaterial engineering due to their similarity in phase composition to that of inorganic bone. Through phase and structural testing, that relationship can be confirmed. The initial α-TCP powder was composed of α-TCP phase (97.0 ± 1.0 wt%) and a small amount of hydroxyapatite (3.0 ± 1.0 wt%), whereas the HA/CTS hybrid granules were composed of HA as the only crystalline phase. In biomicroconcretes, XRD analysis revealed the presence of two crystalline phases: α-TCP and hydroxyapatite, and their proportion varied according to the setting environment (air/SBF) (Figure 2A). Moreover, the amorphous halos originating from polymers were present.

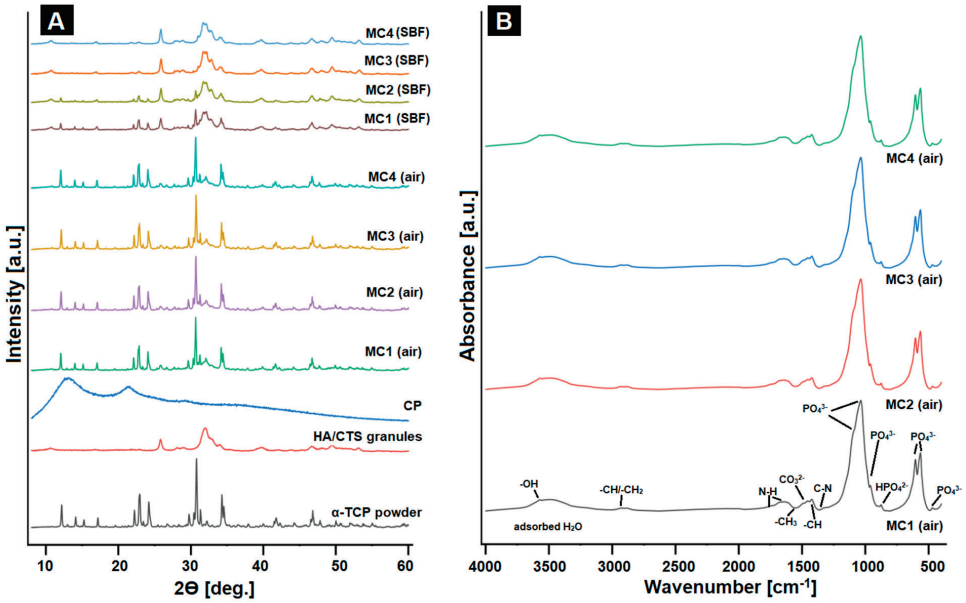

Figure 2. XRD patterns of studied materials (**A**) and FTIR spectra (**B**) of obtained biomaterials after 7 days of setting and hardening in air or in SBF.

The detailed phase compositions of the obtained materials are presented in Table 2.

Table 2. Phase compositions of the obtained materials after 7 days of setting and hardening in air or SBF.

Material	7 Days in Air		7 Days in SBF	
	α-TCP, wt%	Hydroxyapatite, wt%	α-TCP, wt%	Hydroxyapatite, wt%
MC1	54 ± 1	46 ± 1	2 ± 1	98 ± 1
MC2	56 ± 1	44 ± 1	2 ± 1	98 ± 1
MC3	59 ± 1	41 ± 1	3 ± 1	97 ± 1
MC4	61 ± 1	39 ± 1	3 ± 1	97 ± 1

The materials containing citrus pectin in the liquid phase were characterized by slightly slower hydrolysis of α-TCP to hydroxyapatite. The amount of α-TCP phase in the materials after 7 days in air was in the range from 54 ± 1 to 61 ± 1 wt%, while the proportion of the hydroxyapatite phase was in the range from 39 ± 1 to 46 ± 1 wt.

Slower hydrolysis of α-TCP may be explained by water absorption by CP [45,46]. The analysis of the samples' phase compositions after 7 days of incubation in SBF confirmed that α-TCP, as a thermodynamically metastable phase, spontaneously hydrolyzed to calcium-deficient hydroxyapatite. Similar observations were previously reported for α-TCP based bone cements [21,33].

The materials' FTIR spectra (Figure 2B) after setting and hardening showed characteristics bands at ~598, ~559 cm^{-1} (bending), ~965, and ~1020 cm^{-1} (stretching), which corresponded to the vibrations of PO_4^{3-} groups. The wide band in the range of ~3000–3800 cm^{-1} was assigned to the absorbed water. Moreover, the spectra possessed an absorption band at ~870 cm^{-1} that corresponded to HPO_4^{2-} groups, confirming the presence of non-stoichiometric hydroxyapatite. Additionally, in a similar spectral range (~873–875 cm^{-1}), carbonate bonds may have appeared in the material, whereas the existence of a band at 1424 cm^{-1} indicated partial substitution of CO_3^{2-} in the hydroxyapatite structure. Similar results were obtained for calcium phosphate-based biomaterials by Gao et al. [47] and Cichoń et al. [48]. FTIR studies confirmed the presence of chitosan and pectin in the biomaterials. The absorption band with a maximum at ~2930 cm^{-1} can be attributed to alkyl C-H (stretching) vibrations. The band at around 1649 cm^{-1} was assigned to N-H bending vibrations of the primary amine and confirmed the presence of chitosan and amidated citrus pectin in the materials. What is more, the bands around 1315 cm^{-1} and 3573 cm^{-1} corresponded to C-N and O-H stretching vibrations, respectively. For the pectin- and chitosan-containing systems, the formation of electrostatic and/or hydrogen bonding is possible. In the biomicroconcretes, the creation of polyelectrolyte complexes at the hybrid granule/pectin interface took place. Polyelectrolyte complexes between these molecules were previously studied inter alia by Rashidova et al. [49] as well as Dziadek et al. [14]. The presence of electrostatic interactions between components of developed biomicroconcretes allows the creation of a double hybrid system, thus influencing other physicochemical properties of the biomaterials. FT-IR spectroscopy, as a complementary research method, confirmed the XRD results and demonstrated the presence of both polymers, which could not be easily confirmed using diffractometry alone. Moreover, the similarity of the obtained materials to the inorganic part of human bone was also acknowledged.

2.4. Microstructure

By observing the microstructure of the developed materials, we were able to assess their suitability for potential use as a bone tissue substitute. In addition, observations enabled us also to identify the presence of microstructural defects. Scanning microscopy (SEM) observations of the obtained biomaterials were performed both after 7 days of setting and hardening in air (Figure 3), as well as after 7 days of sample incubation in SBF.

The biomicroconcretes possessed a compact and homogeneous microstructure formed by an α-TCP matrix and hybrid hydroxyapatite-chitosan granules. Materials MC2–MC4 where citrus pectin was added were characterized by more intimate contact between hybrid HA/CTS granules and the cementitious matrix, as the formed polymeric bridges linked the mentioned components. The highest number of bridges was observed in the material MC4, with a maximal amount of CP in the liquid phase. Analogous bridges were previously observed by Czechowska et al. [21] where chitosan was introduced in the liquid phase of calcium phosphate bone cement. The presence of polymeric bridges was related not only to the hybrid HA/CTS granules, but also to the electrostatic interactions between the polycationic chitosan contained in the granules and the polyanionic citrus pectin. The confirmation of interaction between the oppositely charged polymers could also be confirmed by the increased presence of polymer bridges in the material. In addition, the presence of such bridges could affect the mechanical strength of the materials. Polymer

bridges can potentially reinforce the material in a manner similar to the fibers commonly used in composites.

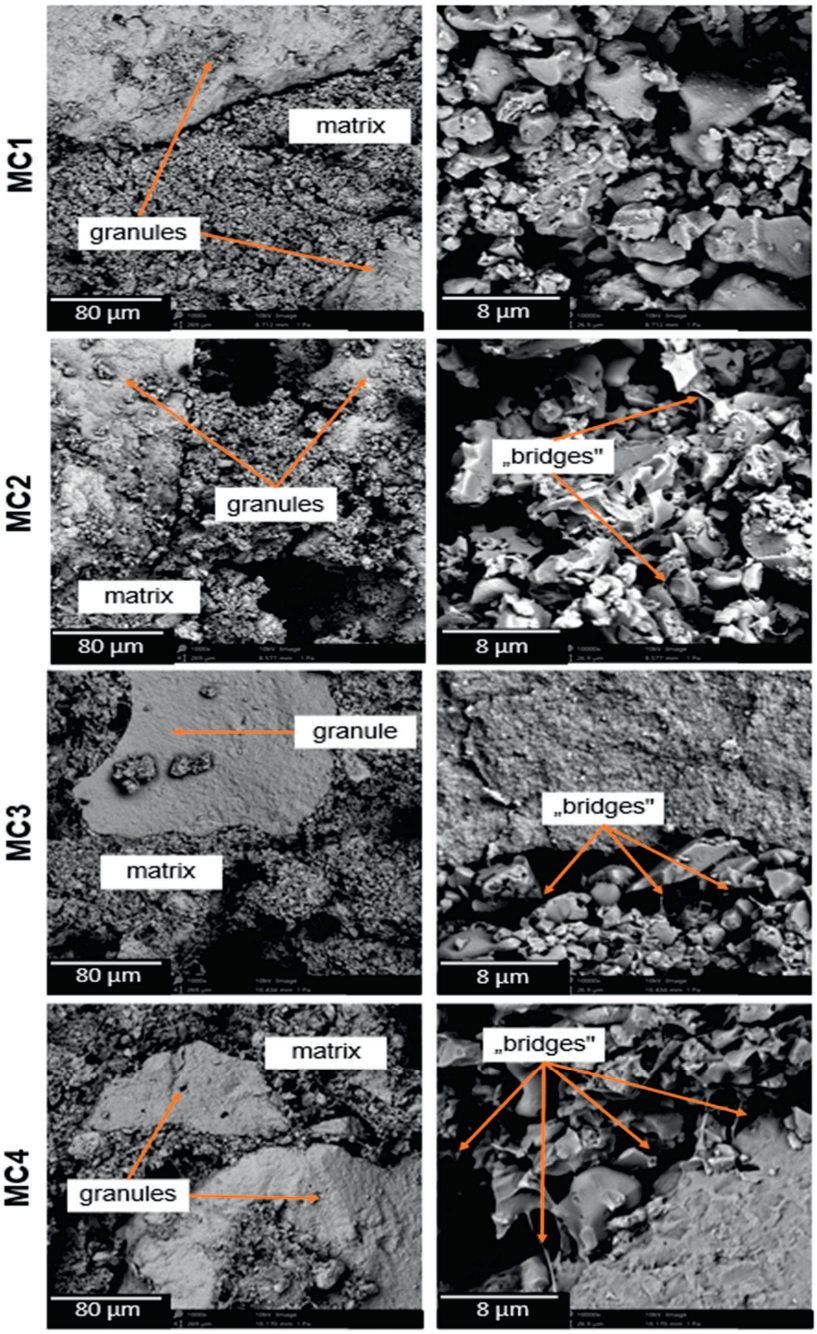

Figure 3. SEM images of the materials' cross-sections after 7 day in air.

2.5. Compressive Strength

Mechanical strength is an important parameter when assessing materials. From the clinical point of view, the mechanical strength of these substitutes must be within the range of the tissue they would be replacing. In the case of ceramic materials such as CPCs, compressive strength is the most commonly measured parameter to determine their mechanical properties [50]. The results of compressive strength measurements of the obtained materials carried out after 7 days of setting and hardening are shown in Figure 4.

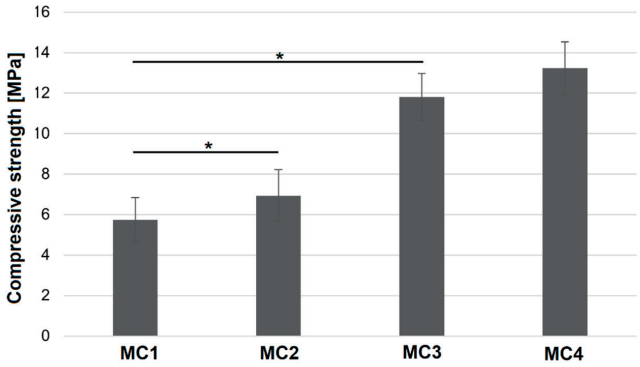

Figure 4. Compressive strength of biomicroconcretes after 7 days of drying in air (* statistically significant difference, $p < 0.05$).

It was found that the compressive strength of MC1 samples, where the liquid phase was based only on 2 wt% Na_2HPO_4 solution, was the lowest (5.75 ± 1.08 MPa). The presence of citrus pectin in the liquid phase of biomicroconcretes significantly improves the mechanical properties of the final materials up to 13.24 ± 1.28 MPa (MC4). Furthermore, the increase in mechanical strength with the increasing amount of pectin was noticed. A similar correlation was observed previously elsewhere [37]. The polymer may provide mechanical improvement in two different ways: firstly, via ensuring better homogenization of cementitious pastes through the presence of citrus pectin (confirmed in SEM studies), and secondly, due to the formation of a double hybrid structure originating from (1) electrostatic interaction between polycationic chitosan and polyanionic pectin as well as (2) the hybrid nature of hydroxyapatite-chitosan granules. The existence of a double hybrid system resulted in better adhesion of the cement phase to the surface of the granules and thus the intimate contact of the components. The mechanical strength of developed materials allows their implantation in non-load or low-load bearing places (compressive strength of cancellous bone is approximately 4–12 MPa) [51]. Summarizing, the improved mechanical properties of the obtained multicomponent scaffolds could be attributed to the higher crosslinking degree promoted by multifaceted interactions between components.

2.6. Chemical Stability and Bioactivity In Vitro

The chemical stability of implantable biomaterials determines their potential clinical applications in the future. To evaluate the chemical stability and bioactivity in vitro, the biomicroconcretes were incubated in SBF at a temperature of 37 °C. The pH changes of SBF during the sample's immersion are demonstrated in Figure 5. Despite the presence of polymeric additive, i.e., citrus pectin, as well as the hybrid HA/CTS granules, the pH values during the sample incubation ranged from 7.34 to 7.43 and remained close to the physiological pH [52].

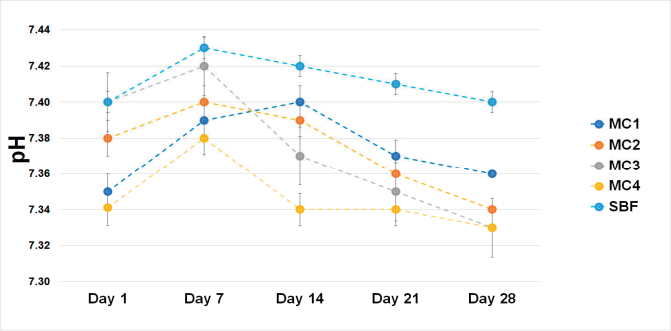

Figure 5. pH vs. sample incubation time in SBF.

After 7 days of incubation in SBF at 37 °C, all biomicroconcretes were fully covered by plate-like apatitic structures (Figure 6). The presence of apatitic forms confirmed the in vitro bioactivity of the developed materials according to the Kokubo and Takadama method [53]. The microstructure observations after the samples' incubation revealed that the developed materials had bioactive potential. It can be stated that the application of polymeric additives, such as chitosan in the hybrid granules and pectin in the liquid phase, allowed obtaining materials with favorable physicochemical properties with bioactive potential.

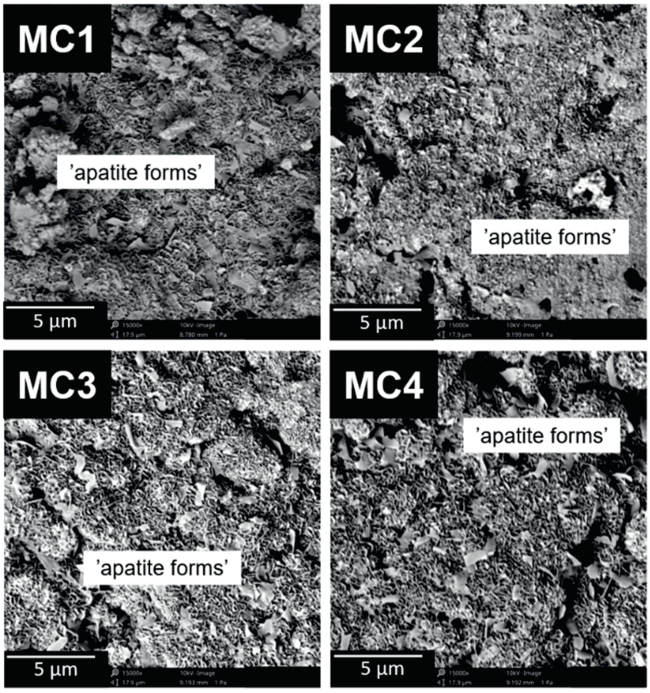

Figure 6. SEM microstructure of material surfaces after 7 days of incubation in SBF.

The ionic conductivity of material MC1 was in the range of ~62–74 µS/cm. It was observed that the ionic conductivity of water around the incubated MC2–MC4 samples increased from ~65–81 µS/cm on the first day of incubation to ~80–91 µS/cm on day 28 (Figure 7).

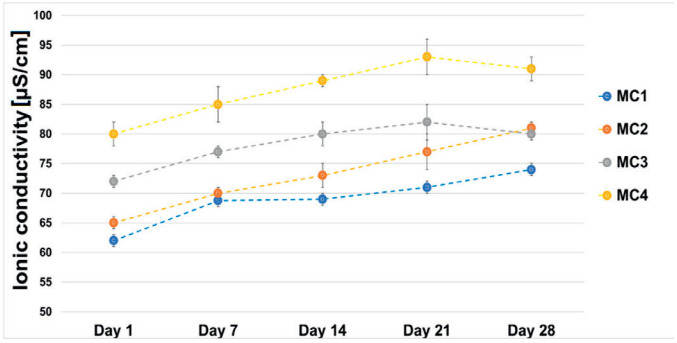

Figure 7. Ionic conductivity vs. sample incubation time in distilled water.

The higher ionic conductivity of biomicroconcretes MC2, MC3, and MC4 compared to MC1 may have been related to the degradation of the citrus pectin. Pectin in aqueous solutions degrades to non-toxic products (i.e., d-galacturonic acid, l-arabinose, d-apiose, d-galactose, l-fructose) that do not have negative effects on cells when the material is implanted into the body [54,55]. Despite slight differences in the ionic conductivity of the distilled water surrounding them, the incubated samples of the biomicroconcretes all remained stable throughout the incubation time. Similar results regarding changes in the ionic conductivity of pectin-containing materials were previously reported elsewhere [56].

3. Materials and Methods

3.1. Materials

As a solid phase of the studied materials, α-tricalcium phosphate (α-TCP) and hybrid hydroxyapatite/chitosan (HA/CTS) granules were used. The highly reactive α-TCP powder was obtained via a wet chemical method described previously [21,57]. As the reagents, $Ca(OH)_2$ (≥99.5%, POCH, Gliwice, Poland) and H_3PO_4 (85.0%, POCH, Gliwice, Poland) were applied. HA/CTS hybrid materials in the form of granules (300–400 µm) were prepared by the modified wet chemical method described by Zima [58]. Briefly, phosphoric acid was introduced directly to the chitosan solutions in acetic acid, and the obtained mixtures were added dropwise to the $Ca(OH)_2$ suspension. The suspension was aged for 24 h and then decanted. The precipitate was washed with distilled water, centrifuged, and frozen for 48 h. After defrosting, the obtained filter cakes were sieved and dried to obtain hybrid granules. The following substrates were used: $Ca(OH)_2$ (≥99.5 wt%, POCH, Gliwice, Poland), H_3PO_4 (85.0 wt%, POCH, Gliwice, Poland), and medium-molecular-weight chitosan (~100,000 kDa, DD ≥ 75.0 wt%, Sigma-Aldrich, St. Louis, MO, USA). As the liquid phases, various mixtures of 2 wt% disodium phosphate (99.9 wt%, Chempur, Piekary Śląskie, Poland) and 5 wt% low esterified amidated citrus pectin gels (Herbstreith & Fox, Werder/Havel, Germany) were applied. In order to optimize the setting time of the developed materials, Na_2HPO_4 was used in the liquid phase as an accelerator of the hydrolysis process, as recommended in other studies [59].

3.2. Preparation of Biomicroconcretes

In this study, five types of biomicroconcretes containing α-TCP powder and hybrid HA/CTS granules as a solid phase and different liquid phases were obtained (Table 3). Samples were prepared by mixing powder phase with the appropriate liquid phase. The liquid-to-powder (L/P) ratio was selected based on preliminary studies, and it was 0.5 g/g. Material MC1 containing solely 2 wt% disodium phosphate solution as a liquid phase was used as a control material. Subsequent materials in addition to disodium phosphate solution contained also a citrus pectin gel.

Table 3. The initial composition of developed materials.

Material	Solid Phase (P)	Liquid Phase (L)
MC1 (Control)	α-TCP: HA/CTS granules 3:2	2.0 wt% Na_2HPO_4 solution
MC2		1.5 wt% Na_2HPO_4 solution in 1.25 wt% citrus pectin gel
MC3		1.0 wt% Na_2HPO_4 solution in 2.5 wt% citrus pectin gel
MC4		0.5 wt% Na_2HPO_4 solution in 3.75 wt% citrus pectin gel
MC5		5.0 wt% citrus pectin gel

3.3. Methods

3.3.1. Setting Times

The setting times of the obtained materials were measured. The initial (t_i) and final (t_f) setting times of the obtained biomaterials were determined using a Gillmore apparatus (Humboldt, Norridge, IL, USA) according to the ASTM-C200-08 standard [60]. All experiments were carried out at 22.0 ± 1.0 °C. Test samples were prepared in 10 mm × 7 mm × 3 mm cuboid form. All measurements were performed in triplicate. The results are presented as the mean ± standard deviation (SD).

3.3.2. Injectability

The injectability of the obtained materials was assessed by injecting cement paste through the 2 mm nozzle of a 20 mL plastic syringe (B. Brown, Melsungen, Germany) directly into the cylinder with simulated body fluid (SBF) solution, preheated to 37 °C. The force applied to the syringe plunger during the injection was determined by a universal testing machine (Instron 3345, Instron, Norwood, MA, USA). The crosshead displacement rate was equal to 1.0 mm min^{-1}. Measurements were performed in triplicate for each material. The value for the injectability of the material was considered to be the constant value of the pressure force during the extrusion of homogenous paste. The results are presented as the mean ± standard deviation (SD). Figure 8 shows the testing equipment for the injectability tests.

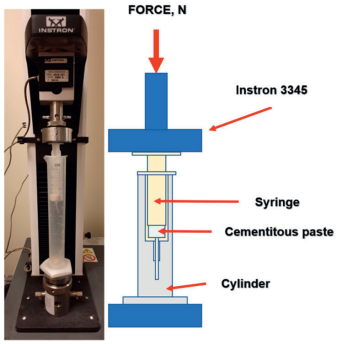

Figure 8. Injectability testing equipment.

3.3.3. Phase Composition

The crystalline phases of obtained biomicroconcretes were analyzed using X-ray diffraction (XRD) with Cu Kα radiation (1.54 Å) at 30 kV and 10 mA (D2 Phaser, Bruker, Billerica, MA, USA) within the 2θ range from 10 to 60° at 0.04 intervals (scanning speed of 2.5°/min). The analyses were performed after 7 days of setting and hardening in air, as

well as after 7 days of incubation in simulated body fluid (SBF). The crystalline phases were identified by comparing the experimental diffractograms to the patterns from International Centre for Diffraction Data α-TCP (00-009-0348) and hydroxyapatite (HA; 01-076-0694). A phase quantification based on Rietveld refinement was performed using TOPAS software (Version 4.2.0.1, 2011, Bruker, Billerica, MA, USA). All measurements were performed in triplicate. The results are presented as the mean ± standard deviation (SD).

3.3.4. Structural Analysis

Structural studies of the obtained biomaterials were performed using Fourier transform infrared (FTIR) spectroscopy, within the scanning range of 400–4000 cm^{-1} and resolution of 4 cm^{-1} using a BioRad FTS 6000 spectrometer (Vertex 70&70v, Bruker, Billerica, MA, USA). Positions of the FTIR bands were measured in accordance with the center of weight. The baseline correction, normalization, and spectral analyses were performed using Spectragryph software (v1.2.15, Friedrich Menges, Oberstdorf, Germany). The measurements were carried out after 7 days of setting and hardening in air, as well as after 7 days of incubation in simulated body fluid (SBF).

3.3.5. Compressive Strength

For the mechanical tests, cylindrical samples 12 mm in height and 6 mm in diameter were prepared in Teflon molds. Samples were removed from the molds between their initial and final setting times and left for 7 days in air. After 7 days, the compressive strength of the samples was examined using a universal testing machine (Instron 3345, Instron, Norwood, MA, USA). Biomicroconcrete samples were subjected to uniaxial compression with a crosshead speed of 1.0 mm min^{-1}. The results of the compressive strength tests are presented as the mean value of 15 measurements ± standard deviation (SD).

3.3.6. Microstructure

Observations of the microstructure of the obtained biomaterials were performed using a scanning electron microscope (SEM, PhenomPure, Thermo Fisher Scientific, Waltham, MA, USA) in backscattered electron (BSE) mode at an acceleration voltage of 10 kV. Before the study, samples were coated with a thin gold layer to avoid overcharging (Manual Sputter Coater 108, Agar Scientific, Stansted, UK).

3.3.7. Chemical Stability and Bioactivity In Vitro

To determine the in vitro chemical stability of cementitious materials, cylindrical samples (3 mm in height and 6 mm in diameter) were placed in plastic containers with 20 mL of SBF or distilled water and stored at 37 °C for 4 weeks. The ionic conductivity and pH of the solutions around the incubated samples were measured using a SevenCompact Duo pH/conductometer (Mettler Toledo, Columbus, OH, USA). In vitro bioactivity of the obtained biomicroconcretes was assessed via SEM observations of the apatite layers on the materials' surfaces after the 7 day sample incubation in SBF.

3.3.8. Statistics

The statistical analysis of obtained results was performed using a one-way analysis of variance (ANOVA) with a post hoc Tukey honestly significant difference (HSD) test for comparing multiple treatments (*—statistically significant difference between the results, $p > 0.05$). All analyses were performed with OriginPro software (version 2021, OriginLab Corporation, Northampton, MA, USA).

4. Conclusions

In this study, materials based on highly reactive α-TCP powder and hybrid hydroxyapatite-chitosan granules with the addition of citrus pectin were developed and examined. The use of citrus pectin introduced with the liquid phase allowed us to to obtain easily moldable, fully injectable calcium phosphate-based biomicroconcretes characterized by good cohesion

and setting times in an acceptable range. Usually, biomicroconcretes containing granules or microspheres are not injectable. Through the careful selection of the liquid phase, we were able to obtain a paste with favorable rheological properties that did not clog the syringe during the injection. The presence of citrus pectin in the liquid phase significantly improved both the injectability and mechanical strength of the materials (from 5.75 MPa to 13.23 MPa). The unique properties of biomicroconcretes containing citrus pectin resulted from both the the dual setting system and the presence of the double hybrid system. The dual setting system originated from α-TCP hydrolysis and citrus pectin crosslinking in the presence of Ca^{2+} ions allowed us to obtain materials characterized by excellent cohesion and chemical stability, whereas the double hybrid system was due to the presence of hybrid granules and interactions between polycationic chitosan in hybrid granules and polyanionic citrus pectin. All developed biomicroconcretes revealed in vitro bioactivity, which makes them good candidates for further biological studies. The MC3 biomicroconcrete is considered to be the most promising among the studied materials. By applying easy-to-functionalize polymers such as chitosan and citrus pectin, further modifications of the proposed materials, for example, attaching other substances to the functionalized polymer groups, will be possible. This research confirmed the beneficial properties of the obtained biomicroconcretes and paves the way for further in vitro and in vivo studies.

Author Contributions: Conceptualization, P.P., J.P.C., E.C. and A.Z.; Methodology, J.P.C., E.C. and A.Z.; Validation, J.P.C., E.C. and A.Z.; Investigation, P.P. and E.C.; Writing—original draft, P.P. and E.C.; Writing—review & editing, J.P.C. and A.Z.; Visualization, P.P.; Supervision, J.P.C. and A.Z.; Project administration, A.Z.; Funding acquisition, A.Z. All authors have read and agreed to the published version of the manuscript.

Funding: Research project supported by the program "Excellence initiative–research university" for the AGH University of Science and Technology, Project Nu. 18.18.160.4159. Research co-funded by the Faculty of Materials Science and Ceramics AGH UST—University of Science and Technology, Kraków, Poland, Project No. 16.16.160.557 (2023).

Institutional Review Board Statement: Not applicable.

Informed Consent Statement: Not applicable.

Data Availability Statement: Not applicable.

Acknowledgments: The authors thank the company Herbstreith & Fox for delivering citrus pectin.

Conflicts of Interest: The authors declare no conflict of interest.

References

1. Kashimbetova, A.; Slámečka, K.; Casas-Luna, M.; Oliver-Urrutia, C.; Ravaszová, S.; Dvořák, K.; Čelko, L.; Montufar, E.B. Implications of unconventional setting conditions on the mechanical strength of synthetic bone grafts produced with self-hardening calcium phosphate pastes. *Ceram. Int.* **2022**, *48*, 6225–6235. [CrossRef]
2. Ambard, A.J.; Mueninghoff, L. Calcium Phosphate Cement: Review of Mechanical and Biological Properties. *J. Prosthodont.* **2006**, *15*, 321–328. [CrossRef] [PubMed]
3. Tronco, M.C.; Cassel, J.B.; Santos, L.A.D. α-TCP-based calcium phosphate cements: A critical review. *Acta Biomater.* **2022**, *151*, 70–87. [CrossRef] [PubMed]
4. Russo, P.; Vitiello, L.; Sbardella, F.; Santos, J.I.; Tirillò, J.; Bracciale, M.P.; Rivilla, I.; Sarasini, F. Effect of Carbon Nanostructures and Fatty Acid Treatment on the Mechanical and Thermal Performances of Flax/Polypropylene Composites. *Polymers* **2020**, *12*, 438. [CrossRef]
5. Goy, R.C.; Morais, S.T.B.; Assis, O.B.G. Evaluation of the antimicrobial activity of chitosan and its quaternized derivative on *E. coli* and *S. aureus* growth. *Rev. Bras. Farmacogn.* **2016**, *26*, 122–127. [CrossRef]
6. Zima, A.; Czechowska, J.; Szponder, T.; Ślósarczyk, A. In vivo behavior of biomicroconcretes based on α-tricalcium phosphate and hybrid hydroxyapatite/chitosan granules and sodium alginate. *J. Biomed. Mater. Res.* **2020**, *108*, 1243–1255. [CrossRef]
7. Czechowska, J.; Cichoń, E.; Belcarz, A.; Ślósarczyk, A.; Zima, A. Effect of Gold Nanoparticles and Silicon on the Bioactivity and Antibacterial Properties of Hydroxyapatite/Chitosan/Tricalcium Phosphate-Based Biomicroconcretes. *Materials* **2021**, *14*, 3854. [CrossRef]
8. De Santis, R.; Russo, T.; Rau, J.V.; Papallo, I.; Martorelli, M.; Gloria, A. Design of 3D Additively Manufactured Hybrid Structures for Cranioplasty. *Materials* **2021**, *14*, 181. [CrossRef]

9. Zhang, J.; Liu, W.; Gauthier, O.; Sourice, S.; Pilet, P.; Rethore, G.; Khairoun, K.; Bouler, J.-M.; Tancret, F.; Weiss, P. A simple and effective approach to prepare injectable macroporous calcium phosphate cement for bone repair: Syringe-foaming using a viscous hydrophilic polymeric solution. *Acta Biomater.* **2016**, *31*, 326–338. [CrossRef]
10. Jang, J.-H.; Shin, S.; Kim, H.-J.; Jeong, J.; Jin, H.-E.; Desai, M.S.; Lee, S.-W.; Kim, S.-Y. Improvement of physical properties of calcium phosphate cement by elastin-like polypeptide supplementation. *Sci. Rep.* **2018**, *8*, 5216. [CrossRef]
11. Saveleva, M.S.; Eftekhari, K.; Abalymov, A.; Douglas, T.E.L.; Volodkin, D.; Parakhonskiy, B.V.; Skirtach, A.G. Hierarchy of Hybrid Materials—The Place of Inorganics-in-Organics in it, Their Composition and Applications. *Front. Chem.* **2019**, *7*, 179. [CrossRef] [PubMed]
12. Hashim, A.F.; Youssef, K.; Roberto, S.R.; Abd-Elsalam, K.A. Hybrid inorganic-polymer nanocomposites: Synthesis, characterization, and plant-protection applications. In *Multifunctional Hybrid Nanomaterials for Sustainable Agri-Food and Ecosystems*; Elsevier: Amsterdam, The Netherlands, 2020; pp. 33–49. [CrossRef]
13. An, J.; Wolke, J.G.C.; Jansen, J.A.; Leeuwenburgh, S.C.G. Influence of polymeric additives on the cohesion and mechanical properties of calcium phosphate cements. *J. Mater. Sci. Mater. Med.* **2016**, *27*, 58. [CrossRef] [PubMed]
14. Dziadek, M.; Dziadek, K.; Salagierski, S.; Drozdowska, M.; Serafim, A.; Stancu, I.-C.; Szatkowski, P.; Kopec, A.; Rajzer, I.; Douglas, T.E.; et al. Newly crosslinked chitosan- and chitosan-pectin-based hydrogels with high antioxidant and potential anticancer activity. *Carbohydr. Polym.* **2022**, *290*, 119486. [CrossRef]
15. Pellis, A.; Guebitz, G.M.; Nyanhongo, G.S. Chitosan: Sources, Processing and Modification Techniques. *Gels* **2022**, *8*, 393. [CrossRef]
16. Ibrahim, H.M.; El-Zairy, E.M.R. Chitosan as a Biomaterial—Structure, Properties, and Electrospun Nanofibers. In *Concepts, Compounds and the Alternatives of Antibacterials*; Bobbarala, V., Ed.; InTech: London, UK, 2015. [CrossRef]
17. Singhal, S.; Hulle, N.R.S. Citrus pectins: Structural properties, extraction methods, modifications and applications in food systems—A review. *Appl. Food Res.* **2022**, *2*, 100215. [CrossRef]
18. Minzanova, S.; Mironov, V.F.; Arkhipova, D.M.; Khabibullina, A.V.; Mironova, L.G.; Zakirova, Y.M.; Milyukov, V.A. Biological Activity and Pharmacological Application of Pectic Polysaccharides: A Review. *Polymers* **2018**, *10*, 1407. [CrossRef]
19. Freitas, C.M.P.; Coimbra, J.S.R.; Souza, V.G.L.; Sousa, R.C.S. Structure and Applications of Pectin in Food, Biomedical, and Pharmaceutical Industry: A Review. *Coatings* **2021**, *11*, 922. [CrossRef]
20. Marudova, M.; MacDougall, A.J.; Ring, S.G. Pectin–chitosan interactions and gel formation. *Carbohydr. Res.* **2004**, *339*, 1933–1939. [CrossRef] [PubMed]
21. Czechowska, J.; Zima, A.; Paszkiewicz, Z.; Lis, J.; Ślósarczyk, A. Physicochemical properties and biomimetic behaviour of α-TCP-chitosan based materials. *Ceram. Int.* **2014**, *40*, 5523–5532. [CrossRef]
22. de Almeida, D.A.; Sabino, R.M.; Souza, P.R.; Bonafé, E.G.; Venter, S.A.; Popat, K.C.; Martins, A.F.; Monteiro, J.P. Pectin-capped gold nanoparticles synthesis in-situ for producing durable, cytocompatible, and superabsorbent hydrogel composites with chitosan. *Int. J. Biol. Macromol.* **2020**, *147*, 138–149. [CrossRef]
23. Martins, J.G.; Camargo, S.E.A.; Bishop, T.T.; Popat, K.C.; Kipper, M.J.; Martins, A.F. Pectin-chitosan membrane scaffold imparts controlled stem cell adhesion and proliferation. *Carbohydr. Polym.* **2018**, *197*, 47–56. [CrossRef] [PubMed]
24. Wong, S.K.; Wong, Y.H.; Chin, K.-Y.; Ima-Nirwana, S. A Review on the Enhancement of Calcium Phosphate Cement with Biological Materials in Bone Defect Healing. *Polymers* **2021**, *13*, 3075. [CrossRef]
25. Nicolle, L.; Journot, C.M.A.; Gerber-Lemaire, S. Chitosan Functionalization: Covalent and Non-Covalent Interactions and Their Characterization. *Polymers* **2021**, *13*, 4118. [CrossRef] [PubMed]
26. Chen, J.; Liu, W.; Liu, C.-M.; Li, T.; Liang, R.-H.; Luo, S.-J. Pectin Modifications: A Review. *Crit. Rev. Food Sci. Nutr.* **2015**, *55*, 1684–1698. [CrossRef] [PubMed]
27. Basak, S.; Annapure, U.S. Trends in "green" and novel methods of pectin modification—A review. *Carbohydr. Polym.* **2022**, *278*, 118967. [CrossRef] [PubMed]
28. Geffers, M.; Barralet, J.E.; Groll, J.; Gbureck, U. Dual-setting brushite–silica gel cements. *Acta Biomater.* **2015**, *11*, 467–476. [CrossRef]
29. Christel, T.; Kuhlmann, M.; Vorndran, E.; Groll, J.; Gbureck, U. Dual setting α-tricalcium phosphate cements. *J. Mater. Sci. Mater. Med.* **2013**, *24*, 573–581. [CrossRef]
30. Ginebra, M.P.; Fernández, E.; Boltong, M.G.; Bermúdez, O.; Planell, J.A.; Driessens, F.C.M. Compliance of an apatitic calcium phosphate cement with the short-term clinical requirements in bone surgery, orthopaedics and dentistry. *Clin. Mater.* **1994**, *17*, 99–104. [CrossRef]
31. Sugawara, A.; Asaoka, K.; Ding, S.-J. Calcium phosphate-based cements: Clinical needs and recent progress. *J. Mater. Chem. B* **2013**, *1*, 1081–1089. [CrossRef]
32. Smith, B.T.; Lu, A.; Watson, E.; Santoro, M.; Melchiorri, A.J.; Grosfeld, E.C.; Beucken, J.J.v.D.; Jansen, J.A.; Scott, D.W.; Fisher, J.P.; et al. Incorporation of fast dissolving glucose porogens and poly(lactic-co-glycolic acid) microparticles within calcium phosphate cements for bone tissue regeneration. *Acta Biomater.* **2018**, *78*, 341–350. [CrossRef]
33. Şahin, E. Calcium Phosphate Bone Cements. In *Cement Based Materials*; Saleh, H.E.-D.M., Rahman, R.O.A., Eds.; InTech: London, UK, 2018. [CrossRef]
34. He, Z.; Zhai, Q.; Hu, M.; Cao, C.; Wang, J.; Yang, H.; Li, B. Bone cements for percutaneous vertebroplasty and balloon kyphoplasty: Current status and future developments. *J. Orthop. Transl.* **2015**, *3*, 1–11. [CrossRef]

35. Durucan, C.; Brown, P.W. Reactivity of α-tricalcium phosphate. *J. Mater. Sci.* **2002**, *37*, 963–969. [CrossRef]
36. Rabiee, S.M.; Baseri, H. Prediction of the Setting Properties of Calcium Phosphate Bone Cement. *Comput. Intell. Neurosci.* **2012**, *2012*, 1–8. [CrossRef] [PubMed]
37. Dziadek, M.; Zima, A.; Cichoń, E.; Czechowska, J.; Ślósarczyk, A. Biomicroconcretes based on the hybrid HAp/CTS granules, α-TCP and pectins as a novel injectable bone substitutes. *Mater. Lett.* **2020**, *265*, 127457. [CrossRef]
38. Larsson, S.; Hannink, G. Injectable bone-graft substitutes: Current products, their characteristics and indications, and new developments. *Injury* **2011**, *42*, S30–S34. [CrossRef]
39. Ginebra, M.-P.; Montufar, E.B. Cements as bone repair materials. In *Bone Repair Biomaterials*; Elsevier: Amsterdam, The Netherlands, 2019; pp. 233–271. [CrossRef]
40. O'Neill, R.; McCarthy, H.; Montufar, E.; Ginebra, M.-P.; Wilson, D.; Lennon, A.; Dunne, N. Critical review: Injectability of calcium phosphate pastes and cements. *Acta Biomater.* **2017**, *50*, 1–19. [CrossRef] [PubMed]
41. Arkin, V.H.; Narendrakumar, U.; Madhyastha, H.; Manjubala, I. Characterization and In Vitro Evaluations of Injectable Calcium Phosphate Cement Doped with Magnesium and Strontium. *ACS Omega* **2021**, *6*, 2477–2486. [CrossRef] [PubMed]
42. Cui, S.; Yao, B.; Gao, M.; Sun, X.; Gou, D.; Hu, J.; Zhou, Y.; Liu, Y. Effects of pectin structure and crosslinking method on the properties of crosslinked pectin nanofibers. *Carbohydr. Polym.* **2017**, *157*, 766–774. [CrossRef]
43. da Silva, M.A.; Bierhalz, A.C.K.; Kieckbusch, T.G. Alginate and pectin composite films crosslinked with Ca^{2+} ions: Effect of the plasticizer concentration. *Carbohydr. Polym.* **2009**, *77*, 736–742. [CrossRef]
44. Zima, A.; Czechowska, J.; Siek, D.; Ślósarczyk, A. Influence of magnesium and silver ions on rheological properties of hydroxyapatite/chitosan/calcium sulphate based bone cements. *Ceram. Int.* **2017**, *43*, 16196–16203. [CrossRef]
45. Stephen, A.M.; Cummings, J.H. Water-holding by dietary fibre in vitro and its relationship to faecal output in man. *Gut* **1979**, *20*, 722–729. [CrossRef]
46. Boulos, N.N.; Greenfield, H.; Wills, R.B.H. Water holding capacity of selected soluble and insoluble dietary fibre. *Int. J. Food Prop.* **2000**, *3*, 217–231. [CrossRef]
47. Gao, J.; Qiao, L.; Li, L.; Wang, Y. Hemolysis effect and calcium-phosphate precipitation of heat-organic-film treated magnesium. *Trans. Nonferrous Met. Soc. China* **2006**, *16*, 539–544. [CrossRef]
48. Cichoń, E.; Ślósarczyk, A.; Zima, A. Influence of Selected Surfactants on Physicochemical Properties of Calcium Phosphate Bone Cements. *Langmuir* **2019**, *35*, 13656–13662. [CrossRef]
49. Rashidova, S.S.; Milusheva, R.Y.; Semenova, L.N.; Mukhamedjanova, M.Y.; Voropaeva, N.L.; Vasilyeva, S.; Faizieva, R.; Ruban, I.N. Characteristics of Interactions in the Pectin?Chitosan System. *Chromatographia* **2004**, *59*, 11–12. [CrossRef]
50. Vaishya, R.; Chauhan, M.; Vaish, A. Bone cement. *J. Clin. Orthop. Trauma* **2013**, *4*, 157–163. [CrossRef]
51. Gerhardt, L.-C.; Boccaccini, A.R. Bioactive Glass and Glass-Ceramic Scaffolds for Bone Tissue Engineering. *Materials* **2010**, *3*, 3867–3910. [CrossRef]
52. Hopkins, E.; Sanvictores, T.; Sharma, S. Physiology, Acid Base Balance. In *StatPearls*; StatPearls Publishing: Treasure Island, FL, USA, 2022. Available online: http://www.ncbi.nlm.nih.gov/books/NBK507807/ (accessed on 25 November 2022).
53. Kokubo, T.; Takadama, H. How useful is SBF in predicting in vivo bone bioactivity? *Biomaterials* **2006**, *27*, 2907–2915. [CrossRef]
54. Li, X.; Bi, J.; Jin, X.; Li, X.; Zhao, Y.; Song, Y. Effect of pectin osmosis or degradation on the water migration and texture properties of apple cube dried by instant controlled pressure drop drying (DIC). *LWT* **2020**, *125*, 109202. [CrossRef]
55. Khattab, A.M. The Microbial Degradation for Pectin. In *Pectins—The New-Old Polysaccharides*; Masuelli, M.A., Ed.; IntechOpen: London, UK, 2022. [CrossRef]
56. Klinchongkon, K.; Khuwijitjaru, P.; Adachi, S. Degradation kinetics of passion fruit pectin in subcritical water. *Biosci. Biotechnol. Biochem.* **2017**, *81*, 712–717. [CrossRef] [PubMed]
57. Kolmas, J.; Kaflak, A.; Zima, A.; Ślósarczyk, A. Alpha-tricalcium phosphate synthesized by two different routes: Structural and spectroscopic characterization. *Ceram. Int.* **2015**, *41*, 5727–5733. [CrossRef]
58. Zima, A. Hydroxyapatite-chitosan based bioactive hybrid biomaterials with improved mechanical strength. *Spectrochim. Acta Part. A Mol. Biomol. Spectrosc.* **2018**, *193*, 175–184. [CrossRef] [PubMed]
59. Komath, M.; Varma, H.K.; Sivakumar, R. On the development of an apatitic calcium phosphate bone cement. *Bull. Mater. Sci.* **2000**, *23*, 135–140. [CrossRef]
60. C01 Committee. *Test Method for Time of Setting of Hydraulic-Cement Paste by Gillmore Needles*; ASTM International: Singapore, 2020. [CrossRef]

Publikacja 2 – *„Influence of Natural Polysaccharides on Properties of the Biomicroconcrete-Type Bioceramics"*

materials

MDPI

Article

Influence of Natural Polysaccharides on Properties of the Biomicroconcrete-Type Bioceramics

Piotr Pańtak, Ewelina Cichoń, Joanna Czechowska and Aneta Zima *

Faculty of Materials Science and Ceramics, AGH University of Science and Technology, Mickiewicza Av. 30, 30-058 Kraków, Poland; pantak@agh.edu.pl (P.P.); ecichon@agh.edu.pl (E.C.); jczech@agh.edu.pl (J.C.)
* Correspondence: azima@agh.edu.pl

Abstract: In this paper, novel hybrid biomicroconcrete-type composites were developed and investigated. The solid phase of materials consisted of a highly reactive α -tricalcium phosphate (α-TCP) powder, hybrid hydroxyapatite-chitosan (HAp-CTS) material in the form of powder and granules (as aggregates), and the polysaccharides sodium alginate (SA) or hydroxypropyl methylcellulose (HPMC). The liquid/gel phase in the studied materials constituted a citrus pectin gel. The influence of SA or HPMC on the setting reaction, microstructure, mechanical as well as biological properties of biomicroconcretes was investigated. Studies revealed that manufactured cement pastes were characterized by high plasticity and cohesion. The dual setting system of developed biomicroconcretes, achieved through α-TCP setting reaction and polymer crosslinking, resulted in a higher compressive strength. Material with the highest content of sodium alginate possessed the highest mechanical strength (~17 MPa), whereas the addition of hydroxypropyl methylcellulose led to a subtle compressive strength decrease. The obtained biomicroconcretes were chemically stable and characterized by a high bioactive potential. The novel biomaterials with favorable physicochemical and biological properties can be prosperous materials for filling bone tissue defects of any shape and size.

Keywords: biomicroconcretes; hybrid materials; calcium phosphate; chitosan; dual setting

Citation: Pańtak, P.; Cichoń, E.; Czechowska, J.; Zima, A. Influence of Natural Polysaccharides on Properties of the Biomicroconcrete-Type Bioceramics. *Materials* **2021**, *14*, 7496. https://doi.org/10.3390/ma14247496

Academic Editor: Francesco Baino

Received: 17 October 2021
Accepted: 3 December 2021
Published: 7 December 2021

1. Introduction

The bone substitutes constitute an important group of biomaterials widely used in orthopedics, craniofacial surgery, and dentistry [1]. Due to the growing demand for implantable materials, researchers are constantly working on improving their properties as well as on developing completely new bone substitutes [2]. Calcium phosphate bone cements (CPCs) are biocompatible, moldable materials, which harden in vivo through a low temperature setting reaction. CPCs, in addition to biocompatibility, bioactivity, and mechanical properties similar to bone tissue, should also possess appropriate rheological properties, injectability, cohesion, and setting times. A major advantage of CPCs over the preformed grafts is their ability to adapt to the complex geometry of the bone defect. Despite the excellent biocompatibility and bioactivity of CPCs, their poor mechanical strength and frequent lack of satisfactory injectability limit their applications [3,4]. In order to overcome poor injectability and compressive strength of CPCs, various polymeric additives, including polyanions (e.g., pectins, sodium alginate, and methylcellulose) and polycations (e.g., chitosan and CTS) can be applied. From the point of view of bone tissue engineering, sodium alginate (SA) and hydroxypropyl methylcellulose (HPMC) have favorable properties (i.e., biocompatibility, low toxicity, and ease of gelation). SA belongs to the group of alginates derived from brown algae cell walls. This anionic polysaccharide is widely used in pharmaceutical [5] and biomedical applications [6–8]. In the field of calcium phosphate-based bone cements, SA is often applied because materials with sodium alginate gain injectability and show beneficial properties in in vitro tests [9,10]. HPMC

(anionic polysaccharide) is a cellulose-derived polymer with a wide range of biomedical applications [11]. In the studies of Burguera et al. [12], the HPMC to the liquid phase of cements allowed to obtain CPCs with better injectability, and Liu et al. [13] pointed out the outstanding cohesion of bone cements containing HPMC. An additional reason for the use of the above-mentioned polymers is their biologically favorable features, such as biocompatibility, biodegradability, and antimicrobial properties [14–17].

An interesting modification of bone cements seems to be biomicroconcretes, i.e., bone cements containing aggregates in the form of microspheres or granules [18–23]. Nezafati et al. [23] investigated tetra calcium phosphate (TTCP) based cement with gelatine microspheres (GMs). They stated that the final setting time and injectability were increased when GMs were added to the CPCs. Meng et al. [21] examined material composed of α-tricalcium phosphate (α-TCP), calcium dihydrogen phosphate monohydrate (DCPM), and $CaCO_3$ incorporated with chitosan microspheres (10%, *w*/*w*). They demonstrated that the biomicroconcretes promote adhesion, proliferation, and differentiation of osteoblasts and had good biocompatibility in the muscles of animals. In the study of Zima et al., biomicroconcretes based on α-TCP and hybrid, hydroxyapatite-chitosan (HAp-CTS) granules were bioactive and supported the growth of bone tissue [18]. Furthermore, the use of chitosan (polycation) together with polyanionic polymers is of great interest due to their unique electrostatic interaction in an aqueous environment [24–26]. Neufeld et al. [27] studied pectin/chitosan physical hydrogels as potential drug delivery vehicles. Dziadek et al. [28] combined α-TCP, hybrid HAp/CTS granules, and pectins receiving injectable biomicroconcretes with improved surgical handiness, due to polyelectrolyte complex formation. The use of pectins in cement-based bone substitutes is still under evaluation. The crosslinking agents have also been studied for the fabrication of particles or composites from chitosan and pectin [29,30]. In this study, polymeric additives, i.e., sodium alginate (SA) and hydroxypropyl methylcellulose (HPMC) as a polyanions will be examined as potential moderators of interactions between polycationic chitosan and citrus pectin. We suspect that the use of polyanionic polymers together with polycationic chitosan can lead to achieving favorable properties of hybrid, biomicroconcrete-type materials due to the formation of polyelectrolyte complexes.

The aim of this study was to develop and obtain biomicroconcretes on the basis of α-tricalcium phosphate, hydroxyapatite, chitosan, and citrus pectin and investigate the influence of natural polysaccharides in the form of sodium alginate and hydroxypropyl methylcellulose (2 and 4 wt%) on their physicochemical and biological properties.

2. Materials and Methods

2.1. Materials

The initial α-tricalcium phosphate (α-TCP) powder was synthesized by the wet chemical method described previously [31,32]. As reagents, $Ca(OH)_2$ (≥99.5%, POCH, Gliwice, Poland) and H_3PO_4 (85.0%, POCH, Gliwice, Poland) were applied. In brief, the α-TCP precipitate was dried, sintered above 1250 °C (5 h), ground in an attritor mill (3 h), and sieved below 63 μm.

Hydroxyapatite-chitosan (HAp-CTS) hybrid materials, containing 21 wt% of chitosan, were obtained by the modified wet chemical method described previously [33]. The following substrates were used: $Ca(OH)_2$ (≥99.5 wt%, POCH, Gliwice, Poland), H_3PO_4 (85.0 wt%, POCH, Gliwice, Poland), and medium-molecular-weight chitosan (~100,000 kDa, DD ≥ 75.0 wt%, Sigma-Aldrich, St. Louis, MO, USA). HAp-CTS hybrids in the form of powder and granules (300–400 μm) were applied as an aggregate in developed materials.

Five types of biomicroconcretes were prepared by mixing the solid phase, i.e., α-TCP, HAp-CTS materials, and polymeric additives with the liquid phase. As polymeric additives, sodium alginate (SA, POCH, Gliwice, Poland) or hydroxypropyl methylcellulose (HPMC, Alfa Aesar, Tewksbury, MA, USA) was used. The polymeric modifiers SA and HPMC were introduced in the form of powder directly during the cement paste mixing. As a liquid phase, a 5 wt% pectin gel in distilled water was used. A low esterified amidated

pectin from citrus peels (CUL) was kindly delivered by Herbstreith & Fox (Herbstreith & Fox, Werder (Havel), Germany). The initial composition of the prepared biomicroconcretes, as well as a liquid to powder ratio (L/P), are presented in Table 1.

Table 1. Initial compositions of developed materials.

Material Label	Solid (Powder) Phase (P)	Liquid Phase (L)	L/P (mL/g)
Control	25 wt% α-TCP: 35 wt% HAp/CTS granules: 40 wt% HAp/CTS powder	5 wt% CUL in distilled water (gel)	0.8
MC-SA2	Control + 2 wt% SA powder		
MC-SA4	Control + 4 wt% SA powder		
MC-HPMC2	Control + 2 wt% HPMC powder		
MC-HPMC4	Control + 4 wt% HPMC powder		

2.2. Methods

2.2.1. Injectability and Setting Times

The injectability of the obtained materials was checked visually by injecting the cement paste through a 20 mL plastic syringe with a 2 mm nozzle (B. Brown, Melsungen, Germany) directly into the SBF solution preheated to 37 °C. The setting times (initial and final) of obtained biomicroconcretes were measured according to ASTM-C200-08 standard using a Gillmore apparatus (Humboldt, Norridge, IL, USA [34]. The results are presented as the average value of three measurements ± standard deviation (SD).

2.2.2. Structural Studies

The crystalline phases were analysed by a powder X-ray diffractometer (XRD, D2 Phaser, Bruker, Ballerica, MA, USA). An XRD analysis was performed using CuK-α radiation (1.54 Å) at 30 kV and 10 mA. The intensity was recorded in a 2θ range from 10° to 90° at 0.04° intervals with a scanning speed of 2.5° min^{-1}. The crystalline phases were identified by comparing the experimental diffractograms to the Joint Committee on Powder Diffraction Standards: α-TCP (JCPDS 00-009-0348) and hydroxyapatite (HAp; JCPDS 01-076-0694). A quantitative phase composition analysis based on Rietveld refinement was performed using Profex software (Version 4.3.5., Nicola Döbelin, Solothurn, Switzerland). The identification and quantification of the crystalline structures of materials nonincubated and incubated in simulated body fluid (SBF) at 37 °C were made after 7 days of setting and hardening.

Structural analyses were performed by Fourier transform infraRed spectroscopy (FTIR), within the scanning range 400–4000 cm^{-1} and resolution of 4 cm^{-1} using a BioRad FTS 6000 spectrometer (Vertex 70&70v, Bruker, Ballerica, MA, USA). The band positions of each result were measured according to the center of weight. The baseline correction, normalisation, and spectra analyses were performed using the Spectragryph software (Vwrsion v1.2.15, Friedrich Menges, Oberstdorf, Germany).

2.2.3. Microstructure

The microstructure observations of the fractured samples were performed with the use of scanning electron microscopy (SEM, PhenomPure, Thermo Fisher Scientific, Waltham, MA, USA). In order to evaluate bioactive potential, the materials' surface after 7 days of incubation in SBF at 37 °C was also assessed. Before the examination, the samples were coated with a thin gold film using a low deposition rate.

2.2.4. Mechanical Strength

The compressive strength was examined using the universal testing machine (Instron 3345, Instron, Norwood, MA, USA). The cylindrical biomicroconcrete samples (6 mm × 12 mm) were subjected to uniaxial compression with a crosshead speed of 1.0 mm min^{-1}. The biomicroconcrete samples were prepared and stored in air at 37 °C for 1 week. For

comparison, samples after 7 days of incubation in SBF at 37 °C were also tested. The results of the compressive strength were presented as the average value of minimal ten measurements ± standard deviation (SD).

2.2.5. Chemical Stability and Bioactivity In Vitro

In order to evaluate the chemical stability and bioactivity of the obtained materials, the cylindrical samples (12 mm × 6 mm) were placed in sterile containers filled with 40 mL of SBF or distilled water and stored at 37 °C for 28 days. The SBF solution was prepared according to Kokubo's protocol [1,35]. The chemical stability of the obtained samples was assessed by measuring the pH of SBF and the ionic conductivity of the distilled water around incubated samples in the function of time using a pH/conductometer (H198129 Combo, Hanna, Smithfield, RI, USA). Measurements were performed at 1, 3, 7, and 28 days of incubation. Each measurement was performed triple times for each material. Results were expressed as the average value of three measurements ± standard deviation (SD).

2.2.6. Statistics

A statistical analysis was performed using one-way ANOVA with a posthoc Tukey HSD (Honestly Significant Difference) test for comparing multiple treatments (* means the statistically significant difference between the results, $p > 0.05$). An analysis was performed with OriginPro 2021 software (Version 2021, OriginLab Corporation, Northampton, MA, USA).

3. Results and Discussion

3.1. Injectability and Setting Times

The novel biomicroconcrete-type biomaterials possessed excellent injectability. No phase separation was observed during the cement paste extrusion from the syringe to SBF. Moreover, it was observed that all developed materials were characterized by high cohesion and maintained their initial shape after extrusion, indicating washout resistance. However, the material MC-SA4, where the polysaccharide additive of 4 wt% of SA was applied, possessed the best injectability and cohesion in comparison to the others (Figure 1). No significant differences among the material groups containing the sodium alginate additive (MC-SA2, MC-SA4) and hydroxypropyl methylcellulose (MC-HPMC2, MC-HPMC4) were observed.

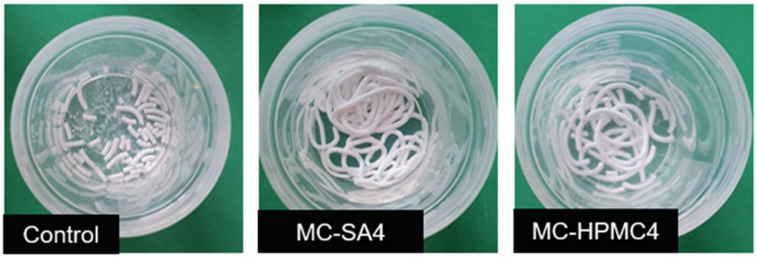

Figure 1. Obtained materials: Control, MC-SA4 and MC-HPMC4 immediately after extrusion from the syringe to SBF.

Outstanding surgical handiness was achieved through the use of natural polymers in the cement compositions. The polymeric additives increased the viscosity of the cement pastes and improved their injectability and cohesion. The ability of SA and HPMC to form hydrogels resulted in increased water resistance during the incubation in SBF, and the pectin crosslinking led to better integrity of the injected paste. Similar observations were reported in previous studies where polymeric additives were applied [18,28,36].

The setting times of the obtained cement-type materials depended on the polymeric additives and varied between 28 and 37 min (initial setting time) and more than 60 min (final setting time) (Table 2).

Table 2. The setting times of the biomicroconcretes.

Material	Initial, t_i [Min]	Final, t_f [Min]
Control	28 ± 2	>60
MC-SA2	33 ± 2	
MC-SA4	36 ± 3	
MC-HPMC2	34 ± 1	
MC-HPMC4	37 ± 2	

The results show that the addition of polysaccharides increased the initial cement setting time. Furthermore, the initial setting times of materials containing 2 wt% (MC-SA2 and MC-HPMC2) and 4 wt% of the polymeric additive (MC-SA4 and MC-HPMC4) were similar in the subgroups. The setting time determined the time in which material was completely hardened. The process that enables setting and hardening is α-TCP hydrolysis. α-TCP contained in the biomicroconcretes reacts with water and forms the calcium-deficient apatite, according to the following Equation (1) [37,38]:

$$3Ca_3(PO_4)_2 + H_2O \rightarrow Ca_9(PO_4)5(HPO_4)OH, \quad (1)$$

Several factors influence the setting reaction of biomicroconcretes. The most important are: the amount of the highly reactive α-TCP phase in material, the presence of the setting accelerator in the liquid phase, the kind of polymeric additive in the liquid phase, and, finally, the presence of polymeric additives in the powder phase of the material [39]. The implantation of CPCs is a complex process with a brief window. Clinically, quick setting times can make the cement paste difficult to apply. Alternately, for the cement formulations with long setting times, the possibility of material washout constitutes a problem. The initial and final setting times of the obtained biomicroconcretes were higher than recommended in the literature (4–8 min for initial, up to 15 min for final) [40]. However, there are some commercially used bone substitutes characterized by longer than recommended setting times (i.e., Bone Source®: t_I = 10–15 min, t_F~4 h; Norian SRS/CRS®: t_I = 10 min, t_F~12 h) [41,42]. The presence of powder-added polymeric additives both in the form of sodium alginate (MC-SA2, MC-SA40) and hydroxypropyl methylcellulose (MC-HPMC2, MC-HPMC4) results in the elongation of the setting times of the obtained materials but also improves their cohesion. Furthermore, the amount of polymeric additive has an impact on the setting process. The higher the number of polysaccharides used, the longer the setting time was. These results are consistent with studies of Czechowska et al. [19]. In order to shorten the setting times, it would be essential to use a setting accelerator (i.e., disodium hydrogen phosphate Na_2HPO_4) [19,43]. Although the setting times of the obtained materials were longer than recommended, the presence of chitosan, citrus pectin, and other polymeric additives ensured good cohesion of the final materials, preventing them from disintegrating on contact with SBF. Moreover, the presence of the above-mentioned polysaccharides interactions and the setting of α-TCP powder caused the initiation of the dual setting process in the obtained biomicroconcretes. This process is based on the hydrolysis of α-TCP and polymer crosslinking simultaneously [44]. Chitosan and pectin interactions were studied previously by Marudova et al. [24], and they are based on the polyelectrolyte nature of those polymers. Chitosan as a natural polycation interacts with polyanionic pectin [27,45]. In addition, an idea for using other polysaccharides such as SA and HPMC as powder additives to biomicroconcretes was also motivated by the occurrence of interactions between them. Polyanionic sodium alginate may interact with polycationic chitosan and in the presence of calcium ions additionally crosslink, which will lead to a

rigid ionic gel formation [14]. It also helps to form homogenous materials with beneficial mechanical properties [9,10].

3.2. Structural Studies

The materials phase composition was determined by XRD studies, whereas FTIR allowed the examination of the biomicroconcrete's chemical composition. The initial α-TCP powder composed of α-TCP phase (98.0 wt%) and a small amount of hydroxyapatite (2.0 wt%). The HAp-CTS hybrid materials were composed of hydroxyapatite as the only crystalline phase. In the case of biomicroconcretes, diffractograms revealed the presence of two different crystalline phases corresponding to α-TCP and HAp, and their proportion varied according to the environment in which the samples were kept. The detailed phase composition is presented in Table 3.

Table 3. Phase composition of tested biomicroconcretes.

Material Label	Phase Composition [wt%]			
	7 Days after Setting and Hardening		After 7 Days of Incubation in SBF (37 °C)	
	α-TCP	HAp	α-TCP	HAp
Control	25.0	75.0	2.0	98.0
MC-SA2	26.0	74.0	2.0	98.0
MC-SA4	29.0	71.0	3.0	97.0
MC-HPMC2	26.0	74.0	2.0	98.0
MC-HPMC4	28.0	72.0	1.0	99.0

The diffractograms of biomicroconcretes revealed two crystalline phases, i.e., α-TCP and hydroxyapatite. In addition, the amorphous halos originating from polymers were present. Very similar results were obtained in previous studies on hybrid HAp-CTS materials [28,33]. Moreover, the analysis of the phase composition after material incubation in SBF confirmed that α-TCP almost completely hydrolyzed to hydroxyapatite (Table 3). As in a simulated environment, the α-TCP phase is thermodynamically metastable and spontaneously hydrolyzes to nonstoichiometric hydroxyapatite [40]. It is suggested that slight differences observed in the phase composition of individual materials were caused by the presence of polymer additives in the biomicroconcretes. The outcome of the FTIR measurements supports the results of the XRD studies. The FTIR analysis of the studied materials confirmed the presence of functional group characteristic for calcium phosphates and polysaccharides, such as chitosan or pectin (Figure 2). Infrared spectra of biomicroconcretes after setting and hardening revealed the presence of characteristic bands at 470, 563, 602, 958 as well as 1101 cm^{-1} that were assigned to the PO_4^{3-} groups. The CO_3^{2-} group forms a weak peak between 870 and 880 cm^{-1} (note: it overlaps here with HPO_4^{2-}) and a more intensive peak at 1424 cm^{-1} (note: overlapping with -CH bending). The absorption band with a maximum at 2928 cm^{-1} can be attributed to alkyl C-H stretching. The band at around 1649 cm^{-1} confirms the presence of N-H bending modes of the primary amine. Furthermore, the band around 1315 cm^{-1} corresponds to C-N stretching. Spectra also revealed a band at 3573 cm^{-1} which is attributed to O-H stretching vibrations, and a wide band around 3500 cm^{-1} indicates the presence of residual water in the studied samples. A low concentration of polymeric additives (i.e., sodium alginate and hydroxypropyl methylcellulose) in the cements, as well as an overlapping of bands, may explain the lack of visible additional bands assigned to these polysaccharides (i.e., C = O). Stretches typical for carboxylic groups at 1610 cm^{-1} (SA) [46] or esters around 3368, 1737, 1227, and 1377 cm^{-1} (HPMC) [47] were not visible.

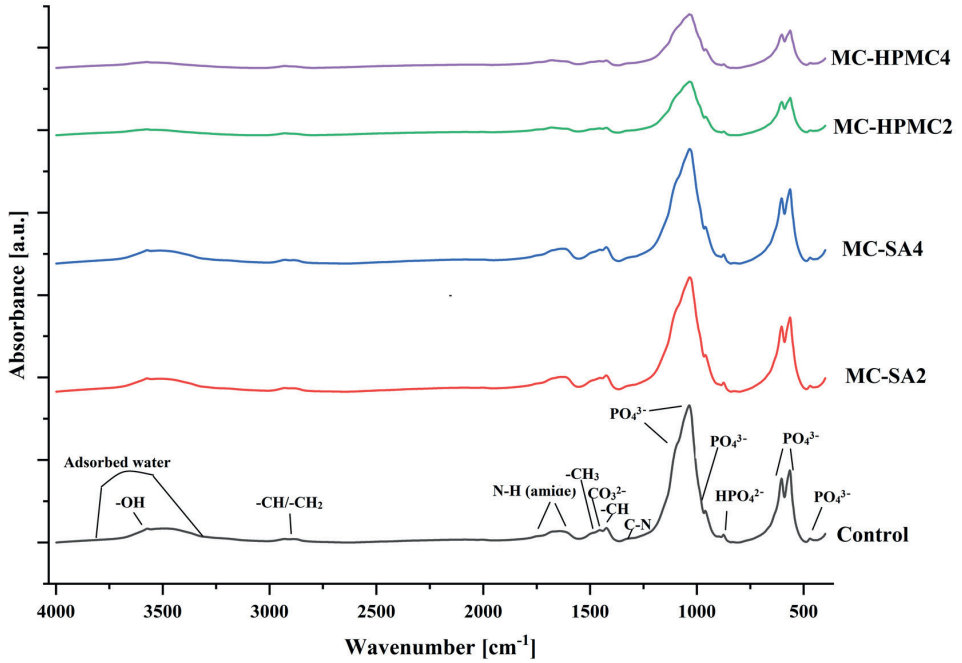

Figure 2. FT-IR spectra of obtained biomicroconcretes: Control, MC-SA2, MC-SA4, MC-HPMC2, and MC-HPMC4.

3.3. Microstructure

SEM observations of the obtained composites after seven days of drying in air revealed that the materials possessed compact, homogenous microstructure formed by hybrid hydroxyapatite-chitosan granules and a cementitious matrix with visible micropores. The microstructure of hybrid HAp-CTS granules and biomicroconcretes was composed of calcium phosphates (CaPs) agglomerated matrix (Figure 3(1a–1c)) and polymers. The polymers present in developed materials were observed in the form of a polymeric film adhering to the calcium phosphate grains as well as polymeric bridges between the granules (Figure 3(2a–2c)). Characteristic polymeric bridges between granules and pectin present in the matrix were observed by others. For example, Zima et al. [33] developed hybrid HAp/CTS granules, while Mickiewicz et al. [48] added various water-soluble polymers to commercial calcium phosphate bone substitutes. The presence of numerous characteristic chitosan bridges is evidence of the interactions among hybrid HAp/CTS materials, citrus pectin, and probably polymeric additives [13,24]. Similar microstructures were observed previously by Czechowska et al. [32] where the addition of chitosan to the liquid phase of α-TCP-based bone cements was investigated.

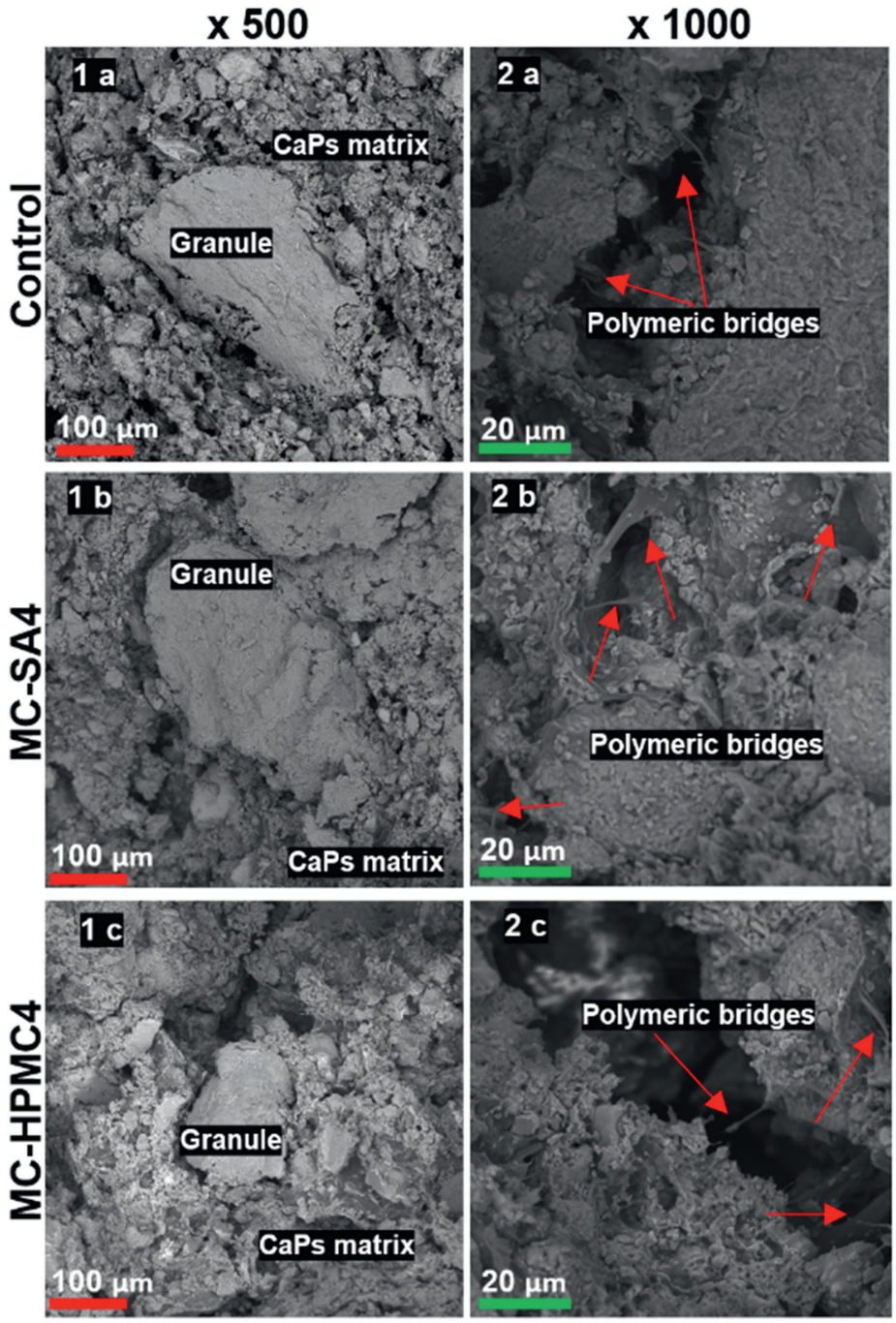

Figure 3. SEM microphotographs of cross-sections of obtained materials. Magnifications 500× (**1a**–**1c**) and 1000× (**2a**–**2c**).

After seven days of incubation in SBF, the surfaces of biomicroconcretes were completely covered by apatitic structures (Figure 4). The materials were characterized by similar microstructures regardless of the content of the polymeric additive. Hybrid granules were in intimate contact with the cementitious matrix, therefore all obtained composites are characterized by good mechanical properties and cohesion in the presence of a simulated biological environment.

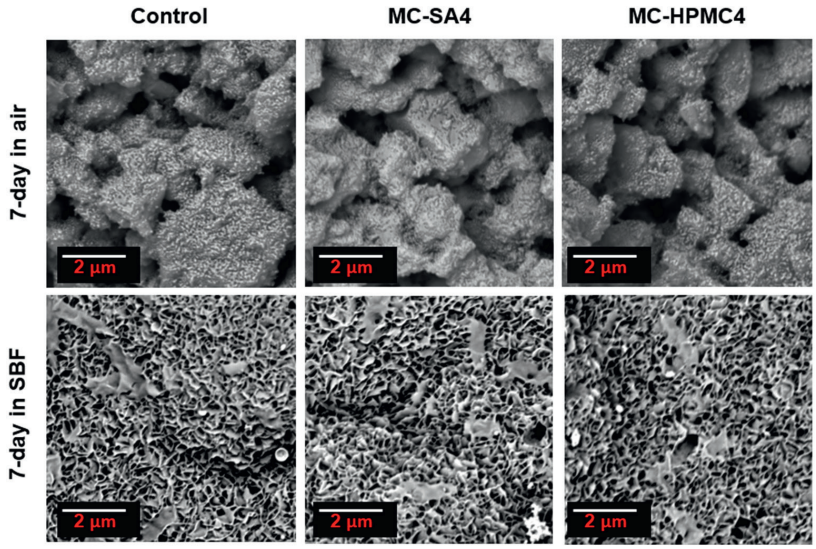

Figure 4. SEM microphotographs of biomicroconcretes surface after 7-day incubation in air or SBF.

3.4. Mechanical Strength

The results of compressive strength tests, both after seven days of drying in air (Figure 5A) and after seven days of incubation in SBF at 37 °C (Figure 5B) are shown bellow.

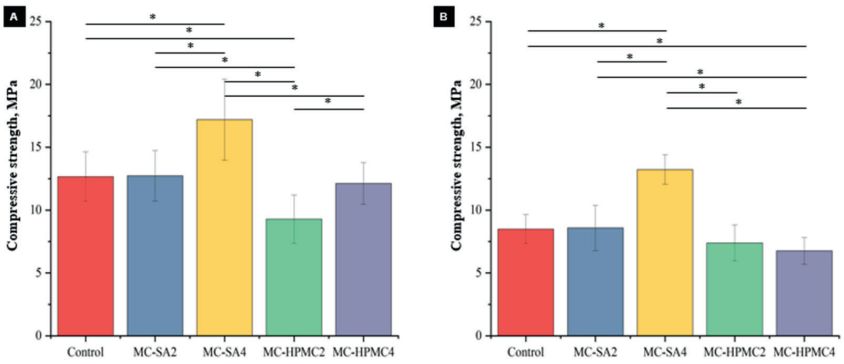

Figure 5. Compressive strength of biomicroconcretes after 7 days of drying in air (**A**) and after 7 days of incubation in SBF (**B**) (*—statistically significant difference, $p < 0.05$).

The compressive strength of the obtained cements ranged from 9.3 ± 2.1 to 17.2 ± 2.6 MPa for materials after seven days of setting and hardening and from 6.6 ± 1.2 to 13.2 ± 1.2 MPa for materials after incubation in SBF. A high compressive strength of the biomicroconcretes was obtained due to the presence of a dual setting system (α-TCP hydrolysis and interaction between sodium alginate and other polymeric additives in the material matrix composition) [24]. The mechanical properties of the obtained biomicroconcretes result not only from their hybrid nature but also from the characteristics of the additional polymer. Sodium alginate, compared to HPMC in an aqueous solution, is characterized by greater rigidity and viscosity, which may have a direct impact on the final properties of the developed biomaterials [49,50]. The highest compressive strength value was recorded for the material MC-SA4, where the 4 wt% addition of sodium alginate was applied (up to 17.2 ± 3.4 MPa). The increased strength with adding sodium alginate compared to the control material was due to the presence of additional interactions between Ca^{2+} cations and anionic sodium alginate. Alternately, materials containing another polymeric additive, hydroxypropyl methylcellulose, were characterized by lower compressive strength. A similar negative influence of HPMC on the material strength was also reported by Perez et al. [51]. It is suggested that the weakening of the strength of the materials with the HPMC addition is caused by the fact that HPMC is a highly hygroscopic polymer [52], thus absorbed water is necessary for α-TCP hydrolysis. Nevertheless, compressive strength values similar to that of human cancellous bone (between 4 and 12 MPa) [53] were obtained. Thus, it makes the obtained biomicroconcretes suitable for low-load bearing applications.

3.5. Chemical Stability and Bioactivity In Vitro

Chemical stability studies are one of the important tests for considering implantable materials for medical applications. Incubating the sample in SBF is considered as a first step for evaluating material characteristics and understanding their degradation mechanisms [54]. In order to evaluate chemical stability and bioactivity in vitro of the obtained biomicroconcretes, materials samples were incubated in simulated body fluid. Figure 6A shows the pH changes of SBF during the immersion of the samples. The pH changes of SBF remained close to the physiological values and ranged from 7.22 to 7.41. The addition of polysaccharides in the form of sodium alginate (MC-SA2 and MC-SA4) or hydroxypropyl methylcellulose (MC-HPMC2and MC-HPMC4) only slightly influenced the solution's pH values. Similar pH values of incubated CPCs were observed elsewhere [32,55]. Ionic conductivity during the incubation in distilled water of the control material was in the range of ~75–87 μS/cm. An additive in the form of sodium alginate (materials MC-SA2 and MC-SA4) caused an increase in ionic conductivity (~87–113 μS/cm), whereas for HPMC (materials MC-HPMC2 and MC-HPMC4), a decrease of ionic conductivity to ~49–69 μS/cm was observed (Figure 6B). This phenomenon can be explained by a higher degradation rate of SA than HPMC in aqueous solutions [18,56,57]. Ionic conductivity of all the obtained materials reached a plateau after seven days of incubation in distilled water.

The results show that polymeric additives did not affect the chemical stability of the developed biomicroconcretes incubated in SBF.

The bioactive potential of materials was estimated through the incubation in SBF according to Kokubo's protocol [35]. The SEM observations show that the evenly distributed, bone-like apatite layer was present on the sample's surface after seven days of incubation in SBF at 37 °C (Figure 4). The materials MC-SA2 and MC-HPMC2 possessed similar microstructure. The study revealed the presence of needle-like crystal structures forming an apatite-like layer after the seven-day incubation in SBF. The presence of apatite forms indirectly indicates the high bioactive potential of the obtained materials. The cement-type materials with hybrid HAp/CTS granules have been proven to be biocompatible in vivo by Zima et al. [18]. The polymeric additives used in the study had no adverse effects on the cells due to their beneficial biological properties. Thus, it may be assumed that the obtained biomaterials also will be biocompatible. To confirm this hypothesis further studies are necessary.

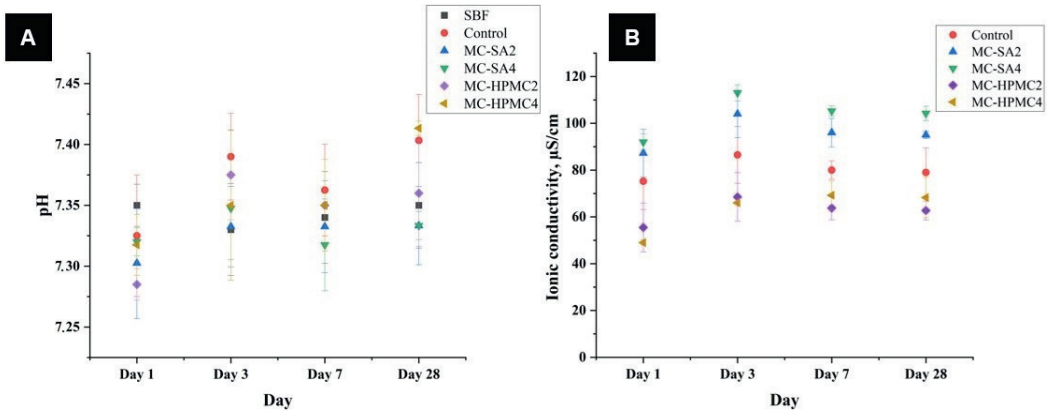

Figure 6. pH vs. time of incubation in SBF (**A**) and ionic conductivity vs. time of incubation in distilled water (**B**).

4. Conclusions

In this study, innovative biomicroconcretes based on highly reactive α-TCP powder, hybrid hydroxyapatite-chitosan hybrids (granules and powder), and citrus pectin gel were developed and examined. Moreover, the influence of polymeric additives in the form of sodium alginate and hydroxypropyl methylcellulose on the obtained materials was investigated. Newly developed biomicroconcretes differ significantly from materials previously described in the literature. Thus, in this paper, the main focus was on investigating the effect of polymer additives on the physicochemical properties of biomicroconcrete-type materials. The idea of using hybrid HAp-CTS granules as aggregates in developed biomaterials with the combination of the use of biopolymers resulted in novel composites characterized by beneficial properties of bioceramics (as calcium phosphates) and biopolymeric materials. It has been demonstrated that the addition of both natural polymers influenced the physicochemical properties of the composites. All obtained biomicroconcretes were characterized by excellent injectability and cohesion in simulated body fluid. It was also observed that the liquid phase in the form of gelled citrus pectin as well as the addition of the polymer influenced the material's setting process. Moreover, it was observed that a polymeric additive in the form of 4 wt% of sodium alginate unlike hydroxypropyl methylcellulose caused the biomicroconcretes to strengthen (up to 17.2 MPa for nonincubated materials and 13.2 MPa for materials incubated in SBF). Unique mechanical properties can be connected to the dual setting system occurring in developed materials, where α-TCP hydrolysis and polymer crosslinking take place simultaneously. The formation of hydrogel complexes during the preparation of the cement pastes allowed for the interaction between the polymers present in the tested materials (i.e., interaction between polycationic and polyanionic polymers). In vitro studies revealed that developed materials were chemically stable and demonstrated bioactive potential by the formation of apatitic layers on their surfaces as early as seven 7 days after incubation in SBF. Thus, the obtained materials can be considered as potentially bioactive. The ionic conductivity changed depending on the presence of the polymeric additive used. Sodium alginate caused an increase in ionic conductivity, unlike hydroxypropyl methylcellulose, which is indirectly connected to the degradation process of these polymers. All these findings confirm the most beneficial influence of the addition of 4 wt% sodium alginate on the character of the obtained biomicroconcretes and pave the way to further in vitro and in vivo studies.

Author Contributions: Conceptualization: P.P., E.C., J.C. and A.Z.; investigation: P.P., E.C., J.C. and A.Z.; writing—original draft preparation: P.P. and E.C.; writing—review and edit: J.C. and A.Z. All authors have read and agreed to the published version of the manuscript.

Funding: Research funded by the Faculty of Materials Science and Ceramics AGH UST—University of Science and Technology, Kraków, Poland, Project No. 16.16.160.557 (2021).

Institutional Review Board Statement: Not applicable.

Informed Consent Statement: Not applicable.

Data Availability Statement: All the data are available within the manuscript.

Acknowledgments: Authors thank the company Herbstreith & Fox for delivering the pectins.

Conflicts of Interest: The authors declare no conflict of interest. The funders had no role in the design of the study; in the collection, analyses, or interpretation of data; in the writing of the manuscript, or in the decision to publish the results.

References

1. Kokubo, T. *Bioceramics and Their Clinical Applications*; Woodhead Publishing: Cambridge, UK, 2008; ISBN 9781845692049.
2. Phillips, M.; Stonoga, Z.J.K. Bone disease. In *Orthopaedic Bone Cements*; Woodhead Publishing: Cambridge, UK, 2008; pp. 3–40. ISBN 9781845693763.
3. Ambard, A.J.; Mueninghoff, L. Calcium phosphate cement: Review of mechanical and biological properties. *J. Prosthodont.* **2006**, *15*, 321–328. [CrossRef]
4. Habraken, W.; Habibovic, P.; Epple, M.; Bohner, M. Calcium phosphates in biomedical applications: Materials for the future? *Mater. Today* **2016**, *19*, 69–87. [CrossRef]
5. Puscaselu, R.G.; Lobiuc, A.; Dimian, M.; Covasa, M. Alginate: From food industry to biomedical applications and management of metabolic disorders. *Polymers* **2020**, *12*, 2417. [CrossRef]
6. Szekalska, M.; Puciłowska, A.; Szymańska, E.; Ciosek, P.; Winnicka, K. Alginate: Current Use and Future Perspectives in Pharmaceutical and Biomedical Applications. *Int. J. Polym. Sci.* **2016**, *2016*. [CrossRef]
7. Abasalizadeh, F.; Moghaddam, S.V.; Alizadeh, E.; Akbari, E.; Kashani, E.; Fazljou, S.M.B.; Torbati, M.; Akbarzadeh, A.; Akbarzadeh, A. Alginate-based hydrogels as drug delivery vehicles in cancer treatment and their applications in wound dressing and 3D bioprinting. *J. Biol. Eng.* **2020**, *14*, 1–22, Erratum in **2020**, *14*, 8. [CrossRef]
8. Mazur, K.; Buchner, R.; Bonn, M.; Hunger, J. Hydration of sodium alginate in aqueous solution. *Macromolecules* **2014**, *47*, 771–776. [CrossRef]
9. Lee, G.S.; Park, J.H.; Won, J.E.; Shin, U.S.; Kim, H.W. Alginate combined calcium phosphate cements: Mechanical properties and in vitro rat bone marrow stromal cell responses. *J. Mater. Sci. Mater. Med.* **2011**, *22*, 1257–1268. [CrossRef] [PubMed]
10. Štulajterová, R.; Medvecký, L.; Giretová, M.; Sopčák, T.; Briančin, J. Influence of Sodium Alginate on Properties of Tetracalcium Phosphate/Nanomonetite Biocement. *Powder Metall. Prog.* **2020**, *19*, 1–11. [CrossRef]
11. Devjak Novak, S.; Šporar, E.; Baumgartner, S.; Vrečer, F. Characterization of physicochemical properties of hydroxypropyl methylcellulose (HPMC) type 2208 and their influence on prolonged drug release from matrix tablets. *J. Pharm. Biomed. Anal.* **2012**, *66*, 136–143. [CrossRef] [PubMed]
12. Burguera, E.F.; Xu, H.H.K.; Weir, M.D. Injectable and rapid-setting calcium phosphate bone cement with dicalcium phosphate dihydrate. *J. Biomed. Mater. Res. Part B Appl. Biomater.* **2006**, *77*, 126–134. [CrossRef]
13. Liu, W.; Zhang, J.; Rethore, G.; Khairoun, K.; Pilet, P.; Tancret, F.; Bouler, J.M.; Weiss, P. A novel injectable, cohesive and toughened Si-HPMC (silanized-hydroxypropyl methylcellulose) composite calcium phosphate cement for bone substitution. *Acta Biomater.* **2014**, *10*, 3335–3345. [CrossRef]
14. Adrian, G.; Mihai, M.; Vodnar, D.C. The Use of Chitosan, Alginate, and Pectin in the Biomedical and Food Sector- Biocompatibility, Bioadheviveness, and Biodegradability. *Polymers* **2019**, *11*, 1837.
15. Vunain, E.; Mishra, A.K.; Mamba, B.B. *Fundamentals of Chitosan for Biomedical Applications*; Elsevier: Amsterdam, The Netherlands, 2017; Volume 1, ISBN 9780081002575.
16. Lee, K.Y.; Mooney, D.J. Alginate: Properties and biomedical applications. *Prog. Polym. Sci.* **2012**, *37*, 106–126. [CrossRef]
17. Wu, H.; Du, S.; Lu, Y.; Li, Y.; Wang, D. The application of biomedical polymer material hydroxy propyl methyl cellulose(HPMC) in pharmaceutical preparations. *J. Chem. Pharm. Res.* **2014**, *6*, 155–160.
18. Zima, A.; Czechowska, J.; Szponder, T.; Ślósarczyk, A. In vivo behavior of biomicroconcretes based on α-tricalcium phosphate and hybrid hydroxyapatite/chitosan granules and sodium alginate. *J. Biomed. Mater. Res. Part A* **2020**, *108*, 1243–1255. [CrossRef]
19. Czechowska, J.; Zima, A.; Ślósarczyk, A. Comparative study on physicochemical properties of alpha-TCP / calcium sulphate dihydrate biomicroconcretes containing chitosan, sodium alginate or methylcellulose. *Acta Bioeng. Biomech.* **2020**, *22*. [CrossRef]
20. Hasan, M.L.; Kim, B.; Padalhin, A.R.; Faruq, O.; Sultana, T.; Lee, B.T. In vitro and in vivo evaluation of bioglass microspheres incorporated brushite cement for bone regeneration. *Mater. Sci. Eng. C* **2019**, *103*, 109775. [CrossRef] [PubMed]
21. Meng, D.; Dong, L.; Yuan, Y.; Jiang, Q. In vitro and in vivo analysis of the biocompatibility of two novel and injectable calcium phosphate cements. *Regen. Biomater.* **2019**, *6*, 13–19. [CrossRef]

22. Wu, T.; Shi, H.; Ye, J. Effect of PLGA/lecithin hybrid microspheres and β-tricalcium phosphate granules on the physicochemical properties, in vitro degradation and biocompatibility of calcium phosphate cement. *RSC Adv.* **2015**, *5*, 47749–47756. [CrossRef]
23. Nezafati, N.; Farokhi, M.; Heydari, M.; Hesaraki, S.; Nasab, N.A. In vitro bioactivity and cytocompatablity of an injectable calcium phosphate cement/silanated gelatin microsphere composite bone cement. *Compos. Part B Eng.* **2019**, *175*, 107146. [CrossRef]
24. Marudova, M.; MacDougall, A.J.; Ring, S.G. Pectin-chitosan interactions and gel formation. *Carbohydr. Res.* **2004**, *339*, 1933–1939. [CrossRef]
25. Amini, A.R.; Laurencin, C.T.; Nukavarapu, S.P. Bone tissue engineering: Recent advances and challenges. *Crit. Rev. Biomed. Eng.* **2012**, *40*, 363–408. [CrossRef] [PubMed]
26. Duan, J.; Liang, X.; Cao, Y.; Wang, S.; Zhang, L. High strength chitosan hydrogels with biocompatibility via new avenue based on constructing nanofibrous architecture. *Macromolecules* **2015**, *48*, 2706–2714. [CrossRef]
27. Neufeld, L.; Bianco-Peled, H. Pectin–chitosan physical hydrogels as potential drug delivery vehicles. *Int. J. Biol. Macromol.* **2017**, *101*, 852–861. [CrossRef] [PubMed]
28. Dziadek, M.; Zima, A.; Cichoń, E.; Czechowska, J.; Ślósarczyk, A. Biomicroconcretes based on the hybrid HAp/CTS granules, α-TCP and pectins as a novel injectable bone substitutes. *Mater. Lett.* **2020**, *265*, 127457. [CrossRef]
29. Chacón-Cerdas, R.; Medaglia-Mata, A.; Flores-Mora, D.; Starbird-Pérez, R. Synthesis of chitosan, pectin, and chitosan/pectin microspheres by two water-in-oil emulsion crosslinking methods. *Chem. Pap.* **2020**, *74*, 509–520. [CrossRef]
30. Andriani, Y. Retracted-Glutaraldehyde-Crosslinked Chitosan-Pectin Nanoparticles as a Potential Carrier for Curcumin Delivery and Its In Vitro Release Study. *Int. J. Drug Deliv.* **2015**, *7*, 167–173. [CrossRef]
31. Kolmas, J.; Kaflak, A.; Zima, A.; Ślósarczyk, A. Alpha-tricalcium phosphate synthesized by two different routes: Structural and spectroscopic characterization. *Ceram. Int.* **2015**, *41*, 5727–5733. [CrossRef]
32. Czechowska, J.; Zima, A.; Paszkiewicz, Z.; Lis, J.; Ślósarczyk, A. Physicochemical properties and biomimetic behaviour of α-TCP-chitosan based materials. *Ceram. Int.* **2014**, *40*, 5523–5532. [CrossRef]
33. Zima, A. Hydroxyapatite-chitosan based bioactive hybrid biomaterials with improved mechanical strength. *Spectrochim. Acta Part A Mol. Biomol. Spectrosc.* **2018**, *193*, 175–184. [CrossRef]
34. Standard Test Method for Time of Setting of Hydraulic-Cement Paste by Gillmore Needles. Available online: https://standards.globalspec.com/std/14347806/astm-c266-20 (accessed on 6 December 2021).
35. Kokubo, T.; Takadama, H. How useful is SBF in predicting in vivo bone bioactivity? *Biomaterials* **2006**, *27*, 2907–2915. [CrossRef]
36. Douglas, T.E.L.; Dziadek, M.; Schietse, J.; Boone, M.; Declercq, H.A.; Coenye, T.; Vanhoorne, V.; Vervaet, C.; Balcaen, L.; Buchweitz, M.; et al. Pectin-bioactive glass self-gelling, injectable composites with high antibacterial activity. *Carbohydr. Polym.* **2019**, *205*, 427–436. [CrossRef] [PubMed]
37. He, Z.; Zhai, Q.; Hu, M.; Cao, C.; Wang, J.; Yang, H.; Li, B. Bone cements for percutaneous vertebroplasty and balloon kyphoplasty: Current status and future developments. *J. Orthop. Transl.* **2015**, *3*, 1–11. [CrossRef] [PubMed]
38. Durucan, C.; Brown, P.W. Reactivity of α-tricalcium phosphate. *J. Mater. Sci.* **2002**, *37*, 963–969. [CrossRef]
39. Rabiee, S.M.; Baseri, H. Prediction of the setting properties of calcium phosphate bone cement. *Comput. Intell. Neurosci.* **2012**, *2012*, 1–8. [CrossRef]
40. Calcium Phosphate Bone Cements. Available online: https://www.intechopen.com/chapters/61543 (accessed on 6 December 2021).
41. Ewald, A.; Hösel, D.; Patel, S.; Grover, L.M.; Barralet, J.E.; Gbureck, U. Silver-doped calcium phosphate cements with antimicrobial activity. *Acta Biomater.* **2011**, *7*, 4064–4070. [CrossRef] [PubMed]
42. Schmitz, J.P.; Hollinger, J.O.; Milam, S.B. Reconstruction of bone using calcium phosphate bone cements: A critical review. *J. Oral Maxillofac. Surg.* **1999**, *57*, 1122–1126. [CrossRef]
43. Komath, M.; Varma, H.K.; Sivakumar, R. On the development of an apatitic calcium phosphate bone cement. *Bull. Mater. Sci.* **2000**, *23*, 135–140. [CrossRef]
44. Christel, T.; Kuhlmann, M.; Vorndran, E.; Groll, J.; Gbureck, U. Dual setting α-tricalcium phosphate cements. *J. Mater. Sci. Mater. Med.* **2013**, *24*, 573–581. [CrossRef]
45. Thibault, J.-F.; Ralet, M.-C. Pectins, their Origin, Structure and Functions. *Adv. Diet. Fibre Technol.* **2008**, *32*, 367–378. [CrossRef]
46. Taha, M.O.; Aiedeh, K.M.; Al-Hiari, Y.; Al-Khatib, H. Synthesis of zinc-crosslinked thiolated alginic acid beads and their in vitro evaluation as potential enteric delivery system with folic acid as model drug. *Pharmazie* **2005**, *60*, 736–742. [PubMed]
47. Bashir, S.; Zafar, N.; Lebaz, N.; Mahmood, A.; Elaissari, A. Hydroxypropyl methylcellulose-based hydrogel copolymeric for controlled delivery of galantamine hydrobromide in Dementia. *Processes* **2020**, *8*, 1350. [CrossRef]
48. Mickiewicz, R.A.; Mayes, A.M.; Knaack, D. Polymer-calcium phosphate cement composites for bone substitutes. *J. Biomed. Mater. Res.* **2002**, *61*, 581–592. [CrossRef] [PubMed]
49. Belalia, F.; Djelali, N.E. Rheological properties of sodium alginate solutions. *Rev. Roum. Chim.* **2014**, *59*, 135–145.
50. Silva, S.M.C.; Pinto, F.V.; Antunes, F.E.; Miguel, M.G.; Sousa, J.J.S.; Pais, A.A.C.C. Aggregation and gelation in hydroxypropyl-methyl cellulose aqueous solutions. *J. Colloid Interface Sci.* **2008**, *327*, 333–340. [CrossRef]
51. Perez, R.A.; Kim, H.W.; Ginebra, M.P. Polymeric additives to enhance the functional properties of calcium phosphate cements. *J. Tissue Eng.* **2012**, *3*, 2041731412439555. [CrossRef] [PubMed]

52. Wang, Y.; Xie, Y.; Xu, D.; Lin, X.; Feng, Y.; Hong, Y. Hydroxypropyl Methylcellulose Reduces Particle Adhesion and Improves Recovery of Herbal Extracts During Spray Drying of Chinese Herbal Medicines. *Dry. Technol.* **2014**, *32*, 557–566. [CrossRef]
53. Chatzistavrou, X.; Newby, P.; Boccaccini, A.R. *Bioactive Glass and Glass-Ceramic Scaffolds for Bone Tissue Engineering*; Woodhead Publishing Limited: Cambridge, UK, 2011; ISBN 9781845697686.
54. Noshadi, I.; Walker, B.W.; Portillo-Lara, R.; Sani, E.S.; Gomes, N.; Aziziyan, M.R.; Annabi, N. Engineering Biodegradable and Biocompatible Bio-ionic Liquid Conjugated Hydrogels with Tunable Conductivity and Mechanical Properties. *Sci. Rep.* **2017**, *7*, 4345. [CrossRef] [PubMed]
55. Czechowska, J.; Zima, A.; Siek, D.; Ślósarczyk, A. Influence of sodium alginate and methylcellulose on hydrolysis and physico-chemical properties of α-TCP based materials. *Ceram. Int.* **2018**, *44*, 6533–6540. [CrossRef]
56. Guarino, V.; Caputo, T.; Altobelli, R.; Ambrosio, L. Degradation properties and metabolic activity of alginate and chitosan polyelectrolytes for drug delivery and tissue engineering applications. *AIMS Mater. Sci.* **2015**, *2*, 497–502. [CrossRef]
57. Joshi, S.C. Sol-gel behavior of hydroxypropyl methylcellulose (HPMC) in ionic media including drug release. *Materials* **2011**, *4*, 1861–1905. [CrossRef] [PubMed]

Publikacja 3 – *„The influence of silane coupling agents on the properties of α-TCP-based ceramic bone substitutes for orthopaedic applications”*

RSC Advances

ROYAL SOCIETY OF CHEMISTRY

PAPER

View Article Online
View Journal | View Issue

Cite this: *RSC Adv.*, 2023, **13**, 34020

The influence of silane coupling agents on the properties of α-TCP-based ceramic bone substitutes for orthopaedic applications

Piotr Pańtak, * Joanna P. Czechowska and Aneta Zima *

Biomaterials based on α-TCP are highly recommended for medical applications due to their ability to bond chemically with bone tissue. However, in order to improve their physicochemical properties, modifications are needed. In this work, novel, hybrid α-TCP-based bone cements were developed and examinated. The influence of two different silane coupling agents (SCAs) – tetraethoxysilane (TEOS) and 3-glycidoxypropyl trimethoxysilane (GPTMS) on the properties of the final materials was investigated. Application of modifiers allowed us to obtain hybrid materials due to the presence of different bonds in their structure, for example between calcium phosphates and SCA molecules. The use of SCAs increased the compressive strength of the bone cements from 7.24 ± 0.35 MPa to 12.17 ± 0.48 MPa. Moreover, modification impacted the final setting time of the cements, reducing it from 11.0 to 6.5 minutes. The developed materials displayed bioactive potential in simulated body fluid. Presented findings demonstrate the beneficial influence of silane coupling agents on the properties of calcium phosphate-based bone substitutes and pave the way for their further *in vitro* and *in vivo* studies.

Received 4th September 2023
Accepted 11th November 2023

DOI: 10.1039/d3ra06027f

rsc.li/rsc-advances

1. Introduction

Alpha tricalcium phosphate (α-TCP) due to its unique properties has been intensively studied as a promising material for bone tissue replacement and regeneration.[1–3] Due to its chemical similarity to the inorganic part of bone tissue and self-setting properties α-TCP is commonly used as a main component of calcium phosphate-based cements (CPCs).[4] CPCs possess excellent biocompatibility, osteoconductivity, and ability to bond with natural bone tissue.[5,6] However, despite their numerous advantages, they still have some drawbacks, including their relatively low mechanical strength and fast resorption rates.[7,8] To address these limitations, various modifications of powder and liquid phase of CPCs have been proposed.

α-TCP powder can be modified in different ways, for example through the incorporation of dopants, such as zinc, magnesium, or strontium, or by mixing with other calcium phosphate powders, such as β-TCP or hydroxyapatite.[7–10] A common modification of CPCs formulation is application of different natural polysaccharides, which additionally provides injectability of cementitious pastes.[11–14] Recently, it has been reported that calcium phosphates can be modified with silane coupling agents (SCAs), which are organosilicon compounds. Silane coupling agents can bond chemically to both the inorganic and organic surfaces, forming strong covalent bonds and improving the interfacial adhesion between different materials.[16,17] SCAs have been widely used to modify the surface properties of various materials, including ceramics, polymers, and metals, to improve their performance in medical applications.[18–22]

Suppakarn *et al.*[23] modified hydroxyapatite (HA) powders with different silane coupling agents, including γ-aminopropyl triethoxysilane (APES), methyl trimethoxysilane (MTMS), and γ-glycidoxypropyl trimethoxysilane (GPMS) to obtain HA/polypropylene composites. The results demonstrated that the silane treatment enhanced the interaction between the HA and PP, resulting in an increase in the stiffness of the composite material. The γ-aminopropyl triethoxysilane (APES) was found to be the most effective silane coupling agent for this application. Ji *et al.*[24] developed hydroxyapatite-based scaffolds by modifying the surface of HA with different silane coupling agents: 3-methacryloxypropyltrimethoxysilane, 3-aminopropyltrimethoxysilane and carboxyethylsilanetriol sodium salt. The using of SCAs modifiers enhanced mechanical strength up to 30 MPa, which was explained by the presence of electrostatic bonds between components. Furthermore, the functionalized silane-coated HAp scaffolds displayed excellent biocompatibility. Ghorbani *et al.*[25] incorporated 3-glycidoxypropyl trimethoxysilane (GPTMS) as a bioactive inorganic crosslinker in chitosan-polyvinyl alcohol scaffolds which led to the improvement of mechanical strength, water uptake, and biodegradation properties. It has been demonstrated that an increase in GPTMS content enhanced the compressive strength of samples, while reducing water uptake and biodegradation of materials. What is

Faculty of Materials Science and Ceramics, AGH University of Science and Technology, Mickiewicza Av. 30, 30-058 Kraków, Poland. E-mail: pantak@agh.edu.pl; azima@agh.edu.pl

more obtained composites possessed excellent biological properties confirmed by different assays. Another common SCA is tetraethoxysilane (TEOS) which is used in the development of biomaterials due to its ability to form biocompatible silica coatings, enhancing their biocompatibility and stability within the cellular environment. Tallia *et al.*[26] developed promising SiO_2–CaO/PTHF/PCL-diCOOH hybrid material with improved mechanical properties, enhanced dissolution behaviour, and cell attachment capability. Fuh *et al.*[27] described novel TEOS treatment method that enhances micro-porosity, reduces sintering shrinkage, and improves biodegradation in hydroxyapatite (HA) scaffolds, making it a promising technique for HA manufacturing.

Despite the potential advantages of using silane coupling agents to modify calcium phosphates powders, to the best of our knowledge, no modification of α-TCP has been carried out yet. The simultaneous hydrolysis of α-TCP and silane coupling agent may potentially lead to the formation of a novel α-TCP-based hybrid materials with improved properties due to presence of additional bonds between the components. The SCAs during hydrolysis can react with the hydroxyl groups on the surface of calcium phosphates, forming covalent bonds and modifying the properties of material. Such interactions, have been described previously in other biomaterials.[28,29] In this work, two different SCAs were examined as potential moderators of interactions between materials components. We believe that the use of SCAs can lead to favourable properties of hybrid, α-TCP-based bone cements due to the formation of new bonds in the materials' structure.

The aim of this study was to develop bone cements on the basis of α-tricalcium phosphate and investigate the influence of tetraethoxysilane (TEOS) and 3-glycidoxypropyl trimethoxysilane (GPTMS) on their physicochemical and biological properties.

2. Materials and methods

2.1. Synthesis of α-TCP

The initial α-TCP powder was synthesized by the wet chemical method described previously.[30] As reagents, $Ca(OH)_2$ (≥99.5%, POCH, Gliwice, Poland) and H_3PO_4 (85.0%, POCH, Gliwice, Poland) were applied. In brief, the α-TCP precipitate after synthesis was dried, sintered above 1250 °C (5 h), ground in an attritor mill (3 h), and sieved below 63 μm.

2.2. Modification of α-TCP

The α-TCP powder was modified with 1, 2 and 5 wt% TEOS (T) (≥99.5%, Sigma-Aldrich, St. Louis, MO, USA) or GPTMS (G) (≥98.0%, Sigma-Aldrich, St. Louis, MO, USA) (Table 1). To modify the initial powders, solutions of the appropriate silane coupling agents were prepared using anhydrous ethanol as a solvent (99.8%, POCH, Gliwice, Poland). The alcoholic solvent was used to avoid hydrolysis of the calcium phosphate powders and SCAs. After adding the powders to the SCA solutions, they were stirred on a magnetic stirrer for 4 hours. The resulting precipitates were subjected to aging (1 h) and subsequently silanised by thermal treatment at 115 °C (4 h). Prior to preparing the samples, the powders were sieved through a sieve below 63 μm.

Table 1 Composition of the initial powders

Label	Description
α-TCP	Non-modified α-TCP powder
α-TCP/T1	α-TCP powder modified with 1 wt% of TEOS
α-TCP/T2	α-TCP powder modified with 2 wt% of TEOS
α-TCP/T5	α-TCP powder modified with 5 wt% of TEOS
α-TCP/G1	α-TCP powder modified with 1 wt% of GPTMS
α-TCP/G2	α-TCP powder modified with 2 wt% of GPTMS
α-TCP/G5	α-TCP powder modified with 5 wt% of GPTMS

2.3. Bone cements preparation

Seven types of materials were prepared by mixing the solid phase, *i.e.*, non-modified and SCA-modified α-TCP with the liquid phase. The initial composition of the prepared cements, as well as a liquid to powder ratio (L/P), are presented in Table 2.

2.4. Methods

2.4.1. Specific surface area. The specific surface area (SSA) of the initial α-TCP and SCAs-modified α-TCP powders was determined by the BET (Brunauer–Emmett–Teller) method using accelerated surface area and porosimetry system ASAP 2010 (Micromeritics, Norcross, GA, USA).

2.4.2. Powders size distribution and zeta potential. The size distribution of the initial α-TCP and SCAs-modified α-TCP powders as well as zeta potential was based on Brownian motion and the Dynamic Light Scattering (DLS) technique and combination of electrophoresis and the Laser Doppler Velocimetry technique using system Zetasizer Nano-ZS (Malvern Panalytical, Malvern, UK).

2.4.3. Chemical and phase composition. The X-ray fluorescence method (XRF) was applied to check the chemical composition of the initial powders (WDXRF Axios Max, PANalytical, Malvern, UK). The X-ray diffraction (XRD) analysis was performed using Cu Kα radiation (1.54 Å) at 30 kV and 10 mA. The analysis was conducted in the 2θ range of 10–60° at 0.04 intervals with a scanning speed of 2.5° min^{-1} using D2 Phaser diffractometer (Bruker, Ballerica, MA, USA). The obtained diffractograms were compared with the International Centre for Diffraction Data α-TCP (00-009-0348) and hydroxyapatite (HA;

Table 2 Composition of the bone cements

Label	Powder phase	Liquid phase	L/P [g g^{-1}]
Cement	α-TCP	Distilled water	0.45
Cem_T1	α-TCP/T1		
Cem_T2	α-TCP/T2		
Cem_T5	α-TCP/T5		
Cem_G1	α-TCP/G1		
Cem_G2	α-TCP/G2		
Cem_G5	α-TCP/G5		

01-076-0694) to identify the crystalline phases. TOPAS software (Bruker, Ballerica, MA, USA) was used for phase quantification based on Rietveld refinement. All measurements were performed in triplicate. The mean ± standard deviation (SD) was used to present the results.

FT-IR and Raman spectroscopy methods were used for the characterization of obtained non-modified and modified powders, as well as the hardened bone cements. FTIR investigations of materials were conducted on a BioRad FTS 6000 spectrometer (Bruker, Ballerica, MA, USA) with the Raman attachment (NdYAG laser excitation line of 1064 nm) in the wavenumber range of 3800–200 cm^{-1}. The transmission technique was used and the samples were prepared as standard KBr pellets. This methodology was used to obtain an accurate and detailed understanding of the chemical and structural properties of the materials, which is crucial for determining their suitability for specific biomedical applications.

2.4.4. Setting times. The setting times were determined in accordance with the ASTM C266-20 standard, using Gilmore Needles (Humbold MFG Co., Norridge, IL, USA).[31] The Gillmore Apparatus, consisting of two steel-weighted needles, was used for this purpose. The initial setting needle weighed 113 g and had a diameter of 2.12 mm, while the final setting needle weighed 453.6 g and had a diameter of 1.06 mm. To determine the setting times, the cementitious pastes were placed in a special form measuring 8 mm × 10 mm × 5 mm, and the needle of the apparatus was lightly applied to its surface. The setting time was measured as the point at which the needle penetrated the surface without leaving a complete circular mark. All experiments were carried out at room temperature (22 ± 1 °C), and the results were presented as the average of three measurements, along with their corresponding standard deviations (SD).

2.4.5. Mechanical strength. To determine the compressive strength of the materials, cylindrical samples with a height of 12 mm and diameter of 6 mm were tested using a universal material testing machine (Instron 3345, Norwood, MA, USA) at a crosshead displacement rate of 1 mm min^{-1}. The compressive strength results were expressed as the mean value ± the standard deviation (SD) of twenty-fold determinations. To determine if there were any statistically significant differences between the materials, a one-way ANOVA followed by post hoc Tukey's Honest Significant Difference (HSD) test was applied with a significance level of $p < 0.01$.

2.4.6. Microstructure. For microstructure observations of the fractured samples, scanning electron microscopy (SEM) was employed using a PhenomPure instrument (Thermo Fisher Scientific, Waltham, MA, USA). To evaluate the bioactive potential of the materials, their surfaces were assessed after 7 days of incubation in simulated body fluid (SBF) at 37 °C. Before examination, the samples were coated with a thin layer of gold film using a low deposition rate to prevent any charge build-up and to enhance the imaging resolution.

2.4.7. *In vitro* bioactivity and chemical stability. To evaluate the chemical stability and bioactivity of the bone cements, they were incubated in distilled water or simulated body fluid (SBF) prepared according to Kokubo's protocol.[32] Cylindrical samples were placed in containers with 20 mL SBF or water and stored at 37 °C. The chemical stability of the materials was determined by measuring the pH and ionic conductivity of the solutions around incubated samples at various time intervals. Measurements were taken using a Seven Compact Duo pH/conductometer (Mettler Toledo, Columbus, OH, USA). Results were expressed as the average value of three measurements ± standard deviation (SD). After immersion, the samples were removed from solution, rinsed with distilled water, and dried at temperatures below 40 °C. To confirm the bioactive potential, the surfaces of the samples were observed using SEM.

3. Results and discussion

3.1. Specific surface area

The specific surface area is an important parameter for characterizing the performance of catalysts, adsorbents, and other porous materials, as it can affect the reactivity, selectivity, and stability.[33,34] The specific surface area of obtained powders is shown in Fig. 1.

The specific surface area of the obtained calcium phosphate powders was in the range of 1.81 ± 0.04 to 3.67 ± 0.04 and decreased with increasing amounts of the silane coupling agent. The highest value of specific surface area was noticed for non-modified α-TCP powder. From the results obtained, it can be seen that the specific surface area of the powders decreases with use and increasing amount of silane coupling agent. Generally, the specific surface area of α-TCP ranged from 2.0 to 11.0 g m^{-2} and depends on many factors, such as synthesis, processing routes and presence of modifiers.[35,36] The decreasing value of the specific surface area of silane coupling agent-modified powders is due to the confinement of micropores in the powder grains with the silane coupling agents. The silane coupling agents form a thin layer on the surface of the grains, which reduce the overall surface area of calcium phosphate powders. Similar results were obtained by Sonn *et al.*[37] and Chuang *et al.*,[38] who modified the surface of silica nanoparticles

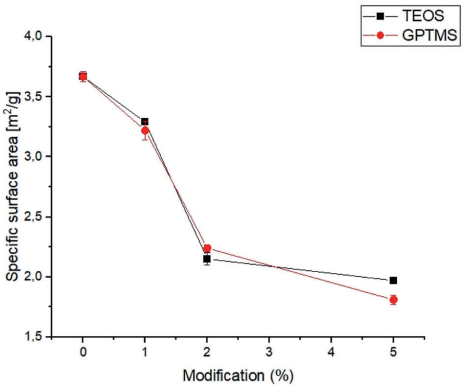

Fig. 1 Specific surface area *vs.* amount of used silane coupling agent.

with various coupling agents. They have also shown that the specific surface area of nanoparticles decreased with increasing concentration of the silane coupling agents due to reduction of micropores in the powders.

3.2. Powders size distribution and zeta potential

The powder size distribution and zeta potential are crucial parameters in powder technology, especially for calcium phosphates, as they can affect the properties and performance of the powders. Optimal values of this parameters depend on specific requirements. The powder size distribution (Fig. 2) and zeta potential (Table 3) of obtained powders are shown below.

It was observed that the surface modification of the α-TCP powders with both silane coupling agents changed a powders size distribution. For non-modified α-TCP pore size were in the range of approximately 1.0 to 100.0 μm. However, the SCA modification caused change of powders size distribution to the range between ~1.0 to 10.0 μm. When silane coupling agents are used to modify the surface of the powder particles, they can form a monolayer or multilayer made of organic molecules, which can reduce the surface energy and enhance the dispersibility of the particles in the surrounding medium.[39] Additionally, as TEOS and GPTMS has a hydrophobic functional groups, what can reduce the water affinity of the particle surface and promote the formation of smaller agglomerates.[40–42] The differences in zeta potential measurements also were observed. The non-modified powder possessed the least electro-negative zeta potential (*i.e.* −4.65 ± 0.3 mV). However, the surface modification caused changes in zeta potential values. As in the case of powders size distribution the changes in zeta potential values were caused by the presence of layer of SCA molecules, which can reduce the electrostatic repulsion between CaPs particles and decrease the zeta potential[43] (up to −24.4 ± 0.9 mV for α-TCP/G5).

Table 3 Zeta potential of obtained powders

Powder label	Zeta potential [mV]
α-TCP	−4.65 ± 0.3
α-TCP/T1	−9.67 ± 0.5
α-TCP/T2	−12.72 ± 0.3
α-TCP/T5	−16.31 ± 0.7
α-TCP/G1	−18.3 ± 1.5
α-TCP/G2	−21.2 ± 1.0
α-TCP/G5	−24.4 ± 0.9

3.3. Chemical and phase composition

The XRD analysis revealed that the initial α-tricalcium phosphate and silane coupling agents modified α-TCP powders composed mainly of α-TCP (97–98 wt%) and a small amount of hydroxyapatite phase (2–3 wt%) (Fig. 3A). As expected, the modification of the powders *via* SCAs in anhydrous medium did not result in hydrolysis of α-TCP to non-stoichiometric hydroxyapatite. Additionally, by using silane coupling agents to modify the surface of the powders, silicon ions were introduced. The applied method of modification allowed for introduction to α-tricalcium phosphate, and no other crystalline phases containing silicon were observed. The X-ray fluorescence method confirmed the presence of silicon in all modified

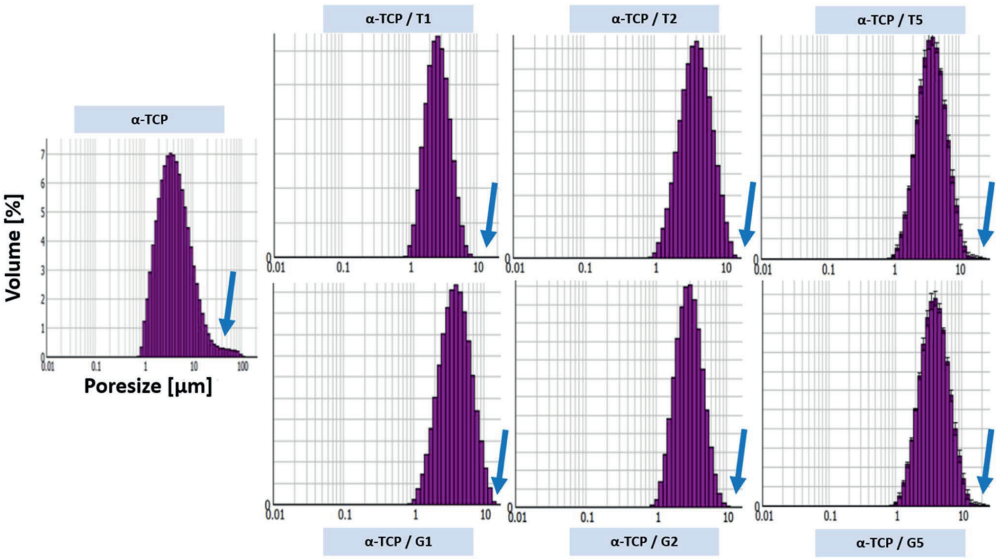

Fig. 2 Powders size distribution of non-modified and modified α-TCP powders.

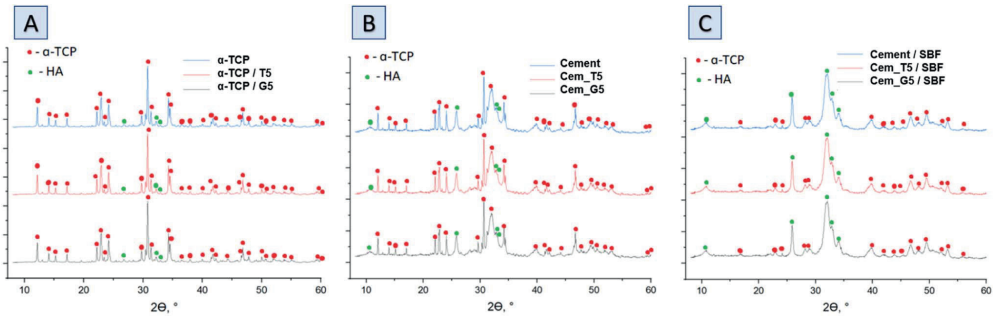

Fig. 3 Diffractograms of obtained materials: powders (A), bone cements after setting and hardening in air for 7 days (B) and bone cements incubated in SBF for 7 days (C).

powders and in amount of 0.035 ± 0.001 wt% for non-modified powder. As expected, the silicon content increased with the increasing amount of SCAs used and was 0.218 ± 0.004 wt% and 0.280 ± 0.002 wt% for powders modified with 5 wt% of TEOS and GPTMS respectively. Presence of silicon may improve the biological properties of the final material, such as osteoconductivity.[44] The modification allowed the powder to be enriched with silicon ions after α-TCP synthesis. Overwhelming majority of scientific publications describe the introduction of silicon ions into calcium phosphate-based materials at the synthesis stage.[45]

The diffractograms of bone cements after setting and hardening in air for 7 days (Fig. 3B and Table 4), as well as cements incubated in SBF for 7 days (Fig. 3C and Table 3), revealed two crystalline phases, *i.e.*, α-TCP and hydroxyapatite, regardless the amount of the silane coupling agents. It has been demonstrated that in the simulated body fluid, the α-TCP phase is thermodynamically metastable and almost completely hydrolyses to nonstoichiometric hydroxyapatite. This transformation is accompanied by a change in the chemical composition and crystallographic structure of the material, which can affect its properties and behaviour in biological and biomedical applications.[46]

Infrared spectra of initial powders (Fig. 4A), cements after setting and hardening (Fig. 4B) as well as cements after 7 days of incubation in simulated body fluid (Fig. 4C) revealed the presence of several characteristic bands, which provided valuable insights into the composition and structure of the materials. Similar results were obtained for all SCAs concentrations, and no significant differences were observed for the various amount of silane coupling agents. Specifically, bands at around 565 and 605 cm^{-1} were observed and assigned to triply degenerate υ4 P–O–P bending modes. Additionally, a strong doublet near 600 and 670 cm^{-1} was connected to SO_4 bending vibrations (υ4). Interestingly, the coincidence of SO_4 and PO_4 bending vibration bands was observed at around 603 cm^{-1}. The other important bands were observed at 1060 cm^{-1} and around 1040 cm^{-1}, which were assigned to υ3 non-symmetric stretching modes of P–O and are characteristic of calcium phosphates. Furthermore, a band at 962 cm^{-1} was observed, which was associated with the υ1 symmetric stretching vibration of P–O bands. In addition, a wide band around 3500 cm^{-1} indicates the presence of residual water in the studied samples. Low concentration of silane coupling agents in the cements, as well as an overlapping of bands, may explain the lack of visible peaks of Si–O–Si, Si–OH, Si–C and C–H bands assigned to SCAs.[47] In addition bone cements after setting and hardening in air, as well as after incubation in SBF possessed the absorption bands arising from HPO_4^{2-}. The weak band at around 870 cm^{-1} assigned as P–OH stretch of HPO_4^{2-} to calcium deficient materials. Thus, obtained data confirmed the presence of calcium-deficient hydroxyapatite (CDHA) in material at the same time shows its bioactive potential due to hydrolysis of α-TCP to non-stoichiometric hydroxyapatite.

Raman spectra of non-modified powder and cements (Fig. 5A), TEOS-modified powder and cements (Fig. 5B) as well as TEOS-modified powder and cements (Fig. 5C) revealed the presence of bands characteristic for calcium phosphates, as well as band unique for TEOS and GPTMS. Specifically, CPCs based on α-TCP are characterised by bands around 450 and 560 cm^{-1} attributed to the symmetric stretching and bending modes of the Ca–O bonds. This bands may shift slightly depending on the conditions. Additionally, phosphate groups at around 960, 1005, and 1080 cm^{-1} are attributed to the symmetric stretching, bending, and asymmetric stretching modes, respectively. The small amounts of carbonate ions, which are confirmed by bands at around 1060 and 1415 cm^{-1}. These bands are attributed to the symmetric stretching and bending modes of the carbonate

Table 4 Phase composition of tested bone cements

Material label	After 7 days of setting and hardening in air (22 ± 1 °C)		After 7 days of incubation in SBF (37 ± 1 °C)	
	α-TCP	Hydroxyapatite	α-TCP	Hydroxyapatite
Cement	90.7 ± 0.5	9.3 ± 0.5	10.4 ± 1.0	89.6 ± 1.0
Cem_T5	87.9 ± 1.0	12.1 ± 1.0	6.4 ± 1.0	93.6 ± 1.0
Cem_G5	85.4 ± 1.0	14.6 ± 1.0	5.8 ± 0.5	94.2 ± 0.5

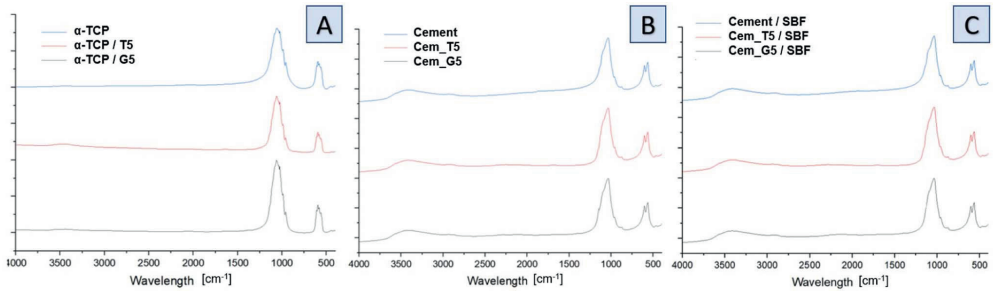

Fig. 4 FT-IR spectra of obtained materials: powders (A), bone cements after setting and hardening in air for 7 days (B) and bone cements incubated in SBF for 7 days (C).

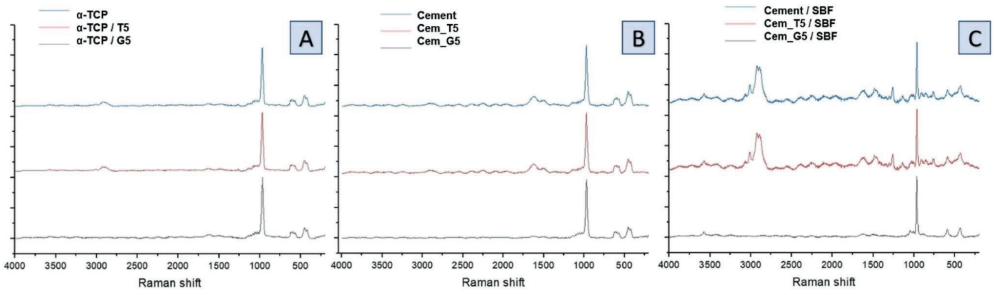

Fig. 5 Raman spectra of obtained materials: non-modified powder and cements (A), TEOS-modified powder and cements (B) and GPTMS-modified powder and cements (C).

ion, especially for cements after its incubation in SBF. The presence of remaining water in CPCs was also confirmed by the presence of characteristic bands at around 3300 and 3500 cm^{-1}. In addition to the bands characteristic for calcium phosphates, bands characteristic for silane coupling agents also were observed. TEOS exhibits a Si–O–Si band at around 1100 cm^{-1}, which is attributed to the symmetric stretching mode of the Si–O–Si bond. It also exhibits band at around 2940 cm^{-1}, attributed to the stretching mode of the Si–CH_3 bond and band around 1250 cm^{-1} is assigned to the stretching mode of the Si–O–CH_3 bond in TEOS. The presence of Si–OH groups in TEOS were confirmed by bands around 3600–3700 cm^{-1}, which is attributed to their stretching mode. On the other hand, GPTMS presence in obtained materials was confirmed by the presence of Raman band at around 910 cm^{-1}, attributed to the stretching mode of the CH_2–O bond. This characteristic bond of epoxide groups is more visible for incubated materials. Similarly, to TEOS, GPTMS also exhibits bands assigned to a Si–O–Si (~1100 cm^{-1}), Si–CH_3 (~2940 cm^{-1}) and Si–O–CH_2 (~1250 cm^{-1}).

During the simultaneous hydrolysis of α-TCP and silane coupling agents several potential new bonds can be formed between the coupling agents and the surface of the α-TCP particles. This includes the Si–O bond, which can be formed when the silanol group of the TEOS or GPTMS molecule reacts with the groups on the surface of CaPs grains. The stretching vibration of the Si–O bond typically appears between 1000–1200 cm^{-1}, while the stretching vibration of the –OH appears around 3500 cm^{-1}. The formation of the Si–O bond results in a shift of the Si–O stretching vibration. Ribeiro *et al.*[48] demonstrated interaction between ultra-fine calcium carbonate and natural rubber by applying a superficial treatment to the calcium carbonate which provides materials with improved properties. They observed the similar bonds between coupling agents and calcium carbonate groups. Bi *et al.*[49] investigated the effects of trimethoxysilanes on the properties of $CaCO_3$-based composites. They confirmed the presence of chemical interaction between components, which allow to improve the tensile strength and abrasion resistance of the materials. Moreover, Bi *et al.* stated that the silanol groups of two coupling agents react with each other and form a covalent bond Si–O–Si, creating the hybrid material. Purcar *et al.*[50] synthesized hybrid nanomaterials based on zinc oxide *via* the sol–gel method, using different silane coupling agents. They confirmed the presence of Si–O–Si bands in the materials and showed their positive influence on the materials' properties. Furthermore, the

presence of Si–O–P bond at 1000 and 1200 cm^{-1} can confirm the interactions between the silanol group on the TEOS or GPTMS molecule and the phosphate groups, forming a covalent bond between the silicon atom of the coupling agent and the oxygen atom of the phosphate group. These bonds can enhance the further properties of the materials, such as mechanical strength and bioactivity. In addition, the introduction of coupling agents to cements composition may allow for its further modification using polymers with different functional groups that can also react with SCAs.

Table 5 Setting times of developed materials

Material	Initial setting time (T_i) [min]	Final setting time (T_f) [min]
Control	6.5 ± 0.5	11.0 ± 1.0
T1	6.5 ± 0.5	11.5 ± 0.5
T2	5.0 ± 1.0	9.0 ± 0.5
T5	4.0 ± 0.5	7.5 ± 1.0
G1	5.0 ± 0.5	9.0 ± 1.0
G2	4.0 ± 1.0	7.5 ± 0.5
G5	3.5 ± 1.0	6.5 ± 0.5

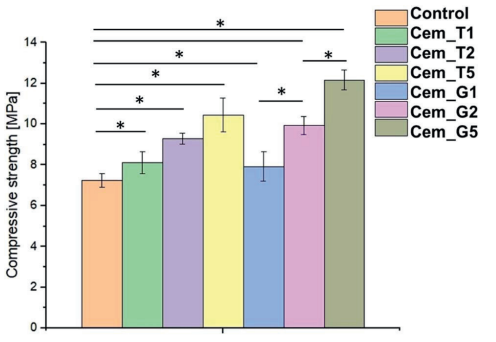

Fig. 6 Compressive strength of obtained bone cements after 7 days of setting and hardening (* – statistically significant difference, $p < 0.01$).

3.4. Setting times

Setting time is critical parameter for calcium phosphate cements because it affects their handling, injectability, and mechanical properties.[51] The setting times of the obtained bone cements depended on the amount of used silane coupling agent and varied between 3.5 and 6.5 min (initial setting time) and 6.5 and 11.5 min (final setting time) (Table 5).

The results showed that the addition of silane coupling agent used for calcium phosphate modification decreased both, the initial and final setting time. The process responsible for setting and hardening of calcium phosphate cements involves α-TCP hydrolysis. When α-TCP reacts with water, it forms calcium-deficient apatite, as described by the following eqn (1):[52,53]

$$3Ca_3(PO_4)_2 + H_2O \rightarrow Ca_9(PO_4)_5(HPO_4)OH \quad (1)$$

Several factors can affect the setting reaction of bone cements, such as the amount of highly reactive α-TCP phase in the material, such as: the presence of setting accelerators in the liquid phase, the type and amount of polymeric additive in the liquid or powder phase, and α-TCP powder modifications.[54] Results of our studies revealed that the presence of silane coupling agents also influence the setting time values. It seems that SCAs accelerate the setting process of α-TCP-based bone cements. Previous studies have demonstrated that the incorporation of silicon into calcium phosphate cement alters its properties in comparison to the non-modified cements. For example, Czechowska *et al.*[45] developed calcium phosphate-based bone fillers based on silicon doped α-TCP with hybrid, gold-modified granules. Their study showed a shortening of both initial and final setting times for silicon-containing materials. The study by Wei *et al.*[55] confirmed a higher solubility of silicon-modified α-TCP, additionally Mestres *et al.*[56] found a faster hydrolysis of silicon-modified α-TCP in comparison with non-modified powders. All this finding corresponds with the results obtained during experiments. Although the measured setting times were reduced due to the use of a silane coupling agent, their values remained in the range suitable for clinical application (4–8 min for initial setting, up to 15 min for final setting time[46]).

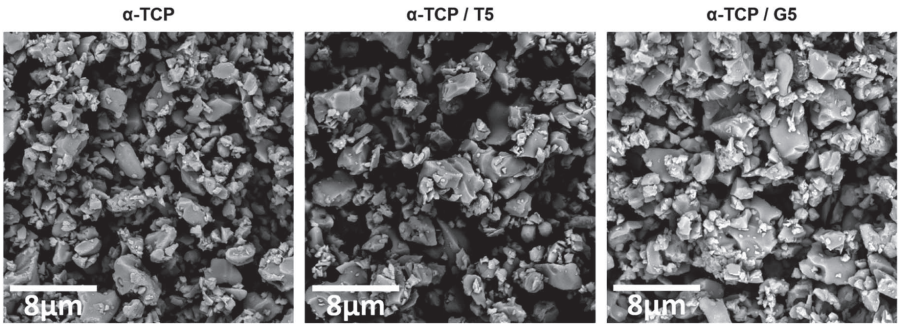

Fig. 7 Morphology of initial α-TCP powders (magnification: 100 00×).

3.5. Mechanical strength

The mechanical strength of calcium phosphate-based bone cements is important parameter, because it determines the ability of the cement to withstand the mechanical forces and stresses in the bone environment, ensuring successful bone repair and regeneration. The compressive strength of obtained biomaterials ranged from 7.24 ± 0.35 MPa to 12.17 ± 0.48 MPa (Fig. 6). The results of the mechanical tests revealed that the presence of SCAs modifier positively affected the compressive strength of the bone cements. The highest values were obtained for material G5 (with 5 wt% of GPTMS). Based on the results of a one-way ANOVA and a subsequent Tukey HSD post-hoc analysis, it can be concluded that the observed differences between the control and SACs modified materials were statistically significant.

The silane coupling agents as modifiers of α-TCP may provide the mechanical improvement of obtained bone cements due to formation of additional bonds in materials' structure during the simultaneous hydrolysis of α-TCP and SCAs. The increase in the mechanical strength of the developed cements is possibly related to the chemical interactions between their components and formation of additional Si–O–Si, Si–O, or Si–O–P bonds what led to creation of hybrid-type materials. Similar, positive influence of using silane coupling agents on mechanical behaviour of different biomaterials where previously described in the literature. In the study by Ma *et al.*[57] the trimethoxysilane was used as a modifier of hydroxyapatite/polyether ether ketone (PEEK) composites to obtain materials with improved mechanical strength. Furthermore, Ma *et al.* shoved promising results from *in vivo* studies. Vaz *et al.*[58]

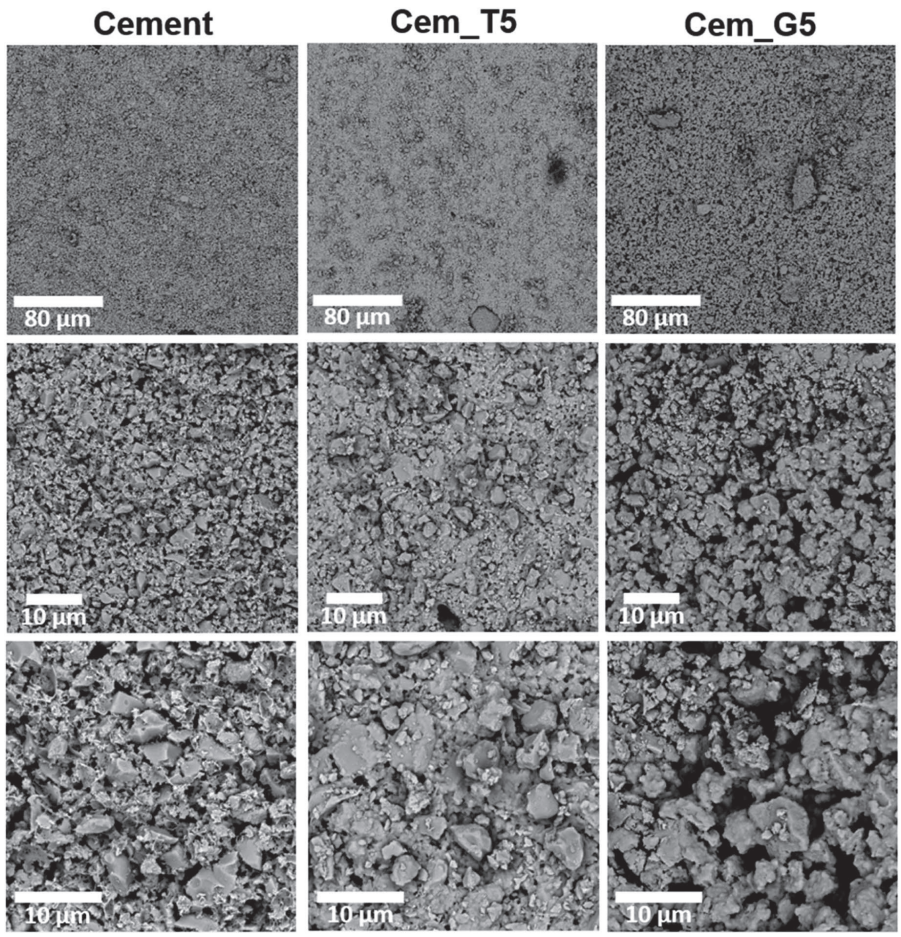

Fig. 8 Microstructure of obtained materials after seven days of setting and hardening in air (cross-sections, magnifications: 1000, 5000, 100 00×).

shoved beneficial application of different coupling agents to obtain starch/ethylene-vinyl alcohol copolymer/hydroxyapatite composites characterised by increased mechanical resistance due to improved adhesion between material components. Harper *et al.*[59] presented the beneficial properties of hydroxyapatite loaded acrylic bone cements. By modification of hydroxyapatite by using 3-trimethoxysilylpropylmethacrylate authors obtained materials characterised by increased mechanical parameters. It should be noted that the compressive strength of cancellous bone ranges from approximately 4 to 12 MPa.[60] Thus, the hybrid-type, SACs modified materials developed in our study possessed mechanical strength suitable for implantation in non-load or low-load bearing locations.

3.6. Microstructure

To evaluate the potential of the developed materials as a bone tissue substitutes and detect any microstructural defects, their microstructure was examined. The initial powders and obtained biomaterials were observed using scanning electron microscopy (SEM) after setting and hardening in air, as well as after incubation in SBF.

SEM observations revealed that the morphology of powder grains of non-modified and TEOS or GPTMS modified α-TCP did not differ significantly (Fig. 7).

The set and hardened materials possessed compact, homogenous microstructure formed by cementitious matrix with visible micropores (Fig. 8). Regardless the amount of silane coupling agent no differences in materials' microstructure were observed. Similar microstructures of α-TCP-based bone cements can be found in other studies.[61]

After 7 days of incubation in simulated body fluid (SBF) all prepared materials were completely covered by plate-like apatitic structure confirmed their bioactivity *in vitro* according to Kokubo and Takadama's criteria (Fig. 9).[62] Furthermore, the microstructure analysis after incubation showed that the developed materials retained their bioactive potential despite the using silane coupling agents as a modifier of α-TCP powders.

3.7. *In vitro* bioactivity and chemical stability

The chemical stability of implantable biomaterials is crucial parameter in determining their potential clinical application. The pH changes of the SBF during the samples' immersion are illustrated in Fig. 10.

The pH changes of SBF around incubated samples remained close to the physiological values and ranged from 7.34 to 7.40. The addition of TEOS and GPTMS only slightly influenced the solution's pH values. Similar pH values of incubated calcium phosphate-based bone substitutes were observed elsewhere.[15]

Ionic conductivity during the incubation in distilled water of the control material was in the range of ~72–81 μS cm^{-1}. A CPCs modifiers caused slightly increase in ionic conductivity to the range of ~73–87 μS cm^{-1} for TEOS, and to the range of ~84–96 for GPTMS (Fig. 11). This phenomenon can be explained by

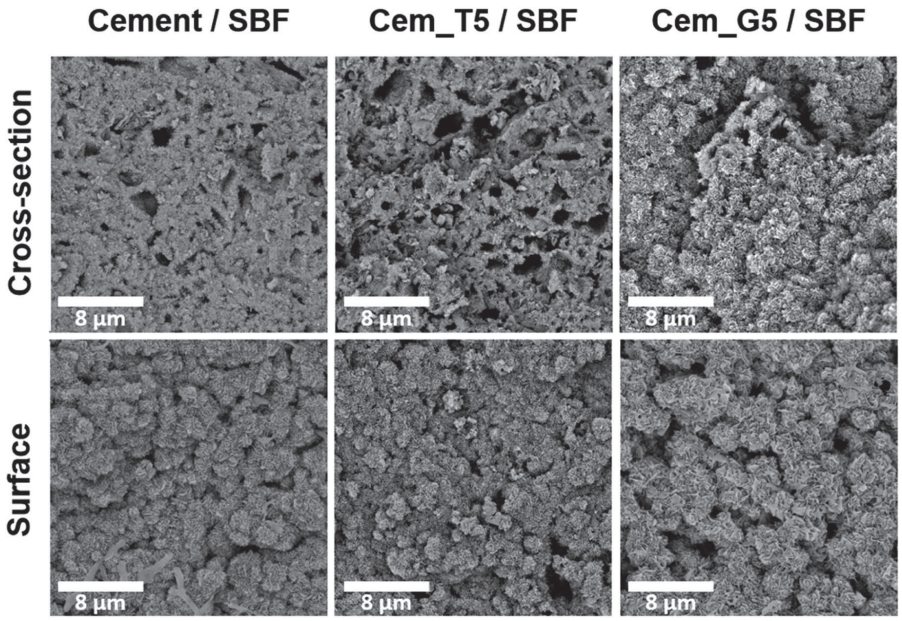

Fig. 9 Microstructure of obtained materials after 7 days incubation in SBF (magnification: 100 00×).

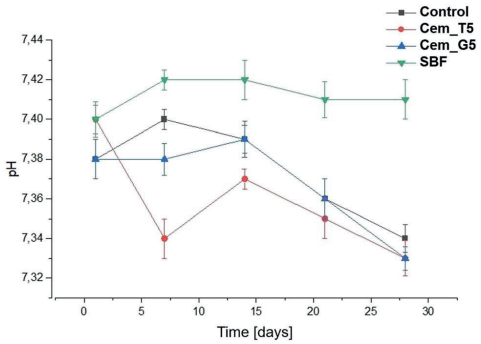

Fig. 10 pH *versus* bone cements' incubation time in SBF.

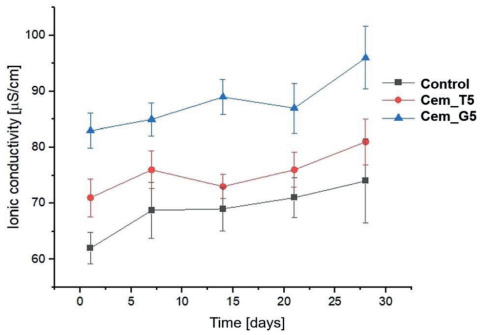

Fig. 11 Ionic conductivity *versus* bone cements' incubation time in distilled water.

a higher degradation rate silane coupling agents and the releasing of ion during its continuous hydrolysis in aqueous solutions.[63] Ionic conductivity of all the obtained materials is in the range typical for α-TCP-based bone cements. It can therefore be concluded that the modification with silane coupling agents did not significantly affect the degradation rate of bone cements.

The bioactive potential of obtained materials was estimated through its incubation in SBF.[62] The SEM observations show that the evenly distributed, bone-like apatite layer was present on the sample's surfaces and cross-sections after seven days of incubation in SBF at 37 °C (Fig. 9). The presence of apatite forms indirectly indicates the high bioactive potential of the obtained materials.

4. Conclusions

The positive effect of silane coupling agents on the mechanical behaviour of various biomaterials has been previously described, but there is little information about the effect of SACs on the properties of calcium phosphate bone cements. In this study, we developed and examined the novel, hybrid-type calcium phosphate bone cements based on α-TCP powders modified with silane coupling agents (SCAs) – tetraethoxysilane (TEOS) or 3-glycidoxypropyl trimethoxysilane (GPTMS). Developed materials, due to their hybrid nature, combine the excellent biological properties and improved physicochemical properties. Application of SACs allowed to increase the compressive strength of the composites from 7.24 ± 0.35 MPa to 12.17 ± 0.48 MPa. The strengthening effect may be explained by the chemical interactions between the components during the simultaneous hydrolysis of α-TCP and silane coupling agents. It has been shown that SCAs during hydrolysis can react with the hydroxyl groups on the surface of calcium phosphates, forming covalent bonds (*e.g.* Si–O–Si, or Si–O–P). In addition, the silanol groups have the tendency to form hydrogen bonding between each other. Furthermore, the results of our studies revealed that modification of α-TCP by SCAs influenced the setting process of bone cements. The decrease of final setting time from 11.0 to 6.5 minutes was observed. SEM observations showed that all of the developed bone substitutes have a homogenous microstructure. All of the studied materials possessed a bioactive potential, proven in *in vitro* studies in simulated body fluid. By using the silane coupling agents, we developed materials containing silicon, which may positively impact their osteoconductivity. Based on the obtained results, it can be concluded that the most favourable enhancement of the physicochemical properties of the developed materials was achieved by the modification of α-TCP with 5 wt% GPTMS.

All presented findings confirm the beneficial influence of silane coupling agents on the properties of calcium phosphate-based bone cements and pave the way to further *in vitro* and *in vivo* studies. Developed hybrid-type materials may be further modified, by introducing natural polymers, what should lead to creation of chemically coupled hybrid-type bone cements.

Conflicts of interest

There are no conflicts to declare.

Acknowledgements

Research project supported by program "Excellence initiative – research university" for the AGH University of Science and Technology. Research co-funded by the Faculty of Materials Science and Ceramics AGH UST—University of Science and Technology, Kraków, Poland, Project No. 16.16.160.557 (2023).

References

1 M. C. Tronco, J. B. Cassel and L. A. dos Santos, *Acta Biomater.*, 2022, **151**, 70–87.
2 R. G. Carrodeguas and S. De Aza, *Acta Biomater.*, 2011, **7**, 3536–3546.
3 W. Habraken, P. Habibovic, M. Epple and M. Bohner, *Mater. Today*, 2016, **19**, 69–87.
4 L. Yubao, Z. Xingdong and K. de Groot, *Biomaterials*, 1997, **18**, 737–741.

5 N. Eliaz and N. Metoki, *Materials*, 2017, **10**, 334.
6 X. Hou, L. Zhang, Z. Zhou, X. Luo, T. Wang, X. Zhao, B. Lu, F. Chen and L. Zheng, *J. Food Biochem.*, 2022, **13**, 187.
7 G. Hannink and J. J. C. Arts, *Injury*, 2011, **42**, S22–S25.
8 L. Schröter, F. Kaiser, S. Stein, U. Gbureck and A. Ignatius, *Acta Biomater.*, 2020, **117**, 1–20.
9 K. Szurkowska, Ł. Szeleszczuk and J. Kolmas, *Int. J. Mater. Sci.*, 2020, **21**, 9164.
10 J. V. Rau, I. V. Fadeeva, A. A. Forysenkova, G. A. Davydova, M. Fosca, Y. Yu. Filippov, I. V. Antoniac, A. Antoniac, A. D'Arco, M. Di Fabrizio, M. Petrarca, S. Lupi, M. Di Menno Di Bucchianico, V. G. Yankova, V. I. Putlayev and M. B. Cristea, *Adv. Mater. Interfaces*, 2022, **9**, 2200803.
11 L. Sinusaite, A. Popov, E. Raudonyte-Svirbutaviciene, J.-C. Yang, A. Kareiva and A. Zarkov, *Ceram. Int.*, 2021, **47**, 12078–12083.
12 K. Sariibrahimoglu, J. G. C. Wolke, S. C. G. Leeuwenburgh, L. Yubao and J. A. Jansen, *J. Biomed. Mater. Res.*, 2014, **102**, 415–422.
13 P. Pańtak, E. Cichoń, J. Czechowska and A. Zima, *Materials*, 2021, **14**, 7496.
14 M. Dziadek, A. Zima, E. Cichoń, J. Czechowska and A. Ślósarczyk, *Mater. Lett.*, 2020, **265**, 127457.
15 J. Czechowska, A. Zima, D. Siek and A. Ślósarczyk, *Ceram. Int.*, 2018, **44**, 6533–6540.
16 P. G. Pape, in *Applied Plastics Engineering Handbook*, Elsevier, 2017, pp. 555–572.
17 E. P. Plueddemann, *Silane Coupling Agents*, Springer US, Boston, MA, 1991.
18 D. S. Franklin and S. Guhanathan, *Iran. Polym. J.*, 2014, **23**, 809–817.
19 T. Nihei, *J. Oral Sci.*, 2016, **58**, 151–155.
20 M. V. Reyes-Peces, A. Pérez-Moreno, D. M. de-los-Santos, M. M. Mesa-Díaz, G. Pinaglia-Tobaruela, J. I. Vilches-Pérez, R. Fernández-Montesinos, M. Salido, N. de la Rosa-Fox and M. Piñero, *Polymers*, 2020, **12**, 2723.
21 L. Mendes, B. Loomans, N. Opdam, C. da Silva, L. Casagrande and T. Lenzi, *J. Adhes. Dent.*, 2020, **22**, 443–453.
22 Y. Xie, C. A. S. Hill, Z. Xiao, H. Militz and C. Mai, *Composites, Part A*, 2010, **41**, 806–819.
23 N. Suppakarn, S. Sanmaung, Y. Ruksakulpiwat and W. Sutapun, *Key Eng. Mater.*, 2007, **361–363**, 511–514.
24 E. Ji, Y. H. Song, J. H. Seo and K. I. Joo, *Korean J. Chem. Eng.*, 2023, **40**, 1709–1714.
25 F. Ghorbani, M. Pourhaghgouy, T. Mohammadi-hafshehjani and A. Zamanian, *Silicon*, 2020, **12**, 3015–3026.
26 F. Tallia, H.-K. Ting, S. J. Page, J. P. Clark, S. Li, T. Sang, L. Russo, M. M. Stevens, J. V. Hanna and J. R. Jones, *Front. Mater.*, 2022, **9**, 901196.
27 L.-J. Fuh, Y.-J. Huang, W.-C. Chen and D.-J. Lin, *Mater. Sci. Eng., C*, 2017, **75**, 798–806.
28 J. Rao, Y. Zhou and M. Fan, *Polymers*, 2018, **10**, 266.
29 K. Marcoen, M. Gauvin, J. De Strycker, H. Terryn and T. Hauffman, *ACS Omega*, 2020, **5**, 692–700.
30 J. Kolmas, A. Kaflak, A. Zima and A. Ślósarczyk, *Ceram. Int.*, 2015, **41**, 5727–5733.
31 C01 Committee, *Test Method for Time of Setting of Hydraulic-Cement Paste by Gillmore Needles*, ASTM International.
32 *Bioceramics and Their Clinical Applications*, ed. T. Kokubo, CRC Press [u.a.], Boca Raton, Fla, 2008, vol. 1.
33 M. Jaroniec, M. Kruk and A. Sayari, in *Studies in Surface Science and Catalysis*, Elsevier, 1998, vol. 117, pp. 325–332.
34 M. Nasrollahzadeh, M. Atarod, M. Sajjadi, S. M. Sajadi and Z. Issaabadi, in *Interface Science and Technology*, Elsevier, 2019, vol. 28, pp. 199–322.
35 T. Martinez, M. Espanol, C. Charvillat, O. Marsan, M. P. Ginebra, C. Rey and S. Sarda, *J. Mater. Sci.*, 2021, **56**, 13509–13523.
36 J. Czechowska, A. Zima and A. Ślósarczyk, *Acta Bioeng. Biomech.*, 2020, **22**, 47–56.
37 J. S. Sonn, J. Y. Lee, S. H. Jo, I.-H. Yoon, C.-H. Jung and J. C. Lim, *Ann. Nucl. Energy*, 2018, **114**, 11–18.
38 W. Chuang, J. Geng-sheng, P. Lei, Z. Bao-lin, L. Ke-zhi and W. Jun-long, *Results Phys.*, 2018, **9**, 886–896.
39 Y. Lu, N. Jiang, X. Li and S. Xu, *RSC Adv.*, 2017, **7**, 46486–46498.
40 M. Khodaei and S. Shadmani, *Surf. Coat. Technol.*, 2019, **374**, 1078–1090.
41 A. V. Rao, R. R. Kalesh and G. M. Pajonk, *J. Mater. Sci.*, 2003, **38**, 4407–4413.
42 S. Shetranjiwalla, A. Vreugdenhil and O. Strong, *Coatings*, 2021, **11**, 306.
43 T. Glawdel and C. Ren, in *Encyclopedia of Microfluidics and Nanofluidics*, ed. D. Li, Springer US, Boston, MA, 2008, pp. 2199–2207.
44 W. Götz, E. Tobiasch, S. Witzleben and M. Schulze, *Pharmaceutics*, 2019, **11**, 117.
45 J. Czechowska, E. Cichoń, A. Belcarz, A. Ślósarczyk and A. Zima, *Materials*, 2021, **14**, 3854.
46 E. Şahin, in *Cement Based Materials*, ed. H. E.-D. M. Saleh and R. O. A. Rahman, InTech, 2018.
47 X. Gui-Long, D. Changyun, L. Yun, P. Pi-Hui, H. Jian and Y. Zhuoru, *Nanomater. Nanotechnol.*, 2011, **1**, 21.
48 G. D. Ribeiro, C. T. Hiranobe, J. F. R. da Silva, G. B. Torres, L. L. Paim, A. E. Job, F. C. Cabrera and R. J. dos Santos, *Crystals*, 2022, **12**, 1552.
49 W. Bi, C. Goegelein, M. Hoch, J. Kirchhoff and S. Zhao, *Polymers*, 2022, **14**, 3393.
50 V. Purcar, R. Şomoghi, S. Niţu, C.-A. Nicolae, E. Alexandrescu, I. Gîfu, A. Gabor, H. Stroescu, R. Ianchiş, S. Căprărescu and L. Cinteză, *Nanomaterials*, 2017, **7**, 439.
51 H. H. Xu, P. Wang, L. Wang, C. Bao, Q. Chen, M. D. Weir, L. C. Chow, L. Zhao, X. Zhou and M. A. Reynolds, *Bone Res.*, 2017, **5**, 17056.
52 C. Durucan and P. W. Brown, *J. Mater. Sci.*, 2002, **37**, 963–969.
53 Z. He, Q. Zhai, M. Hu, C. Cao, J. Wang, H. Yang and B. Li, *J. Orthop. Transl.*, 2015, **3**, 1–11.
54 S. M. Rabiee and H. Baseri, *Comput. Intell. Neurosci.*, 2012, **2012**, 1–8.
55 X. Wei, O. Ugurlu, A. Ankit, H. Y. Acar and M. Akinc, *Mater. Sci. Eng., C*, 2009, **29**, 126–135.

56 G. Mestres, C. Le Van and M.-P. Ginebra, *Acta Biomater.*, 2012, **8**, 1169–1179.
57 R. Ma, Q. Li, L. Wang, X. Zhang, L. Fang, Z. Luo, B. Xue and L. Ma, *Mater. Sci. Eng., C*, 2017, **73**, 429–439.
58 C. M. Vaz, R. L. Reis and A. M. Cunha, *Biomaterials*, 2002, **23**, 629–635.
59 E. J. Harper, M. Braden and W. Bonfield, *J. Mater. Sci.: Mater. Med.*, 2000, **11**, 491–497.
60 X. Chatzistavrou, P. Newby and A. R. Boccaccini, in *Bioactive Glasses*, Elsevier, 2011, pp. 107–128.
61 D. Moreno, F. Vargas, J. Ruiz and M. E. López, *Bol. Soc. Esp. Ceram. Vidrio*, 2020, **59**, 193–200.
62 T. Kokubo and H. Takadama, *Biomaterials*, 2006, **27**, 2907–2915.
63 C. Lee, S. Yamaguchi and S. Imazato, *J. Prosthodont. Res.*, 2023, **67**, 55–61.

Publikacja 4 – *„The Synergistic Effect of Polysaccharides and Silane Coupling Agents on the properties of Calcium Phosphate-Based Bone Substitutes”*

International Journal of *Molecular Sciences*

MDPI

Article

The Synergistic Effect of Polysaccharides and Silane Coupling Agents on the Properties of Calcium Phosphate-Based Bone Substitutes

Piotr Pańtak [1], Joanna P. Czechowska [1], Vladyslav Vivcharenko [2], Annett Dorner-Reisel [3] and Aneta Zima [1,*]

[1] Faculty of Materials Science and Ceramics, AGH University of Krakow, al. A. Mickiewicza 30, 30-059 Krakow, Poland
[2] Department of Tissue Engineering and Regenerative Medicine, Faculty of Medical Sciences, Medical University of Lublin, Chodzki 1, 20-093 Lublin, Poland
[3] Faculty of Mechanical Engineering, Schmalkalden University of Applied Sciences, 98574 Schmalkalden, Germany
* Correspondence: azima@agh.edu.pl

Abstract

In this study, novel hybrid cementitious materials composed of calcium phosphates and polysaccharides were obtained and developed. Moreover, the impact of two distinct silane coupling agents—tetraethyl orthosilicate (TEOS) and 3-glycidoxypropyltrimethoxysilane (GPTMS)—on the physicochemical and biological properties of the resulting materials was systematically analyzed. Comprehensive assessments were conducted to evaluate the chemical and phase compositions (using XRF, XRD, FTIR), setting behavior, mechanical strength, microstructure (SEM), porosity, in vitro chemical stability, and biological performance of bone cements. Notably, the synergistic effect of polysaccharides and silane coupling agents significantly enhanced the compressive strength of the cements, increasing it to 19.34 MPa. Additionally, the integration of citrus pectin into the liquid phase, along with the inclusion of hybrid hydroxyapatite–chitosan granules, not only enabled the formation of materials with high surgical handiness but also improved the materials' physicochemical characteristics. The findings from this study emphasize the beneficial role of silane coupling agents in improving the properties of calcium phosphate-based bone substitutes. The developed materials demonstrate substantial potential for use in bone tissue engineering according to ISO 10993. However, further in vitro and in vivo studies are required to confirm their safety and effectiveness.

Keywords: calcium phosphates; bioceramics; polysaccharides; hybrid materials; silane coupling agents

Academic Editors: Kazuaki Hashimoto and Mamoru Aizawa

Received: 21 July 2025
Revised: 23 August 2025
Accepted: 26 August 2025
Published: 12 September 2025

Citation: Pańtak, P.; Czechowska, J.P.; Vivcharenko, V.; Dorner-Reisel, A.; Zima, A. The Synergistic Effect of Polysaccharides and Silane Coupling Agents on the Properties of Calcium Phosphate-Based Bone Substitutes. *Int. J. Mol. Sci.* **2025**, *26*, 8910. https://doi.org/10.3390/ijms26188910

1. Introduction

Calcium phosphate cements (CPCs) based on α-tricalcium phosphate (α-TCP) are widely used in contemporary regenerative medicine, particularly in the management of bone defects [1]. A key advantage of CPCs lies in their inherent bioactivity, which facilitates direct interaction with bone tissue and promotes regenerative processes of bone healing. The superior biological performance of calcium phosphate cements is intrinsically linked to their chemical composition, which closely resembles that of natural bone mineral. The bioactivity of CPCs is primarily attributed to their capacity to form a hydroxyapatite layer on their surface upon contact with physiological fluids, thereby fostering integration with

the surrounding bone matrix [2]. Additionally, their properties promote the growth of new bone tissue at the site of application, which makes CPCs highly suitable for various clinical applications, including defect repair, bone stabilization, and controlled drug delivery [3–5].

Despite their outstanding biological properties, calcium phosphate bone cements (CPCs) exhibit certain limitations that hinder their widespread application in orthopedic and dental surgery [6]. The biggest disadvantage of CPCs is their low mechanical strength and pronounced brittleness [7]. These mechanical deficiencies are particularly troublesome in load-bearing regions or areas exposed to significant and dynamic mechanical forces, thereby limiting CPCs' efficacy and durability in such environments [8]. To overcome these limitations, research on CPC modification focuses on improving their mechanical properties while maintaining their bioactivity. One of the most promising approaches is the introduction of polymers, whether synthetic or natural, into the composition of calcium phosphate cements [9,10]. For example, Czechowska et al. [11] investigated the influence of one of the polysaccharides, namely sodium alginate and methylcellulose, on the physiochemical properties and in vitro behavior of α-TCP-based cementitious materials and confirmed the beneficial influence of polymeric addition on their compressive strength. Watanabe et al. [12] examined α-TCP-based bone cements modified with polyvinyl alcohol. They determined that higher concentrations of polyvinyl alcohol significantly enhanced the mechanical properties of the developed materials. Dziadek et al. [13], through the addition of another example of polysaccharides, low-esterified pectin, developed novel bone substitutes with high surgical handiness and improved mechanical properties. Polymers also enhance the flexibility and mechanical resistance of CPCs, making them more suitable for dynamically loaded areas. However, they may accelerate material degradation [14]. Another approach to strengthening CPCs involves adding fillers, such as fibers or granules, which improve mechanical properties and modify stress distribution within the material [15–17]. A particularly interesting material solution involving bone substitute materials based on calcium phosphates containing aggregates in the form of granules is biomicroconcrete, where the granules acting as aggregates enhance the resistance to the brittle fracture of these materials, like the behavior observed in technical concrete applications [18].

Although the use of polymers and aggregates significantly improves the mechanical properties of CPCs, these composites still have limitations, prompting the ongoing search for new solutions. One of the latest and most promising approaches is the use of silane coupling agents (SCAs) as cement modifiers [19]. SCAs are chemical compounds capable of reacting with both organic and inorganic components of materials, which influences both physicochemical and biological properties of composites [20]. For example, Kouhi et al. [21] modified bredigite (BR) nanoparticles with 3-glycidoxypropyltrimethoxysilane (GPTMS) to improve their dispersibility in a polyhydroxybutyrate-co-hydroxyvalerate (PHBV) matrix. They demonstrated that the PHBV scaffolds containing GPTMS-modified bredigite (G-BR) exhibited enhanced mechanical properties and better nanoparticle dispersion. Furthermore, materials demonstrated improved cell attachment and proliferation, which makes them promising candidates for bone tissue engineering. On the other hand, Bravaya et al. [22] modified alumina nanofibers with various silane agents to create hybrid ethylene–propylene copolymer materials. In this study, trialkoxysilanes with alkenyl and alkyl functional groups were used for the modification of silane coupling agents, improving the mechanical properties of the final materials and nanofiller dispersion. Varghese et al. [23] optimized the surface treatment of glass fibers in dental composites using three different silane coupling agents (3-methacryloxypropyltrimethoxysilane (3-MPS), 3-glycidoxipropyltrimethoxysilane (3-GPS), or 8-methacryloxyoctyltrimethoxysilane (8-MOTS)), incorporating the treated fibers

into a dental resin. They found that the presence of silane in certain concentrations (1.4 wt.% for 8_MOTS and 0.8 wt.% for 3-MPS) significantly improved the overall mechanical performance of the composites.

Thus, although silane coupling agents are not yet widely used in bone substitute materials, the scientific literature suggests their potential benefits. It is believed that their incorporation can significantly enhance the mechanical properties of cementitious materials, primarily by improving the bonding between the individual components. These features make SCAs promising candidates for further research and development in biomaterial engineering.

The objective of this study was to develop, obtain, and evaluate novel hybrid bone substitute materials based on highly reactive, self-setting α-TCP (α-tricalcium phosphate) powder combined with hybrid hydroxyapatite–chitosan granules. The liquid phase consisted of a blend of citrus pectin gel and disodium phosphate. Additionally, this study aimed to investigate how the modification of α-TCP with two different silane coupling agents, specifically tetraethyl orthosilicate (TEOS) and 3-glycidoxypropyltrimethoxysilane (GPTMS), influences their physicochemical and biological properties.

2. Results and Discussion

2.1. Chemical and Phase Composition

The X-ray fluorescence analysis confirmed the presence of silicon in all modified powders, with a baseline level of 0.029 ± 0.002 wt.% in the non-modified powder. As anticipated, the silicon content increased with the addition of silane coupling agents (SCAs), reaching 0.223 ± 0.006 wt.% and 0.286 ± 0.004 wt.% for powders modified with 5 wt.% TEOS and GPTMS, respectively. The presence of silicon may enhance the biological properties of the final material, such as osteoconductivity [24,25]. This modification facilitated the enrichment of the powder with silicon ions following α-TCP synthesis, whereas most of the scientific literature focuses on introducing silicon ions during the synthesis of calcium phosphate-based materials [26,27].

The XRD analysis showed that both the initial α-TCP and SCA-modified α-TCP powders were primarily composed of α-TCP (97–98 wt.%), with a minor presence of hydroxyapatite (2–3 wt.%). In contrast, the hybrid HA-CTS powder contained only one crystalline phase, hydroxyapatite (Figure 1A). The diffractograms of the cementitious materials, after setting and hardening in air for 7 days and after 7 days of incubation in SBF, revealed the presence of two crystalline phases: hydroxyapatite and a small amount of α-TCP (Figure 1B,C). No additional silicon-containing crystalline phases were identified by XRD.

The quantitative analysis of the diffractograms indicated that in a humid environment, the α-TCP phase displayed thermodynamic metastability and underwent near-complete hydrolysis, leading to the formation of calcium-deficient hydroxyapatite (CDHA) (Table 1). This transformation was previously observed inter alia by E. Şahin [28] and L. Yubao [29]. The process of hydrolysis is believed to affect the material's properties and performance in biological applications.

The FTIR study results support the XRD findings and confirm the presence of functional groups characteristic of calcium phosphates and polymers. The infrared spectra of the developed materials, after setting and hardening in air for 7 days, as well as after incubation in simulated body fluid (SBF), are shown in Figure 2.

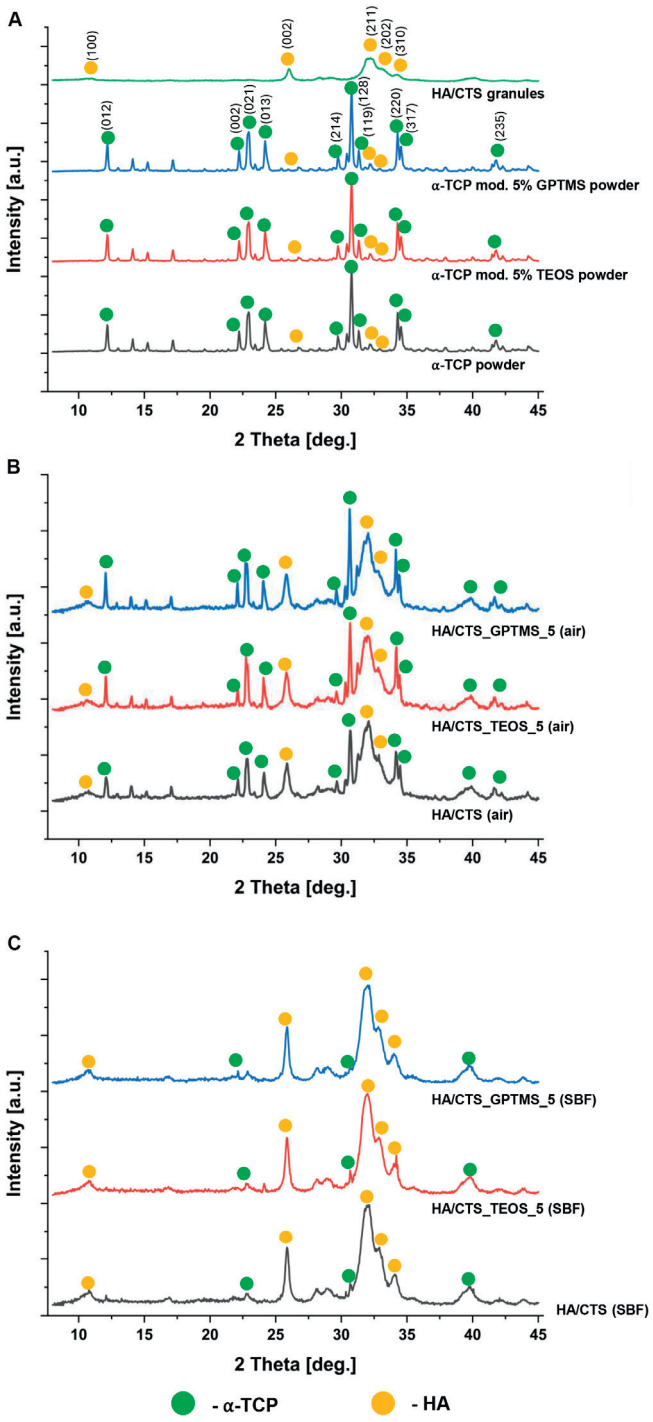

Figure 1. X-ray diffraction (XRD) patterns: initial powders and granules (**A**), cementitious materials after 7 days of setting and hardening in air (**B**), and incubation in SBF for 7 days (**C**).

Table 1. Phase composition of the obtained materials after 7 days of setting and hardening in air or after 7 days of incubation in SBF.

Material	7 Days in Air		7 Days in SBF	
	α-TCP, wt.%	*Hydroxyapatite, wt.%*	*α-TCP, wt.%*	*Hydroxyapatite, wt.%*
HA/CTS	58 ± 2	42 ± 2	8 ± 2	92 ± 2
HA/CTS_TEOS_5	52 ± 1	48 ± 1	7 ± 1	93 ± 1
HA/CTS_GPTMS_5	51 ± 2	49 ± 2	6 ± 1	94 ± 2

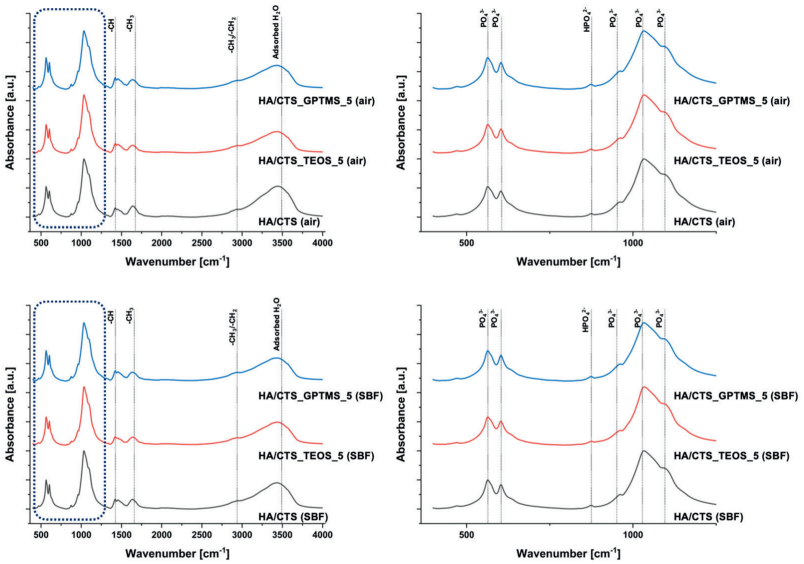

Figure 2. FT-IR spectra of investigated materials.

The FTIR spectra of the materials revealed distinct bands at approximately 600 and 560 cm^{-1}, corresponding to the bending vibrations of the PO_4^{3-} groups, and around 965 and 1020 cm^{-1}, associated with the stretching vibrations of these groups. A broad band in the range of approximately 3000–3800 cm^{-1} was attributed to absorbed water. Additionally, an absorption band at around 870 cm^{-1} was linked to the HPO_4^{2-} groups, indicating the presence of non-stoichiometric hydroxyapatite. In the same spectral range (approximately 873–875 cm^{-1}), there were also possible carbonate bonds in the material. The band at 1424 cm^{-1} suggested partial substitution of CO_3^{2-} within the hydroxyapatite structure. FTIR analysis also confirmed the presence of chitosan and amidated citrus pectin, with an absorption band at approximately 2930 cm^{-1} corresponding to alkyl C-H stretching vibrations and the band around 1650 cm^{-1} attributed to N-H bending vibrations of primary amines. The presence of these bands suggests the formation of electrostatic and/or hydrogen bonds, likely forming polyelectrolyte complexes at the interface between the hybrid powder and pectin within the cements. The low concentration of silane coupling agents in the pastes, combined with overlapping bands from phosphates, may account for the absence of visible peaks corresponding to Si–O–Si, Si-OH, Si–C, and C–H bonds associated with the silane coupling agents [30–32].

2.2. Setting Times

The setting process of self-setting calcium phosphate-based cementitious pastes begins upon mixing the powder and liquid phases, resulting in a viscous paste whose rheological properties evolve until the material fully hardens. The setting times of the bone cements ranged from 5.5 to 12.0 min for the initial setting time and 11.5 to 19.5 min for the final setting time (Table 2).

Table 2. Setting times of developed materials.

Material	Initial Setting Time (ti) [min]	Final Setting Time (tf) [min]
HA/CTS	11.0 ± 1.0	19.5 ± 1.5
HA/CTS_TEOS_1	8.5 ± 0.5	17.5 ± 0.5
HA/CTS_TEOS_2	12.0 ± 1.5	15.0 ± 0.5
HA/CTS_TEOS_5	6.5 ± 1.0	15.0 ± 1.0
HA/CTS_GPTMS_1	10.0 ± 1.5	17.5 ± 1.5
HA/CTS_GPTMS_2	7.5 ± 0.5	14.5 ± 1.0
HA/CTS_GPTMS_5	5.5 ± 0.5	11.5 ± 1.0

The solid phase of the developed pastes consisted of highly reactive α-tricalcium phosphate powder. When this powder comes into contact with the water, it hydrolyzes to calcium-deficient hydroxyapatite, as described by the following Equation (1) [33,34]:

$$3Ca_3(PO_4)_2 + H_2O \rightarrow Ca_9(PO_4)_5(HPO_4)OH \quad (1)$$

During hydrolysis, the paste undergoes a setting and hardening process, which involves the nucleation and growth of CDHA crystals. Initially, the powder particles within the paste undergo restructuring, transforming the fluid paste into a rigid, yet weak, monolith. Subsequently, the strength of the material increases as the hardening process continues.

The setting process of cementitious materials based on α-TCP is influenced by many factors. Primarily, it is dependent on the amount of highly reactive α-TCP powder in the materials' formulation. Additional factors, such as the presence of setting accelerators in the liquid phase or polymers in the mixture, also play significant roles. In the developed materials, disodium hydrogen phosphate was used to accelerate setting and counteract the elongation of the setting process caused by citrus pectin [35]. Since the same liquid phase was used for all formulations, variations in setting times were attributed to differences in the solid phase composition, especially the incorporation of silane coupling agents as modifiers of α-TCP powders. It appears that the presence of SCAs slightly reduced the setting time of the cement pastes. This effect may be attributed to the hydrolysis of silane coupling agents upon exposure to water, leading to their condensation and potentially contributing to a minor acceleration in the setting process. This phenomenon is well-described in previous studies [27,36]. Another possible explanation involves the SCAs acting as sources of silicon ions, which are known to enhance the solubility of α-TCP and accelerate its setting compared to unmodified powders.

2.3. Mechanical Strength

The compressive strength of the developed biomaterials ranged from 11.42 ± 1.12 MPa to 19.34 ± 0.94 MPa. It was observed that the compressive strength of the materials depended on the amount of coupling agents used. An increase in the quantity of the modifier resulted in higher mechanical strength, regardless of the type of coupling agent

employed. The inclusion of silane coupling agents (SCAs) enhanced the strength of the bone cements, with the highest value recorded for the material HA/CTS_GPTMS_5, which contained 5 wt.% of GPTMS (Figure 3). Statistical analysis using one-way ANOVA and Tukey's HSD post hoc tests revealed that the differences between the control and modified materials were significant.

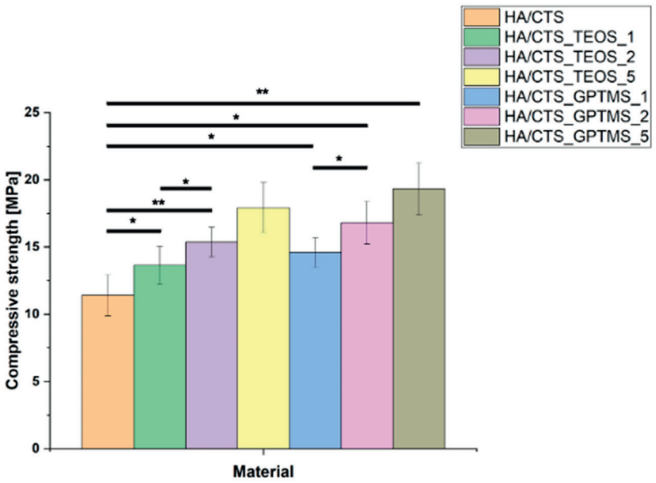

Figure 3. Compressive strength of developed bone substitutes. Statistical significance is indicated as $p < 0.05$ (*) and $p < 0.01$ (**).

Silane coupling agents used as modifiers for α-TCP can synergistically enhance the mechanical properties of the resulting bone cements by forming additional bonds within the material structure and causing better adhesion between the material's compounds. Moreover, the use of natural polymers in the composition of the developed cementitious materials further reinforced this effect due to synergistic interactions between the functional groups of the polymers and those originating from the coupling agents.

The improvement in mechanical strength likely arises from chemical interactions between the components, leading to the creation of Si-O-Si, Si-O, or Si-O-P bonds, which result in hybrid-type materials. A similar positive effect of silane coupling agents on the mechanical performance of various biomaterials has also been reported in previous studies. For example, Ji et al. [37] developed hydroxyapatite-based scaffolds by modifying the surface of HA pellets with silane coupling agents containing methacrylate, amine, and carboxylic acid functional groups to enhance their mechanical properties for dental and bone regeneration applications. They found that coating with carboxylic acid-functionalized silane significantly improved the mechanical strength and biocompatibility of the scaffolds, making them suitable as bone filler composites in tissue engineering. Vaz et al. [38] showed beneficial application of different coupling agents to obtain starch/ethylene-vinyl alcohol copolymer/hydroxyapatite composites characterized by increased mechanical resistance due to improved adhesion between material components. On the other hand, Kotha et al. [39] evaluated the impact of using a silane coupling agent (methacryloxypropyltrichlorosilane) on the mechanical properties of steel fiber-reinforced acrylic bone cements. They studied the tensile and fracture properties of cements reinforced with silane-coated or uncoated 316 L stainless steel fibers and found that the interfacial shear strength and mechanical properties were significantly improved with silane-coated fibers. Furthermore, the improvement in the mechanical strength of the developed bone cement materials was

achieved due to interactions between the chitosan present in the hybrid granules and the citrus pectin incorporated in the liquid phase, as well as the functional groups derived from the silane coupling agents. A similar effect was previously observed by Pańtak et al. [40]. The authors developed and evaluated hybrid bone scaffolds fabricated using the robocasting technique. In their study, it was demonstrated that the use of silane coupling agents and citrus pectin enhanced the mechanical strength of the biomaterials through interactions between calcium phosphates, polymers, and the silane coupling agents.

2.4. Porosity

In the developed materials, the incorporation of silane coupling agents resulted in a noticeable reduction in porosity. The HA/CTS biomaterial without SCA modification exhibited a porosity of 58.3 ± 0.5 vol.%, while materials modified with TEOS and GPTMS showed significantly lower porosity values of 47.6 ± 0.5 vol.% and 46.4 ± 0.5 vol.%, respectively. The observed decrease in porosity closely correlated with the compressive strength results. Specifically, the reduction in porosity in materials containing silane coupling agents contributed to an improvement in their mechanical strength.

Additionally, the pore size distribution plots revealed distinct differences: the unmodified HA/CTS cement displayed a bimodal porosity distribution with larger pores, approximately 10 microns in size, while no such large pores were observed in the SCA-modified materials (Figure 4).

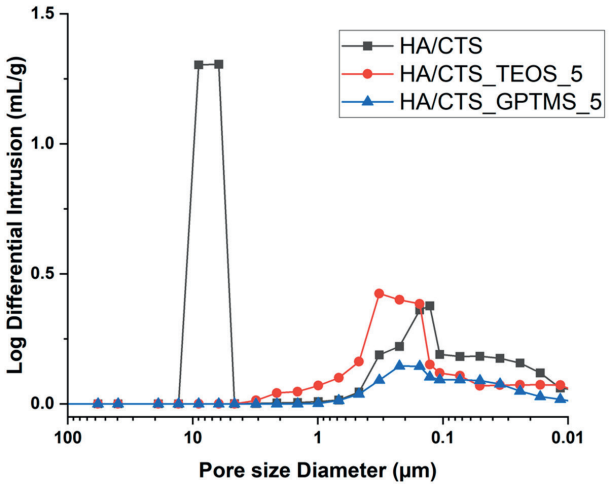

Figure 4. Distribution and size of pores in the obtained bone substitutes.

The observed decrease in porosity and the absence of large pores in the modified materials can be attributed to the use of SCAs, which are known to enhance adhesion between different components of a material [41]. In this case, the application of SCAs likely improved the adhesion of the α-TCP powder to the hybrid granules, resulting in a more compact structure with fewer and smaller pores. Silane coupling agents are commonly used to promote interfacial bonding in composite materials, thereby improving mechanical properties and reducing porosity, as reported in previous studies [42,43].

2.5. Microstructure

The set and hardened materials displayed a uniform microstructure, consisting of hybrid granules embedded in a cementitious matrix with both macro- and micropores. The

hybrid granules were visible and evenly distributed in the material (Figure 5). Interestingly, the use of SCAs improved the adhesion between the cementitious matrix and hybrid granules (highlighted with arrows). Similar microstructures in α-TCP-based biomaterials intended for bone tissue replacement have been reported in other studies [35].

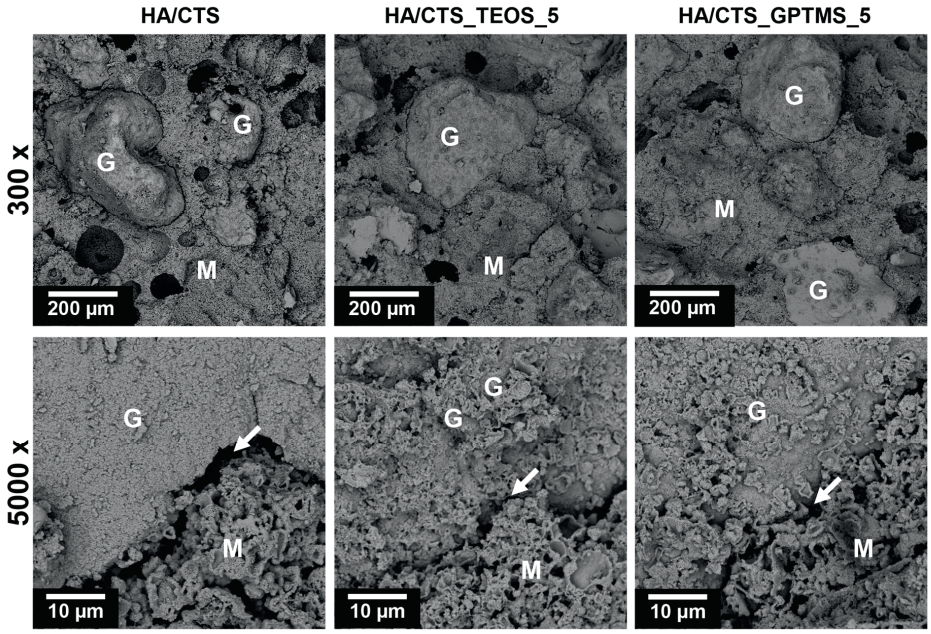

Figure 5. Microstructure of developed bone cements (M—cementitious matrix; G—hybrid HA/CTS granules, arrows—matrix/granule interface).

2.6. Chemical Stability and Bioactivity In Vitro

Evaluating the chemical stability of candidate materials for bone substitution is crucial, as it helps predict how the material will behave after the implantation procedure. Figure 6 illustrates the pH changes in the SBF and the ionic conductivity variations in distilled water during the immersion of the samples.

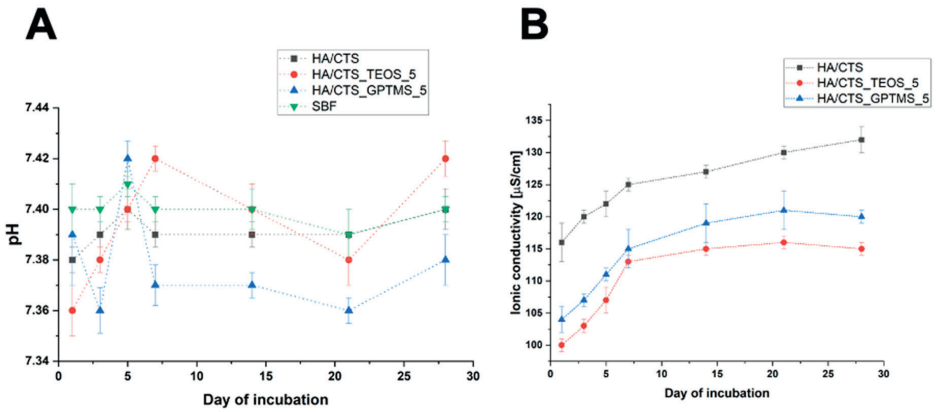

Figure 6. pH (**A**) and ionic conductivity (**B**) vs. time of incubation of developed biomaterials.

The pH levels of the SBF surrounding the incubated samples remain near the physiological values, fluctuating between 7.36 and 7.42. The introduction of TEOS and GPTMS only had a minor effect on the pH of the solution. Comparable pH levels for incubated calcium phosphate-based bone substitutes have been reported in other studies [11].

The ionic conductivity during the samples' incubation in distilled water also depended on their composition (Figure 6B). The ionic conductivity of the distilled water around the incubated HA/CTS was the highest and ranged from approximately 140 to 181 μS/cm. In the case of SCA-modified materials, these values were slightly lower: between 100 and 116 μS/cm for HA/CTS_TEOS_5 and 116 and 133 μS/cm for HA/CTS_GPTMS_5. The observed phenomenon could be attributed to the faster degradation and hydrolysis of HA/CTS cement agents in aqueous solutions [44]. The ionic conductivity of all tested biomaterials was comparable to previously studied chemically bonded biomaterials based on α-TCP.

After 7 days of incubation in simulated body fluid (SBF), all prepared materials were fully covered by a plate-like apatitic structure, which, according to Kokubo and Takadama's criteria, confirms in vitro bioactive potential of composites (Figure 7) [45].

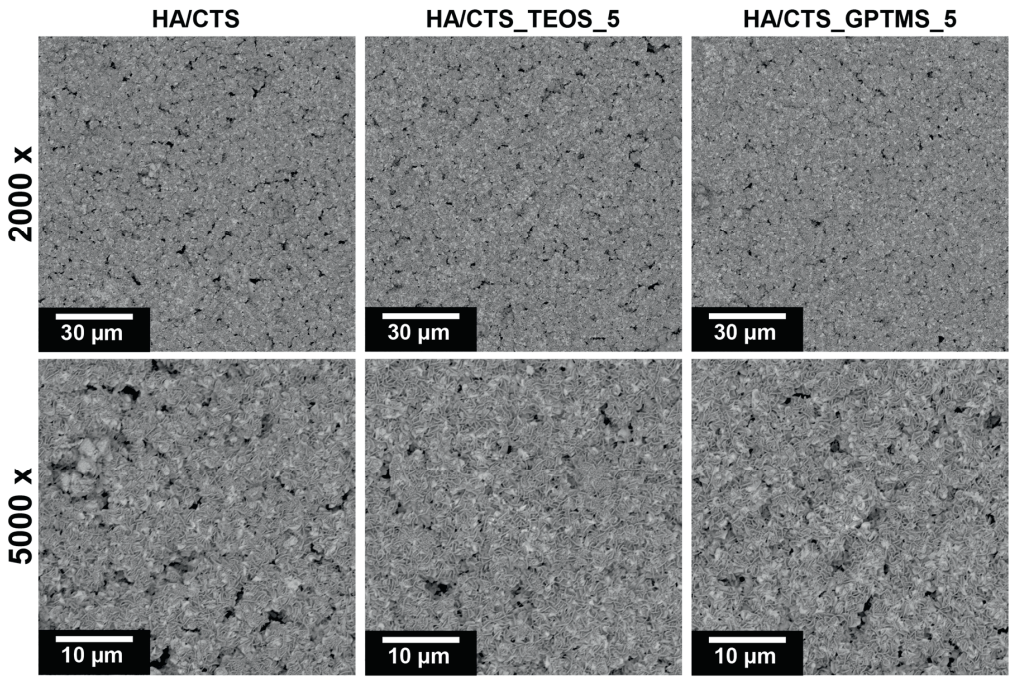

Figure 7. Microstructure of materials' surfaces after 7 days of incubation in SBF.

2.7. Cytotoxicity Tests

The cytotoxicity of the tested cementitious samples was evaluated based on the metabolic activity of MC3T3-E1 cells after exposure to biomaterial extracts, using the WST-8 test. Cell viability in all tested samples was high, exceeding 90%, which indicates a lack of cytotoxicity, as defined by ISO 10993-5:2009 (Figure 8A).

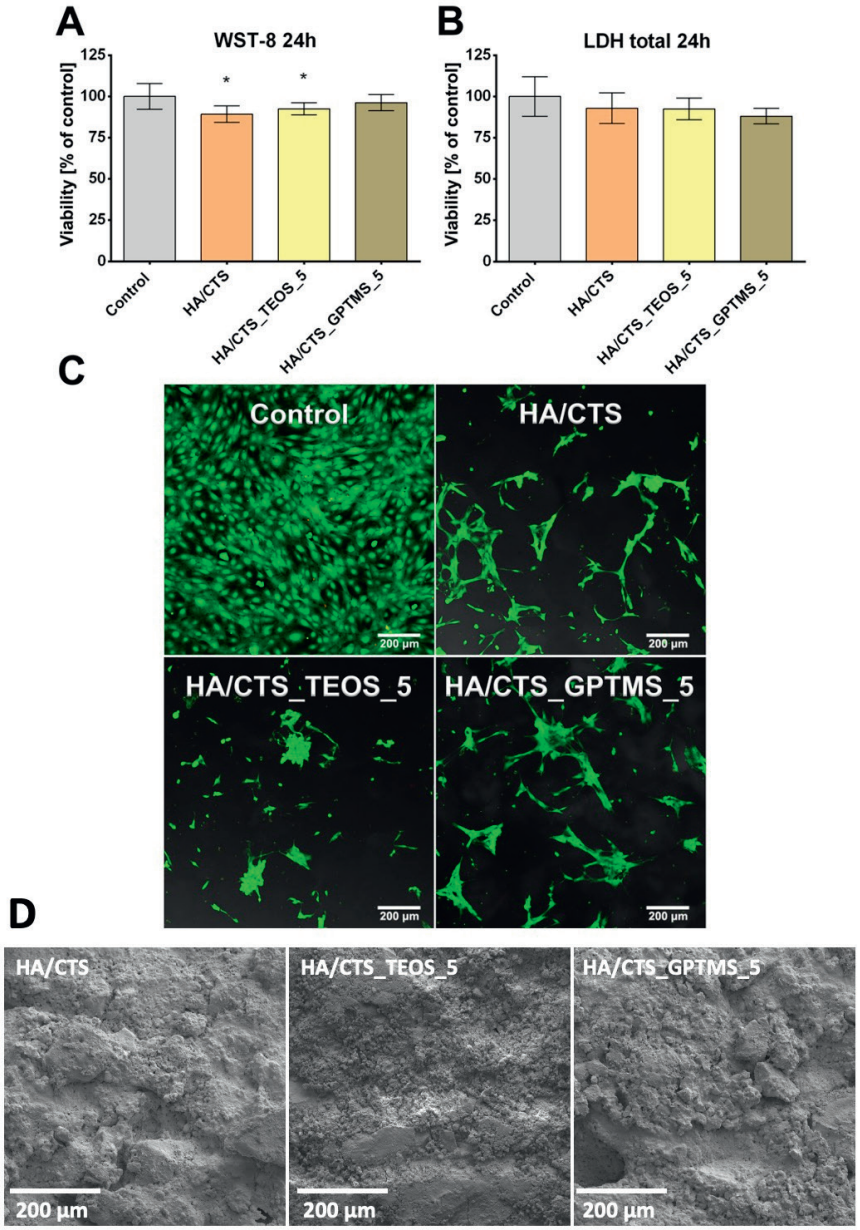

Figure 8. Cytocompatibility evaluation of the tested cementitious samples against mouse calvarial preosteoblast cell line: (**A**) WST-8 test conducted using scaffold extracts (* statistically significant results compared to the control, $p < 0.05$, one-way ANOVA followed by Tukey's test); (**B**) LDH total test conducted using scaffold extracts; (**C**) direct contact cytotoxicity assay performed with a Live/Dead staining kit (green fluorescence indicating viable cells, red fluorescence indicating dead cells); (**D**) SEM of developed materials' surfaces.

HA/CTS and HA/CTS_TEOS_5 samples exhibited slightly lower viability values in the WST-8 assay compared to the control, which can be attributed to the negative

effect of biomaterial extracts on mitochondrial dehydrogenase activity measured during the experiment. The absence of cytotoxicity was further confirmed by the LDH total assay performed after cell lysis, where the measured LDH activity correlated with the cell number in the population. The conducted test revealed no statistically significant differences between the scaffolds and the negative control, confirming the non-cytotoxic character of the samples (Figure 8B). The cytotoxicity of the tested samples was further evaluated using a direct contact test. Mouse preosteoblasts were cultured on the scaffolds for 2 days and then visualized through fluorescent staining (Figure 8C). The distribution of the observed calvarial preosteoblasts reflects the microstructure of the surface of the cementitious materials. It can be noted that the cells spread out within the depressions present on the surface of the analyzed materials (Figure 8D).

3. Materials and Methods

3.1. Materials

3.1.1. Synthesis of α-TCP and SCA-Modified α-TCP Powders

The initial α-TCP powder was synthesized via a wet chemical method following a previously described procedure [46,47]. $Ca(OH)_2$ (≥99.5%, POCH, Gliwice, Poland) and H_3PO_4 (85.0%, POCH, Gliwice, Poland) at the Ca/P molar ratio of 1.5 were applied as reagents. After aging and drying, the precipitate underwent a calcination at 1250 °C for 5 h, grinding in an attritor mill for 4 h, and sieving below 63 μm. To modify the surface of α-TCP powder, the 1, 2, and 5 wt.% solutions of TEOS (T) or GPTMS (G) (≥99.5%, Sigma-Aldrich, St. Louis, MO, USA) in ethanol (99.8 wt.%, POCH, Gliwice, Poland) were applied according to Pańtak et al. [19]. The anhydride solvent was used to avoid the hydrolysis of both α-TCP and silane coupling agents. α-TCP powder was added to the SCA solution at the liquid-to-powder (L/P) ratio of 0.25 and stirred in a magnetic stirrer for 4 h. The sedimented powder was then aged for 1 h and silanized at 115 °C for 4 h. Prior to preparing the samples, the powders were sieved below 63 μm.

3.1.2. Synthesis of Hybrid Hydroxyapatite/Chitosan Granules

Hybrid HA/chitosan (CTS) granules, containing 17 wt.% CTS, were synthesized using a modified wet chemical method, following the procedure outlined previously by Zima [48]. Briefly, phosphoric acid (85.0%, POCH, Gliwice, Poland) was directly added to a 10 wt.% CTS solution in 0.5 wt.% acetic acid (98.0%, POCH, Gliwice, Poland). This mixture was then carefully dripped into a suspension of $Ca(OH)_2$ (Merck, Darmstadt, Germany) for HA precipitation. The molar ratio of Ca/P during the synthesis was within the range of 1.65–1.67. The CTS used was of medium molecular weight (~100,000 kDa) with a deacetylation degree of ≥75.0% and a viscosity ranging from 200 to 800 CPS (Sigma-Aldrich, St. Louis, MO, USA). After aging the suspension for 24 h, it was decanted. The HA/CTS precipitate was washed with distilled water, centrifuged, and dried. Prior to preparing the samples, the granules were ground and sieved. For the preparation of the samples, granules of sizes 300–400 μm were used.

3.2. Preparation of Bone Cements

Developed biomaterials are composed of solid phase (setting powder and aggregate) and liquid phase, and when mixed, they create a paste that sets in situ. In this study, seven types of powder batches containing α-TCP, modified α-TCP, and HA/CTS granules were used as the solid phase (Table 3). The liquid-to-powder (L/P) ratio was selected based on preliminary studies, and it was 0.5 g/g.

Table 3. The initial composition of developed materials.

Material	Solid Phase (P)	Liquid Phase (L)	L/P [g/g]
HA/CTS	α-TCP: HA/CTS granules 3:2 by weight	1.0 wt.% Na_2HPO_4 solution in 2.5 wt.% citrus pectin gel	0.5
HA/CTS_TEOS_1	α-TCP (1 wt.% TEOS): HA/CTS granules 3:2 by weight		
HA/CTS_TEOS_2	α-TCP (2 wt.% TEOS): HA/CTS granules 3:2 by weight		
HA/CTS_TEOS_5	α-TCP (5 wt.% TEOS): HA/CTS granules 3:2 by weight		
HA/CTS_GPTMS_1	α-TCP (1 wt.% GPTMS): HA/CTS granules 3:2 by weight		
HA/CTS_GPTMS_2	α-TCP (2 wt.% GPTMS): HA/CTS granules 3:2 by weight		
HA/CTS_GPTMS_5	α-TCP (5 wt.% GPTMS): HA/CTS granules 3:2 by weight		

3.3. Methods

3.3.1. Chemical and Phase Composition

The chemical composition of the initial powders was examined using X-ray fluorescence (XRF) with the WDXRF Axios Max (PANalytical, Malvern, UK). X-ray diffraction (XRD) was used to identify crystalline phases, employing Cu Kα radiation (1.54 Å) at 30 kV and 10 mA. The analysis covered a 2θ range of 5–45° with 0.04 intervals, scanning at a speed of 2.5°/min, using a D2 Phaser diffractometer (Bruker, Ballirica, MA, USA). Diffractograms were compared with the International Centre for Diffraction Data for α-TCP (00-009-0348) and hydroxyapatite (HA; 01-076-0694). Phase quantification was performed using TOPAS software (Bruker, Billerica, MA, USA) based on Rietveld refinement. All measurements were performed in triplicate, with results presented as mean ± SD.

The structural analysis of the obtained biomaterials after setting and hardening was carried out using Fourier Transform Infrared (FTIR) spectroscopy, covering a scanning range of 400–4000 cm^{-1} with a resolution of 4 cm^{-1}, using a BioRad FTS 6000 spectrometer (Vertex 70&70v, Bruker, Billerica, MA, USA). The positions of the FTIR bands were determined based on the center of weight. Baseline correction, normalization, and spectral analysis were conducted using Spectragryph software (v1.2.15, Friedrich Menges, Oberstdorf, Germany).

3.3.2. Setting Times

The setting times were determined according to the ASTM C266-20 standard using Gilmore Needles (Humbold MFG Co., Norridge, IL, USA) [49]. The apparatus included two steel-weighted needles: the initial setting needle, weighing 113 g with a diameter of 2.12 mm, and the final setting needle, weighing 453.6 g with a diameter of 1.06 mm. Cement pastes were placed in a form measuring 8 mm × 10 mm × 5 mm, and the needle was gently applied to the surface. The setting time was recorded when the needle no longer left a complete circular mark. All tests were conducted at 22 ± 1 °C, with results averaged over three measurements, including standard deviations (SDs).

3.3.3. Mechanical Strength

For mechanical testing, cylindrical samples with dimensions of 12 mm in height and 6 mm in diameter were fabricated using Teflon molds. The samples were extracted from the molds between their initial and final setting times and allowed to cure in air for 7 days. Following this curing period, compressive strength was evaluated using a universal testing machine (Instron 3345, Instron, Norwood, MA, USA). The cementitious samples were subjected to uniaxial compression at a crosshead speed of 1.0 mm/min. The compressive strength values were presented as the averages of 15 measurements, along with their standard deviations (SDs).

3.3.4. Porosity

The open porosity and pore size distribution of the foamed cements were evaluated using mercury intrusion porosimetry (MIP) with the AutoPore IV porosimeter (Micrometrics, Norcross, GA, USA). Dried sample fragments were placed in the penetrometer, which was then positioned in the low-pressure chamber of the apparatus and degassed. Mercury was introduced into the penetrometer, and the volume of mercury intrusion was recorded as the pressure increased. After completing the low-pressure measurements, the penetrometer was moved to the high-pressure chamber for additional testing. All measurements were performed in triplicate.

3.3.5. Microstructure

To observe the microstructures of the fractured samples and assess the bioactive potential of the materials, a PhenomPure scanning electron microscope (SEM) from Thermo Fisher Scientific (Waltham, MA, USA) was employed. Before examination, the samples were coated with a thin layer of gold using a low deposition rate to prevent charge accumulation and enhance image resolution.

3.3.6. Chemical Stability and Bioactivity

To assess the in vitro chemical stability of the materials, cylindrical samples with dimensions of 3 mm in height and 6 mm in diameter were placed in plastic containers with 20 mL of either simulated body fluid (SBF) or distilled water and incubated at 37 °C for 4 weeks. During this period, the ionic conductivity and pH of the surrounding solutions were monitored using a Seven Compact Duo pH/conductometer (Mettler Toledo, Columbus, OH, USA). The in vitro bioactivity of the bone substitutes was evaluated through scanning electron microscopy (SEM), focusing on the formation of apatite layers on the material surfaces after 7 days of incubation in SBF.

3.3.7. Cell Studies

In vitro cytocompatibility studies were performed using a mouse primary calvarial preosteoblast cell line (MC3T3-E1 Subclone 4, CRL-2593, ATCC-LGC standards, Teddington, UK). MC3T3-E1 cells were cultured in Alpha Minimum Essential Medium (GIBCO, Life Technologies, Carlsbad, CA, USA) supplemented with 10% fetal bovine serum (FBS, PanBiotech GmbH, Aidenbach, Bavaria, Germany) and antibiotics (100 U/mL of penicillin and 0.1 mg/mL of streptomycin) (Sigma-Aldrich Chemicals, Warsaw, Poland). The cells were maintained at 37 °C with 5% CO_2 in an air atmosphere.

Before the cell culture experiments, all samples were sterilized by ethylene oxide. The cytotoxicity of the fabricated cementitious samples was evaluated based on MC3T3-E1 viability after the cells were exposed to the liquid biomaterial extracts in accordance with ISO 10993-5 (2009). First, mouse preosteoblasts at a concentration of 1.5×10^5 cells/mL were seeded in flat-bottom 96-multiwell plates and cultured for 24 h. Next, the culture

medium was replaced with sample extracts prepared according to ISO 10993-12:2021. The cell culture medium incubated in a polystyrene plate served well as a negative control. After 24 h, the cytotoxicity of the bone cement samples was assessed using WST-8 and LDH total assays, according to the manufacturers' instructions (Sigma-Aldrich Chemicals, Warsaw, Poland). The cytotoxicity of the tested samples was also estimated using a Live/Dead Double Staining Kit (Sigma-Aldrich Chemicals, St. Louis, MO, USA). The study was conducted in direct contact of mouse preosteoblasts with biomaterials. First, cells were seeded directly on the pre-soaked samples at a concentration of 1×10^5 and cultured for 48 h. Next, the cells were fluorescently stained using a Live/Dead Double Staining Kit according to the manufacturer's instructions and visualized using a confocal laser scanning microscope (CLSM, Olympus Fluoview equipped with FV1000, Olympus Corporation, Tokyo, Japan). Cells seeded on the polystyrene surface were used as a control.

3.3.8. Statistics

The statistical analysis of the obtained results was performed using a one-way analysis of variance (ANOVA) with a post hoc Tukey Honestly Significant Difference (HSD) test for comparing multiple treatments. Statistically significant differences were indicated by * ($p < 0.05$) and ** ($p < 0.01$). In the case of in vitro cell culture tests, statistical significance was considered at $p < 0.05$.

4. Conclusions

In this research, innovative hybrid bone substitutes were developed and investigated. The cementitious materials produced consisted of highly reactive α-TCP powder (either unmodified or modified with silane coupling agents), hybrid hydroxyapatite–chitosan granules, and citrus pectin used with disodium phosphate as the liquid phase. This study focused on the impact of two distinct coupling agents—tetraethyl orthosilicate (TEOS) and 3-glycidoxypropyltrimethoxysilane (GPTMS)—on the physicochemical and biological properties of the bone substitutes. The unique characteristics of these materials stem from the hybrid system, which synergistically relies on chemical interactions between the hybrid granules, pectin, and SCA-modified tricalcium phosphates. These chemical interactions contribute to reducing porosity and strengthening the bone substitutes, resulting in an increase in compressive strength from approximately 11.42 to 19.34 MPa. Notably, the silane coupling agents had beneficial effects on the materials' microstructure, chemical stability, or biological performance. All the developed cements exhibited bioactive potential in vitro, indicating their suitability for further biological research. Additionally, the use of easily functionalizable polymers like chitosan and citrus pectin, alongside silane coupling agents, allows for future modifications of the materials with drugs or other bioactive compounds. This research highlights the favorable properties of the bone substitutes, laying the groundwork for future in vitro and in vivo investigations.

Author Contributions: Conceptualization, P.P. and J.P.C.; Funding Acquisition, A.D.-R. and A.Z.; Investigation, P.P., V.V., J.P.C., A.D.-R. and A.Z.; Methodology, P.P. and J.P.C.; Project Administration, A.D.-R. and A.Z.; Supervision, J.P.C. and A.Z.; Validation, J.P.C. and A.Z.; Visualization, P.P. and V.V.; Writing—Original Draft, P.P. and V.V.; Writing—Review and Editing, J.P.C., A.D.-R. and A.Z. All authors have read and agreed to the published version of the manuscript.

Funding: Research project supported by the program "The Excellence Initiative – Research University" for the AGH University of Science and Technology. The authors are thankful to the Deutsche Forschungsgemeinschaft DFG for the financial support of the projects Do-660/7-1 and Do-660/7-2. This work was supported by the NAWA STER Programme Internationalization of the Doctoral School of AGH University of Kraków (12.12.455.00710). Research co-funded by the Faculty of Materials Science and Ceramics, AGH University of Kraków, Kraków, Poland, Project No. 16.16.160.557 (2025).

Institutional Review Board Statement: Not applicable.

Informed Consent Statement: Not applicable.

Data Availability Statement: The data presented in this study are available on request from the corresponding author.

Conflicts of Interest: The authors declare no conflicts of interest.

References

1. Tronco, M.C.; Cassel, J.B.; dos Santos, L.A. α-TCP-based calcium phosphate cements: A critical review. *Acta Biomater.* **2022**, *151*, 70–87. [CrossRef]
2. Zhao, X. Introduction to bioactive materials in medicine. In *Woodhead Publishing Series in Biomaterials, Bioactive Materials in Medicine*; Woodhead Publishing: Sawston, UK, 2011; pp. 1–13. [CrossRef]
3. Pylostomou, A.; Demir, Ö.; Loca, D. Calcium phosphate bone cements as local drug delivery systems for bone cancer treatment. *Mater. Sci. Eng. C* **2023**, *148*, 213367. [CrossRef] [PubMed]
4. Schröter, L.; Kaiser, F.; Stein, S.; Gbureck, U.; Ignatius, A. Biological and mechanical performance and degradation characteristics of calcium phosphate cements in large animals and humans. *Acta Biomater.* **2020**, *117*, 1–20. [CrossRef]
5. Steinacker, V.C.; Weichhold, J.; Renner, T.; Gubik, S.; Vollmer, A.; Breitenbücher, N.; Fuchs, A.; Straub, A.; Hartmann, S.; Kübler, A.C.; et al. Biological and mechanical performance of calcium phosphate cements modified with phytic acid. *J. Mater. Sci. Mater. Med.* **2024**, *35*, 36. [CrossRef]
6. Graça, M.P.F.; Gavinho, S.R. Calcium Phosphate Cements in Tissue Engineering. In *Contemporary Topics About Phosphorus in Biology and Materials*; IntechOpen: London, UK, 2020. [CrossRef]
7. Ginebra, M.; Rilliard, A.; Fernández, E.; Elvira, C.; Román, J.S.; Planell, J.A. Improvement of the Mechanical Properties of an α-TCP Cement by the Addition of a Polymeric Drug Containing Salicylic Acid. *Key Eng. Mater.* **2000**, *192-195*, 781–784. [CrossRef]
8. Geffers, M.; Groll, J.; Gbureck, U. Reinforcement Strategies for Load-Bearing Calcium Phosphate Biocements. *Materials* **2015**, *8*, 2700–2717. [CrossRef]
9. Dos Santos, L.; De Oliveira, L.; Rigo, E.; Carrodeguas, R.; Boschi, A.; De Arruda, A. Influence of polymeric additives on the mechanical properties of α-tricalcium phosphate cement. *Bone* **1999**, *25*, 99S–102S. [CrossRef] [PubMed]
10. A Perez, R.; Kim, H.-W.; Ginebra, M.-P. Polymeric additives to enhance the functional properties of calcium phosphate cements. *J. Tissue Eng.* **2012**, *3*, 2041731412439555. [CrossRef]
11. Czechowska, J.; Zima, A.; Siek, D.; Ślósarczyk, A. Influence of sodium alginate and methylcellulose on hydrolysis and physicochemical properties of α-TCP based materials. *Ceram. Int.* **2018**, *44*, 6533–6540. [CrossRef]
12. Watanabe, M.; Tanaka, M.; Sakurai, M.; Maeda, M. Development of calcium phosphate cement. *J. Eur. Ceram. Soc.* **2006**, *26*, 549–552. [CrossRef]
13. Dziadek, M.; Zima, A.; Cichoń, E.; Czechowska, J.; Ślósarczyk, A. Biomicroconcretes based on the hybrid HAp/CTS granules, α-TCP and pectins as a novel injectable bone substitutes. *Mater. Lett.* **2020**, *265*, 127457. [CrossRef]
14. Guo, L.; Liang, Z.; Yang, L.; Du, W.; Yu, T.; Tang, H.; Li, C.; Qiu, H. The role of natural polymers in bone tissue engineering. *J. Control. Release* **2021**, *338*, 571–582. [CrossRef]
15. Gu, T.; Shi, H.; Ye, J. Reinforcement of calcium phosphate cement by incorporating with high-strength β-tricalcium phosphate aggregates. *J. Biomed. Mater. Res. Part B Appl. Biomater.* **2011**, *100B*, 350–359. [CrossRef]
16. Xu, H.H.; Quinn, J.B. Calcium phosphate cement containing resorbable fibers for short-term reinforcement and macroporosity. *Biomaterials* **2002**, *23*, 193–202. [CrossRef]
17. Boehm, A.V.; Meininger, S.; Gbureck, U.; Müller, F.A. Self-healing capacity of fiber-reinforced calcium phosphate cements. *Sci. Rep.* **2020**, *10*, 9430. [CrossRef]
18. Czechowska, J.P.; Dorner-Reisel, A.; Zima, A. Hybrid Bone Substitute Containing Tricalcium Phosphate and Silver Modified Hydroxyapatite–Methylcellulose Granules. *J. Funct. Biomater.* **2024**, *15*, 196. [CrossRef]
19. Pańtak, P.; Czechowska, J.P.; Zima, A. The influence of silane coupling agents on the properties of α-TCP-based ceramic bone substitutes for orthopaedic applications. *RSC Adv.* **2023**, *13*, 34020–34031. [CrossRef]
20. Tang, Q.; Xiao, P.; Kou, C.; Lou, K.; Kang, A.; Wu, Z. Physical, chemical and interfacial properties of modified recycled concrete aggregates for asphalt mixtures: A review. *Constr. Build. Mater.* **2021**, *312*, 125357. [CrossRef]
21. Kouhi, M.; Reddy, V.J.; Ramakrishna, S. GPTMS-Modified Bredigite/PHBV Nanofibrous Bone Scaffolds with Enhanced Mechanical and Biological Properties. *Appl. Biochem. Biotechnol.* **2018**, *188*, 357–368. [CrossRef]

22. Bravaya, N.; Saratovskikh, S.; Panin, A.; Faingol'D, E.; Zharkov, I.; Babkina, O.; Vasil'EV, S.; Bubnova, M.; Volkov, V.; Lobanov, M. Influence of silane coupling agent on the synthesis and properties of nanocomposites obtained via in situ catalytic copolymerization of ethylene and propylene in the presence of modified Nafen™ Al_2O_3 nanofibers. *Polymer* **2019**, *174*, 114–122. [CrossRef]
23. Varghese, J.T.; Cho, K.; Raju; Farrar, P.; Prentice, L.; Prusty, B.G. Influence of silane coupling agent on the mechanical performance of flowable fibre-reinforced dental composites. *Dent. Mater.* **2022**, *38*, 1173–1183. [CrossRef] [PubMed]
24. Götz, W.; Tobiasch, E.; Witzleben, S.; Schulze, M. Effects of Silicon Compounds on Biomineralization, Osteogenesis, and Hard Tissue Formation. *Pharmaceutics* **2019**, *11*, 117. [CrossRef] [PubMed]
25. Lim, P.; Konishi, T.; Wang, Z.; Feng, J.; Wang, L.; Han, J.; Yang, Z.; Thian, E. Enhancing osteoconductivity and biocompatibility of silver-substituted apatite in vivo through silicon co-substitution. *Mater. Lett.* **2018**, *212*, 90–93. [CrossRef]
26. Reid, J.W.; Tuck, L.; Sayer, M.; Fargo, K.; Hendry, J.A. Synthesis and characterization of single-phase silicon-substituted α-tricalcium phosphate. *Biomaterials* **2006**, *27*, 2916–2925. [CrossRef]
27. Mestres, G.; Le Van, C.; Ginebra, M.P. Silicon-stabilized α-tricalcium phosphate and its use in a calcium phosphate cement: Characterization and cell response. *Acta Biomater.* **2012**, *8*, 1169–1179. [CrossRef]
28. Şahin, E. Calcium Phosphate Bone Cements. In *Cement Based Materials*; InTech Open: London, UK, 2018. [CrossRef]
29. Yubao, L.; Xingdong, Z.; de Groot, K. Hydrolysis and phase transition of alpha-tricalcium phosphate. *Biomaterials* **1997**, *18*, 737–741. [CrossRef]
30. Casagrande, C.A.; Jochem, L.F.; Repette, W.L. Analysis of the 3-Glycidoxypropyltrimethoxysilane (GPTMS) hydrolysis by infrared spectroscopy. *Mater. De Jan.* **2020**, *25*, e-12811. [CrossRef]
31. Rubio, F.; Rubio, J.; Oteo, J.L. A FT-IR Study of the Hydrolysis of Tetraethylorthosilicate (TEOS). *Spectrosc. Lett.* **1998**, *31*, 199–219. [CrossRef]
32. Gui-Long, X.; Changyun, D.; Yun, L.; Pi-Hui, P.; Jian, H.; Zhuoru, Y. Preparation and Characterization of Raspberry-like SiO_2 Particles by the Sol-Gel Method. *Nanomater. Nanotechnol.* **2011**, *1*, 21. [CrossRef]
33. He, Z.; Zhai, Q.; Hu, M.; Cao, C.; Wang, J.; Yang, H.; Li, B. Bone cements for percutaneous vertebroplasty and balloon kyphoplasty: Current status and future developments. *J. Orthop. Transl.* **2015**, *3*, 1–11. [CrossRef]
34. Durucan, C.; Brown, P.W. Reactivity of α-tricalcium phosphate. *J. Mater. Sci.* **2002**, *37*, 963–969. [CrossRef]
35. Pańtak, P.; Cichoń, E.; Czechowska, J.; Zima, A. Influence of Natural Polysaccharides on Properties of the Biomicroconcrete-Type Bioceramics. *Materials* **2021**, *14*, 7496. [CrossRef]
36. Wei, X.; Ugurlu, O.; Ankit, A.; Acar, H.Y.; Akinc, M. Dissolution behavior of Si,Zn-codoped tricalcium phosphates. *Mater. Sci. Eng. C* **2009**, *29*, 126–135. [CrossRef]
37. Ji, E.; Song, Y.H.; Seo, J.H.; Joo, K.I. Utilization of functionalized silane coatings for enhanced mechanical properties of hydroxyapatite filler. *Korean J. Chem. Eng.* **2023**, *40*, 1709–1714. [CrossRef]
38. Vaz, C.; Reis, R.; Cunha, A. Use of coupling agents to enhance the interfacial interactions in starch–EVOH/hydroxylapatite composites. *Biomaterials* **2002**, *23*, 629–635. [CrossRef]
39. Kotha, S.P.; Lieberman, M.; Vickers, A.; Schmid, S.R.; Mason, J.J. Adhesion enhancement of steel fibers to acrylic bone cement through a silane coupling agent. *J. Biomed. Mater. Res. Part A* **2005**, *76A*, 111–119. [CrossRef]
40. Pańtak, P.; Czechowska, J.P.; Kashimbetova, A.; Čelko, L.; Montufar, E.B.; Wójcik, Ł.; Zima, A. Improving the processability and mechanical strength of self-hardening robocasted hydroxyapatite scaffolds with silane coupling agents. *J. Mech. Behav. Biomed. Mater.* **2024**, *161*, 106792. [CrossRef]
41. Pape, P.G.; Promoters, A. *Plastics Design Library, Applied Plastics Engineering Handbook*; William Andrew Publishing: Norwich, NY, USA, 2011; pp. 503–517. [CrossRef]
42. Wu, J.-K.; Zheng, K.-W.; Nie, X.-C.; Ge, H.-R.; Wang, Q.-Y.; Xu, J.-T. Promoters for Improved Adhesion Strength between Addition-Cured Liquid Silicone Rubber and Low-Melting-Point Thermoplastic Polyurethanes. *Materials* **2022**, *15*, 991. [CrossRef] [PubMed]
43. Matinlinna, J.P.; Lung, C.Y.K.; Tsoi, J.K.H. Silane adhesion mechanism in dental applications and surface treatments: A review. *Dent. Mater.* **2018**, *34*, 13–28. [CrossRef] [PubMed]
44. Lee, C.; Yamaguchi, S.; Imazato, S. Quantitative evaluation of the degradation amount of the silane coupling layer of CAD/CAM resin composites by water absorption. *J. Prosthodont. Res.* **2023**, *67*, 55–61. [CrossRef]
45. Kokubo, T.; Takadama, H. How useful is SBF in predicting in vivo bone bioactivity? *Biomaterials* **2006**, *27*, 2907–2915. [CrossRef] [PubMed]
46. Kolmas, J.; Kaflak, A.; Zima, A.; Ślósarczyk, A. Alpha-tricalcium phosphate synthesized by two different routes: Structural and spectroscopic characterization. *Ceram. Int.* **2015**, *41*, 5727–5733. [CrossRef]
47. Czechowska, J.; Zima, A.; Paszkiewicz, Z.; Lis, J.; Ślósarczyk, A. Physicochemical properties and biomimetic behaviour of α-TCP-chitosan based materials. *Ceram. Int.* **2014**, *40*, 5523–5532. [CrossRef]

48. Zima, A. Hydroxyapatite-chitosan based bioactive hybrid biomaterials with improved mechanical strength. *Spectrochim. Acta Part A: Mol. Biomol. Spectrosc.* **2018**, *193*, 175–184. [CrossRef] [PubMed]
49. *ASTM C266-20*; Standard Test Method for Time of Setting of Hydraulic-Cement Paste by Gillmore Needles. ASTM International: West Conshohocken, PA, USA, 2021. Available online: https://store.astm.org/c0266-20.html (accessed on 10 July 2025).

Publikacja 5 – *„The influence of titanium and cooper on physiochemical and antibacterial properties of bioceramic-based composites for orthopaedic applications”*

Ceramics International 51 (2025) 1214–1226

Contents lists available at ScienceDirect

Ceramics International

journal homepage: www.elsevier.com/locate/ceramint

The influence of titanium and cooper on physiochemical and antibacterial properties of bioceramic-based composites for orthopaedic applications

Piotr Pańtak [a,*], Joanna P. Czechowska [a], Anna Belcarz [b], Aneta Zima [a]

[a] Faculty of Materials Science and Ceramics, AGH University of Krakow, Mickiewicza Av. 30, 30-058, Kraków, Poland
[b] Chair and Department of Biochemistry and Biotechnology, Medical University of Lublin, Chodźki 1,20-093, Lublin, Poland

ARTICLE INFO

Handling Editor: Dr P. Vincenzini

Keywords:
Bioceramic
Bone cements
Calcium phosphates
Hybrid materials
Cooper
Titanium

ABSTRACT

This study examines the impact of titanium and copper ion modifications on the properties of hybrid hydroxyapatite/chitosan granules, which serve as components of novel injectable bone substitutes - biomicroconcretes. In addition to the hybrid granules, the powdered phase of the composites comprises highly reactive α-tricalcium phosphate (α-TCP) powder. The utilization of a mixture consisting of citrus pectin and disodium phosphate as the liquid phase of bone substitutes facilitated the development of easily mouldable, fully injectable biomicroconcretes based on calcium phosphate, characterized by distinct properties. The resulting biomicroconcretes demonstrated favourable cohesion and setting times falling within acceptable parameters. Furthermore, the incorporation of citrus pectin into the liquid phase significantly augmented the mechanical strength of the materials. The unique attributes of biomicroconcretes containing citrus pectin arise from the presence of both a dual setting system and a double hybrid system. The dual setting mechanism, stemming from the hydrolysis of α-TCP and the crosslinking of citrus pectin in the presence of Ca^{2+} ions, yielded materials distinguished by excellent cohesion and chemical stability. Conversely, the double hybrid system emerged from the coexistence of hybrid granules and interactions between polycationic chitosan within the hybrid granules and polyanionic citrus pectin. All obtained biomicroconcretes exhibited *in vitro* bioactivity, positioning them as promising candidates for further biological investigations. Notably, the integration of antibacterial copper ions into hybrid hydroxyapatite/chitosan granules significantly enhances their potential utility as bone substitute materials, effectively reducing the risk of *S. aureus* and *E. coli* infection during surgical procedures. It has been found that titanium modified composites reduced adhesion of *S. aureus* but did not reduce the adhesion of *E. coli* cells. This research validates the advantageous properties of the synthesized ceramic-based biomaterials and sets the stage for subsequent *in vitro* and *in vivo* studies.

1. Introduction

Calcium phosphate (CaPs) ceramics have wide applications, particularly in bone tissue engineering, due to properties that make them superior to other bone substitutes [1]. Their biological characteristics, including the ability to form a durable bond with bone tissue, allow their use in fields like orthopedics, maxillofacial surgery, and dentistry [2,3]. Calcium phosphates are available as ceramic blocks, porous sponges, granules, or calcium phosphate-based bone cements (CPCs) [4]. Bone cements, composed of powder and liquid phases, form a plastic paste upon mixing, enabling easy implantation into defects of various shapes and sizes [5]. Bone cements based on α-tricalcium phosphate (α-TCP) are notable for their self-setting capability and their ability to hydrolyze into calcium-deficient hydroxyapatite. However, due to the brittleness, their use is limited to non-load-bearing applications [6]. Various modifications have been explored to enhance the mechanical strength of calcium phosphate-based bone cements. Recent research has focused on introducing aggregates such as granules, fibers, or microspheres, which act as crack-arresting inclusions, creating composites similar to concrete in construction materials. These composites can be referred to as biomicroconcretes [7–10]. Another method to improve CPC strength is the use of polymer additives [11,12]. Previous studies highlighted the beneficial effects of citrus pectin gel, combined with a setting accelerator (disodium hydrogen phosphate), resulting in acceptable setting times and enhanced mechanical strength [13]. Additionally, citrus pectin allows to obtain injectability of biomaterials, which is a desirable

* Corresponding author.
E-mail address: pantak@agh.edu.pl (P. Pańtak).

https://doi.org/10.1016/j.ceramint.2024.11.102
Received 6 August 2024; Received in revised form 17 October 2024; Accepted 7 November 2024
Available online 8 November 2024

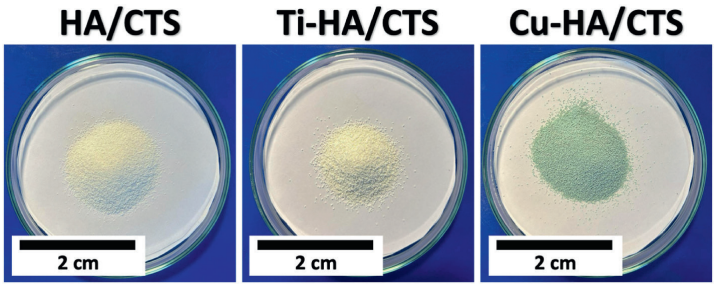

Fig. 1. The hybrid inorganic-organic hydroxyapatite-chitosan granules modified with titanium (Ti-HA/CTS) and cooper (Cu-HA/CTS) ions.

feature for minimally invasive surgeries [14].

Despite the beneficial properties of calcium phosphate-based bone cements, infections frequently occur due to improper implantation procedures or inadequate sterilization, which can hinder subsequent patient treatment [15]. To mitigate this risk, various strategies have been applied to obtain antibacterial or bactericidal activity of biomaterials, including using antibiotics, metal nanoparticles (eg.AuNPs, AgNPs, CuNPs) or antibacterial ions [16,17]. Despite the beneficial impact of antibiotics on the antibacterial properties of bone substitutes, the potential for allergies in some patients and the limited spectrum of antibacterial action necessitate exploration of other strategies. Furthermore, the emergence of multidrug-resistant bacterial strains makes it crucial to investigate other biologically active substances as alternatives to antibiotics. In recent years, a promising strategy for imparting antibacterial properties to implantable materials designed for bone tissue regeneration has been the use of copper and titanium ions.

In 2017 Rau et al. [18] obtained calcium phosphate cement containing β-TCP doped with copper ions, which inhibited apatite formation and exhibited antibacterial effects against Gram-negative bacteria. The antibacterial activity was attributed to copper ions, while the enhanced viability of human cells suggested a dual effect of copper: toxic to bacteria yet beneficial to healthy cells, likely due to differences in the protection mechanisms of prokaryotes and eukaryotes. Numerous studies confirmed beneficial impact of cooper ions on antibacterial properties biomaterials for bone tissue regeneration. For example, in 2019 Foroutan et al. [19] synthesized novel calcium phosphate glasses containing 0, 2, 4, and 6 mol % Cu^{2+}. They investigated the physicochemical properties of developed materials, as well as enhanced antibacterial activity against *S. aureus*. Fadeeva et al. [20] developed copper-substituted tricalcium phosphate ceramics with antibacterial properties to combat antibiotic resistance. Cu-TCP demonstrated antibacterial activity against *Escherichia coli* and *Salmonella enteritidis*, while showing good cytocompatibility in cell culture studies. Jacobs et al. [21] investigated the cytotoxicity and antibacterial properties of Cu-doped Biphasic Calcium Phosphate (BCP) powders, composed mainly of hydroxyapatite and β-tricalcium phosphate. Authors confirmed strong antibacterial effect of copper against both Gram-positive (*Staphylococcus aureus*) and Gram-negative (*Escherichia coli* and *Pseudomonas aeruginosa*) bacteria.

Copper ions exhibit a strong antibacterial effect; however, the potential application of other metal ions, such as titanium, is intriguing. Nonetheless, the antibacterial activity of titanium ions has not yet been fully explored. Stipniece et al. [22] synthesized Ag- and/or Ti-doped apatitic-tricalcium phosphate powders using a wet chemical precipitation method. The authors determined the minimum inhibitory concentration and antibacterial activity of the doped powders against *Staphylococcus aureus*, demonstrating that the inclusion of both Ti and Ag imparts antibacterial properties to β-tricalcium phosphate against this Gram-positive bacterium. The same research group presented the results of studies on effect of titanium on the antibacterial properties of highly porous bioceramic scaffolds. They confirmed the beneficial effect of titanium on the antibacterial activity of the materials [23,24]. In the literature, the obtaining of most ion-doped calcium phosphates is associated with high-temperature treatment. However, the development of hybrid-type, antibacterial ion-enriched materials without thermal treatment represents a relatively new branch in the field of biomaterials engineering.

The aim of this study was to develop, obtain, and investigate novel injectable hybrid-type bone substitute materials based on highly reactive, self-setting α-TCP powder and hydroxyapatite-chitosan granules, and to assess the influence of their modification with titanium and copper ions on their physicochemical properties and antibacterial potential. The liquid phase of the materials consisted of a mixture of citrus pectin gel and disodium phosphate. This composition allowed for the development of dual hybrid bone substitutes, consisting of hybrid granules and hybrids derived from polyelectrolyte interactions, with a dual setting mechanism. The careful selection of the liquid phase enabled the development of fully injectable materials containing hybrid granules. Furthermore, the ion modification, resulted in composites with antibacterial properties.

2. Materials and methods

2.1. Materials

As a solid phase of developed materials, α-tricalcium phosphate powder (α-TCP) and hybrid hydroxyapatite/chitosan (HA/CTS) granules, also modified with titanium (Ti-HA/CTS) or cooper (Cu-HA/CTS) were used. The highly reactive α-TCP powder was obtained via a wet chemical method described previously [25]. As the reagents, $Ca(OH)_2$ (≥99.5 %, Merck, Darmstadt, Germany) and H_3PO_4 (85.0 %, POCH, Gliwice, Poland) were applied. HA/CTS hybrid materials, in the form of granules (300–400 μm) were prepared by the modified wet chemical method described previously [26]. The following substrates: $Ca(OH)_2$ (≥99.5 wt%, Merck, Darmstadt, Germany), H_3PO_4 (85.0 wt%, POCH, Gliwice, Poland), and medium-molecular-weight chitosan (~100,000 kDa, DD ≥ 75.0 wt%, Sigma-Aldrich, St. Louis, MO, USA) were used. To maintain the reaction environment above a pH level of 10, a 5 wt% solution of sodium hydroxide (pure p.a., POCH, Gliwice, Poland) was utilized. Titanium chloride, $TiCl_3$ (15.0 %, Merck, Darmstadt, Germany), and copper nitrate, $Cu(NO_3)_2*3H_2O$ (pure p.a., Chempur, Piekary Śląskie, Poland), were employed as sources of titanium and copper ions, respectively. The amount of titanium or copper introduced into the material was 5.0 wt%. The resulting hybrid inorganic-organic hydroxyapatite-chitosan granules modified with titanium (Ti-HA/CTS) and cooper (Cu-HA/CTS) ions are presented in Fig. 1. The mixture of 1 wt% disodium phosphate (99.9 wt%, Chempur, Piekary Śląskie, Poland) in 2.5 wt% low esterified amidated citrus pectin gel (Herbstreith & Fox, Werder/Havel, Germany) was applied as the liquid phase.

Table 1
The initial composition of developed materials.

Material	Solid phase (P)	Liquid phase (L)	L/P [g/g]
BM-C	α-TCP: HA/CTS granules 3:2 by weight	1.0 wt% Na_2HPO_4 solution in 2.5 wt % citrus pectin gel	0.5
BM-Ti	α-TCP: Ti-HA/CTS granules 3:2 by weight		
BM-Cu	α-TCP: Cu-HA/CTS granules 3:2 by weight		

2.2. Preparation of biomicroconcretes

Biomicroconcreates are composed of solid phase (setting powder and aggregate) and liquid phase, which when are mixed, create a paste that sets in situ. In this study, three types of powder batches containing: α-TCP and HA/CTS, Ti-HA/CTS or Cu-HA/CTS granules were used as solid phase (Table 1). The liquid to powder (L/P) ratio was selected based on preliminary studies and it was 0.5 g/g.

2.3. Methods

2.3.1. Injectability

The injectability test of the cementitious materials was carried out by extruding cement paste through a 2 mm nozzle of 20 mL plastic syringe (B. Brown, Melsungen, Germany) directly into the cylinder with simulated body fluid (SBF) solution, preheated to 37 °C, as described in previous study [13]. The force applied to syringe plunger during injection was assessed using an Instron 3345 universal testing machine (Instron, Norwood, MA, USA) at a crosshead displacement rate of 1.0 mm/min. Triplicate measurements were conducted for each material. The injectability of the material was determined by the constant pressure force during homogeneous paste extrusion. Results are expressed as mean of three measurements ± standard deviation (SD).

2.3.2. Setting times

The setting times of obtained materials were measured. The initial (t_i) and final (t_f) setting times of the obtained biomaterials were determined using Gillmore apparatus (Humboldt, Norridge, IL, USA) according to ASTM C266-20 standard [27]. All experiments were carried out at 22.0 ± 1.0 °C. Test samples were prepared in 10 mm × 7 mm x 3 mm cuboids form. All measurements were performed in triplicate. The results are presented as the mean ± standard deviation (SD).

2.3.3. Chemical and phase composition

The X-ray fluorescence method (XRF) was applied to check the chemical composition of the initial powders (WDXRF Axios Max, PANalytical, Malvern, UK). The X-ray diffraction (XRD) analysis was performed using Cu Kα radiation (1.54 Å) at 30 kV and 10 mA. The analysis was conducted in the 2θ range of 10–60° at 0.04 intervals with a scanning speed of 2.5°/min using D2 Phaser diffractometer (Bruker, Ballerica, MA, USA). The XRD powder method was applied. The obtained diffractograms were compared with the International Centre for Diffraction Data α-TCP (00-009-0348) and hydroxyapatite (HA; 01-076-0694) to identify the crystalline phases. TOPAS software (Bruker, Ballerica, MA, USA) was used for phase quantification based on Rietveld refinement. All measurements were performed in triplicate. The mean ± standard deviation (SD) was used to present the results.

The structural studies of obtained biomaterials after setting and hardening were performed using Fourier Transform Infrared (FTIR) spectroscopy, within the scanning range of 400–4000 cm^{-1} and resolution of 4 cm^{-1} using a BioRad FTS 6000 spectrometer (Vertex 70&70v, Bruker, Ballerica, MA, USA). Positions of the FTIR bands were measured in accordance with the centre of weight. The baseline correction, normalization, and spectra analyses were performed using Spectragryph software (v1.2.15, Friedrich Menges, Oberstdorf, Germany).

2.3.4. Mechanical properties

For the mechanical tests the cylindrical samples, 12 mm in height and 6 mm in diameter, were prepared in Teflon molds. Samples were removed from the molds between their initial and final setting times and left for 7 days in air. After 7 days, the compressive strength of the samples was examined using the universal testing machine (Instron 3345, Instron, Norwood, MA, USA). Biomicroconcrete samples were subjected to uniaxial compression with a crosshead speed of 1.0 mm/min. The results of the compressive strength are presented as the mean value of 15 measurements ± standard deviation (SD).

2.3.5. Microstructure

The observations of the microstructure of obtained biomaterials were performed using a scanning electron microscope Scios 2 (SEM, PhenomPure, Thermo Fisher Scientific, Waltham, MA, USA). Before the study, samples were coated with a 10 nm carbon layer to avoid overcharging (EM ACE600 sputter coater, Leica Microsystems, Wetzlar, Germany) then observed at an accelerated voltage of 10–15 kV, under low vacuum, using in-column detector (T2) and opti-plane mode. The EDS detector was used for the elemental analysis in microareas, as well as for EDS elemental mapping.

2.3.6. Porosity

The open porosity and pore size distribution of the obtained bone cements were assessed via mercury intrusion porosimetry (MIP) using an AutoPore IV porosimeter (Micrometrics, Norcross, GA, USA). Dried fragments of the samples were placed in the penetrometer, which was subsequently placed in the low-pressure chamber for degassing. Mercury was then introduced into the penetrometer, and the volume of mercury intrusion was recorded as the pressure increased. Once the low-pressure phase was completed, the penetrometer was transferred to the high-pressure chamber for further testing. All measurements were repeated three times.

2.3.7. Chemical stability and bioactivity in vitro

To determine the *in vitro* chemical stability of materials, the cylindrical samples (3 mm in height and 6 mm in diameter) were placed in plastic containers with 20 mL of SBF or distilled water and stored at 37 °C for 4 weeks. Ionic conductivity and pH of the solutions around incubated samples were measured using Seven Compact Duo pH/conductometer (Mettler Toledo, Columbus, OH, USA). *In vitro* bioactivity of obtained biomicroconcretes was assessed via SEM observations of the apatite layers on the materials' surfaces after the 7-day samples incubation in SBF.

2.3.8. Ions release studies

The release of titanium and copper ions from the cementitious material powder was evaluated by immersing hardened materials in distilled water, with periodic collection of 25 μL aliquots. These aliquots were combined with 25 μL of hydrogen peroxide and concentrated ammonia, serving as complexing agents for titanium and copper, respectively. The mixture was placed in 96-well plates, and absorbance at λ = 600 nm was measured using a UV/Vis spectrophotometer (UV-2600i, Shimadzu, Japan). The absorbance values were then converted to concentrations using a calibration curve generated from titanium and copper salt solutions of known concentrations.

2.3.9. Antibacterial activity studies

2.3.9.1. Strains and maintenance. Staphylococcus aureus ATCC 25923 and *Escherichia coli* ATCC 25922 reference bacterial strains were used in

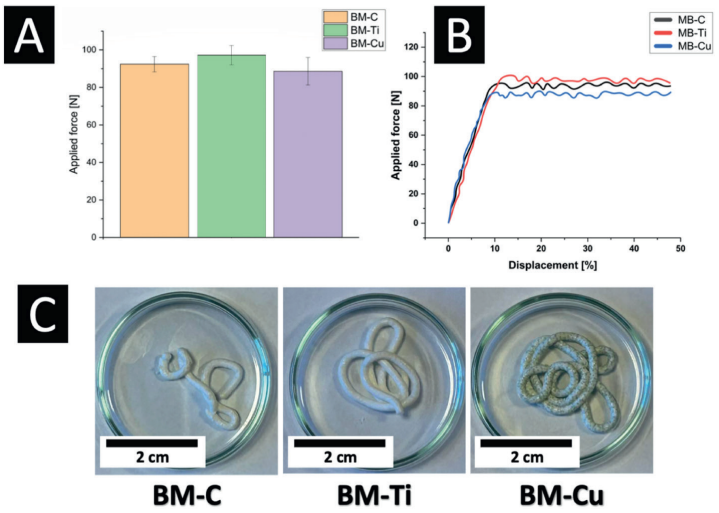

Fig. 2. Force required for pastes extrusion (A), the force-displacement curves of extruded pastes (B)and pastes immediately after injection into SBF (C).

all experiments. Both microorganisms were maintained in microbanks at −80 °C prior to the tests and then cultured on Mueller-Hinton agar plates (Biomaxima, Poland) at 37 °C (20–24 h). Approx. 3–4 CFUs (colony forming units) were finally transferred from the plates to Mueller-Hinton (M − H) broth (Biomaxima, Poland) and incubated for 24 h at 37 °C. The resulting suspensions were appropriately diluted before the experiments, individually for each strain. Tested biomaterials were sterilized by EthO (ethylene oxide) before the tests.

2.3.9.2. Agar plate test. Wells (ø = 7.5 mm) were drilled in Mueller-Hinton agar (Biomaxima, Poland) in 90 mm Petri dishes (thickness: 5–6 mm). Sterilized HAP/CTS, HAP/CTS/Ti and HAP/CTS/Cu samples were placed inside the wells (one per well). Then the wells were filled with melted Mueller-Hinton agar medium (approx. 40 °C). After medium setting, 500 µl of bacterial inoculate in sterile 0.9 % NaCl (0.1 McFarland standard – an equivalent of approx. 3.0 × 107 CFU/ml) was evenly spread onto the agar. Then plates were incubated at 37 °C for 20–24 h and diameters of bacterial growth inhibition zones were measured. The test was performed individually for each bacterial strain.

2.3.9.3. Antibacterial activity test (AATCC Test Method 100–2004 "antibacterial finishes on textile materials: assessment of"). Evaluation of antibacterial activity of tested samples was performed on basis of AATCC Test Method 100–2004 for textile materials, adapted for porous ceramic materials. Bacterial suspension (1.5 × 105 CFU/ml) of each strain was prepared in M − H broth diluted 250-fold in sterile 0.9 % NaCl. Samples (in triplicate) were placed on sterile microscope slides (Chemland, Poland) and soaked with 40 µl bacterial inoculate (the liquid was completely absorbed by the samples). In parallel, 40 µl of bacterial suspension of each strain was placed in sterile 50 ml Falcon tubes, to control the viability of bacteria without contact with tested materials (control). All samples were protected against evaporation and incubated at 37 °C, 24 h. Afterwards, the samples were transferred into 50 ml Falcon tubes containing 5 ml of sterile 0.9 % NaCl. For controls, 5 ml of sterile 0.9 % NaCl was added to 50 ml Falcon tubes. All tubes (with samples and controls) were vigorously shaken (1 min) to elute the bacterial cells and mix them with 0.9 % NaCl. Finally, 50 µl aliquots of all eluates were plated exponentially onto M − H agar Petri dishes using EasySpiral Dilute (Interscience, France) automatic plater (each sample in triplicate). M − H agar plates with plated bacteria eluted from the samples or controls were incubated at 37 °C for 20–28 h. CFUs were counted for each plate using Scan 300 colony counter (Interscience, France).

2.3.9.4. Bacterial adhesion test. Sterilized HAP/CTS, HAP/CTS/Ti and HAP/CTS/Cu were incubated with 1 ml of sterile suspension of bacterial cells (approx. 3.0×10^8 cells/ml) in Mueller-Hinton broth. After 2 h incubation at 37 °C, 50 rpm, in Innova 42 (New Brunswick Scientific, USA), non-adhered bacteria were gently washed away with 0.9 % NaCl (50 ml, 4 times) and samples were incubated with Viability/Cytotoxicity Assay Kit for Bacteria Live & Dead Cells (Biotium, USA) in 0.9 % NaCl (according to the instructions of producer). After staining at R/T, 10 min, in darkness, samples were washed in 0.9 % NaCl to remove non-absorbed dye and adhered bacteria were visualized by laser confocal scanning microscopy (LCSM) Olympus Fluoview FV1000; Olympus, Japan). Area of samples showing green fluorescence (indicating the presence of viable bacteria) as percent of total image area was quantified using ImageJ program.

2.3.10. Statistics

The statistical analysis of obtained results was done using a one-way analysis of variance (ANOVA) with a posthoc Tukey Honestly Significant Difference (HSD) test for comparing multiple treatments (* - statistically significant difference between the results, $p < 0.05$). All analyses were performed with OriginPro software (Version 2021, OriginLab Corporation, Northampton, MA, USA).

3. Results and discussion

3.1. Injectability

The injectability of bone substitutes is desirable feature as it offers a less invasive approach to stabilizing bone fractures, reinforcing weakened bone structures, and accelerating bone healing, due to the reduced surgical site [28]. The term injectability not only refers to the force required to extrude cement paste through a syringe needle but also the percentage of remaining paste in the syringe cylinder. From a practical point of view, the maximum force required to inject the paste should not

Table 2
Setting time of developed materials.

Material	*Initial setting time (t_i) [min]*	*Final setting time (t_f) [min]*
BM-C	11.5 ± 1.0	19.0 ± 1.5
BM-Ti	11.0 ± 0.5	18.5 ± 1.0
BM-Cu	12.0 ± 1.5	21.0 ± 1.0

exceed the force that a surgeon can generate with one hand during surgery. In the literature, the upper limit of this value is defined as 100N [29]. The outcomes of the injectability test and the visual characteristic of the cement pastes post-injection directly into simulated body fluid (SBF) at 37 °C are presented in Fig. 2.

Because calcium phosphate-based bone cements are predominantly non-injectable, various modifications of composition have been employed to improve the injectability of pastes [30]. In our study the addition of a polymeric modifier to the liquid phase sufficiently altered the rheological properties the material, which ultimately become injectable. Other researchers have also applied natural polymers to ensure injectability. For instance, Zhong et al. [31] incorporated oxidized sodium alginate into calcium phosphate bone cements, improving the rheological properties of the cementitious pastes and enabling the production of injectable materials. However, despite numerous scientific reports on injectable bone substitutes, the number of materials incorporating aggregates, such as granules, remains limited as they may potentially disrupt paste flow through a syringe and be a cause a filter-pressing phenomenon (liquid phase separation mechanism). In the case of designed materials, despite the presence of hybrid granules, pastes were fully injectable, and the force required for paste injection was below the recommended 100 N. In our study, by employing a mixture of citrus pectin and sodium hydrogen phosphate in the liquid phase, fully injectable, self-setting pastes were obtained. Furthermore, all pastes retained cohesion upon contact with simulated body fluid (SBF). The excellent cohesion of the pastes in SBF was determined by both hydrolysis of α-TCP to CDHA and the crosslinking of citrus pectin in the presence of calcium ions [32,33]. Modification with titanium and copper had no detrimental effect on injectability and cohesion of pastes.

3.2. Setting times

Apart from injectability, setting time is a significant parameter, especially during surgical procedures, because it determines the period during which the surgeon can manipulate the cement paste in its plastic state. Ideally, the surgeon should apply the paste into the defect between the initial and final setting times, during the so-called 'dough time' [34]. Under optimal conditions, the initial setting time (ti) should be around 15 min, while the final setting time should not exceed 30 min [35,36]. Despite some literature suggests that the final setting time should not exceed 15 min, it is convenient for the surgeon to have longer period for application of the injectable cement [37]. This allows for more precise application, often in hard-to-reach areas. The results of setting times for developed bone substitute materials are presented in Table 2.

The initial setting times of the investigated cement pastes ranged from 11.0 ± 0.5 to 12.0 ± 1.5 min, while the final setting times ranged from 18.5 ± 1.0 to 21.0 ± 1.0 min. Even though the developed materials exhibited slightly prolonged setting times, no negative influence of the complex composition on the cement setting process was observed. In the case of materials based solely on α-TCP, the setting process relies on the hydrolysis of this component to non-stoichiometric hydroxyapatite. Various factors influence the setting process of cementitious materials, including both material composition and external conditions [38]. The presence of polymers in cement mixtures, in both liquid and powder phases, improves their injectability but usually also increase setting times. One of the mechanisms that may prolong the setting process of α-TCP-based materials is the water absorption by polymers, which

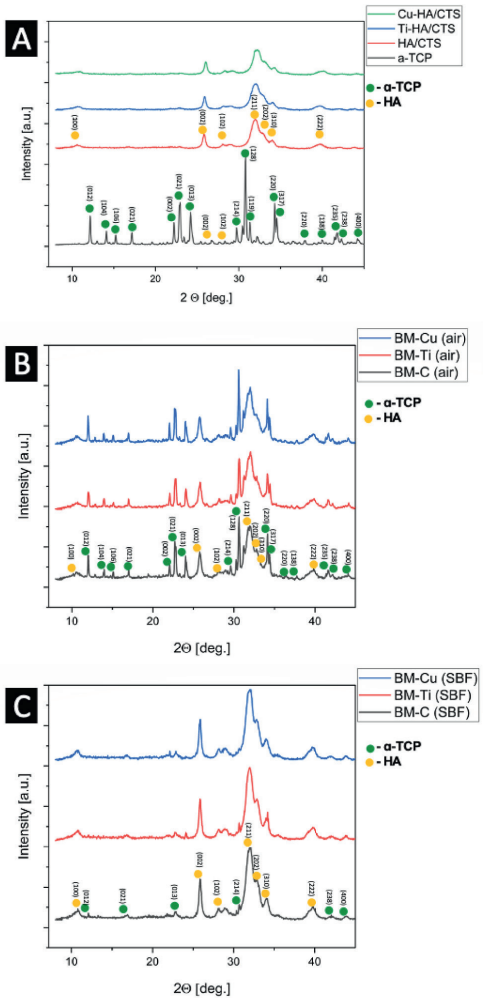

Fig. 3. XRD patterns of initial materials (a), materials after setting and hardening in air for 7 days (B), and materials after incubation in SBF for 7 days (C).

restrict the water availability crucial for α-TCP hydrolysis. To counteract prolonged setting it is recommended to apply substances known as setting accelerators (e.g., Na_2HPO_4) [39]. Through the simultaneous usage of citrus pectin gel and Na_2HPO_4, the materials demonstrated acceptable setting times. The developed biomicroconcretes possessed a dual setting system, which involved the simultaneous hydrolysis of α-TCP to non-stoichiometric hydroxyapatite and pectin cross-linking facilitated by Ca^{2+} ions [40]. The formation of complex between pectin and copper can also take place, as revealed inter alia by Seslija et al. [41], and Kohila rani et al. [42], which might contribute to slightly longer setting times in the case of BM-Cu.

3.3. Phase composition and structural studies

Study of the chemical and phase composition of calcium phosphate-based bone substitute materials allows for assessing their similarity to

Table 3
Phase composition of the obtained materials after 7 days of setting and hardening in air or SBF.

Material	7 days in air		7 days in SBF	
	α-TCP, wt. %	*Hydroxyapatite, wt. %*	*α-TCP, wt. %*	Hydroxyapatite, wt. %
BM-C	54 ± 1	46 ± 1	3 ± 1	97 ± 1
BM-Ti	56 ± 1	44 ± 1	2 ± 1	98 ± 1
BM-Cu	53 ± 1	47 ± 1	3 ± 1	98 ± 1

the inorganic component of bone tissue. The X-ray fluorescence method confirmed the presence of titanium and cooper in hybrid hydroxyapatite-chitosan granules. As expected, the amount of modifier was 4.87 ± 0.003 wt% and 5.11 ± 0.007 wt% for granules modified with 5 wt% of titanium and cooper respectively. Most studies describe doping calcium phosphates with various ions during their synthesis, however, effective incorporation of ions into the material structure typically requires post-synthesis thermal processing [43]. In our study, we employed wet chemical synthesis with no additional thermal treatment to obtain titanium and copper-modified hybrid granules with nearly expected amounts of modifiers, as no other crystalline phases containing titanium or copper were found.

The initial α-TCP powder primarily consisted of the α-TCP phase (97.0 ± 1.0 wt%) with a minor presence of hydroxyapatite (3.0 ± 1.0 wt %). In contrast, the hybrid granules (HA/CTS, Ti-HA/CTS, and Cu-HA/CTS) consisted solely of hydroxyapatite as the crystalline phase. No adverse effects of granules modification were observed, and no additional phases appeared in the material during synthesis.

The phase composition of the developed biomicroconcretes was strongly influenced by the sample storage environment. However, XRD analysis of set and hardened materials, showed only two crystalline phases: α-TCP and hydroxyapatite. The presence of polymers: chitosan and citrus pectin, was evident as the characteristic amorphous halos observed in the diffraction patterns. Fig. 3 depicts the diffraction patterns of the starting materials, as well as biomicroconcretes stored in air and incubated in SBF.

The detailed phase composition of obtained materials is presented in Table 3.

No significant differences in phase composition were observed between materials. The amount of α-TCP phase in the materials after 7 days in air was in the range from 53 ± 1 to 56 ± 1 wt%, while the proportion of hydroxyapatite phase was in the range from 44 ± 1 to 47 ± 1 wt. The analysis of samples' phase composition after 7 days of incubation in simulated body fluid (SBF) confirmed that α-TCP, undergoes spontaneous hydrolysis to form calcium-deficient hydroxyapatite. Similar observations were previously made for α-TCP-based cementitious bone substitutes [44,45].

Materials' FTIR spectra (Fig. 4) after setting and hardening, as well as after incubation in SBF showed characteristics bending bands at ~600 cm^{-1} and ~560 cm^{-1} and stretching bands around 967 and 1024 cm^{-1}, which corresponds to the vibrations of PO_4^{3-} groups. The wide band in the range of ~3000–3800 cm^{-1} is assigned to the absorbed water in the samples. Moreover, the spectra possess an absorption band at around 872 cm^{-1} which corresponds to HPO_4^{2-} groups, confirming the presence of non-stoichiometric hydroxyapatite. Additionally, in a similar spectral range between 870 and 875 cm^{-1}, carbonate bonds may appear in the material. Whereas the existence of a band at 1425 cm^{-1} indicates partial substitution of CO_3^{2-} in the hydroxyapatite structure during the transformation during its hydrolysis. Similar findings were reported for calcium phosphate-based biomaterials previously for example by Ślósarczyk et al. [46], and Durucan et al. [47]. FTIR studies confirm the presence of polymers in examined biomaterials. The absorption band with a maximum at ~2933 cm^{-1} can be attributed to stretching alkyl C-H bands. The band at around 1650 $cm^{-1}$was assigned to N-H bending vibrations of the primary amine from chitosan and amidated citrus pectin. What is more, the band around 1315 cm^{-1} and 3573 cm^{-1} corresponds to C-N and O-H stretching vibrations, respectively. In the systems containing pectin and chitosan, the formation of electrostatic and/or hydrogen bonding is possible. In the studied biomicroconcretes, the creation of polyelectrolyte complexes occurred at the hybrid granule/pectin interface. The formation of polyelectrolyte complexes between these molecules has been previously studied by Rashidova et al. [48] as well as Dziadek et al. [49]. The presence of electrostatic interactions among the components of the developed biomicroconcretes facilitates the creation of a double hybrid system, thereby influencing other physicochemical properties of the biomaterials. Despite the modification of hybrid granules with ions, no additional bands as well as

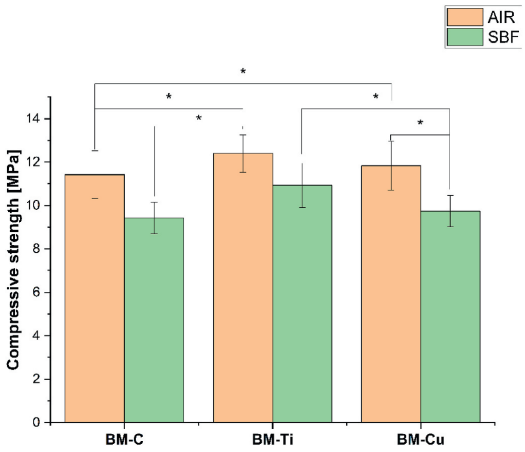

Fig. 5. Compressive strength of biomicroconcretes after 7-days of setting in air and after 7 days of incubation in SBF (* - statistically significant difference, $p < 0.05$).

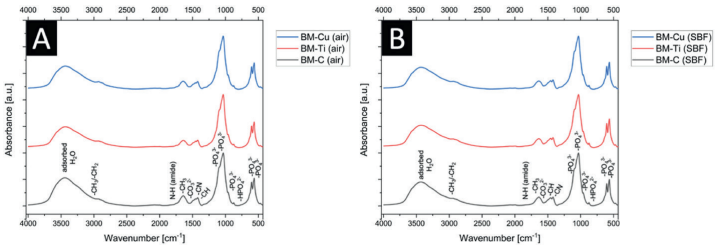

Fig. 4. FTIR spectra of obtained biomaterials: after setting and hardening in air for 7 days (A), and materials after incubation in SBF for 7 days (B).

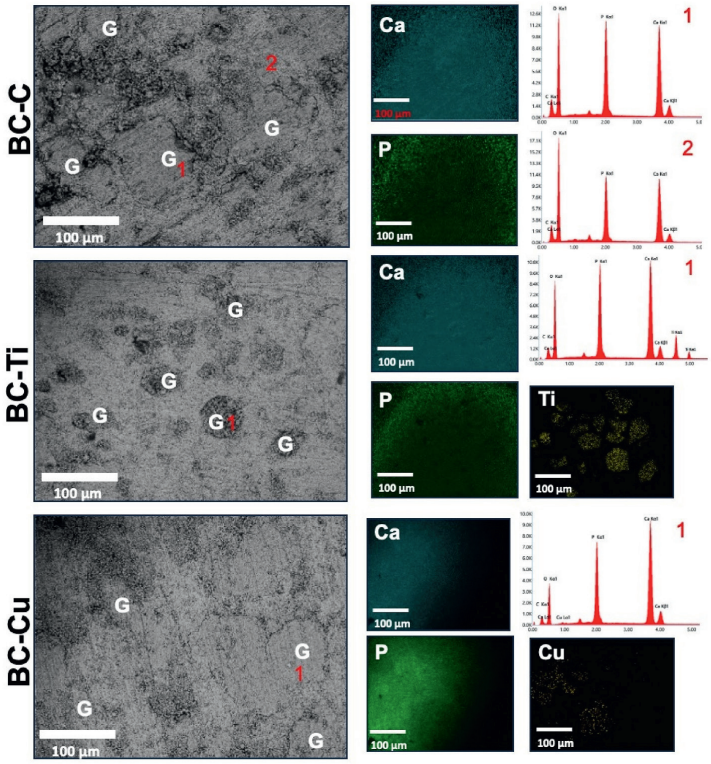

Fig. 6. SEM images of the materials' cross-section with EDS analysis after 7 days in air.

no significant shift in band positions was detected in the spectra of the investigated materials. This could be due to the masking of weak bands by strong bands originating from phosphates.

3.4. Mechanical properties

Mechanical strength is a crucial parameter in material evaluation. The mechanical strength of biomaterials should align with the properties of the tissue they are intended to replace. The results of compressive strength measurements of biomicroconcretes carried out after 7 days of setting and hardening as well as after 7 days of incubation in simulated body fluid are shown in Fig. 5.

The compressive strength of developed bone substitutes varied from 11.4 ± 1.1 MPa up to 12.4 ± 0.9 MPa. After 7 days of incubation in SBF compressive strength of developed materials slightly decreased and ranged 9.4 ± 0.7 MPa up to 10.9 ± 1.0 MPa. A slight decrease in compressive strength of the materials after incubation in SBF is associated with material degradation and the leaching of polymers into the incubation environment. The mechanical strength of materials depends on their microstructure, which in the case of biomicroconcretes is formed by matrix and aggregate(granules). The microstructure of matrix evolves during the setting process and is significantly affected by the composition of the materials. In the case of examined biomicroconcretes the dual setting takes place, due to the hydrolysis of α-TCP and the cross-linking of polymers within the material. The formation of a double hybrid structure originates from the electrostatic interaction between polycationic chitosan and polyanionic pectin, enhances the adhesion of the cement phase to the surface of the hydroxyapatite-chitosan granules. This interaction improves the intimate contact between the components, promoting overall material cohesion. The dual hybrid system specifically involves the combination of: (1) hybrid hydroxyapatite-chitosan-based granules and (2) the interactions between the polycationic chitosan within the granules and the polyanionic pectin introduced with the liquid phase. Furthermore, a statistically significant increase in mechanical strength was observed with the modification of hybrid granules using titanium and copper ions, further validating the effectiveness of these modifications in enhancing the performance of the biomicroconcretes. The mechanical strength of the developed materials enables their implantation in non-load or low-load bearing sites, as the compressive strength of cancellous bone typically ranges from approximately 4 to 12 MPa [50].

3.5. Microstructure

The results of the microstructure observation of the developed bone substitutes using a scanning electron microscopy (SEM) after 7 days of setting and hardening in air, along with EDS elemental analysis in microareas and EDS elemental mapping, are presented in Fig. 6. Moreover, the detailed microphotographs of cementitious samples are shown in Fig. 7.

The results of the SEM observation confirmed that the developed biomicroconcretes exhibit a homogeneous microstructure consisting of visible hybrid granules closely surrounded by a cementitious matrix based on α-TCP. The absence of macropores suggests that the employed

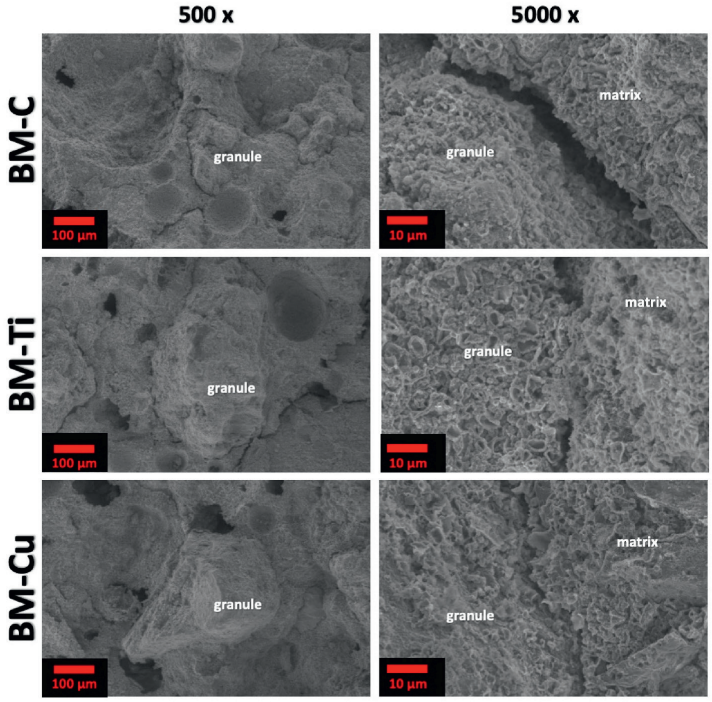

Fig. 7. SEM microphotographs od obtained materials and detailed granule-matrix interface at the magnification of 5000×.

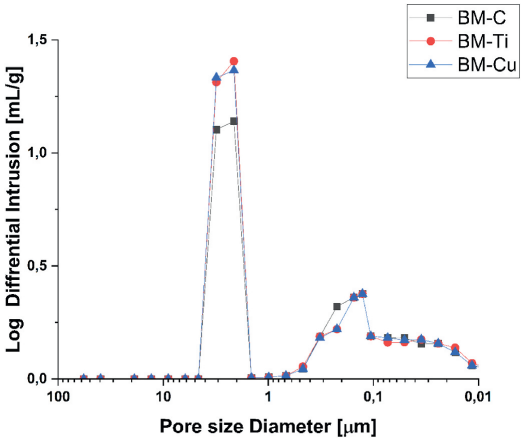

Fig. 8. Distribution and size of pores in obtained bone cements.

liquid phase, in the form of a mixture of citrus pectin gel and disodium phosphate, allowed for thorough mixing of the individual components of the biomicroconcretes. Similar microstructure observations were previously reported for cementitious materials based α-TCP and hybrid granules [51]. Elemental analysis conducted through mapping and EDS analysis in microareas demonstrated and confirmed the presence of titanium and cooper used for modifying the hybrid hydroxyapatite-chitosan granules.

3.6. Porosity

The porosity of developed biomaterials ranged from 56.7 ± 0.5 vol% for BM_C to 55.2 ± 0.5 vol% and 51.2 ± 0.5 vol% for BM_Ti and BM-Cu respectively. Additionally, the pore size distribution plots revealed that all developed materials displayed a bimodal porosity distribution with larger pores, approximately 2 µm in size, and small pores within the range under 1 µm (Fig. 8).

The porosity plays a crucial role in bone substitute materials, as it significantly influences their integration with natural tissue. Properly tailored porosity enables the ingrowth of bone tissue into the implant material, thereby supporting the regeneration process [52,53]. In the case of cementitious materials, it is also essential that the porosity does not lead to a substantial reduction in mechanical strength [54]. The observed porosity is comparable to that seen in similar calcium phosphate-based implant materials [55,56]. No significant differences between biomicroconcretes containing non-modified and copper or titanium modified granules were observed.

3.7. Chemical stability and bioactivity in vitro

Assessing the chemical stability of potential bone substitute materials is crucial as it helps determine how the material will behave post-implantation. To evaluate the chemical stability and bioactive potential *in vitro*, the obtained samples of cementitious materials were incubated in simulated body fluid (SBF) at 37 °C following the Kokubo protocol [57]. Changes in the pH of SBF surrounding the incubated samples are depicted in Fig. 9. Despite the simultaneous presence of polymers (citrus

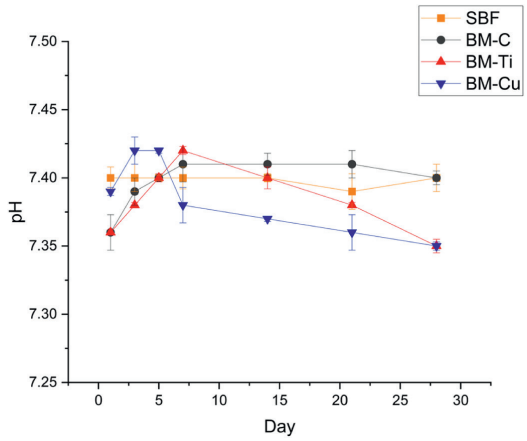

Fig. 9. pH vs. time of samples incubation in SBF.

pectin, chitosan) as well as titanium and copper ions in the materials structure, the pH values during the incubation of the materials remained within the range of 7.35–7.42, which is close to physiological [58].

Incubating materials in SBF, besides determining potential changes in pH values around the incubated samples, also enables an indirect assessment of the materials' bioactive potential. After a week-long incubation of the set cementitious material samples in SBF at 37 °C, it was observed that the surfaces of all tested materials were completely covered with cauliflower-like apatite layers (Fig. 10). The presence of apatite structures indirectly indicates and confirms a high *in vitro* bioactive potential according to the Kokubo and Takadama [59]. Thus, it can be concluded that both the presence of polymer in the liquid phase and antibacterial modifiers in the hybrid hydroxyapatite-chitosan granules do not negatively affect the bioactive potential of calcium phosphate-based materials.

The ionic conductivity of materials during incubation in distilled water allows for determining the amount of ions leached into the incubation environment. The specific ionic conductivity values during the incubation of the developed materials strongly depended on which element the granules, included in the biomicroconcretes, were modified with. For materials containing unmodified hydroxyapatite-chitosan granules, the specific ionic conductivity values ranged from 116 to 133 μS/cm. In the case of modification with ions, the specific conductivity values ranged from 100 to 116 μS/cm and 140–181 μS/cm, for materials containing titanium (BM-Ti) and cooper (BM-Cu) respectively (Fig. 11).

The highest values of ionic conductivity were observed during the incubation of the material containing hybrid hydroxyapatite-chitosan granules modified with copper. This is attributed to the rapid release of ions from the BM-Cu material into the incubation environment. A similar effect of copper action was previously observed in studies on self-setting cementitious materials based on calcium phosphates [60]. Additionally, the observed values of ionic conductivity of the materials may result from the presence of citrus pectin, which degrades in aqueous solutions to non-toxic products (such as d-galacturonic acid, l-arabinose, d-apiose, d-galactose, l-fructose) that do not have negative effects on cells when the material is implanted into the body [61].

3.8. Ion release

The evaluation of ion release with antibacterial properties serves as a preliminary step for more comprehensive *in vitro* studies of the materials. In the obtained materials, the release profile of titanium ions differs significantly from that of copper ions. For the former, a notably lower amount of ions was observed. Despite the difference in ion concentrations, the highest release for both ions occurred on the first day. The release curves for titanium and copper ions were generated through incubation of the materials in distilled water and are shown in Fig. 12A and B, respectively, for BM-Ti and BM-Cu materials.

The observed differences in the release profiles of titanium and copper ions may be attributed to the differing chemical properties of these elements and their ability to form stable compounds within cementitious biomaterials. Titanium ions, due to their stronger and more stable bonding within the material structure, may be released at a slower rate [62,63]. The observed release of titanium ions suggests that antibacterial effect of titanium may be observed for a longer incubation period. Although the release of titanium ions occurs at a slower rate and in smaller quantities, this may have positive implications for patient

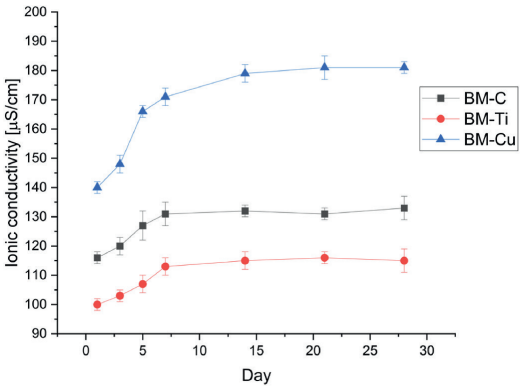

Fig. 11. Ionic conductivity vs. time of samples incubation in distilled water.

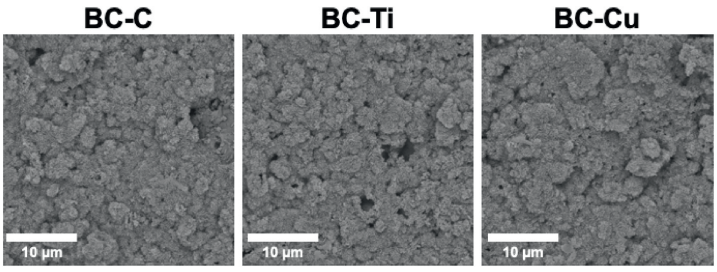

Fig. 10. SEM microstructure of materials' surface after 7-day incubation in SBF.

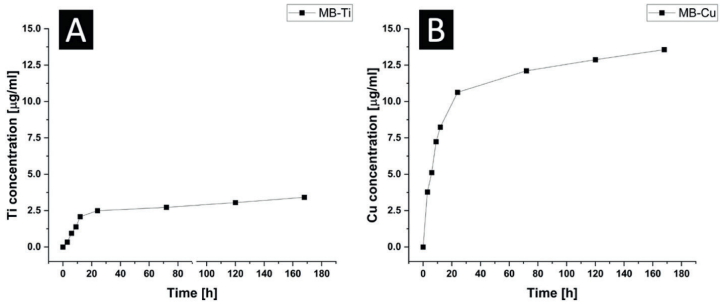

Fig. 12. Ion release from BM-Ti (A) and BM-Cu (B) vs. time of materials' immersion in distilled water.

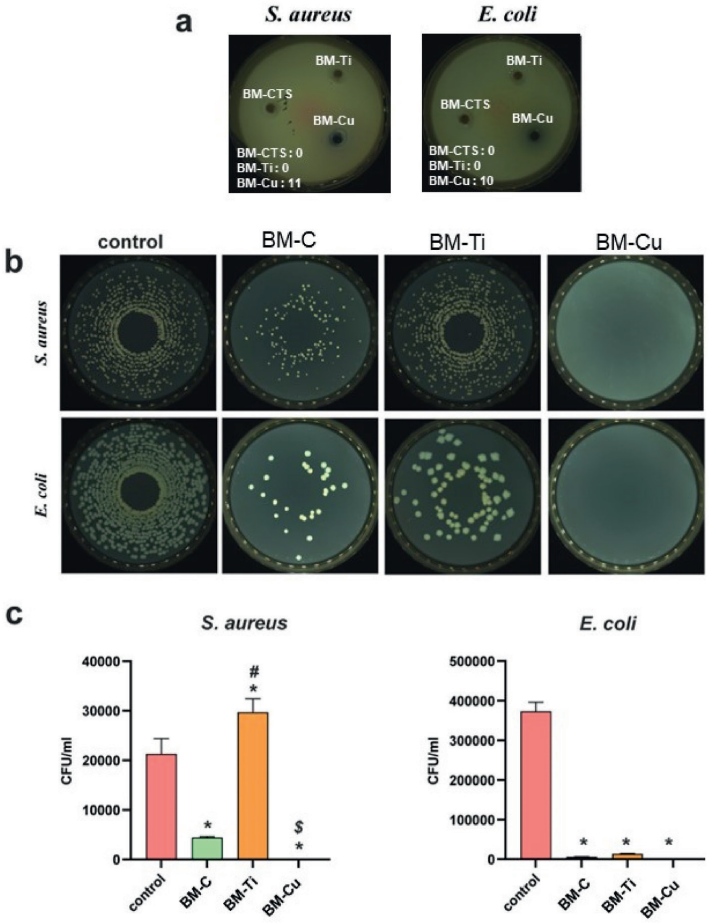

Fig. 13. Antibacterial activity of the cements: zones of bacterial growth inhibition (a) and results of AATCC Test Method 100–2004 as plate images (b) and graph (c). (*) symbol indicates statistically significant differences between the samples and control, (#) symbol indicates statistically significant results between BM-C and the samples, ($) symbol indicates statistically significant results between BM-Ti and the samples; according to one-way ANOVA with post-hoc Tukey's test ($p < 0.05$).

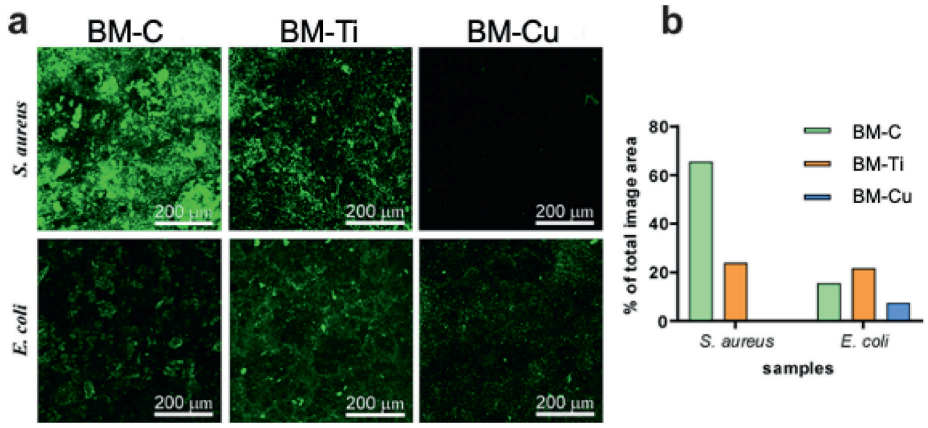

Fig. 14. Adhesion of bacterial cells to the cements: images of LCSM with viable bacteria stained green (a) and area of green fluorescence as percent of total image area (b). (For interpretation of the references to color in this figure legend, the reader is referred to the Web version of this article.)

treatment over an extended period, as the sustained release of ions can provide prolonged antibacterial effects, thereby enhancing the safety and efficacy of bone substitute materials in clinical practice. In contrast, copper ions were released at a significantly faster rate. It is likely due to their greater mobility of copper ions and their ability to dissolve more readily in water [21,64]. Studies of Rau et al. [18] found that the copper-doped bone cement exhibited similar kinetics of cooper ions release.

3.9. Antibacterial activity

Pilot experiment on agar plate tests showed that only BM-Cu inhibited the growth of *S. aureus* and *E. coli* (growth inhibition zones for both bacteria were 11 mm and 10 mm, respectively; Fig. 13). Moreover, the darkened, dirty-green color of inhibition area was observed around BM-Cu biomicroconcrete, which probably resulted from the release of Cu^{+2} ions to the agar medium. This may be caused by absorption of copper ions by medium proteins, similarly to the phenomenon noted by Irawati et al. [65] for bacterial CopA protein color change to blue caused by Cu^{+2} ions absorption. However, BM-C and BM-Ti materials did not show any antibacterial activity in this test. Weak response of tested composites in term of antibacterial activity probably resulted from the low rate of cooper and titanium ions release from the concretes. However, it was shown that at least HAP/CTS/Cu are expected to exhibit notable antibacterial activity.

The results of antibacterial activity measurement according to the standard adapted for porous materials provided more information. For both bacterial strains, very significant reduction of viable bacteria was observed for BM-C and complete elimination of bacteria for BM-Cu material. Both chitosan and copper ions are well known for their antimicrobial properties [66–69], thus they are probably responsible for notable antibacterial activity of these cements [69]. Interestingly, addition of titanium caused the increase of viable bacteria number. Surprisingly, in the case of *S. aureus*, the number of these bacteria exceeded the number in the control. These results suggested that titanium ions support rather than reduce the viability of tested bacterial strains which is in general agreement with common observations that titanium is inert and antibacterially inactive [70].

Bacterial adhesion to biomaterial surfaces is the first step leading to the formation of biofilm, one of the most dangerous phenomena causing the resistance of microorganisms to antibacterial agents [71,72]. Fig. 14 shows the images of cements incubated with the bacteria (green fluorescence indicates the presence of viable bacteria). In comparison with BM-C concretes, BM-Ti and BM-Cu surfaces showed the reduction of *S. aureus* adhesion, the most significantly for the copper-containing material. Quantification of fluorescence area revealed that area of the material covered by green fluorescence was reduced to 23.9 % and 0.3 % of total sample area for BM-Ti and BM-Cu, respectively, compared to 65.5 % for BM-C. For *E. coli* strain, the relationships were different. Bacterial adhesion was more distinct between all samples and the area of the material covered by green fluorescence was 21.7 % and 7.6 % of total sample area for BM-Ti and BM-Cu, respectively, compared to 15.6 % for BM-C. The observations lead to the conclusions that: i) adhesion of *E. coli* to the cements is less sensitive to the ions content in materials and ii) titanium ions did not reduce but rather enhance the adhesion of *E. coli* cells, opposite to *S. aureus* cells. However, BM-Cu were the least favourable to adhesion of both microorganisms which is in good agreement with earlier reports that copper suppresses the bacterial adhesion to surfaces [73].

4. Conclusions

In this study, materials based on highly reactive α-TCP powder and hybrid hydroxyapatite-chitosan granules modified with titanium and copper ions were developed and examined. The use of a mixture of citrus pectin and disodium phosphate as the liquid phase of obtained bone substitutes allowed to obtain easily mouldable, fully injectable calcium phosphate-based biomicroconcretes. Developed biomaterials possessed setting times within an acceptable range. Additionally, the presence of citrus pectin in the liquid phase significantly improved their mechanical strength. The unique properties of biomicroconcretes containing citrus pectin resulted from both the occurrence of the dual setting system and the presence of the double hybrid system. The dual setting system originated from α-TCP hydrolysis and citrus pectin crosslinking in the presence of Ca^{2+} ions, allowed for obtaining materials characterized by excellent cohesion and chemical stability. Whereas the double hybrid system is due to the presence of hybrid granules and interactions between polycationic chitosan in hybrid granules and polyanionic citrus pectin. All developed biomicroconcretes revealed *in vitro* bioactivity, making them good candidates for further biological studies. The application of hybrid hydroxyapatite/chitosan granules suppresses the bacterial adhesion to surfaces. Copper modified biomaterials possessed the highest antibacterial activity and are the least favourable to adhesion of both *E. coli* and S. aureus. Titanium modified materials reduced

adhesion of *S. aureus* but did not reduce but rather enhance the adhesion of *E. coli* cells. This research confirms the beneficial properties of obtained biomicroconcretes and paves the way for further *in vitro* and *in vivo* studies.

CRediT authorship contribution statement

Piotr Pańtak: Writing – original draft, Visualization, Methodology, Investigation, Formal analysis, Conceptualization. **Joanna P. Czechowska:** Writing – review & editing, Visualization, Validation, Methodology, Investigation, Funding acquisition, Conceptualization. **Anna Belcarz:** Writing – review & editing, Visualization, Methodology, Investigation. **Aneta Zima:** Writing – review & editing, Supervision, Project administration, Funding acquisition, Formal analysis, Conceptualization.

Declaration of competing interest

The authors declare that they have no known competing financial interests or personal relationships that could have appeared to influence the work reported in this paper.

Acknowledgment

Research project supported by program „Excellence initiative – research university" for the AGH University of Science and Technology (IDs: 4159, 4222 – PI: A. Zima). Research co-funded by the Faculty of Materials Science and Ceramics AGH UST—University of Science and Technology, Kraków, Poland, Project No. 16.16.160.557 (2024). This research was funded in part by National Science Centre, Poland (Project MINIATURA7 No.2023/07/X/ST11/00705). For the purpose of Open Access, the author has applied a CC-BY public copyright licence to any Author Accepted Manuscript (AAM) version arising from this submission. Evaluation of antibacterial activity was supported by the Ministry of Education and Science in Poland within the statutory activity of the Medical University of Lublin (DS6/2024). Evaluation of microstructure was supported by the program „Excellence initiative – research university" for the AGH University of Science and Technology (ID: 1449 – PI: M. Ziąbka). The authors thank the company Herbstreith & Fox for delivering citrus pectin.

References

[1] S. Samavedi, A.R. Whittington, A.S. Goldstein, Calcium phosphate ceramics in bone tissue engineering: a review of properties and their influence on cell behavior, Acta Biomater. 9 (2013) 8037–8045, https://doi.org/10.1016/j.actbio.2013.06.014.
[2] J. Jeong, J.H. Kim, J.H. Shim, N.S. Hwang, C.Y. Heo, Bioactive calcium phosphate materials and applications in bone regeneration, Biomater. Res. 23 (2019) 4, https://doi.org/10.1186/s40824-018-0149-3.
[3] P. Frayssinet, Calcium phosphates in orthopedic surgery, in: Biomechanics and Biomaterials in Orthopedics, Springer London, London, 2004, pp. 101–108, https://doi.org/10.1007/978-1-4471-3774-0_9.
[4] L. Yang, B. Harink, P. Habibovic, Calcium phosphate ceramics with inorganic additives, in: Comprehensive Biomaterials, Elsevier, 2011, pp. 299–312, https://doi.org/10.1016/B978-0-08-055294-1.00032-5.
[5] M.C. Tronco, J.B. Cassel, L.A. dos Santos, α-TCP-based calcium phosphate cements: a critical review, Acta Biomater. 151 (2022) 70–87, https://doi.org/10.1016/j.actbio.2022.08.040.
[6] R. Harrison, Z.K. Criss, L. Feller, S.P. Modi, J.G. Hardy, C.E. Schmidt, L.J. Suggs, M. B. Murphy, Mechanical properties of α-tricalcium phosphate-based bone cements incorporating regenerative biomaterials for filling bone defects exposed to low mechanical loads, J. Biomed. Mater. Res. B Appl. Biomater. 104 (2016) 149–157, https://doi.org/10.1002/jbm.b.33362.
[7] H.H. Xu, P. Wang, L. Wang, C. Bao, Q. Chen, M.D. Weir, L.C. Chow, L. Zhao, X. Zhou, M.A. Reynolds, Calcium phosphate cements for bone engineering and their biological properties, Bone Res 5 (2017) 17056, https://doi.org/10.1038/boneres.2017.56.
[8] A.V. Boehm, S. Meininger, U. Gbureck, F.A. Müller, Self-healing capacity of fiber-reinforced calcium phosphate cements, Sci. Rep. 10 (2020) 9430, https://doi.org/10.1038/s41598-020-66207-2.
[9] R. Krüger, J. Groll, Fiber reinforced calcium phosphate cements – on the way to degradable load bearing bone substitutes? Biomaterials 33 (2012) 5887–5900, https://doi.org/10.1016/j.biomaterials.2012.04.053.
[10] A. Ślósarczyk, J. Czechowska, E. Cichoń, A. Zima, New hybrid bioactive composites for bone substitution, Processes 8 (2020) 335, https://doi.org/10.3390/pr8030335.
[11] D.L. Alge, T.G. Chu, Calcium phosphate cement reinforcement by polymer infiltration and *in situ* curing: a method for 3D scaffold reinforcement, J. Biomed. Mater. Res. 94A (2010) 547–555, https://doi.org/10.1002/jbm.a.32742.
[12] Y. Huang, J. Zhang, W. Zhang, S. Zeng, H. Shi, T. Yu, C. Zhou, Formulation of α-tricalcium phosphate bone cement based on an alginate–chitosan gel system, Cryst. Growth Des. 20 (2020) 1400–1404, https://doi.org/10.1021/acs.cgd.0c00005.
[13] P. Pańtak, J.P. Czechowska, E. Cichoń, A. Zima, Novel double hybrid-type bone cements based on calcium phosphates, chitosan and citrus pectin, Int. J. Mol. Sci. 24 (2023) 13455, https://doi.org/10.3390/ijms241713455.
[14] Ö. Demir-Oğuz, A.R. Boccaccini, D. Loca, Injectable bone cements: what benefits the combination of calcium phosphates and bioactive glasses could bring? Bioact. Mater. 19 (2023) 217–236, https://doi.org/10.1016/j.bioactmat.2022.04.007.
[15] A. Giacometti, O. Cirioni, A.M. Schimizzi, M.S. Del Prete, F. Barchiesi, M. M. D'Errico, E. Petrelli, G. Scalise, Epidemiology and Microbiology of surgical wound infections, J. Clin. Microbiol. 38 (2000) 918–922, https://doi.org/10.1128/JCM.38.2.918-922.2000.
[16] M. Wekwejt, A. Michno, K. Truchan, A. Pałubicka, B. Świeczko-Żurek, A. M. Osyczka, A. Zieliński, Antibacterial activity and cytocompatibility of bone cement enriched with antibiotic, nanosilver, and nanocopper for bone regeneration, Nanomaterials 9 (2019) 1114, https://doi.org/10.3390/nano9081114.
[17] A. Bistolfi, G. Massazza, E. Verné, A. Massè, D. Deledda, S. Ferraris, M. Miola, F. Galetto, M. Crova, Antibiotic-Loaded Cement in Orthopedic Surgery: A Review, ISRN Orthop 2011, 2011, pp. 1–8, https://doi.org/10.5402/2011/290851.
[18] J.V. Rau, V.M. Wu, V. Graziani, I.V. Fadeeva, A.S. Fomin, M. Fosca, V. Uskoković, The Bone Building Blues: self-hardening copper-doped calcium phosphate cement and its in vitro assessment against mammalian cells and bacteria, Mater. Sci. Eng. C 79 (2017) 270–279, https://doi.org/10.1016/j.msec.2017.05.052.
[19] F. Foroutan, J. McGuire, P. Gupta, A. Nikolaou, B.A. Kyffin, N.L. Kelly, J.V. Hanna, J. Gutierrez-Merino, J.C. Knowles, S.-Y. Baek, E. Velliou, D. Carta, Antibacterial copper-doped calcium phosphate glasses for bone tissue regeneration, ACS Biomater. Sci. Eng. 5 (2019) 6054–6062, https://doi.org/10.1021/acsbiomaterials.9b01291.
[20] I.V. Fadeeva, B.I. Lazoryak, G.A. Davidova, F.F. Murzakhanov, B.F. Gabbasov, N. V. Petrakova, M. Fosca, S.M. Barinov, G. Vadalà, V. Uskoković, Y. Zheng, J.V. Rau, Antibacterial and cell-friendly copper-substituted tricalcium phosphate ceramics for biomedical implant applications, Mater. Sci. Eng. C 129 (2021) 112410, https://doi.org/10.1016/j.msec.2021.112410.
[21] A. Jacobs, G. Renaudin, N. Charbonnel, J.-M. Nedelec, C. Forestier, S. Descamps, Copper-doped biphasic calcium phosphate powders: dopant release, cytotoxicity and antibacterial properties, Materials 14 (2021) 2393, https://doi.org/10.3390/ma14092393.
[22] L. Stipniece, I. Skadins, M. Mosina, Silver- and/or titanium-doped β-tricalcium phosphate bioceramic with antibacterial activity against Staphylococcus aureus, Ceram. Int. 48 (2022) 10195–10201, https://doi.org/10.1016/j.ceramint.2021.12.232.
[23] Stipniece, et al., Highly porous Ag- and/or Ti-doped calcium phosphate bioceramic scaffolds: from physicochemical to biological properties, in: XVIII ECerS Conference & Exhibition of European Ceramic Society Full Conference Book, Lyon, 2023.
[24] Stipniece, et al., Silver- and/or titanium-doped calcium phosphate highly porous bioceramic with antibacterial activity, in: 31st Annual Conference of the European Society for Biomaterials (ESB 2021), 2021. Berlin.
[25] J. Czechowska, A. Zima, Z. Paszkiewicz, J. Lis, A. Ślósarczyk, Physicochemical properties and biomimetic behaviour of α-TCP-chitosan based materials, Ceram. Int. 40 (2014) 5523–5532, https://doi.org/10.1016/j.ceramint.2013.10.142.
[26] A. Zima, Hydroxyapatite-chitosan based bioactive hybrid biomaterials with improved mechanical strength, Spectrochim. Acta Mol. Biomol. Spectrosc. 193 (2018) 175–184, https://doi.org/10.1016/j.saa.2017.12.008.
[27] ASTM International, ASTM C266-20 - Standard Test Method for Time of Setting of Hydraulic-Cement Paste by Gillmore Needles, n.d.
[28] S. Larsson, G. Hannink, Injectable bone-graft substitutes: current products, their characteristics and indications, and new developments, Injury 42 (2011) S30–S34, https://doi.org/10.1016/j.injury.2011.06.013.
[29] M.-P. Ginebra, E.B. Montufar, Cements as bone repair materials, in: Bone Repair Biomaterials, Elsevier, 2019, pp. 233–271, https://doi.org/10.1016/B978-0-08-102451-5.00009-3.
[30] R. O'Neill, H.O. McCarthy, E.B. Montufar, M.-P. Ginebra, D.I. Wilson, A. Lennon, N. Dunne, Critical review: injectability of calcium phosphate pastes and cements, Acta Biomater. 50 (2017) 1–19, https://doi.org/10.1016/j.actbio.2016.11.019.
[31] W. Zhong, L. Sun, T. Yu, C. Zhou, Preparation and characterization of calcium phosphate cement with enhanced tissue adhesion for bone defect repair, Ceram. Int. 47 (2021) 1712–1720, https://doi.org/10.1016/j.ceramint.2020.08.288.
[32] M.A. da Silva, A.C.K. Bierhalz, T.G. Kieckbusch, Alginate and pectin composite films crosslinked with Ca2+ ions: effect of the plasticizer concentration, Carbohydr. Polym. 77 (2009) 736–742, https://doi.org/10.1016/j.carbpol.2009.02.014.
[33] S. Cui, B. Yao, M. Gao, X. Sun, D. Gou, J. Hu, Y. Zhou, Y. Liu, Effects of pectin structure and crosslinking method on the properties of crosslinked pectin nanofibers, Carbohydr. Polym. 157 (2017) 766–774, https://doi.org/10.1016/j.carbpol.2016.10.052.

[34] M.P. Ginebra, E. Fernández, M.G. Boltong, O. Bermúdez, J.A. Planell, F.C. M. Driessens, Compliance of an apatitic calcium phosphate cement with the short-term clinical requirements in bone surgery, orthopaedics and dentistry, Clin. Mater. 17 (1994) 99–104, https://doi.org/10.1016/0267-6605(94)90018-3.
[35] A. Sugawara, K. Asaoka, S.-J. Ding, Calcium phosphate-based cements: clinical needs and recent progress, J. Mater. Chem. B 1 (2013) 1081–1089, https://doi.org/10.1039/C2TB00061J.
[36] B.T. Smith, A. Lu, E. Watson, M. Santoro, A.J. Melchiorri, E.C. Grosfeld, J.J.J.P. van den Beucken, J.A. Jansen, D.W. Scott, J.P. Fisher, A.G. Mikos, Incorporation of fast dissolving glucose porogens and poly(lactic-co-glycolic acid) microparticles within calcium phosphate cements for bone tissue regeneration, Acta Biomater. 78 (2018) 341–350, https://doi.org/10.1016/j.actbio.2018.07.054.
[37] Q. Quan, X. Gongping, N. Ruisi, L. Shiwen, New research progress of modified bone cement applied to vertebroplasty, World Neurosurg 176 (2023) 10–18, https://doi.org/10.1016/j.wneu.2023.04.048.
[38] S.M. Rabiee, H. Baseri, Prediction of the setting properties of calcium phosphate bone cement, Comput. Intell. Neurosci. 2012 (2012) 1–8, https://doi.org/10.1155/2012/809235.
[39] M. Fathi, A. Kholtei, S. EL Youbi, B. Chafik El Idrissi, Setting properties of calcium phosphate bone cement, Mater Today Proc 13 (2019) 876–881, https://doi.org/10.1016/j.matpr.2019.04.051.
[40] A. Nesic, S. Meseldzija, A. Onjia, G. Cabrera-Barjas, Impact of crosslinking on the characteristics of pectin monolith cryogels, Polymers 14 (2022) 5252, https://doi.org/10.3390/polym14235252.
[41] S. Seslija, D. Veljovic, M. Kalagasidis Krusic, J. Stevanovic, S. Velickovic, I. Popovic, Cross-linking of highly methoxylated pectin with copper: the specific anion influence, New J. Chem. 40 (2016) 1618–1625, https://doi.org/10.1039/C5NJ03320A.
[42] K. Kohila rani, Y.-X. Liu, R. Devasenathipathy, C. Yang, S.-F. Wang, Simple preparation of gold nanoparticle-decorated copper cross-linked pectin for the sensitive determination of hydrogen peroxide, Ionics 25 (2019) 309–317, https://doi.org/10.1007/s11581-018-2573-8.
[43] K.-H. Yoo, Y. Kim, Y.-I. Kim, M.-K. Bae, S.-Y. Yoon, Lithium doped biphasic calcium phosphate: structural analysis and osteo/odontogenic potential in vitro, Front. Bioeng. Biotechnol. 10 (2022), https://doi.org/10.3389/fbioe.2022.993126.
[44] J. Czechowska, A. Zima, Z. Paszkiewicz, J. Lis, A. Ślósarczyk, Physicochemical properties and biomimetic behaviour of α-TCP-chitosan based materials, Ceram. Int. 40 (2014) 5523–5532, https://doi.org/10.1016/j.ceramint.2013.10.142.
[45] E. Şahin, Calcium phosphate bone cements, in: Cement Based Materials, InTech, 2018, https://doi.org/10.5772/intechopen.74607.
[46] A. Ślósarczyk, C. Paluszkiewicz, M. Gawlicki, Z. Paszkiewicz, The FTIR spectroscopy and QXRD studies of calcium phosphate based materials produced from the powder precursors with different ratios, Ceram. Int. 23 (1997) 297–304, https://doi.org/10.1016/S0272-8842(96)00016-8.
[47] C. Durucan, P.W. Brown, α-Tricalcium phosphate hydrolysis to hydroxyapatite at and near physiological temperature, J. Mater. Sci. Mater. Med. 11 (2000) 365–371, https://doi.org/10.1023/A:1008934024440.
[48] S.Sh Rashidova, R.Yu Milusheva, L.N. Semenova, M.Yu Mukhamedjanova, N. L. Voropaeva, S. Vasilyeva, R. Faizieva, I.N. Ruban, Characteristics of interactions in the Pectin?Chitosan system, Chromatographia 59 (2004), https://doi.org/10.1365/s10337-004-0289-6.
[49] M. Dziadek, K. Dziadek, S. Salagierski, M. Drozdowska, A. Serafim, I.-C. Stancu, P. Szatkowski, A. Kopec, I. Rajzer, T.E.L. Douglas, K. Cholewa-Kowalska, Newly crosslinked chitosan- and chitosan-pectin-based hydrogels with high antioxidant and potential anticancer activity, Carbohydr. Polym. 290 (2022) 119486, https://doi.org/10.1016/j.carbpol.2022.119486.
[50] L.-C. Gerhardt, A.R. Boccaccini, Bioactive glass and glass-ceramic scaffolds for bone tissue engineering, Materials 3 (2010) 3867–3910, https://doi.org/10.3390/ma3073867.
[51] P. Pańtak, E. Cichoń, J. Czechowska, A. Zima, Influence of natural polysaccharides on properties of the biomicroconcrete-type bioceramics, Materials 14 (2021) 7496, https://doi.org/10.3390/ma14247496.
[52] E. Cichoń, B. Mielan, E. Pamuła, A. Ślósarczyk, A. Zima, Development of highly porous calcium phosphate bone cements applying nonionic surface active agents, RSC Adv. 11 (2021) 23908–23921, https://doi.org/10.1039/D1RA04266A.
[53] H.H. Xu, P. Wang, L. Wang, C. Bao, Q. Chen, M.D. Weir, L.C. Chow, L. Zhao, X. Zhou, M.A. Reynolds, Calcium phosphate cements for bone engineering and their biological properties, Bone Res 5 (2017) 17056, https://doi.org/10.1038/boneres.2017.56.
[54] A. Vezenkova, J. Locs, Sudoku of porous, injectable calcium phosphate cements – path to osteoinductivity, Bioact. Mater. 17 (2022) 109–124, https://doi.org/10.1016/j.bioactmat.2022.01.001.
[55] M. Espanol, R.A. Perez, E.B. Montufar, C. Marichal, A. Sacco, M.P. Ginebra, Intrinsic porosity of calcium phosphate cements and its significance for drug delivery and tissue engineering applications, Acta Biomater. 5 (2009) 2752–2762, https://doi.org/10.1016/j.actbio.2009.03.011.
[56] M. Kamitakahara, K. Asahara, H. Matsubara, Calcium phosphate cements comprising spherical porous calcium phosphate granules: synthesis, structure, and properties, Journal of Asian Ceramic Societies 10 (2022) 731–738, https://doi.org/10.1080/21870764.2022.2123514.
[57] T. Kokubo, Bioceramics and Their Clinical Applications, first ed., 2008.
[58] E. Hopkins, T. Sanvictores, S. Sharma, Physiology Acid Base Balance, in: StatPearls, Treasure Island (FL): StatPearls Publishing, 2022. https://www.ncbi.nlm.nih.gov/books/NBK507807.
[59] T. Kokubo, H. Takadama, How useful is SBF in predicting in vivo bone bioactivity? Biomaterials 27 (2006) 2907–2915, https://doi.org/10.1016/j.biomaterials.2006.01.017.
[60] J.V. Rau, V.M. Wu, V. Graziani, I.V. Fadeeva, A.S. Fomin, M. Fosca, V. Uskoković, The Bone Building Blues: self-hardening copper-doped calcium phosphate cement and its in vitro assessment against mammalian cells and bacteria, Mater. Sci. Eng. C 79 (2017) 270–279, https://doi.org/10.1016/j.msec.2017.05.052.
[61] X. Li, J. Bi, X. Jin, X. Li, Y. Zhao, Y. Song, Effect of pectin osmosis or degradation on the water migration and texture properties of apple cube dried by instant controlled pressure drop drying (DIC), LWT 125 (2020) 109202, https://doi.org/10.1016/j.lwt.2020.109202.
[62] H.J. Haugen, S.P. Lyngstadaas, Antibacterial effects of titanium dioxide in wounds, in: Wound Healing Biomaterials, Elsevier, 2016, pp. 439–450, https://doi.org/10.1016/B978-1-78242-456-7.00021-0.
[63] O. Mbanga, E. Cukrowska, M. Gulumian, Dissolution of titanium dioxide nanoparticles in synthetic biological and environmental media to predict their biodurability and persistence, Toxicol. Vitro 84 (2022) 105457, https://doi.org/10.1016/j.tiv.2022.105457.
[64] S. Gomes, C. Vichery, S. Descamps, H. Martinez, A. Kaur, A. Jacobs, J.-M. Nedelec, G. Renaudin, Cu-doping of calcium phosphate bioceramics: from mechanism to the control of cytotoxicity, Acta Biomater. 65 (2018) 462–474, https://doi.org/10.1016/j.actbio.2017.10.028.
[65] W. Irawati, E.S. Djojo, L. Kusumawati, T. Yuwono, R. Pinontoan, Optimizing bioremediation: elucidating copper accumulation mechanisms of acinetobacter sp. IrC2 isolated from an industrial waste treatment center, Front. Microbiol. 12 (2021), https://doi.org/10.3389/fmicb.2021.713812.
[66] J. Li, S. Zhuang, Antibacterial activity of chitosan and its derivatives and their interaction mechanism with bacteria: current state and perspectives, Eur. Polym. J. 138 (2020) 109984, https://doi.org/10.1016/j.eurpolymj.2020.109984.
[67] M. Kong, X.G. Chen, K. Xing, H.J. Park, Antimicrobial properties of chitosan and mode of action: a state of the art review, Int. J. Food Microbiol. 144 (2010) 51–63, https://doi.org/10.1016/j.ijfoodmicro.2010.09.012.
[68] C. Ortega-Nieto, N. Losada-Garcia, B.C. Pessela, P. Domingo-Calap, J.M. Palomo, Design and synthesis of copper nanobiomaterials with antimicrobial properties, ACS bio &amp, Med Chem Au 3 (2023) 349–358, https://doi.org/10.1021/acsbiomedchemau.2c00089.
[69] N. Bisht, N. Dwivedi, P. Kumar, M. Venkatesh, A.K. Yadav, D. Mishra, P. Solanki, N. K. Verma, R. Lakshminarayanan, S. Ramakrishna, D.P. Mondal, A.K. Srivastava, C. Dhand, Recent advances in copper and copper-derived materials for antimicrobial resistance and infection control, Curr Opin Biomed Eng 24 (2022) 100408, https://doi.org/10.1016/j.cobme.2022.100408.
[70] P.A. Pesode, S.B. Barve, Recent advances on the antibacterial coating on titanium implant by micro-Arc oxidation process, Mater Today Proc 47 (2021) 5652–5662, https://doi.org/10.1016/j.matpr.2021.03.702.
[71] A. Jolivet-Gougeon, M. Bonnaure-Mallet, Biofilms as a mechanism of bacterial resistance, Drug Discov. Today Technol. 11 (2014) 49–56, https://doi.org/10.1016/j.ddtec.2014.02.003.
[72] N. Venkatesan, G. Perumal, M. Doble, Bacterial resistance in biofilm-associated bacteria, Future Microbiol. 10 (2015) 1743–1750, https://doi.org/10.2217/fmb.15.69.
[73] Y. Wu, W. Wu, W. Zhao, X. Lan, Revealing the antibacterial mechanism of copper surfaces with controllable microstructures, Surf. Coat. Technol. 395 (2020) 125911, https://doi.org/10.1016/j.surfcoat.2020.125911.

Publikacja 6 – *„Improving the processability and mechanical strength of self-hardening robocasted hydroxyapatite scaffolds with silane coupling agents”*

journal of the mechanical behavior of biomedical materials 161 (2025) 106792

Contents lists available at ScienceDirect

Journal of the Mechanical Behavior of Biomedical Materials

journal homepage: www.elsevier.com/locate/jmbbm

Improving the processability and mechanical strength of self-hardening robocasted hydroxyapatite scaffolds with silane coupling agents

Piotr Pańtak [a,*], Joanna P. Czechowska [a,**], Adelia Kashimbetova [b], Ladislav Čelko [b], Edgar B. Montufar [b], Łukasz Wójcik [a], Aneta Zima [a]

[a] Faculty of Materials Science and Ceramics, AGH University of Krakow, Mickiewicza Av. 30, 30-058, Kraków, Poland
[b] Central European Institute of Technology, Brno University of Technology, Purkyňova 123, 612 00, Brno, Czech Republic

ARTICLE INFO

Keywords:
α-TCP
Biopolymers
Silane coupling agents
Hybrid materials
3d printing
Robocasting

ABSTRACT

Bone cements are the subject of intensive research, primarily due to their versatility and the increasing importance for personalized medicine. In this study, novel hybrid self-setting scaffolds, based on calcium phosphates and natural polymers, were fabricated using the robocasting technique. Additionally, the influence of two different silane coupling agents, tetraethyl orthosilicate (TEOS) and 3-glycidoxypropyltrimethoxysilane (GPTMS), on the physicochemical and biological properties of the obtained materials was thoroughly investigated. The chemical and phase compositions (XRF, XRD, FTIR), setting process, rheological properties, mechanical strength, microstructure (SEM), and chemical stability *in vitro* were comprehensively examined. The use of silane coupling agents improved compressive strength of the scaffolds from 5.20 to 9.26 MPa. The incorporation of citrus pectin into the liquid phase of the materials, along with the use of a hybrid hydroxyapatite-chitosan powder, not only facilitated the development of printable pastes suitable for robocasting but also enhanced the physicochemical properties of the robocasted scaffolds. The results presented in this study underscore the beneficial influence of silane coupling agents on the characteristics of calcium phosphate-based bone scaffolds. Developed robocasted scaffolds hold great potential for applications in the field of bone tissue engineering and personalized medicine. Further *in vitro* and *in vivo* studies are necessary to validate their suitability for clinical applications.

1. Introduction

Due to the increase incidence of lifestyle-related bone loss, there is a continuous need for the replacement of damaged tissue with synthetic bone substitutes (Fernandez De Grado et al., 2018), (Sohn and Oh, 2019). Calcium phosphates have been a significant group of biomaterials used for hard tissue augmentation due to their chemical similarity to the inorganic part of bone. Among them, α-tricalcium phosphate (α-TCP) stands out due to its self-setting properties and ability to hydrolyse to calcium deficient hydroxyapatite (CDHA) (Tronco et al., 2022). α-TCP is commonly used as a component of calcium phosphate cements (CPCs) (Cervantes-Uc et al., 2015). Over the years, α-TCP-based CPCs have undergone numerous modifications to enhance their physicochemical and biological properties. For example, addition of natural polymers, such as citrus pectin and chitosan, allowed to obtain injectable materials with enhanced mechanical properties (An et al., 2016), (Perez et al., 2012), (Wong et al., 2021), (Huang et al., 2020). Another approach to improving the performance of CPCs involves addition of biologically active substances such as ions, drugs or nanoparticles. These additions aim to enhance the cellular response post-implantation and introduce antibacterial properties (Xia et al., 2019), (Xia et al., 2018), (Liu et al., 2023), (Dapporto et al., 2022).

One promising application for CPCs is their implementation in additive manufacturing methods. The use of additive manufacturing opens new perspectives, as it allows for the personalized adaptation of the shape and porosity of the implant to meet individual patient needs (Drevet et al., 2023), (Bergmann et al., 2010). Among the many techniques of adhesively forming implant matrices for bone regeneration such as stereolithography, fused deposition modeling (FDM), selective laser melting (SLS), and binder jetting, the robocasting technique has a certain uniqueness (Kumar et al., 2019). Particularly interesting is the robocasting technique. Robocasting involves the precise layer-by-layer

* Corresponding author.
** Corresponding author.
E-mail addresses: pantak@agh.edu.pl (P. Pańtak), jczech@agh.edu.pl (J.P. Czechowska).

https://doi.org/10.1016/j.jmbbm.2024.106792
Received 14 August 2024; Received in revised form 21 October 2024; Accepted 28 October 2024
Available online 9 November 2024

deposition of materials in the form of viscous paste or gel, enabling the creation of three-dimensional structures with porosity-controlled complex geometries (Paterlini et al., 2021). Balance between injectability through the printing nozzle and shape retention of the printed layers is a crucial factor in robocasting. Appropriate rheological properties of calcium phosphates-based pastes can be achieved by utilizing natural and synthetic polymers. For example, Martínez-Vázquez et al. (2010) used hydroxypropyl methylcellulose for robocasting of biphasic β-TCP/calcium pyrophosphate scaffolds. Similarly, Montelongo et al. (2021) and Maazouz et al. (2014) utilized gelatine for robocasting the self-hardening scaffolds. Unfortunately, polymer additives often disrupt the hardening process entirely. Therefore, it becomes necessary to employ additional compounds that accelerate the hardening and enhance the strength of the final prints.

The incorporation of a silane coupling agent (SCA) is an interesting alternative respect to previously applied modifications of CPC-based inks for robocasting. SCAs are organosilicon compounds that have the unique ability to chemically bond with both inorganic and organic surfaces, resulting in interfacial adhesion through the formation of robust covalent bonds (Pape, 2017), (Plueddemann, 1991). So far SCAs find extensive application in the alteration of surface properties for a range of materials, such as ceramics, polymers, and metals, aimed at improving their suitability for medical applications (Nihei, 2016), (Xie et al., 2010).

Suppakarn et al. (2007) enhanced the homogeneity between hydroxyapatite (HA) powders and polypropylene (PP) in HA/polypropylene composites by employing various silane coupling agents, including γ-aminopropyl triethoxysilane (APES), methyl trimethoxysilane (MTMS), and γ-glycidoxypropyl trimethoxysilane (GPMS). The outcomes revealed that the silane treatment significantly improved the interaction between HA and PP, leading to a notable increase in the composite's stiffness. Rakmae et al. (2012) investigated the impact of SCA treatment on the *in vitro* degradation and bioactivity of PLA composites containing bovine bone-based carbonated hydroxyapatite (CHA). The results showed that the strong interfacial bonding between the silane-treated CHA and PLA significantly slowed down the *in vitro* degradation of composites. Houaoui et al. (2021) developed hybrid-type bone scaffolds consist of bioactive glass particles bonded to gelatine through covalent linkage, using 3-glycidoxypropyltrimethoxysilane (GPTMS). Thongchai et al. (2020) produced chitosan and collagen-based hydrogel, crosslinked with tetraethyl orthosilicate (TEOS), for potential pharmaceutical applications. Considering positive results of previous studies, it is reasonable to expect that a SCA can potentially interact with the components of the self-setting pastes, enriching final scaffolds with improved mechanical properties due to presence of different chemical interaction within materials' structure.

The aim of this study was to develop, robocast, and characterize novel hybrid bioceramic scaffolds based on α-TCP, hybrid hydroxyapatite-chitosan powder, citrus pectin and SCAs. Furthermore, the study aimed to examine the impact of two distinct SCAs, TEOS and GPTMS, on the physicochemical and biological properties of the resulting scaffolds. We expect that the use of SCAs will allow for improved physicochemical properties of final biomaterials due to the occurrence of additional interactions between SCAs and components of the cementitious pastes. To best of our knowledge, the combination of a hybrid hydroxyapatite-chitosan powder with the SCAs-modified α-TCP for the robocasting of self-hardening hydroxyapatite scaffolds has not been previously reported.

2. Experimental

2.1. Synthesis of α-TCP and SCA-modified α-TCP powders

The initial α-TCP powder was synthesized via a wet chemical method following a previously described procedure (Czechowska et al., 2014), (Kolmas et al., 2015). $Ca(OH)_2$ (≥99.5%, POCH, Gliwice, Poland) and H_3PO_4 (85.0%, POCH, Gliwice, Poland) at the Ca/P molar ratio of 1.5 were applied as reagents. After ageing and drying, the precipitate underwent a calcination at 1250 °C for 5 h, grinding in an attritor mill for 4 h, and sieving below 63 μm. To modify the surface of α-TCP powder, the 5 wt% solutions of TEOS (T) and GPTMS (G) (≥99.5%, Sigma-Aldrich, St. Louis, MO, USA) in ethanol (99.8 wt%, POCH, Gliwice, Poland) were applied according to Pańtak et al. (2023a). The anhydride solvent was used to avoid hydrolysis of both α-TCP and silane coupling agents. α-TCP powder was added to the SCA solution at the liquid to powder (L/P) of 0.25 and stirred on a magnetic stirrer for 4 h. The sedimented powder was then aged for 1 h and silanised at 115 °C for 4 h. Prior to preparing the samples, the powders were sieved below 63 μm.

2.2. Synthesis of hybrid hydroxyapatite/chitosan powder

The hybrid HA/chitosan (CTS) powder, containing 17 wt% CTS, was synthesized using a modified wet chemical method, following the procedure outlined previously by Zima (2018). Shortly, phosphoric acid (85.0%, POCH, Gliwice, Poland) was directly added to 10 wt% CTS solution in 0.5 wt% acetic acid (98.0%, POCH, Gliwice, Poland). This mixture was then carefully dripped into a suspension of $Ca(OH)_2$ (Merck, Darmstadt, Germany) for HA precipitation. The molar ratio of Ca/P during the synthesis was within the range of 1.65–1.67. The CTS used was of medium molecular weight (~100,000 kDa) with a deacetylation degree of ≥75.0% and a viscosity ranging from 200 to 800 CPS (Sigma-Aldrich, St. Louis, MO, USA). After aging process the suspension for 24 h, it was decanted. The HA/CTS precipitate was washed with distilled water, centrifuged, and dried. Prior to preparing the samples, the powders were grinded and sieved through a sieve below 63 μm.

2.3. Self-setting pastes preparation

The mixture of 1.0 wt% Na_2HPO_4 solution in 2.5 wt% citrus pectin gel (Herbstreith &Fox, Werder, Germany) was used as a liquid phase for paste preparation. Six types of different pastes for robocasting were prepared by mixing the powder phase with the liquid phase at a liquid to powder ratio (L/P) of 0.65 g/g (see Table 1 for details). After homogenization the pastes were either transferred carefully by spatula into moulds (8 mm × 10 mm × 5 mm) for the determination of the setting times, or into 3 ml syringes (Optimum Syringe Barrels, Nordson EFD, Westlake, OH, USA) for robocasting of scaffolds.

2.4. Self-setting pastes characterisation

The setting times of the pastes were determined in accordance with the ASTM C266-20 standard, using Gilmore Needles apparatus (Humbold MFG Co., Norridge, IL, USA) at room temperature (21 ± 1 °C) (C01 Committee). The Gillmore Apparatus, consisting of two steel-weighted needles, was used for this purpose. The initial setting needle weighed 113 g and had a diameter of 2.12 mm, while the final setting needle weighed 453.6 g and had a diameter of 1.06 mm. To determine the

Table 1
Initial composition of the self-setting pastes.

Material	Powder phase	Liquid phase	L/P ratio [g/g]
C	α-TCP	1.0 wt% Na_2HPO_4 solution in 2.5 wt% citrus pectin gel	0.65
C_T5	α-TCP/TEOS_5		
C_G5	α-TCP/GPTMS_5		
H	α-TCP + HA/CTS powder (3:2 by weight)		
H_T5	α-TCP/TEOS_5 + HA/CTS powder (3:2 by weight)		
H_G5	α-TCP/GPTMS_5 + HA/CTS powder (3:2 by weight)		

setting times, the cementitious pastes were placed in a special 8 mm × 10 mm × 5 mm forms, and the needle of the apparatus was lightly applied to its surface. The setting time was noticed as the shortest time at which the needle does not leave a mark on the surface. The results are presented as the average of three measurements, along with their corresponding standard deviations (SD). The viscosity of the pastes was studied as a function of time during at a constant share rate of $1s^{-1}$. The experiments were performed using Anton Paar rheometer MCR 301 with parallel-disks-plates (0.4 mm gap) and temperature (22.0 ± 0.5 °C). Time of pastes preparation (mixing powders and liquids) and loading was approximately 0.5 min.

2.5. Robocasting of the scaffolds

Cubic scaffolds (12 mm length) with a primitive cubic cell, 50% porosity, equivalent to a surface-to-surface distance between the deposited strands in the printing plane of 1000 μm, and 2% overlapping between consecutive layers to achieve rigid strand interconnections without deforming the support layer, were designed in silico. For fabrication, the syringes containing the pastes were loaded in the microextrusion devise (BSN3D+, Fundación CIM, Spain) and the scaffolds were automatically deposited in the air on an aluminium foil at speed of 20 mm/s with a dispensing nozzle of 585 μm in aperture (SmoothFlow Tapered Tips, Nordson EFD, USA). The scaffolds were placed immediately directly into containers with 100% humidity at 37 °C for 24h. Afterwards, one set of scaffolds were incubation in simulated body fluid at 37 °C for 7 days. The scaffolds were characterized after incubation in 100% humidity in dry and wet state, and after incubation in simulated body fluid (SBF) only in wet state.

2.6. Scaffolds characterisation

2.6.1. Phase and chemical composition

The X-ray fluorescence method (XRF) was applied to check the chemical composition of the initial powders (WDXRF Axios Max, PANalytical, Malvern, UK). The X-ray diffraction (XRD) analysis was performed to identify the crystalline phases using Cu Kα radiation (1.54 Å) at 30 kV and 10 mA. The analysis was conducted in the 2θ range of 5–45° at 0.04 intervals with a scanning speed of 2.5°/min using D2 Phaser diffractometer (Bruker, Ballerica, MA, USA). The obtained diffractograms were compared with the International Centre for Diffraction Data α-TCP (00-009-0348) and hydroxyapatite (HA; 01-076-0694) to identify the crystalline phases. TOPAS software (Bruker, Ballerica, MA, USA) was used for phase quantification based on Rietveld refinement. All measurements were performed in triplicate. The mean ± SD was used to present the results.

Fourier-transform infrared (FTIR) spectroscopy was used for the chemical characterization of the scaffolds. FTIR investigations were conducted on a BioRad FTS 6000 spectrometer (Bruker, Ballerica, MA, USA) in the midinfrared spectral region from 4000 to 400 cm^{-1}. The samples were prepared as standard KBr pellets.

2.6.2. Particle size distribution

The size distribution of the initial α-TCP, SCAs-modified α-TCP as well as hybrid hydroxyapatite-chitosan powders was based on Brownian motion and the Dynamic Light Scattering (DLS) technique using laser particle size analyser Mastersizer 2000 with Hydro 2000S module (Malvern Panalytical, Malvern, United Kingdom). All measurements were conducted three times in distilled water at 24.0 ± 0.5 °C, and representative data are shown.

2.6.3. Mechanical properties

The compressive strength of the scaffolds was determined using a universal material testing machine (Instron 3345, Norwood, MA, USA) at a crosshead speed of 1 mm min^{-1}. The scaffolds were compacted perpendicularly to the printing plane. The results were expressed as the mean value ± SD of ten measurements.

2.6.4. Microstructure and pore architecture

For microstructure observations of the fractured samples, and assessment of the bioactive potential of the materials, a PhenomPure scanning electron microscope (SEM) from Thermo Fisher Scientific (Waltham, MA, USA) was used. Before examination, the samples were coated with a thin layer of gold film using a low deposition rate to prevent any charge build-up and to enhance the imaging resolution.

2.6.5. Chemical stability and in vitro bioactivity

To evaluate the chemical stability and bioactivity of the scaffolds, they were incubated in distilled water or simulated body fluid (SBF) prepared according to Kokubo's protocol (Kokubo and Takadama, 2006). Cubical samples were placed in containers with 60 mL SBF or distilled water and stored at 37 ± 1 °C. The chemical stability of the scaffolds was determined by measuring the pH and ionic conductivity of the immersion solutions at various time intervals during incubation in water or SBF. Measurements were conducted using a Seven Compact Duo pH/conductometer (Mettler Toledo, Columbus, OH, USA). Each measurement was repeated three times. After incubation, the scaffolds were removed from the liquid, rinsed with distilled water, and dried at 37 °C. The formation of an appetite layer on the scaffolds surfaces was addressed by observing the samples by SEM.

2.6.6. Statistics

The statistical analysis of obtained results was performed using a one-way analysis of variance (ANOVA) with a post hoc Tukey honestly significant difference (HSD) test for comparing multiple treatments at the significance level of $p = 0.05$. All analyses were performed with OriginPro software (version 2023, OriginLab Corporation, Northampton, MA, USA).

3. Results and discussion

3.1. Particle size distribution

The particle size distribution is a very important factor in biomaterials technology, particularly in robocasting, as it influences the properties and performance of the resulting printing pastes. The ideal size distribution varies depending on specific needs, such as the composition, rheological properties of the paste, the degree of homogenization, and the nozzle diameter used for printing. The powder size distribution of obtained powders is shown in Fig. 1.

The surface modification of α-TCP powders with silane coupling agents (SCAs) altered the particle size distribution. In unmodified α-TCP, the particle size ranged from approximately 0.5 to 100.0 μm. However, after modification with SCAs, the distribution shifted to a range of about 0.5–40.0 μm. The silane agents form a mono- or multilayer of organic molecules on the particle surface, reducing surface energy and improving the dispersibility of the particles in the medium (Lu et al., 2017). Additionally, since TEOS and GPTMS possess hydrophobic functional groups, they lower the particles' affinity for water, promoting the formation of smaller agglomerates (Rao et al., 2003), (Khodaei and Shadmani, 2019). The particle size distribution of the hybrid hydroxyapatite-chitosan powder differed slightly from that of the α-TCP powders. The use of chitosan during synthesis led to the formation of larger agglomerates due to the polymer binding particles together. Nevertheless, all synthesized powders exhibited a similar particle size distribution, enabling the preparation of pastes suitable for robocasting.

3.2. Setting process and rheology of the pastes

The solid phase of the developed pastes was composed of highly reactive α-tricalcium phosphate powder, which, upon contact with the water present in the liquid phase, undergoes hydrolysis to calcium

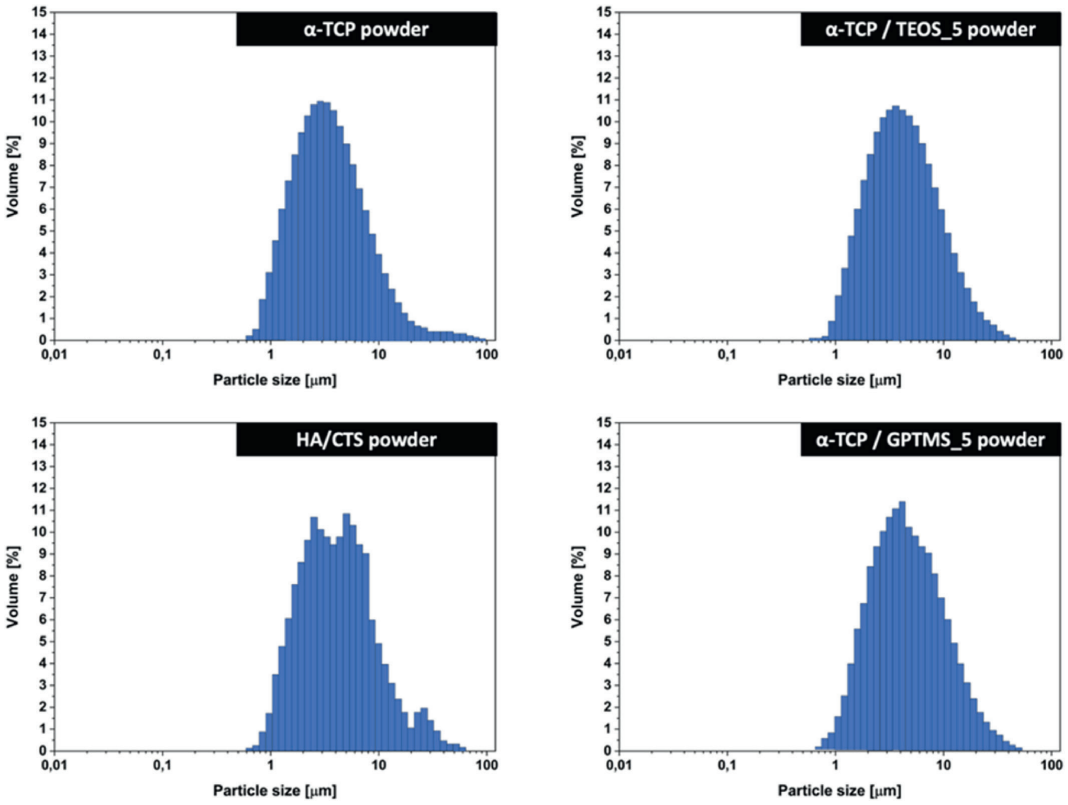

Fig. 1. Powders size distribution of powders used for paste preparation.

deficient hydroxyapatite (CDHA) following equation (1) (Durucan and Brown, 2002), (He et al., 2015):

$$3Ca_3(PO_4)_2 + H_2O \rightarrow Ca_9(PO_4)_5(HPO_4)OH \quad (1)$$

During the hydrolysis the paste undergoes a setting and hardening process related to the nucleation and growth of CDHA crystals. During setting the powder particles in the paste undergone a restructuration that transform the fluid paste into a rigid and weak monolith. Then the strength of the monolith increases during hardening. The initial and final setting times of the pastes ranged from 9.0 ± 1.0 to 27.0 ± 0.5 min and from 28.0 ± 1.0 to 51.0 ± 2.0 min, respectively (Table 2).

The setting process of self-setting calcium phosphate-based cementitious pastes begins upon mixing the powder phase with the liquid phase, resulting in a viscose paste with its rheological properties changing until complete material hardening. The process of α-TCP hydrolysis is influenced by several factors. The most critical factor is the content of highly reactive α-TCP powder in materials' composition. However, the presence of other factors is equally important, such as the presence of setting accelerators in the liquid phase or the presence of polymers in the mixture (C01 Committee). In the developed materials disodium hydrogen phosphate was employed to accelerate the setting process and mitigated the effect of setting time increase caused by the presence of citrus pectin. As the same liquid phase was used for all materials the setting times varied only due to differences in the solid phase composition. Materials based solely on α-TCP (C, C_T5, C_G5) exhibited significantly shorter setting times compared to pastes containing the hybrid hydroxyapatite/chitosan component (Table 2). The cements with hybrid powder (H, H_T5, H_G5) showed more than twofold increase in setting times, which was attributed to the lower amount of the setting phase (α-TCP) and presence of chitosan. Chitosan is a highly water-absorbent polymer and might impede the access of water to α-TCP, affecting its setting process.

Table 2
Setting times of self-setting pastes used for scaffolds robocasting.

Material	Initial setting time (t_i) [min]	Final setting time (t_f) [min]
C	11.5 ± 0.5	32.0 ± 2.0
C_T5	9.0 ± 1.0	28.0 ± 1.0
C_G5	10.5 ± 1.0	29.0 ± 1.0
H	27.0 ± 0.5	48.0 ± 0.5
H_T5	26.5 ± 1.0	51.0 ± 2.0
H_G5	24.0 ± 1.5	45.0 ± 1.0

It seems that the presence of SCAs, slightly shortened the setting process of cement pastes. This phenomenon may relate to the silicon coupling agent serving as a source of silicon ions. The XRF method confirmed the presence of silicon in modified α-TCP powders. The silicon content was 0.227 ± 0.003 wt% and 0.291 ± 0.001 wt% for powders modified with 5 wt% of TEOS and GPTMS respectively. According to the literature, the addition of silicon increases the solubility of α-TCP and accelerates its hydrolysis in comparison to unmodified powders (Wei et al., 2009), (Mestres et al., 2012). For instance, in the study conducted by Czechowska et al. (2021), a decrease in setting times was

observed for silicon-doped α-TCP. Another possible explanation might involve the hydrolysis of silane coupling agents upon contact with water, and their simultaneous condensation, potentially contributing to a slight acceleration in the setting of materials. This process is well established in the literature (Kaur et al., 2022), (Casagrande et al., 2020). The long setting times are advantageous for robocasting because provide a longer printing window in which the rheological properties are nearly constant, facilitating a continuous flow through the printing nozzle. This is a significant factor in planning larger-scale production without the need for frequent preparation of additional paste batches for printing.

The rheology of pastes is of great importance in the field of 3D printed bone scaffolds. Self-setting pastes exhibit a multifaceted rheological behaviour, ultimately solidifying into a solid form. By appropriately adjusting rheological properties of the printing paste, which include viscosity and shear-thinning behaviour, it becomes possible to achieve precise control over paste flow, accurate deposition, and optimize scaffold geometry for improved mechanical properties. The results of the time dependent viscosity measurements of the cementitious pastes for 3D printing are presented in Fig. 2. The viscosity of the tested materials was influenced by the paste composition and fell within the range of 60 Pa*s to 260 Pa*s (C) or to 390 Pa*s (H). The addition of silane coupling agents, both TEOS and GPTMS, resulted in slightly reduced paste viscosities. In all tested materials, the viscosity remained constant for a time and then increased rapidly. The materials containing HA/CTS hybrid powders exhibited extended periods of consistent viscosity, therefore they displayed a wider printing window, up to ~3000s (50min).

The viscosity of cementitious pastes based on calcium phosphates for robocasting is widely described. The rheological properties strongly effect the printing process, as well as characteristics of final materials (del-Mazo-Barbara and Ginebra, 2021), (Dos Santos et al., 2024).

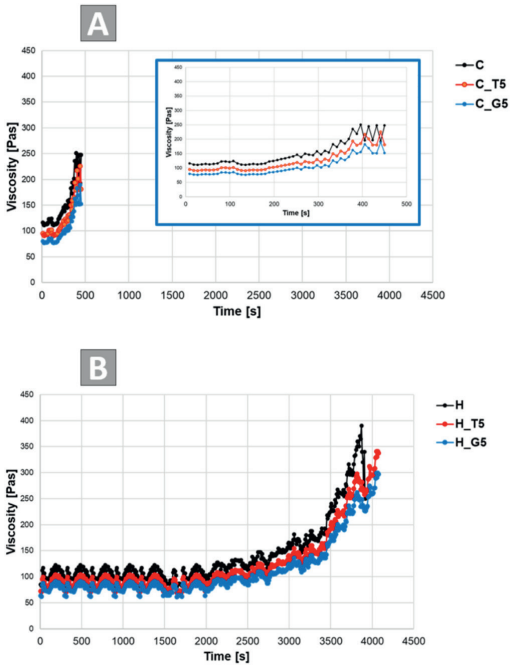

Fig. 2. Viscosity of the α-TCP pastes at constant shear rate ($1*s^{-1}$).

Calcium phosphate bone cements are typically characterized as viscoelastic and thixotropic, displaying time-dependent shear thinning behaviour with the capability to regain viscosity during resting periods. In cases where full recovery does not occur, it is described as pseudo-thixotropic (Bartos, 1992), (Maas et al., 2014). The obtained rheological measurements align closely with the observations of setting times for self-setting pastes based on α-TCP. The results are in accordance with those obtained by Dziadek et al. (2020), in which the utilization of citrus and apple pectins led to an increased injectability of calcium phosphate-based materials containing hybrid granules.

3.3. Microstructure of the scaffolds

To check the feasibility of pastes for robocasting of bone scaffold and to identify any inherent microstructural cracks, an examination of their microstructure was conducted. The set and hardened materials, after 24 h of exposure to 100% humidity, exhibited an uniform microstructure characterized by a cementitious matrix with macro- and micropores (Fig. 3). The scaffold architecture conformed to the predefined model criteria. No adverse influence of the hybrid hydroxyapatite-chitosan powder or silane coupling agents on printed scaffolds morphology was observed. Comparable microstructures of α-TCP-based biomaterials intended for bone tissue substitution can be found in other studies (Espanol et al., 2023), (Moreno et al., 2020).

3.4. Phase and chemical composition of robocasted scaffolds

The XRD analysis revealed that the initial α-TCP and SCAs-modified α-TCP powders composed mainly of α-TCP (97–98 wt%) and a small amount of hydroxyapatite (2–3 wt.%), whereas hybrid HA-CTS powder contained only one crystalline phase, i.e. hydroxyapatite (Fig. 4A). The diffractograms of robocasted scaffolds after setting and hardening in 100% humidity (24h), as well as incubated in SBF (7 days) revealed presence of two crystalline phases, i.e., hydroxyapatite and small amount of α-TCP (Fig. 4B and C). No additional silicon-containing crystalline phases were detected by XRD.

Quantitative analysis revealed that in a humid environment, the α-TCP phase exhibited thermodynamic metastability and underwent near-complete hydrolysis, resulting in the formation of CDHA (Table 3). This transformation led to alterations in the phase composition and crystallographic structure, influencing its properties and performance in biological applications (Şahin et al., 2018).

The results of the FTIR studies align with the findings observed in the XRD and confirmed the presence of functional groups characteristic for calcium phosphates and polymers. Infrared spectra of developed materials, both after setting and hardening in 100% humidity as well as after incubation in simulated body fluid are present at Fig. 5.

The FTIR spectra of the materials showed characteristic bands at approximately 600 and 560 cm^{-1} (bending), as well as around 965 and 1020 cm^{-1} (stretching), corresponding to the vibrations of PO_4^{3-} groups. The broad band in the range of approximately 3000–3800 cm^{-1} was attributed to absorbed water. Furthermore, the spectra exhibited an absorption band at around 870 cm^{-1} associated with HPO_4^{2-} groups, confirming the presence of non-stoichiometric hydroxyapatite. Additionally, within a similar spectral range (approximately 873–875 cm^{-1}), carbonate bonds may have been present in the material. The presence of a band at 1424 cm^{-1} indicated partial substitution of CO_3^{2-} within the hydroxyapatite structure. The detected bands originating from calcium phosphates are characteristic of these types of materials and have been observed previously (Carrodeguas and De Aza, 2011), (Kovrlija et al., 2023). FTIR analyses confirmed the presence of chitosan and pectin. The absorption band at approximately 2930 cm^{-1} was associated with alkyl C-H (stretching) vibrations. The band around 1650 cm^{-1} was attributed to N-H bending vibrations of primary amine, affirming the presence of chitosan and amidated citrus pectin within the materials, as described in previous studies (Manrique and Lajolo, 2002), (Kozioł et al., 2022).

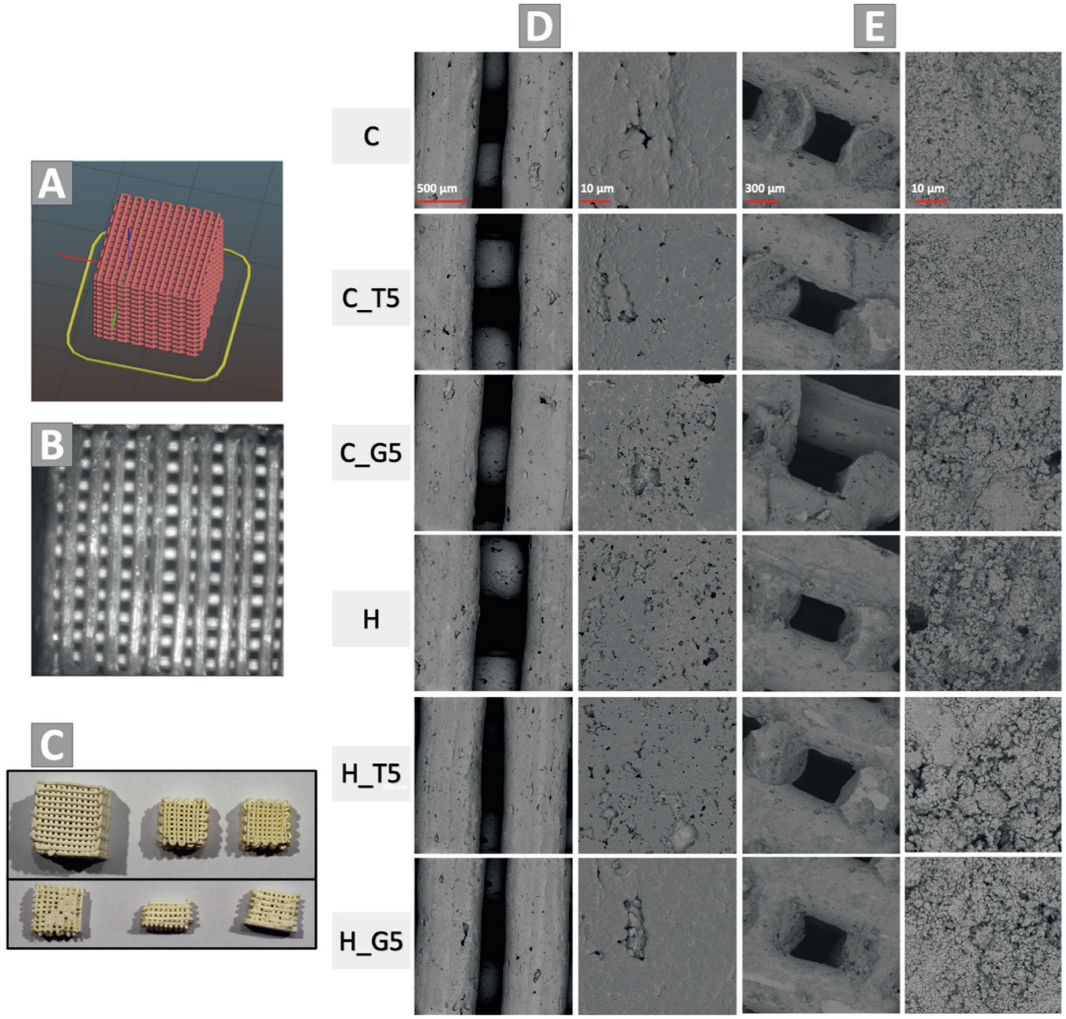

Fig. 3. Designed model (A) and SEM images of the printed scaffold overview (B, C), surface (D) and cross-sections (E) after 24h in 100% humidity.

Furthermore, the bands c.a. 1320 cm^{-1} and 3570 cm^{-1} corresponded to C-N and O-H stretching vibrations, respectively. In the pectin and chitosan containing systems, the formation of electrostatic and/or hydrogen bonding was feasible. The polyelectrolyte complexes are expected to form that within the scaffolds, at the hybrid powder and pectin interface. Low concentration of silane coupling agents in the pastes, as well as an overlapping of bands by corresponding phosphates bands, may explain the lack of visible peaks of Si–O–Si, Si-OH, Si–C and C–H bands assigned to silane coupling agents (Gui-Long et al., 2011).

3.5. Mechanical properties of the scaffolds

The mechanical strength of robocasted bone scaffolds based on calcium phosphate is a main determinant of their capacity to withstand the mechanical forces and stresses inherent in the bone microenvironment. Understanding of the mechanical behavior under various conditions allows for the selection of the most favorable manufacturing, storage, and pre-implantation processing conditions. The compressive strength values depended on the materials composition as well as setting and testing conditions and ranged from 5.20 ± 0.77 MPa to 9.26 ± 0.54 MPa (Fig. 6). Scaffolds displayed their highest compressive strength values when stored for 24 h in a 100% humidity environment (in wet condition), whereas the lowest strength was obtained for scaffolds that set and hardened in SBF. A reduction in the compressive strength of the materials following incubation in SBF is linked to their degradation and the release of polymers into the surrounding environment.

The obtained results confirm, that use of silane coupling agents as modifiers for α-TCP powders enhances the mechanical properties of the scaffolds. It can be concluded that the strengthening effect is not dependent on the type of SCAs, as based on the results of a one-way ANOVA and a subsequent Tukey HSD post-hoc analysis, the differences between the materials modified with TEOS (C_T5, H_T5) and

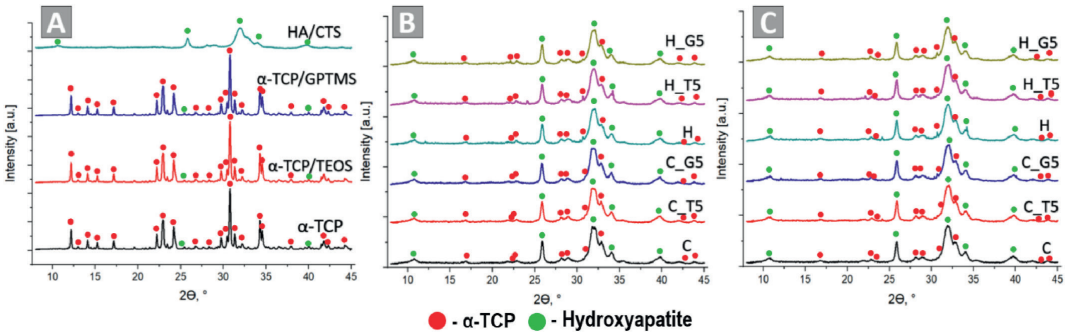

Fig. 4. Diffractograms of obtained materials: initial powders (A), scaffolds after setting and hardening for 24 h in 100% humidity (B) and incubation in SBF for 7 days (C).

Table 3
Phase composition of robocasted scaffolds.

Material	Phase composition, wt.%			
	after 24h in 100% humidity at 37 ± 1 °C		after 7 days of incubation in SBF at 37 ± 1 °C	
	α-TCP	Hydroxyapatite	α-TCP	Hydroxyapatite
C	3.7 ± 1.0	96.3 ± 1.0	0.8 ± 0.5	99.2 ± 0.5
C_T5	5.9 ± 0.5	94.1 ± 0.5	1.2 ± 1.0	98.8 ± 1.0
C_G5	6.4 ± 1.0	93.6 ± 1.0	0.2 ± 0.5	99.8 ± 0.5
H	3.9 ± 0.5	96.1 ± 0.5	0.6 ± 1.0	99.4 ± 1.0
H_T5	2.8 ± 1.0	97.1 ± 1.0	1.6 ± 0.5	98.4 ± 0.5
H_G5	2.4 ± 1.0	97.6 ± 1.0	1.2 ± 0.5	98.8 ± 0.5

GPTMS (C_G5, H_G5) were not statistically significant (Fig. 6). The observed increase in mechanical strength is likely a result of the chemical interactions between the components, leading to the formation of hybrid-type materials. The presence of biopolymers with different electrolytic potential may enhance mechanical properties through two distinct mechanisms: firstly, by facilitating better paste homogenization, and secondly, by creating a dual hybrid structure stemming from both electrostatic interaction between polycationic chitosan and polyanionic pectin, and the hybrid characteristics of hydroxyapatite-chitosan powders (Pańtak et al., 2023b). Similar beneficial effects of silane coupling agents on the mechanical properties of biomaterials have been previously documented in the literature. For instance, Vaz et al. (2002) demonstrated the advantageous application of various zirconate coupling agents to obtain starch/ethylene-vinyl alcohol copolymer/hydroxyapatite composites with improved mechanical resistance, attributed to enhanced adhesion among material constituents. Reyes Peces et al. (Reyes-Peces et al., 2020) significantly improved the compressive strength of chitosan-silica hybrid aerogels by adding GPTMS, indicating the formation of a covalent crosslinked hybrid structure. Whereas, Ghorbani et al. (2020) examined chitosan-polyvinyl alcohol scaffolds with varying GPTMS content and observed improved mechanical properties of the developed scaffolds with an increased amount of the silane coupling agent. It should be noted that the compressive strength of cancellous bone ranges from approximately 4 to 12 MPa (Chatzistavrou et al., 2011). Thus, the hybrid-type, robocasted scaffolds developed in our study possessed mechanical strength suitable for implantation in non-load or low-load bearing applications.

3.6. Chemical stability and in vitro bioactivity or the scaffolds

The chemical stability of robocasted bioceramic scaffolds is crucial parameter in determining their potential clinical application. The pH changes of the SBF during the samples' immersion are illustrated in Fig. 7A.

The pH levels of the SBF fluctuating between 7.33 and 7.43 during the immersion test, and were close the physiological range described in literature (Hopkins et al., 2023). The incorporation of the hybrid HA/CTS powder and SCAs had a minimal impact on the pH values of the

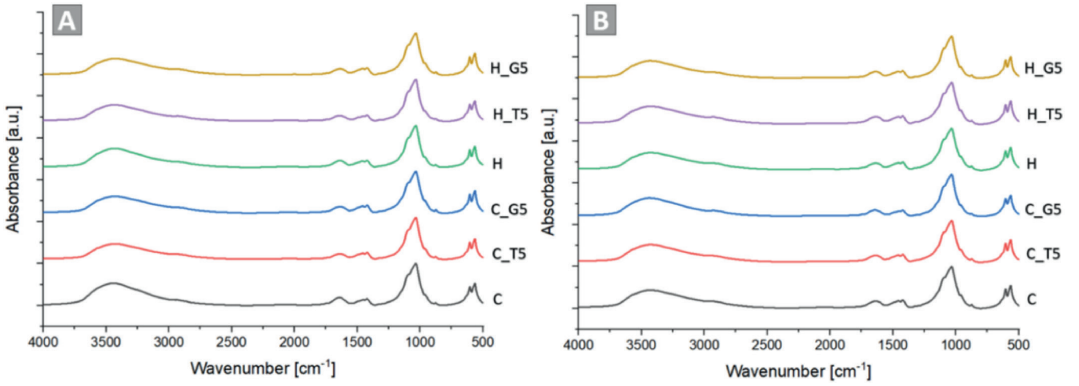

Fig. 5. FT-IR spectra of obtained scaffolds: after 24h setting and hardening in 100% humidity (A)and incubated in SBF for 7 days (B).

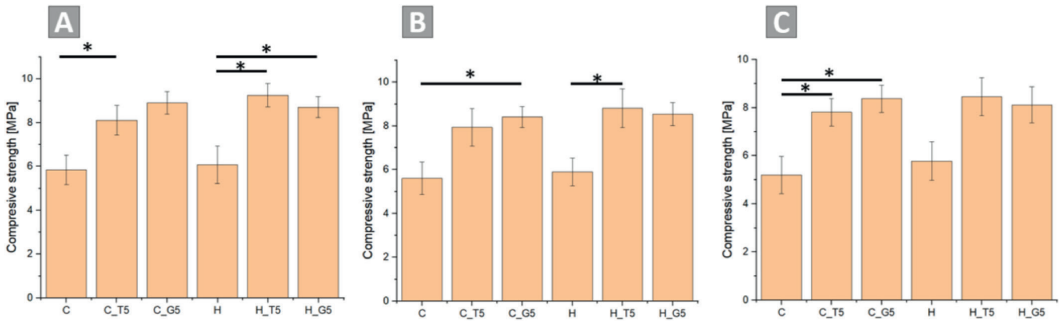

Fig. 6. Compressive strength of robocasted scaffolds after 24h in 100% humidity – tested in wet (A), after 24h in 100% humidity and dried (B) and after incubation in SBF (C) conditions (*p < 0.01).

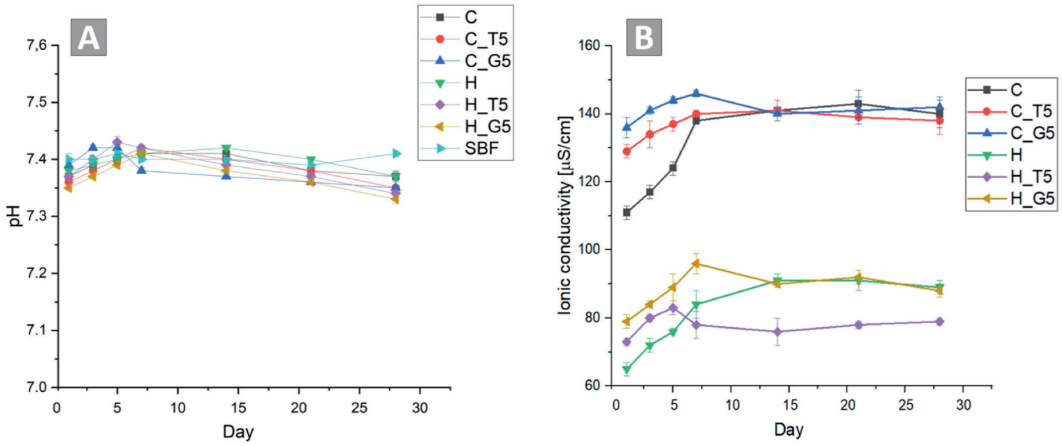

Fig. 7. pH versus bone scaffolds' incubation time in SBF (A) and ionic conductivity versus scaffolds' incubation time in distilled water (B).

solution. Comparable pH levels in the incubated calcium phosphate-based bone substitutes have been reported in previous studies (Czechowska et al., 2018). Ionic conductivity during the scaffolds' incubation in distilled water of also depended on the its composition (Fig. 7B). The ionic conductivity of distilled water around incubated samples ranging up to ~111–146 µS/cm. The presence of hybrid HA/CTS powder decreased the values to the range ~65–96 µS/cm, probably due to lower dissolution rate of hydroxyapatite compared to α-TCP and because of hindering the diffusion of ions into the incubation environment by chitosan. For scaffolds containing SCAs-modified α-TCP we observed slightly higher ionic conductivity during the first 7 days of incubation. This phenomenon may be explained by the faster degradation of silane coupling agents and their hydrolysis in aqueous solutions (Lee et al., 2023). The ionic conductivity of all the tested scaffolds is similar to previously examined chemically bonded biomaterials on the basis of α-TCP (Zima et al., 2020).

Following a 7-day incubation at 37 °C in SBF, all developed robocasted scaffolds were completely covered by plate-like apatitic structures, as illustrated in Fig. 8. The presence of these apatite confirmed the *in vitro* bioactive potential of the materials, according to the criteria established by Kokubo and Takadama (2006). The presence of silane coupling agents did not cause any negative effect on the *in vitro* bioactivity of novel hybrid robocasted scaffolds printed with self-setting injectable pastes.

4. Conclusions

In this study, novel hybrid-type robocasted bone scaffolds were developed and thoroughly investigated. The scaffolds were printed using cementitious, self-setting inks composed of highly reactive α-TCP powder (either non-modified or modified with silane coupling agents), hybrid hydroxyapatite-chitosan powder, and mixture of citrus pectin with disodium phosphate solution as the liquid phase. The effects of two different coupling agents -tetraethyl orthosilicate (TEOS) and 3-glycidoxypropyltrimethoxysilane (GPTMS) - on the physicochemical and biological properties of the scaffolds were examined. The modification of α-TCP with silane coupling agents, combined with natural polymers, allowed for the development of pastes with optimal rheological properties, enabling the fabrication of biomaterials through the robocasting technique. The unique properties of these scaffolds derived from the hybrid system, which depends on chemical interactions between the hybrid powders, pectin, and SCAs-modified tricalcium phosphate. These interactions include electrostatic attraction between the oppositely charged groups of chitosan and citrus pectin, as well as bond formation between silane groups and the functional groups present in calcium phosphates and polymers. These chemical interactions contribute to

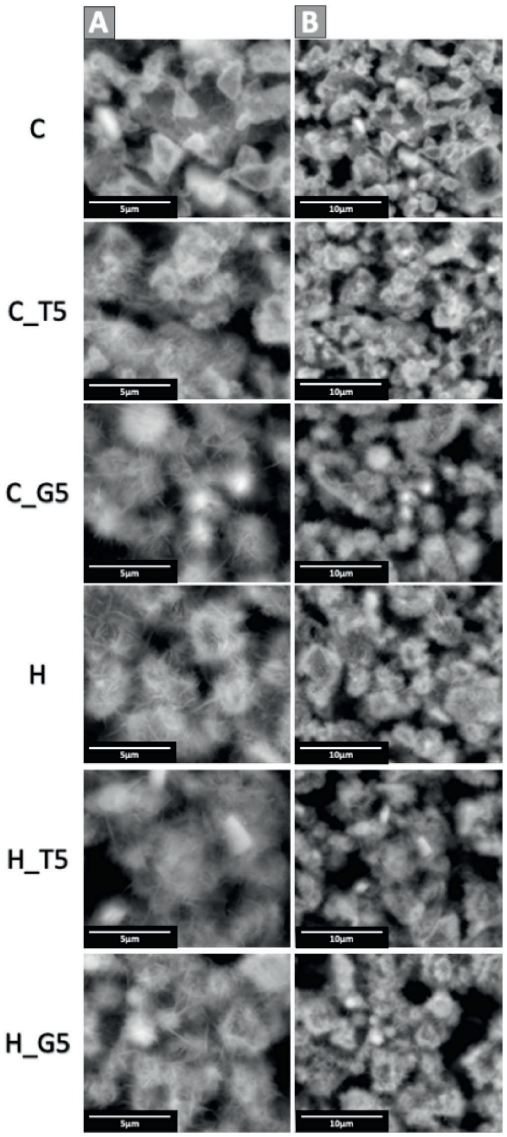

Fig. 8. SEM microstructure of material surfaces after 7 days of incubation in SBF at magnification: 10 000x (A) and 5 000x (B).

improved rheological properties, providing a longer printing window and ensuring a continuous flow through the printing nozzle. Scaffolds with a homogeneous microstructure were successfully printed in less than 2 min, with no issues encountered during the printing process. The hybrid nature of self-setting ink increased also the mechanical strength of the scaffolds, nearly doubling the compressive strength (from approximately 5.20 to 9.26 MPa). Importantly, no negative impact of the silane coupling agents on the microstructure or *in vitro* chemical stability of the materials was observed. All the robocasted scaffolds demonstrated bioactive potential *in vitro*, making them promising candidates for further biological studies. Moreover, the incorporation of easily functionalized polymers such as chitosan and citrus pectin, along with silane coupling agents, allows for future modifications of the materials with drugs or other biologically active agents. This study highlights the favorable properties of the scaffolds and lays the groundwork for further *in vitro* and *in vivo* investigations.

CRediT authorship contribution statement

Piotr Pańtak: Writing – original draft, Visualization, Methodology, Investigation, Funding acquisition, Formal analysis, Conceptualization. **Joanna P. Czechowska:** Writing – review & editing, Validation, Supervision, Methodology, Conceptualization. **Adelia Kashimbetova:** Methodology, Investigation, Conceptualization. **Ladislav Čelko:** Writing – review & editing, Validation, Resources. **Edgar B. Montufar:** Writing – review & editing, Supervision, Resources, Methodology, Investigation, Conceptualization. **Łukasz Wójcik:** Methodology, Investigation. **Aneta Zima:** Writing – review & editing, Validation, Supervision, Project administration, Methodology, Funding acquisition, Conceptualization.

Declaration of competing interest

The authors declare that they have no known competing financial interests or personal relationships that could have appeared to influence the work reported in this paper.

Acknowledgment

Research project supported by program „Excellence initiative – research university" for the AGH University of Science and Technology (grant IDs: 4159, 4222 and 5352). Research co-funded by the Faculty of Materials Science and Ceramics AGH UST—University of Science and Technology, Kraków, Poland, Project No. 16.16.160.557 (2024). Adelia Kashimbetova acknowledges the Brno University of Technology's project CEITEC VUT/FAST-J-23-8309. Acknowledgments to the GlaCerHub project funded by the Horizon Europe program (101087154).

Data availability

Data will be made available on request.

References

An, J., Wolke, J.G.C., Jansen, J.A., Leeuwenburgh, S.C.G., 2016. Influence of polymeric additives on the cohesion and mechanical properties of calcium phosphate cements. J. Mater. Sci. Mater. Med. 27 (3), 58. https://doi.org/10.1007/s10856-016-5665-x.

Bartos, P., 1992. Fresh concrete: properties and tests. In: Developments in Civil Engineering, vol. 38. Elsevier, Amsterdam ; New York.

Bergmann, C., et al., 2010. 3D printing of bone substitute implants using calcium phosphate and bioactive glasses. J. Eur. Ceram. Soc. 30 (12), 2563–2567. https://doi.org/10.1016/j.jeurceramsoc.2010.04.037.

C01 Committee, 'Test Method for Time of Setting of Hydraulic-Cement Paste by Gillmore Needles', ASTM International. doi: 10.1520/C0266-20.

Carrodeguas, R.G., De Aza, S., 2011. α-Tricalcium phosphate: synthesis, properties and biomedical applications. Acta Biomater. 7 (10), 3536–3546. https://doi.org/10.1016/j.actbio.2011.06.019.

Casagrande, C.A., Jochem, L.F., Repette, W.L., 2020. Analysis of the 3-Glycidoxypropyltrimethoxysilane (GPTMS) hydrolysis by infrared spectroscopy. Materia 25 (3). https://doi.org/10.1590/s1517-707620200003.1111 e-12811.

Cervantes-Uc, J.M., Cauich-Rodríguez, J.V., Hernández-Sánchez, F., Chan-Chan, L.H., 2015. Bone cements: formulation, modification, and characterization. In: Encyclopedia of Biomedical Polymers and Polymeric Biomaterials. Taylor & Francis, pp. 1053–1066. https://doi.org/10.1081/E-EBPP-120050598.

Chatzistavrou, X., Newby, P., Boccaccini, A.R., 2011. Bioactive glass and glass-ceramic scaffolds for bone tissue engineering. In: Bioactive Glasses. Elsevier, pp. 107–128. https://doi.org/10.1533/9780857093318.2.107.

Czechowska, J., Zima, A., Paszkiewicz, Z., Lis, J., Ślósarczyk, A., 2014. Physicochemical properties and biomimetic behaviour of α-TCP-chitosan based materials. Ceram. Int. 40 (4), 5523–5532. https://doi.org/10.1016/j.ceramint.2013.10.142.

Czechowska, J., Zima, A., Siek, D., Ślósarczyk, A., 2018. Influence of sodium alginate and methylcellulose on hydrolysis and physicochemical properties of α-TCP based materials. Ceram. Int. 44 (6), 6533–6540. https://doi.org/10.1016/j.ceramint.2018.01.055.

Czechowska, J., Cichoń, E., Belcarz, A., Ślósarczyk, A., Zima, A., 2021. Effect of gold nanoparticles and silicon on the bioactivity and antibacterial properties of hydroxyapatite/chitosan/tricalcium phosphate-based biomicroconcretes. Materials 14 (14), 3854. https://doi.org/10.3390/ma14143854.

Dapporto, M., et al., 2022. Strontium-doped apatitic bone cements with tunable antibacterial and antibiofilm ability. Front. Bioeng. Biotechnol. 10. https://www.frontiersin.org/articles/10.3389/fbioe.2022.969641. (Accessed 14 October 2023).

del-Mazo-Barbara, L., Ginebra, M.-P., 2021. Rheological characterisation of ceramic inks for 3D direct ink writing: a review. J. Eur. Ceram. Soc. 41 (16), 18–33. https://doi.org/10.1016/j.jeurceramsoc.2021.08.031.

Dos Santos, V.I., Chevalier, J., Fredel, M.C., Henriques, B., Gremillard, L., 2024. Ceramics and ceramic composites for biomedical engineering applications via Direct Ink Writing: Overall scenario, advances in the improvement of mechanical and biological properties and innovations. Mater. Sci. Eng. R Rep. 161, 100841. https://doi.org/10.1016/j.mser.2024.100841.

Drevet, R., Fauré, J., Benhayoune, H., 2023. Bioactive calcium phosphate Coatings for bone implant applications: a review. Coatings 13 (6), 1091. https://doi.org/10.3390/coatings13061091.

Durucan, C., Brown, P.W., 2002. Reactivity of α-tricalcium phosphate. J. Mater. Sci. 37 (5), 963–969. https://doi.org/10.1023/A:1014347814241.

Dziadek, M., Zima, A., Cichoń, E., Czechowska, J., Ślósarczyk, A., 2020. Biomicroconcretes based on the hybrid HAp/CTS granules, α-TCP and pectins as a novel injectable bone substitutes. Mater. Lett. 265, 127457. https://doi.org/10.1016/j.matlet.2020.127457.

Espanol, M., Davis, E., Meslet, E., Mestres, G., Montufar, E.B., Ginebra, M.-P., 2023. Effect of moisture on the reactivity of alpha-tricalcium phosphate. Ceram. Int. 49 (11), 18228–18237. https://doi.org/10.1016/j.ceramint.2023.02.193.

Fernandez De Grado, G., et al., 2018. Bone substitutes: a review of their characteristics, clinical use, and perspectives for large bone defects management. J. Tissue Eng. 9, 204173141877681. https://doi.org/10.1177/2041731418776819.

Ghorbani, F., Pourhaghgouy, M., Mohammadi-hafshehjani, T., Zamanian, A., 2020. Effect of silane-coupling modification on the performance of chitosan-poly vinyl alcohol-hybrid scaffolds in bone tissue engineering. Silicon 12 (12), 3015–3026. https://doi.org/10.1007/s12633-020-00397-2.

Gui-Long, X., Changyun, D., Yun, L., Pi-Hui, P., Jian, H., Zhuoru, Y., 2011. Preparation and characterization of Raspberry-like SiO $_2$ particles by the Sol-gel method. Nanomater. Nanotechnol. 1, 21. https://doi.org/10.5772/45813.

He, Z., et al., 2015. Bone cements for percutaneous vertebroplasty and balloon kyphoplasty: Current status and future developments. Journal of Orthopaedic Translation 3 (1), 1–11. https://doi.org/10.1016/j.jot.2014.11.002.

Hopkins, E., Sanvictores, T., Sharma, S., 2023. Physiology, acid Base Balance. In: *StatPearls*, Treasure Island (FL). StatPearls Publishing. Accessed: Oct. 14, 2023. [Online]. Available: http://www.ncbi.nlm.nih.gov/books/NBK507807/.

Houaoui, A., et al., 2021. New Generation of hybrid materials based on Gelatin and bioactive glass particles for bone tissue regeneration. Biomolecules 11 (3), 444. https://doi.org/10.3390/biom11030444.

Huang, Y., et al., 2020. Formulation of α-tricalcium phosphate bone cement based on an alginate–chitosan gel system. Cryst. Growth Des. 20 (3), 1400–1404. https://doi.org/10.1021/acs.cgd.0c00005.

Kaur, H., Chaudhary, S., Kaur, H., Chaudhary, M., Jena, K.C., 2022. Hydrolysis and condensation of tetraethyl orthosilicate at the air–aqueous Interface: Implications for silica nanoparticle formation. ACS Appl. Nano Mater. 5 (1), 411–422. https://doi.org/10.1021/acsanm.1c03250.

Khodaei, M., Shadmani, S., 2019. Superhydrophobicity on aluminum through reactive-etching and TEOS/GPTMS/nano-Al2O3 silane-based nanocomposite coating. Surf. Coating. Technol. 374, 1078–1090. https://doi.org/10.1016/j.surfcoat.2019.06.074.

Kokubo, T., Takadama, H., 2006. How useful is SBF in predicting in vivo bone bioactivity? Biomaterials 27 (15), 2907–2915. https://doi.org/10.1016/j.biomaterials.2006.01.017.

Kolmas, J., Kaflak, A., Zima, A., Ślósarczyk, A., 2015. Alpha-tricalcium phosphate synthesized by two different routes: Structural and spectroscopic characterization. Ceram. Int. 41 (4), 5727–5733. https://doi.org/10.1016/j.ceramint.2014.12.159.

Kovrlija, I., et al., 2023. Exploring the formation Kinetics of Octacalcium phosphate from alpha-tricalcium phosphate: synthesis scale-up, determination of Transient phases, their morphology and Biocompatibility. Biomolecules 13 (3), 462. https://doi.org/10.3390/biom13030462.

Kozioł, A., Środa-Pomianek, K., Górniak, A., Wikiera, A., Cyprych, K., Malik, M., 2022. Structural determination of pectins by spectroscopy methods. Coatings 12 (4), 546. https://doi.org/10.3390/coatings12040546.

Kumar, A., Kargozar, S., Baino, F., Han, S.S., 2019. Additive manufacturing methods for producing hydroxyapatite and hydroxyapatite-based composite scaffolds: a review. Front. Mater. 6, 313. https://doi.org/10.3389/fmats.2019.00313.

Lee, C., Yamaguchi, S., Imazato, S., 2023. Quantitative evaluation of the degradation amount of the silane coupling layer of CAD/CAM resin composites by water absorption. J Prosthodont Res 67 (1), 55–61. https://doi.org/10.2186/jpr.JPR_D_21_00236.

Liu, H., et al., 2023. Study on injectable silver-incorporated calcium phosphate composite with enhanced antibacterial and biomechanical properties for fighting bone cement-associated infections. Colloids Surf. B Biointerfaces 227, 113382. https://doi.org/10.1016/j.colsurfb.2023.113382.

Lu, Y., Jiang, N., Li, X., Xu, S., 2017. Effect of inorganic–organic surface modification of calcium sulfate whiskers on mechanical and thermal properties of calcium sulfate whisker/poly(vinyl chloride) composites. RSC Adv. 7 (73), 46486–46498. https://doi.org/10.1039/C7RA09193A.

Maas, M., Hess, U., Rezwan, K., 2014. The contribution of rheology for designing hydroxyapatite biomaterials. Curr. Opin. Colloid Interface Sci. 19 (6), 585–593. https://doi.org/10.1016/j.cocis.2014.09.002.

Maazouz, Y., et al., 2014. Robocasting of biomimetic hydroxyapatite scaffolds using self-setting inks. J. Mater. Chem. B 2 (33), 5378–5386. https://doi.org/10.1039/C4TB00438H.

Manrique, G.D., Lajolo, F.M., 2002. FT-IR spectroscopy as a tool for measuring degree of methyl esterification in pectins isolated from ripening papaya fruit. Postharvest Biol. Technol. 25 (1), 99–107. https://doi.org/10.1016/S0925-5214(01)00160-0.

Martínez-Vázquez, F.J., Perera, F.H., Miranda, P., Pajares, A., Guiberteau, F., 2010. Improving the compressive strength of bioceramic robocast scaffolds by polymer infiltration. Acta Biomater. 6 (11), 4361–4368. https://doi.org/10.1016/j.actbio.2010.05.024.

Mestres, G., Le Van, C., Ginebra, M.-P., 2012. Silicon-stabilized α-tricalcium phosphate and its use in a calcium phosphate cement: characterization and cell response. Acta Biomater. 8 (3), 1169–1179. https://doi.org/10.1016/j.actbio.2011.11.021.

Montelongo, S.A., Chiou, G., Ong, J.L., Bizios, R., Guda, T., 2021. Development of bioinks for 3D printing microporous, sintered calcium phosphate scaffolds. J. Mater. Sci. Mater. Med. 32 (8), 94. https://doi.org/10.1007/s10856-021-06569-9.

Moreno, D., Vargas, F., Ruiz, J., López, M.E., 2020. Solid-state synthesis of alpha tricalcium phosphate for cements used in biomedical applications. Bol. Soc. Espanola Ceram. Vidr. 59 (5), 193–200. https://doi.org/10.1016/j.bsecv.2019.11.004.

Nihei, T., 2016. Dental applications for silane coupling agents. J. Oral Sci. 58 (2), 151–155. https://doi.org/10.2334/josnusd.16-0035.

Pańtak, P., Czechowska, J.P., Zima, A., 2023a. The influence of silane coupling agents on the properties of α-TCP-based ceramic bone substitutes for orthopaedic applications. RSC Adv. 13 (48), 34020–34031. https://doi.org/10.1039/D3RA06027F.

Pańtak, P., Czechowska, J.P., Cichoń, E., Zima, A., 2023b. Novel Double hybrid-type bone cements based on calcium phosphates, chitosan and citrus pectin. IJMS 24 (17), 13455. https://doi.org/10.3390/ijms241713455.

Pape, P.G., 2017. Adhesion Promoters: silane coupling agents. In: Applied Plastics Engineering Handbook. Elsevier, pp. 555–572. https://doi.org/10.1016/B978-0-323-39040-8.00026-2.

Paterlini, A., Le Grill, S., Brouillet, F., Combes, C., Grossin, D., Bertrand, G., 2021. Robocasting of self-setting bioceramics: from paste formulation to 3D part characteristics. Open Ceramics 5, 100070. https://doi.org/10.1016/j.oceram.2021.100070.

Perez, R.A., Kim, H.-W., Ginebra, M.-P., 2012. Polymeric additives to enhance the functional properties of calcium phosphate cements. J. Tissue Eng. 3 (1), 204173141243955. https://doi.org/10.1177/2041731412439555.

Plueddemann, E.P., 1991. Silane Coupling Agents. Springer US, Boston, MA. https://doi.org/10.1007/978-1-4899-2070-6.

Rakmae, S., Ruksakulpiwat, Y., Sutapun, W., Suppakarn, N., 2012. Effect of silane coupling agent treated bovine bone based carbonated hydroxyapatite on in vitro degradation behavior and bioactivity of PLA composites. Mater. Sci. Eng. C 32 (6), 1428–1436. https://doi.org/10.1016/j.msec.2012.04.022.

Rao, A.V., Kalesh, R.R., Pajonk, G.M., 2003. Hydrophobicity and physical properties of TEOS based silica aerogels using phenyltriethoxysilane as a synthesis component. J. Mater. Sci. 38 (21), 4407–4413. https://doi.org/10.1023/A:1026311905523.

Reyes-Peces, M.V., et al., 2020. Chitosan-GPTMS-silica hybrid Mesoporous aerogels for bone tissue engineering. Polymers 12 (11), 2723. https://doi.org/10.3390/polym12112723.

Şahin, E., 2018. Calcium phosphate bone cements. In: Saleh, H.E.-D.M., Rahman, R.O.A. (Eds.), Cement Based Materials. InTech. https://doi.org/10.5772/intechopen.74607.

Sohn, H.-S., Oh, J.-K., 2019. Review of bone graft and bone substitutes with an emphasis on fracture surgeries. Biomater. Res. 23 (1), 9. https://doi.org/10.1186/s40824-019-0157-y.

Suppakarn, N., Sanmaung, S., Ruksakulpiwat, Y., Sutapun, W., 2007. Effect of surface modification on properties of natural hydroxyapatite/polypropylene composites. KEM 361–363, 511–514. https://doi.org/10.4028/www.scientific.net/KEM.361-363.511.

Thongchai, K., Chuysinuan, P., Thanyacharoen, T., Techasakul, S., Ummartyotin, S., 2020. Integration of collagen into chitosan blend film composites: physicochemical property aspects for pharmaceutical materials. SN Appl. Sci. 2 (2), 255. https://doi.org/10.1007/s42452-020-2052-5.

Tronco, M.C., Cassel, J.B., Dos Santos, L.A., 2022. α-TCP-based calcium phosphate cements: a critical review. Acta Biomater. 151, 70–87. https://doi.org/10.1016/j.actbio.2022.08.040.

Vaz, C.M., Reis, R.L., Cunha, A.M., 2002. Use of coupling agents to enhance the interfacial interactions in starch–EVOH/hydroxylapatite composites. Biomaterials 23 (2), 629–635. https://doi.org/10.1016/S0142-9612(01)00150-8.

Wei, X., Ugurlu, O., Ankit, A., Acar, H.Y., Akinc, M., 2009. Dissolution behavior of Si,Zn-codoped tricalcium phosphates. Mater. Sci. Eng. C 29 (1), 126–135. https://doi.org/10.1016/j.msec.2008.05.020.

Wong, S.K., Wong, Y.H., Chin, K.-Y., Ima-Nirwana, S., 2021. A review on the Enhancement of calcium phosphate cement with biological materials in bone Defect Healing. Polymers 13 (18), 3075. https://doi.org/10.3390/polym13183075.

Xia, Y., et al., 2018. Gold nanoparticles in injectable calcium phosphate cement enhance osteogenic differentiation of human dental pulp stem cells. Nanomed. Nanotechnol. Biol. Med. 14 (1), 35–45. https://doi.org/10.1016/j.nano.2017.08.014.

Xia, Y., et al., 2019. Iron oxide nanoparticle-calcium phosphate cement enhanced the osteogenic activities of stem cells through WNT/β-catenin signaling. Mater. Sci. Eng. C 104, 109955. https://doi.org/10.1016/j.msec.2019.109955.

Xie, Y., Hill, C.A.S., Xiao, Z., Militz, H., Mai, C., 2010. Silane coupling agents used for natural fiber/polymer composites: a review. Compos. Appl. Sci. Manuf. 41 (7), 806–819. https://doi.org/10.1016/j.compositesa.2010.03.005.

Zima, A., 2018. Hydroxyapatite-chitosan based bioactive hybrid biomaterials with improved mechanical strength. Spectrochim. Acta Mol. Biomol. Spectrosc. 193, 175–184. https://doi.org/10.1016/j.saa.2017.12.008.

Zima, A., Czechowska, J., Szponder, T., Ślósarczyk, A., 2020. In vivo behavior of biomicroconcretes based on α-tricalcium phosphate and hybrid hydroxyapatite/chitosan granules and sodium alginate. J. Biomed. Mater. Res. 108 (5), 1243–1255. https://doi.org/10.1002/jbm.a.36898.

Oświadczenia autorów

Kraków, dnia 03.12.2025

mgr inż. Piotr Pańtak
Katedra Ceramiki i Materiałów Ogniotrwałych
Wydział Inżynierii Materiałowej i Ceramiki
Akademia Górniczo-Hutnicza im. Stanisława Staszica w Krakowie
Al. Mickiewicza 30, 20-059 Kraków

OŚWIADCZENIE

Oświadczam, że mój wkład w powstanie niżej wymienionych publikacjach polegał na opracowaniu koncepcji i planu badań wraz z doborem metodyki badawczej, wytworzeniu materiałów do badań materiałowych oraz biologicznych, przeprowadzeniu badań materiałowych, opracowaniu, analizie i interpretacji wyników badań materiałowych, opracowaniu graficznym wyników badań materiałowych, przygotowaniu przeglądu literatury oraz dyskusji wyników badań materiałowych i biologicznych, opracowaniu statystycznym wyników badań materiałowych, przygotowaniu pierwotnej i ostatecznej wersji manuskryptu, wysłaniu manuskryptu do czasopism, przygotowaniu odpowiedzi na recenzje.

1. *Influence of Natural Polysaccharides on Properties of the Biomicroconcrete-Type Bioceramics*, **Piotr Pańtak**, Ewelina Cichoń, Joanna P. Czechowska, Aneta Zima, Materials, 2021, vol. 14, iss. 24, art. no. 7496, s. 1–14, doi: 10.3390/ma14247496.

2. *Novel Double Hybrid-Type Bone Cements Based on Calcium Phosphates, Chitosan and Citrus Pectin*, **Piotr Pańtak**, Joanna P. Czechowska, Ewelina Cichoń, Aneta Zima, International Journal of Molecular Sciences, 2023, vol. 24, iss. 17, art. no. 13455, s. 1–15, doi: 10.3390/ijms241713455.

3. *The influence of silane coupling agents on the properties of α-TCP-based ceramic bone substitutes for orthopaedic applications*, **Piotr Pańtak**, Joanna P. Czechowska, Aneta Zima, RSC Advances, 2023, vol. 13, iss. 48, s. 34020–34031, doi: 10.1039/d3ra06027f.

4. *The Synergistic Effect of Polysaccharides and Silane Coupling Agents on the properties of Calcium Phosphate-Based Bone Substitutes*, **Piotr Pańtak**, Joanna P. Czechowska, Vladyslav Vivcharenko, Annett Dorner-Reisel, Aneta Zima, International Journal of Molecular Sciences, 2025, vol. 26, iss. 18, art. no. 8910, s. 1–18, doi: 10.3390/ijms26188910.

5. *The influence of titanium and copper on physiochemical and antibacterial properties of bioceramic-based composites for orthopaedic applications*, **Piotr Pańtak**, Joanna P. Czechowska, Anna Belcarz, Aneta Zima, Ceramics International, 2025, vol. 51, iss. 1, s. 1214–1226, doi: 10.1016/j.ceramint.2024.11.102.

6. *Improving the processability and mechanical strength of self-hardening robocasted hydroxyapatite scaffolds with silane coupling agents*, **Piotr Pańtak**, Joanna P. Czechowska, Adelia Kashimbetova, Ladislav Čelko, Edgar B. Montufar, Łukasz Wójcik, Aneta Zima, Journal of the Mechanical Behavior of Biomedical Materials, 2025, vol. 161, art. no. 106792, s. 1–11, doi: 10.1016/j.jmbbm.2024.106792.

03.12.2025 Piotr Pańtak

…….. ……..

Data Podpis

Kraków, dnia 03.12.2025

dr hab. inż. Aneta Zima, prof. AGH
Katedra Ceramiki i Materiałów Ogniotrwałych
Wydział Inżynierii Materiałowej i Ceramiki
Akademia Górniczo-Hutnicza im. Stanisława Staszica w Krakowie
Al. Mickiewicza 30, 20-059 Kraków

OŚWIADCZENIE

Wyrażam zgodę na wykorzystanie danych zawartych w wymienionych publikacjach na potrzeby rozprawy doktorskiej mgr. inż. Piotra Pańtaka. Jednocześnie oświadczam, że mój wkład w powstanie niżej wymienionych publikacji polegał na opracowaniu ich koncepcji, analizie i interpretacji wyników badań, sprawowaniu opieki merytorycznej podczas realizacji badań materiałowych, pomocy przy przygotowaniu manuskryptów, dyskusji z recenzentami oraz pozyskanie finansowania na prowadzenie badań.

1. *Influence of Natural Polysaccharides on Properties of the Biomicroconcrete-Type Bioceramics*, Piotr Pańtak, Ewelina Cichoń, Joanna P. Czechowska, **Aneta Zima**, Materials, 2021, vol. 14, iss. 24, art. no. 7496, s. 1–14, doi: 10.3390/ma14247496.

2. *Novel Double Hybrid-Type Bone Cements Based on Calcium Phosphates, Chitosan and Citrus Pectin*, Piotr Pańtak, Joanna P. Czechowska, Ewelina Cichoń, **Aneta Zima**, International Journal of Molecular Sciences, 2023, vol. 24, iss. 17, art. no. 13455, s. 1–15, doi: 10.3390/ijms241713455.

3. *The influence of silane coupling agents on the properties of α-TCP-based ceramic bone substitutes for orthopaedic applications*, Piotr Pańtak, Joanna P. Czechowska, **Aneta Zima**, RSC Advances, 2023, vol. 13, iss. 48, s. 34020–34031, doi: 10.1039/d3ra06027f.

4. *The Synergistic Effect of Polysaccharides and Silane Coupling Agents on the properties of Calcium Phosphate-Based Bone Substitutes*, Piotr Pańtak, Joanna P. Czechowska, Vladyslav Vivcharenko, Annett Dorner-Reisel, **Aneta Zima**, International Journal of Molecular Sciences, 2025, vol. 26, iss. 18, art. no. 8910, s. 1–18, doi: 10.3390/ijms26188910.

5. *The influence of titanium and copper on physiochemical and antibacterial properties of bioceramic-based composites for orthopaedic applications*, Piotr Pańtak, Joanna P. Czechowska, Anna Belcarz, **Aneta Zima**, Ceramics International, 2025, vol. 51, iss. 1, s. 1214–1226, doi: 10.1016/j.ceramint.2024.11.102.

6. *Improving the processability and mechanical strength of self-hardening robocasted hydroxyapatite scaffolds with silane coupling agents*, Piotr Pańtak, Joanna P. Czechowska, Adelia Kashimbetova, Ladislav Čelko, Edgar B. Montufar, Łukasz Wójcik, **Aneta Zima**, Journal of the Mechanical Behavior of Biomedical Materials, 2025, vol. 161, art. no. 106792, s. 1–11, doi: 10.1016/j.jmbbm.2024.106792.

03.12.2025 r.
Data

Aneta Zima
Podpis

Kraków, dnia 03.12.2025

dr inż. Joanna Czechowska
Katedra Ceramiki i Materiałów Ogniotrwałych
Wydział Inżynierii Materiałowej i Ceramiki
Akademia Górniczo-Hutnicza im. Stanisława Staszica w Krakowie
Al. Mickiewicza 30, 20-059 Kraków

OŚWIADCZENIE

Wyrażam zgodę na wykorzystanie danych zawartych w wymienionych publikacjach na potrzeby rozprawy doktorskiej mgr. inż. Piotra Pańtaka. Jednocześnie oświadczam, że mój wkład w powstanie niżej wymienionych publikacji polegał na: opracowaniu ich koncepcji, sprawowaniu opieki merytorycznej podczas planowania i realizacji badań, analizie i interpretacji wyników badań, pomocy w przygotowaniu manuskryptów oraz dyskusji z recenzentami, a także pozyskaniu finansowania na prowadzenie badań.

1. *Influence of Natural Polysaccharides on Properties of the Biomicroconcrete-Type Bioceramics*, Piotr Pańtak, Ewelina Cichoń, **Joanna P. Czechowska**, Aneta Zima, Materials, 2021, vol. 14, iss. 24, art. no. 7496, s. 1–14, doi: 10.3390/ma14247496.

2. *Novel Double Hybrid-Type Bone Cements Based on Calcium Phosphates, Chitosan and Citrus Pectin*, Piotr Pańtak, **Joanna P. Czechowska**, Ewelina Cichoń, Aneta Zima, International Journal of Molecular Sciences, 2023, vol. 24, iss. 17, art. no. 13455, s. 1–15, doi: 10.3390/ijms241713455.

3. *The influence of silane coupling agents on the properties of α-TCP-based ceramic bone substitutes for orthopaedic applications*, Piotr Pańtak, **Joanna P. Czechowska**, Aneta Zima, RSC Advances, 2023, vol. 13, iss. 48, s. 34020–34031, doi: 10.1039/d3ra06027f.

4. *The Synergistic Effect of Polysaccharides and Silane Coupling Agents on the properties of Calcium Phosphate-Based Bone Substitutes*, Piotr Pańtak, **Joanna P. Czechowska**, Vladyslav Vivcharenko, Annett Dorner-Reisel, Aneta Zima, International Journal of Molecular Sciences, 2025, vol. 26, iss. 18, art. no. 8910, s. 1–18, doi: 10.3390/ijms26188910.

5. *The influence of titanium and copper on physiochemical and antibacterial properties of bioceramic-based composites for orthopaedic applications*, Piotr Pańtak, **Joanna P. Czechowska**, Anna Belcarz, Aneta Zima, Ceramics International, 2025, vol. 51, iss. 1, s. 1214–1226, doi: 10.1016/j.ceramint.2024.11.102.

6. *Improving the processability and mechanical strength of self-hardening robocasted hydroxyapatite scaffolds with silane coupling agents*, Piotr Pańtak, **Joanna P. Czechowska**, Adelia Kashimbetova, Ladislav Čelko, Edgar B. Montufar, Łukasz Wójcik, Aneta Zima, Journal of the Mechanical Behavior of Biomedical Materials, 2025, vol. 161, art. no. 106792, s. 1–11, doi: 10.1016/j.jmbbm.2024.106792.

03.12.2025 ..... Data

..... Czechowska ..... Podpis

Kraków, dnia 03.12.2025

dr inż. Ewelina Cichoń
Instytut Katalizy i Fizykochemii Powierzchni im. Jerzego Habera
Polskiej Akademii Nauk w Krakowie
ul. Niezapominajek 8, 30-239 Kraków

OŚWIADCZENIE

Wyrażam zgodę na wykorzystanie danych zawartych w poniżej wymienionych publikacjach na potrzeby rozprawy doktorskiej mgr. inż. Piotra Pańtaka. Jednocześnie oświadczam, że mój wkład w powstanie poniżej wymienionych publikacji polegał na syntezie oraz przygotowaniu materiałów do badań materiałowych, opracowaniu metodologii badań, opracowaniu i interpretacji wyników badań materiałowych, redagowaniu i korekcie manuskryptu oraz opracowaniu odpowiedzi dla recenzentów.

1. *Influence of Natural Polysaccharides on Properties of the Biomicroconcrete-Type Bioceramics*, Piotr Pańtak, **Ewelina Cichoń**, Joanna P. Czechowska, Aneta Zima, Materials, 2021, vol. 14, iss. 24, art. no. 7496, s. 1–14, doi: 10.3390/ma14247496.
2. *Novel Double Hybrid-Type Bone Cements Based on Calcium Phosphates, Chitosan and Citrus Pectin*, Piotr Pańtak, Joanna P. Czechowska, **Ewelina Cichoń**, Aneta Zima, International Journal of Molecular Sciences, 2023, vol. 24, iss. 17, art. no. 13455, s. 1–15, doi: 10.3390/ijms241713455.

3.12.2025 ..... Data

Ewelina Cichoń ..... Podpis

Lublin, dnia 03.12.2025

dr hab. n. farm. Anna Belcarz-Romaniuk, prof. UML
Katedra i Zakład Biochemii i Biotechnologii
Wydział Farmaceutyczny
Uniwersytet Medyczny w Lublinie

OŚWIADCZENIE

Wyrażam zgodę na wykorzystanie danych zawartych w poniżej wymienionej publikacji na potrzeby rozprawy doktorskiej mgr. inż. Piotra Pańtaka. Jednocześnie oświadczam, że mój wkład w powstanie poniżej wymienionej publikacji polegał na planowaniu i doborze metodyki badań biologicznych, przeprowadzeniu badań biologicznych, ich analizie i interpretacji uzyskanych wyników, redagowaniu tej części manuskryptu i jego korekcie językowej.

1. *The influence of titanium and copper on physiochemical and antibacterial properties of bioceramic-based composites for orthopaedic applications*, Piotr Pańtak, Joanna P. Czechowska, **Anna Belcarz**, Aneta Zima, Ceramics International, 2025, vol. 51, iss. 1, s. 1214–1226, doi: 10.1016/j.ceramint.2024.11.102.

Signed by / Podpisano przez:
Anna Agnieszka Belcarz-Romaniuk
Uniwersytet Medyczny w Lublinie
Date / Data: 2025-12-03 09:46

……03.12.2025…….. ……
Data Podpis

Brno, 03.12.2025

Edgar Benjamin Montufar Jimenez, PhD
Central European Institute of Technology
Brno University of Technology
Purkyňova 123, 612 00 Brno
Czech Republic

DECLARATION

I hereby consent to the use of the data contained in the publication listed below for the purposes of the doctoral dissertation of Mr. Piotr Pańtak, M.Sc., B.Eng. I also declare that my contribution to its creation involved the development of the overall research concept, participation in the analysis and interpretation of the material research results, as well as oversight of the scientific and methodological aspects during the planning and execution of the material studies and the preparation of the manuscript.

1. *Improving the processability and mechanical strength of self-hardening robocasted hydroxyapatite scaffolds with silane coupling agents*, Piotr Pańtak, Joanna P. Czechowska, Adelia Kashimbetova, Ladislav Čelko, **Edgar B. Montufar**, Łukasz Wójcik, Aneta Zima, Journal of the Mechanical Behavior of Biomedical Materials, 2025, vol. 161, art. no. 106792, s. 1–11, doi: 10.1016/j.jmbbm.2024.106792.

03.12.2025
.....
Date

.....
Signature

Brno, 08.12.2025

Adelia Kashimbetova
Central European Institute of Technology
Brno University of Technology
Purkyňova 123, 612 00 Brno
Czech Republic

DECLARATION

I hereby consent to the use of the data contained in the publication listed below for the purposes of the doctoral dissertation of Mr. Piotr Pańtak, M.Sc., B.Eng. I also declare that my contribution to its creation involved the development of the concept of work, participation in the analysis and interpretation of the material research results, as well as oversight of the scientific and methodological aspects during the planning and execution of the material studies.

1. *Improving the processability and mechanical strength of self-hardening robocasted hydroxyapatite scaffolds with silane coupling agents*, Piotr Pańtak, Joanna P. Czechowska, **Adelia Kashimbetova**, Ladislav Čelko, Edgar B. Montufar, Łukasz Wójcik, Aneta Zima, Journal of the Mechanical Behavior of Biomedical Materials, 2025, vol. 161, art. no. 106792, s. 1–11, doi: 10.1016/j.jmbbm.2024.106792.

8.12.2025
..... Date

..... Signature

Brno, 03.12.2025

Ladislav Čelko, PhD
Central European Institute of Technology
Brno University of Technology
Purkyňova 123, 612 00 Brno
Czech Republic

DECLARATION

I hereby consent to the use of the data contained in the publication listed below for the purposes of the doctoral dissertation of Piotr Pańtak, M.Sc., B.Eng. I also declare that my contribution to its creation involved oversight of the scientific and methodological aspects during the planning and execution of the material studies, as well as during the preparation of the manuscript.

1. *Improving the processability and mechanical strength of self-hardening robocasted hydroxyapatite scaffolds with silane coupling agents*, Piotr Pańtak, Joanna P. Czechowska, Adelia Kashimbetova, **Ladislav Čelko**, Edgar B. Montufar, Łukasz Wójcik, Aneta Zima, Journal of the Mechanical Behavior of Biomedical Materials, 2025, vol. 161, art. no. 106792, s. 1–11, doi: 10.1016/j.jmbbm.2024.106792.

- 3 -12- 2025
Date

Signature

Kraków, dnia 03.12.2025

dr inż. Łukasz Wójcik
Katedra Ceramiki i Materiałów Ogniotrwałych
Wydział Inżynierii Materiałowej i Ceramiki
Akademia Górniczo-Hutnicza im. Stanisława Staszica w Krakowie
Al. Mickiewicza 30, 20-059 Kraków

OŚWIADCZENIE

Wyrażam zgodę na wykorzystanie danych zawartych w poniżej wymienionej publikacji na potrzeby rozprawy doktorskiej mgr. inż. Piotra Pańtaka. Jednocześnie oświadczam, że mój wkład w powstanie poniżej wymienionej publikacji polegał na planowaniu i wyborze metodyki badań reologicznych, przeprowadzeniu badań reologicznych, ich analizie i interpretacji uzyskanych wyników, redagowaniu tej części manuskryptu i jego korekcie językowej.

1. *Improving the processability and mechanical strength of self-hardening robocasted hydroxyapatite scaffolds with silane coupling agents*, Piotr Pańtak, Joanna P. Czechowska, Adelia Kashimbetova, Ladislav Čelko, Edgar B. Montufar, **Łukasz Wójcik**, Aneta Zima, Journal of the Mechanical Behavior of Biomedical Materials, 2025, vol. 161, art. no. 106792, s. 1–11, doi: 10.1016/j.jmbbm.2024.106792.

03.12.2025 ..... Data

..... Podpis

Schmalkalden, 05.12.2025

Prof. Dr. -Ing. habil Annett Dorner-Reisel
Faculty of Mechanical Engineering
Schmalkalden University of Applied Sciences
Blechhammer 4–9, Schmalkalden D-98574
Germany

DECLARATION

I hereby consent to the use of the data contained in the publication listed below for the purposes of the doctoral dissertation of Piotr Pańtak, M.Sc., B.Eng. I also declare that my contribution to its creation involved proofreading and editing of the manuscript, as well as to securing funding.

1. *The Synergistic Effect of Polysaccharides and Silane Coupling Agents on the properties of Calcium Phosphate-Based Bone Substitutes*, Piotr Pańtak, Joanna P. Czechowska, Vladyslav Vivcharenko, **Annett Dorner-Reisel**, Aneta Zima, International Journal of Molecular Sciences, 2025, vol. 26, iss. 18, art. no. 8910, s. 1–18, doi: 10.3390/ijms26188910.

8.12.25
Date

Signature

Lublin, dnia 03.12.2025

dr n. farm. Vladyslav Vivcharenko
Zakład Inżynierii Tkankowej i Medycyny Regeneracyjnej
Wydział Nauk Medycznych
Uniwersytet Medyczny w Lublinie
ul. Chodźki 1, 20-093 Lublin

OŚWIADCZENIE

Wyrażam zgodę na wykorzystanie danych zawartych w poniżej wymienionej publikacji na potrzeby rozprawy doktorskiej mgr. inż. Piotra Pańtaka. Jednocześnie oświadczam, że mój wkład w powstanie poniżej wymienionej publikacji polegał na planowaniu i wyborze metodyki badań biologicznych, przeprowadzeniu badań biologicznych, ich analizie i interpretacji uzyskanych wyników, redagowaniu tej części manuskryptu i jego korekcie językowej.

1. *The Synergistic Effect of Polysaccharides and Silane Coupling Agents on the properties of Calcium Phosphate-Based Bone Substitutes*, Piotr Pańtak, Joanna P. Czechowska, **Vladyslav Vivcharenko**, Annett Dorner-Reisel, Aneta Zima, International Journal of Molecular Sciences, 2025, vol. 26, iss. 18, art. no. 8910, s. 1–18, doi: 10.3390/ijms26188910.

3.12.2025
Data

Vladyslav Vivcharenko
Podpis